1-1-2000

The effect of branch distribution on morphology, chain dynamics and rheological behavior of metallocene and Ziegler-Natta linear low density polyethylenes.

Mikhail Y. Gelfer
University of Massachusetts Amherst

THE EFFECT OF BRANCH DISTRIBUTION ON MORPHOLOGY, CHAIN DYNAMICS AND RHEOLOGICAL BEHAVIOR OF METALLOCENE AND ZIEGLER-NATTA LINEAR LOW DENSITY POLYETHYLENES

A Dissertation Presented

by

MIKHAIL Y. GELFER

Submitted to the Graduate School of the University of Massachusetts Amherst
in partial fulfillment of the requirements for the degree of

DOCTOR OF PHILOSOPHY

September 2000

Polymer Science and Engineering

THE EFFECT OF BRANCH DISTRIBUTION ON MORPHOLOGY, CHAIN DYNAMICS AND RHEOLOGICAL BEHAVIOR OF METALLOCENE AND ZIEGLER-NATTA LINEAR LOW DENSITY POLYETHYLENES

A Dissertation Presented
by

MIKHAIL Y. GELFER

Approved as to style and content by:

Klaus Schmidt-Rohr, Chair

Henning H. Winter, Member

Samuel P. Gido, Member

Richard J. Farris, Department Head
Department of Polymer Science
And Engineering

ACKNOWLEDGMENTS

I would like to acknowledge the guidance and encouragement provided to me by my advisors, Professors Klaus Schmidt-Rohr and Henning H. Winter throughout the course of this research. I am grateful to them for giving me the opportunity to work on this project. I would also like to thank professor Samuel Gido for his many helpful suggestions.

I wish to thank my wife Polina and daughter Rebecca, whose love and support helped me a great deal during these years. I wish to thank my brother Lev and my parents for believing in me.

I wish to thank many fellow researchers for the great deal of help and support I received in this research. In particular I express appreciation to Roland Horst, Amy Heintz, Frederic Bayer, Douglas Harris and Dan Mowery for many helpful scientific discussions and much experimental assistance.

ABSTRACT

THE EFFECT OF BRANCH DISTRIBUTION ON MORPHOLOGY, CHAIN DYNAMICS AND RHEOLOGICAL BEHAVIOR OF METALLOCENE AND ZIEGLER-NATTA LINEAR LOW DENSITY POLYETHYLENES

SEPTEMBER 2000

MIKHAIL Y. GELFER, B.S. MOSCOW STATE UNIVERSITY

M.S. UNIVERSITY OF MASSACHUSETTS AMHERST

Ph.D. UNIVERSITY OF MASSACHUSETTS AMHERST

Directed by: Professors K. Schmidt-Rohr; H.H. Winter

The effects of the branching distribution in ethylene–α-olefin copolymers (LLDPEs) on morphology and molecular mobility in the solid state, and rheological properties in the melt and during crystallization were studied. Two types of ethylene-α-olefin-copolymers were examined: (I) Ziegler-Natta LLDPE containing significant amounts of highly and low-branched chains, and (II) metallocene LLDPE where branched α-olefin units are statistically distributed among the molecules.

Solid-state NMR techniques, WAXS, DSC, TEM and Raman spectroscopy were utilized to characterize LLDPEs in the solid state. A novel solid-state NMR technique for the determination of the lamellar thickness distribution was developed and tested during this investigation. The crystallization kinetics was measured by DSC. Rheological properties in the

melt and during crystallization were characterized using oscillatory and steady shear techniques.

In Ziegler-Natta copolymers the crystalline domains are predominantly formed by almost linear chains while highly branched molecules are excluded into the amorphous region. In the metallocene system, crystalline and amorphous domains are formed by segments belonging to the same chains. So numerous covalent links exist between crystalline and amorphous regions. As a result, the metallocene system has thinner crystalline and amorphous domains. It shows lower molecular mobility in the amorphous phase than its more branched Ziegler-Natta analog.

The existence of a crystalline-amorphous interface formed by all-trans yet partially mobile chains was proven for LLDPEs by NMR. The morphological partitioning of branched units and local chain conformation near the crystalline defects in LLDPEs was characterized by solid-state NMR techniques.

It was shown that for both metallocene and Ziegler-Natta LLDPEs the critical crystallinity ϕ_{cr}, at the gel point, i.e. the melt-solid transition, does not exceed 5% [w/w]. A higher crystallization rate and a narrower solidification interval is observed for a Ziegler-Natta copolymer and can be related to the significant content of almost linear molecules. Step-crystallization and partial melting temperature programs for the preparation of stable near-critical physical gels, whose crystallinity remains in the vicinity of ϕ_{cr} on the timescale of hours, were developed. The overall crystallinity and local chain conformation in stable

near-critical gels prepared from metallocene LLDPE were studied using Raman spectroscopy.

TABLE OF CONTENTS

ACKNOWLEDGEMENTS iv

ABSTRACT v

LIST OF TABLES xiii

LIST OF FIGURES xiv

Chapter

1. REVIEW OF MORPHOLOGICAL AND RHEOLOGICAL STUDIES OF ETHYLENE–α–OLEFIN COPOLYMERS FOCUSING ON BRANCHING DISTRIBUTION-PROPERTIES RELATIONSHIP 1

1.1 Background and motivation 1
1.2 Metallocene and Ziegler-Natta catalysis for synthesis of LLDPEs 5
1.3 Branching and crystallization rates in LLDPEs 7
1.4 Structural development during crystallization of HDPE and LLDPE 11
1.5 Possibility of liquid-liquid phase separation in LLDPE melts 12
1.6 Effect of the catalyst type on the rheological properties of LLDPE and HDPE in the melt 14
1.7 Avrami parameters for the crystallization of HDPE 14
1.8 Rheological models for the description of liquid-to solid transition induced by crystallization 15
1.9 The effect of branch content on LLDPE morphology 19

1.9.1 Melting temperatures 20
1.9.2 Lattice structure 21
1.9.3 Crystallinity 22
1.9.4 Lamellar structure 23
1.9.5 Interfacial structure 24
1.9.6 Supramolecular structure 25

1.10 Investigation of LLDPE morphology by solid-state NMR 27

1.10.1 Phase composition 28
1.10.2 Solid-state NMR analysis of morphological partitioning of branched units in LLDPEs 34

1.11 Motivation for the thesis work 37
1.12 References 38

2. BASIC CHARACTERISTICS OF MATERIALS, USED IN THIS INVESTIGATION 51
2.1 Properties of HDPEs and LLDPEs under investigation 51
2.2 References 53

3. EFFECT OF BRANCHING DISTRIBUTION ON EVOLUTION OF VISCOELASTIC PROPERTIES OF LLDPES DURING ISOTHERMAL AND NON-ISOTHERMAL CRYSTALLIZATION AND PARTIAL MELTING 56
3.1 Abstract 56
3.2 Introduction 57
3.3 Background information 59

3.3.1 Factors, controlling the lineshape in static ^{13}C NMR spectra of LLDPEs 59
3.3.2 Physical gelation by crystallization 60

3.4 Experimental 61

3.4.1 Materials 61
3.4.2 NMR 62
3.4.3 DSC 62
3.4.4 Rheometry 62
3.4.5 FT Raman measurements 64

3.5 Experimental results and discussions 65

3.5.1 Absence of liquid-liquid phase separation during isothermal melt-crystallization of LLDPEs 65
3.5.2 Melt rheology 67
3.5.3 Isothermal crystallization 68
3.5.4 Non-isothermal crystallization (cooling ramp) 71
3.5.5 Step-crystallization procedure 73
3.5.6 Partial melting procedure 78

3.6 Conclusions 80
3.7 References 83

4. DETERMINATION OF THE CRYSTALLITE-THICKNESS DISTRIBUTION IN POLYETHYLENES FROM ^{1}H NMR ROTATING FRAME RELAXATION 106

4.1 Abstract 106
4.2 Introduction 107
4.3 Experimental 110

4.3.1 Materials and sample preparation 110
4.3.2 DSC 110
4.3.3 TEM 111
4.3.4 Raman LAM 113
4.3.5 NMR 113

4.4 Results and Discussion 115

4.4.1 Sensitivity of $T_{1\rho}$ relaxation to PE structure 115
4.4.2 Mechanism of crystallite-thickness dependence of $T_{1\rho}$ 116
4.4.3 Crystallite thickness distribution from TEM 117
4.4.4 Fitting procedures to determine $p(T_{1\rho})$. 117
4.4.5 Empirical $T_{1\rho}(L)$ curve 120
4.4.6 $V(L)$ from TEM and NMR 121
4.4.7 Summary of calculation procedure 123
4.4.8 Comparison of lamellar thicknesses from DSC, Raman LAM, TEM, and NMR 124
4.4.9 Relaxation by chain flips vs. spin diffusion 125
4.4.10 $T_{1\rho}$ selection experiments with spin diffusion and $T_{1\rho}$ measurement 126
4.4.11 Perspective 128

4.5 Conclusions 130
4.6 References 131

5. EFFECTS OF THE BRANCHING DISTRIBUTION ON LOCAL MORPHOLOGY AND MOLECULAR MOBILITY IN LLDPES AS CHARACTERIZED BY SOLID-STATE NMR 145

5.1 Abstract 145
5.2 Introduction 146
5.3 Background information. Solid-state NMR techniques 147

5.3.1 Crystallinity measurement 147
5.3.2 Morphology and molecular mobility 149

5.3.3 ^{1}H $T_{1\rho}$ technique for the determination of the lamellar thickness distriibution..... 151

5.4 Experimental..... 152

5.4.1 Materials..... 152
5.4.2 DSC..... 152
5.4.3 NMR..... 153

5.5 Experimental Results..... 153

5.5.1 Crystallinity and crystallite thickness distributions... 153
5.5.2 Molecular mobility in the amorphous domain..... 155

5.6 Discussions..... 157
5.7 Conclusions..... 159
5.8 References..... 161

6. BRANCH DEFECTS IN LLDPE CRYSTALLITES AND THE STRUCTURE OF THE INTERFACIAL DOMAIN IN LLDPEs..... 175

6.1 Abstract..... 175
6.2 Introduction..... 176
6.3 Background information. NMR techniques used in this study..... 177

6.3.1 ^{1}H spin-diffusion and combined spin-diffusion-relaxation techniques..... 177
6.3.2 CODEX..... 179
6.3.3 2D exchange spectroscopy..... 181

6.4 Experimental..... 182
6.4.1 Materials..... 182
6.4.2 WAXS..... 183
6.4.3 NMR..... 183

6.5 Experimental Results and Discussions..... 183

6.5.1 Branch partitioning in the ethene-propene co-polymers..... 183
6.5.2 Dependence of lattice dimensions on the crystallite thickness..... 184

6.5.3 Molecular motion and local chain conformation in the vicinity of crystalline branch defect in ethene-propene co-polymers. 185
6.5.4 Investigation of the structure of the crystalline-amorphous interface by spin-diffusion and relaxation techniques. 188

6.6 Conclusions 190
6.7 References 192

7. CONCLUSIONS AND PROPOSED SUBSEQUENT RESEARCH .. 211

7.1 Effect of Branch distribution on the evolution of viscoelastic properties of LLDPEs during isothermal and non-isothermal crystallization and partial melting 211

7.1.1 Conclusions 211
7.1.2 Proposed further research. 213

7.2 Effect of the branch distribution on the morphology and local molecular mobility in LLDPEs. 215

7.2.1 Conclusions 215
7.2.2 Proposed further research. 216

7.3 Morphological partitioning of branched units and structure of the interfacial domain in LLDPEs. 217

7.3.1 Conclusions 217
7.3.2 Proposed further research. 218

7.4 References 220

BIBLIOGRAPHY 221

LIST OF TABLES

Table | Page

2.1 Characteristics of the investigated ethylene-α-olefin copolymers 54

3.1 Rheological characteristics of the investigated ethylene α-olefin copolymers 87

5.1. $^{13}C\ T_1$ relaxation times for LLDPEs and HDPE. $^{13}C\ T_1$ values calculated from the slope of the final ($t > 50$ s) part of the $I(t)$ curve . 163

LIST OF FIGURES

Figure Page

1.1 Synthesis of a metallocene catalyst; he cation form $[L_2Zr(CH_3)]^+$ is catalytically active 48

1.2 Methylene region of the ^{13}C CP MAS spectrum of Ziegler-Natta LLDPE. The narrow signal at 32.8 ppm corresponds to all-trans chains in the crystalline domain . The broad signal at 31 ppm corresponds to chains in the amorphous phase, having mixed trans and gauche conformations 49

1.3 Lineshape analysis of the non-crystalline spectrum of hydrogenated polybutadiene. (M_W = 420 kg/mol); Dotted curves at 30.5 ppm represent Lorentzians for the "rubbery phase" and "interfacial domain". Lorentzians centered at 39, 34, 28 and 26 ppm are sidechain signals (From Kitamaru et al. 1996 [88]) 50

2.1 Intermolecular branching distributions in ethylene-hexene co-polymers PE-M and PE-ZN as determined by TREF (Temperature Raising Elution Fractionation) at Exxon. 55

3.1 Isothermal and non-isothermal temperature programs utilized in rheological and DSC experiments: (a) isothermal crystallization; (b)non-isothermal crystallization; (c) step-crystallization; (d) partial melting; the samples for partial melting were slowly cooled from 160 °C to 30°C with a cooling rate of 1°C/min 88

3.2 Static ^{13}C direct polarization spectra, acquired during isothermal crystallization of LLDPEs (plots have been offset to show details of time evolution) 89

3.3 (a) frequency dependence of the storage modulus for ethylene co-polymers. T_{ref}=140 °C; a_T : logarithmic shift factor (b) the shear rate dependence of steady shear viscosity for ethylene co-polymers T = 160 °C 90

3.4 Isothermal crystallization kinetics for LLDPEs (by DSC) symbols: experimental data; lines: Avrami fit. (a)PE-M; (b) PE-ZN 91

3.5 Dependence of the viscoelastic properties of critical gel on the crystallization temperature ;solid symbol: PE-M; open symbol: PE-ZN: (a)gel time; (b) crystallinity at gel point; (c) gel stiffness S_c and relaxation exponent n_c. 92

3.6 Crystallinity dependence of dynamic viscoelastic properties of LLDPEs during the isothermal crystallization *(ω = 1 [rad/s])*; (a) PE-M *(ω = 1rad/s)*;(b) PE-ZN 93

3.7 Temperature dependence of dynamic viscoelastic properties of LLDPEs during non-isothermal crystallization (cooling ramp 4 °C/hr); lines: *G'*; symbols: *tan* δ
ω= 0.2 [rad/s] – – · ○ ; 1.26: ····· ◇ ; 5: —— △ ; and 20 rad/s: —— ■ .The samples are: (a) PE-M; (b) PE-ZN; (c) HDPE-ZN..... 94

3.8 DSC exotherms acquired during nonisothermal crystallization of LLDPEs. (a)PE-M; (b)PE-ZN. 95

3.9 Temperature dependence of storage modulus *G'(T)* during non-isothermal crystallization in PE-M:HDPE-ZN blends. 96

3.10 Rheological patterns of physical gels, prepared during step-crystallization (time evolution of viscoelastic properties during the isothermal steps)
(a) PE-M; (b) PE-ZN; (c)HDPE-ZN. 97

3.11 Time evolution of storage modulus during the isothermal and step-crystallization; open symbols: isothermal crystallization, solid symbols: step-crystallization. (a) PE-M ;(b) PE-ZN; (c) HDPE-ZN..... 98

3.12 Crystallization kinetics for isothermal and step-crystallization of PE-M. For step-crystallization the duration of the final isothermal step at 119.5 [°C] was used as the crystallization time..... 99

3.13 Sequence probability distributions for the statistic co-polymers having different average branching *x*[%mol]; ξ- number of consecutive methylene units in a sequence; W_ξ-weight fraction of a sequence, containing ξ units; $W_\xi = \xi(1-p)^2 p^\xi$; here $p = \left(\frac{100\% - x}{100\%}\right)$ the probability for the methylene group to be succeeded by another methylene group in a random co-polymer containing *x* [% mol] branched units. 100

3.14 Structural model describing behavior of metallocene and Ziegler-Natta LLDPEs during step-crystallization.
In PE-M longer and shorter linear sequences belong to the same molecules i.e. they are covalently bound. During the step-crystallization the crystallization of long methylene sequences decreases the molecular mobility and hinders crystallization of short sequences; in PE-ZN longer and shorter linear segments form separate crystallites, so their mutual influence is minimal 101

3.15 Steady-Shear properties of critical gels formed during step-crystallization of PE-M. (a) temperature dependence of yield stress τ_Y; (b) temperature dependence of creep viscosity η_{cr} (determined from the final slope of the creep viscosity curves at τ_{cr} = 12 kPa); E_α-flow activation energy 102

3.16 Dynamic viscoelastic properties of stable physical gels formed during partial melting of LLDPEs. (a) PE-ZN; (b) PE-M 103

3.17 Raman spectra acquired during partial melting of PE-M 104

3.18 Temperature dependence of Raman Crystallinity during partial melting of PE-M determined based on the intensity ratio of the 1416 cm^{-1} band to the overall intensity of CH_2 twisting signal[47] ■ and from the the intensity ratio for 1060 cm^{-1} band[50] ○ 105

4.1 NMR pulse sequences used in this work. (a) Standard $^1H\ T_{1\rho}$ experiment with ^{13}C detection. (b) Selection of long $T_{1\rho}$ components, spin diffusion during t_m, and subsequent $^1H\ T_{1\rho}$ measurement with ^{13}C detection. 134

4.2 $T_{1\rho}$ relaxation curves *I(t)* obtained by plotting the peak height of the all-trans peak at 32.8 ppm as a function of the spin-lock time *t*. (a) *I(t)* for LLDPEs. The strong effect of thermal history observed for the PE-ZN material, isothermally crystallized (PE-ZN b.i.) and as a quenched film (PE-ZN film), is striking. (b) I(t) curves for four HDPE: HDPE-Mi isothermally cryst.; HDPE-NBS1484 isothermally cryst.; HDPE-S solution crystallized. 135

4.3 Micrographs (partial views) with circles indicating sampling of lamellae for thickness measurements..... 136

4.4 (a) Lamellar thickness distribution $p(L)$ determined by TEM. (b) Distribution of relaxation times $p(T_{1\rho})$ determined by Williams-Watts fitting of ^1H $T_{1\rho}$ relaxation curves. (c) Distribution of relaxation times $p(T_{1\rho})$ determined by Gaussian fitting of ^1H $T_{1\rho}$ relaxation curves. The good qualitative agreement between $p(T_{1\rho})$ and $p(L)$ indicates a simple $T_{1\rho}$ (L) correlation. 137

4.5 (a) $T_{1\rho}$ decay data (squares) for PE-ZN b.i., showing pronouncedly nonexponential behavior, with single-exponential fit (straight line), Gaussian distribution fit (dashed curve), and stretched-exponential fit (full curve). The stretched-exponential provides clearly the best fit. (b) Corresponding distributions of relaxation times for the Williams-Watts fit (solid line), the Gaussian distribution fit (dashed line), and the single-exponential fit (delta-function). 138

4.6 Empirical calibration curve for converting $T_{1\rho}$ times to crystallite thicknesses. The points indicate average $T_{1\rho}$ and L values of the samples measured by both NMR and TEM. (a) Linear $T_{1\rho}$ scale. (b) Logarithmic $T_{1\rho}$ scale. Filled symbols: TEM data; open symbols: Raman data. 139

4.7 Comparison of thickness distributions $V(L)$ of LLDPEs as determined by NMR and by TEM: (a) PE-M film; (b) PE-ZN film; (c) PE-ZN b.i. (bulk. isothermally crystallized). 140

4.8 $T_{1\rho}$-relaxation curves $I(t)$ and corresponding thickness distributions V(L): (a) solution crystallized HDPE-S. b) Isothermally melt-crystallized Ziegler-Natta HDPE-ZNi; (c) Isothermally melt-crystallized metallocene HDPE-Mi; (d) isothermally melt-crystallized HDPE-NBS1484; the bimodal Gaussian distribution shown on the right with 4% of small crystallites gives better fit than the KWW function (stretched exponential); 141

4.9 DSC melting curves for several LLDPE samples used in this study. The DSC lamellar thicknesses were estimated from the maxima in the melting curves, using the Gibbs-Thomson relation. 142

4.10 Comparison of lamellar thicknesses determined by NMR (x-axis) with those from DSC, Raman LAM, and TEM (vertical axis). Open symbols: HDPEs, for which the interpretation of the relationship between lamellar thickness and melting temperature is controversial. 143

4.11. $T_{1\rho}$ selection, spin-diffusion during t_m and $T_{1\rho}$ measurement for (a) PE-ZN b.i., (b) PE-M film. For each sample, the curve without selection is compared with curves after 30-ms spin lock selection and mixing times of 1 ms, 20 ms, and 100 ms. The invariance of the PE-ZN b.i. curves to mixing time shows that spin diffusion and the resulting magnetization distribution do no affect the decay under spin lock; this means that it is not significantly affected by spin diffusion. 144

5.1 NMR technique for crystallinity measurement. LLDPE-PE-ZNq. is used as an example.
a) The lineshape of the amorphous signal in the fully relaxed spectrum is obscured by noise b) The lineshape of the amorphous signal in the partially relaxed spectrum (the recycle delay t_0 = 50s) is fitted by the gated decoupled spectrum (t_0 = 5s, t_f = 20 μs). The correction factor f is determined. $f = \frac{\left(\frac{I_{gd}}{I_{pr}}\right)}{\left(\frac{NS_{gd}}{NS_{pr}}\right)}$
Here I_{gd} and I_{pr} are the intensities of gated decoupled and partially relaxed spectra; NS_{gd} and NS_{pr} are corresponding numbers of scans
c) Noisy amorphous signal in fully relaxed spectrum (t_0 = 5000 s) is fitted by the lineshape of the gated decoupled spectrum, using the correction factor f determined in a).
The intensity of gated decoupled spectrum is scaled f× (NS_{sp}/NS_{gd}) times 164

5.2 Pulse programs, used in this study: (a) MAS *CP* T_1 filtering; t_f: T_1 filter; (b) MAS gated decoupling; t_f: dipolar dephasing (T_2 filter); t_m: mixing time (c) ^1H spin-diffusion with ^{13}C detection; t_f: dipolar dephasing ; t_m: mixing time 165

5.3 Effect of branching distribution and thermal history on crystallinity. Error in NMR crystallinity ± 3% [w/w]..... 166

5.4 Effect of thermal history on the line shape of crystalline and amorphous Signals. Heavy line: quenched sample. Thin line: isothermally crystallized sample.
Crystalline peak (31.-36 ppm): from ^{13}C direct polarization experiment t_0 = 5000 s. Amorphous peak (28-31.5): from gated decoupled experiment t_f = 20 μs; t_0 = 5s..... 167

5.5 Volume-averaged lamellar thickness distributions in LLDPEs, as determined from $^{1}H\ T_{1\rho}$ relaxation data. 168

5.6 *CP MAS* vs. ^{1}H spin diffusion with ^{13}C detection
— CP MAS; ▬ ^{1}H spin diffusion with ^{13}C detection, t_m = 100ms
(a) PE-M b.i.; (b) PE-M b.q.; (c) PE-M film; (d) PE-ZN b.i.; (e) PE-ZN b.q.; (f) PE-ZN film 169

5.7 $^{13}C\ T_1$ relaxation in ethylene co-polymers
I — MAS *CP* T_1 filtered spectra with ^{1}H decoupling
— t_f = 1s; ▬ t_f = 500s
(a) HDPE-M b.i. ; (b) PE-ZN b.i. ; c) PE-M b.q.
II ..... T_1 relaxation curves for the crystalline phase in ethylene copolymers; 170

5.8 The dependence of the lineshape in static ^{1}H spectra of LLDPEs on composition and thermal history. 171

5.9 ^{13}C MAS spectra of isothermally crystallized LLDPEs after gated decoupling..... 172

5.10 CP MAS spectra with ^{1}H decoupling
—— isothermally crystallized; ▬ quenched
(a) PE-M (b) PE PE-ZN 173

5.11 Proposed morphological structure for metallocene and Ziegler-Natta LLDPEs. 174

6.1 ^{1}H spin-diffusion with ^{13}C detection pulse sequences for the investigation of the phase composition in LLDPEs. 90° pulses are filled black. White: CP-cross-polarization, DD: dipolar decoupling. (a) ^{1}H spin-diffusion with ^{13}C detection; t_f-$^{1}H\ T_2$ filter
(b) ^{1}H spin-diffusion combined with $^{1}H\ T_2$ relaxation with ^{13}C detection. The $^{1}H\ T_2$ relaxation behavior in the domains selected by t_m is determined from the dependence of signal intensity on t_1
(c) ^{1}H spin-diffusion combined with $^{13}C\ T_1$ selection with ^{13}C detection. t_{f1}: $^{13}C\ T_1$ filter 195

6.2 Pulse sequence for CODEX NMR: 90° pulses are filled black. White: CP-cross-polarization, DD: dipolar decoupling. t_r: rotor period. Pure-exchange spectra are obtained by measuring a reference spectrum with t_m and Δ interchanged and subtracting the CODEX spectrum from it. 196

6.3 Pulse sequence for 2D exchange NMR: 90° pulses are filled black White: CP-cross-polarization, DD: dipolar decoupling, 180° pulses. t_f: chemical shift filter, with $t_f = 1/(4\,\Delta\omega)$. Here $\Delta\omega$ is the difference between the resonance frequencies for the crystalline methylene and crystalline propene α-site; t_{fl}-$^{13}C\ T_1$ filter 197

6.4 ^{13}C MAS NMR spectra of ^{13}C labeled ethene-propene co-polymer Pe-PrL:
(a) Cross-polarization; the overall content of propene units is ~1% mol.;(b) CP/T_1 filtered spectrum with t_f = 2s; the content of the propene units in the crystalline phase is 0.46 % mol.;
(c) Direct polarization spectrum, with short recycle delay t_o = 2s; the content of the propene units in the amorphous phase is 2 % mol..... 198

6.5 (a) WAXS pattern for PE-ZN b.q. Scattering maxima are labeled with corresponding Bragg's indices. (b) Unit cell structure for the orthorhombic crystalline lattice (c) Lattice base area *ab* vs. reciprocal crystallite thickness for the HDPE and ethylene co-polymers; symbols: experimental data; straight line: least-squares fit of the *ab(1/L)* dependence calculated for HDPE and ethylene-hexene co-polymers (Pe-PrL excluded). The degree of lattice expansion is distinctly higher for the ethylene-propene co-polymer than for other polymers with similar lamellar thickness. 199

6.6 Investigation of the crystalline mobility in PE-PrL by CODEX
(a) CP/T_1 filtered spectrum (t_f= 2s) vs. pure exchange- CODEX spectrum The relative intensity of the methylene backbone signal is far weaker in CODEX spectrum (b) Normalized CODEX exchange intensities $I(t_m) = (I_{ref.} - I_{CODEX}(t_m))/I_{ref.})$ as a function of t_m for the propene α-site (solid symbols) and crystalline backbone methylene (open symbols). At 292 K many defects undergo chain flips on a 30-ms time scale. 200

6.7 Model for the polymer chain conformation in the crystallite near a branch crystalline defect in ethylene-propene co-polymer; ψ: torsion angle;
The stems on each side of the defect are parallel. The axis denotes the orientation of the principal-axes system (PAS) of the chemical shift tensor for the labeled α-methylene site. The PAS orientation in the molecular frame was drawn according to Schmidt-Rohr et al.[25] 201

6.8. Normalized CODEX amplitude build-up for the crystalline propene α-site in PE-PrL as a function of $\delta N t_r$. Here I_α is normalized CODEX exchange intensity. The functional form of the ordinate axis $(1- I_\alpha)/4$ corresponds to 50% of crystalline defects undergoing two-site jump..... 202

6.9 ^{13}C MAS spectra for PE-PrL, at 260 K to avoid motional broadening. ▬ crystalline signal CP/T_1 filtered ,t_f = 2s; — amorphous signal; direct polarization with short recycle delay t_0 =2s.
(a)α-site methylene, (b) backbone methylene.
The crystalline α-site signal is shifted upfield compared to the amorphous α-site resonance. This indicates higher gauche content in the vicinity of crystalline defects than in the disordered phase.[18] 203

6.10 2D Exchange spectra of the crystalline α-site methylene in PE-PrL; (a) t_m = 300 ms (b) t_m = 1 ms (reference)..... 204

6.11 ^{1}H spin-diffusion with ^{13}C detection in PE-ZN b.q. The corresponding pulse sequence described in Fig.6.1a. t_f = 195 μs; CP =28μs.
(a) Dependence of the ^{13}C lineshape on the mixing time t_m.
t_m = 2 ms and 5 ms correspond to spin diffusion into the crystalline-amorphous interface.
(b) Dependence of the normalized integral intensity of all-trans and gauche-containing components on the mixing time t_m 205

6.12 ^{1}H spin-diffusion with ^{13}C detection in PE-M b.q. The corresponding pulse sequence described at Fig.6.1a. t_f = 250 μs; CP = 28μs.
(a) Dependence of the ^{13}C lineshape on the mixing time t_m.
t_m = 2 ms and 5 ms correspond to spin diffusion into the crystalline-amorphous interface.
(b) Dependence of the normalized integral intensity of all-trans and gauche-containig components on the mixing time t_m 206

6.13 Interfacial (heavy line) vs. crystalline (thin line) lineshape in the methylene region . The interfacial signal was acquired using ^{1}H spin-diffusion with ^{13}C detection technique (Fig.6.1.a), t_m = 2 ms, CP=28 μs. The crystalline spectrum was obtained by cross-polarization. CP=28 μs. (a) PE-ZN b.q.; (b) PE-M b.q. The broad lineshape of the all-trans interfacial signal indicates that at the interface all-trans chains are surrounded by molecules in a disordered conformation. 207

6.14 ^{1}H T_2 relaxation behavior in PE-ZN b.q. Spectra acquired using combined ^{1}H spin-diffusion -^{1}H T_2 relaxation technique (Fig.6.1.b.) ;t_1 increments of 5μs were used in all measurements. (a) Interfacial component. t_f=195 μs; t_m = 5ms; CP=28μs. (b) Crystalline core (reference) t_f=1 μs; t_m = 5ms; CP=28μs (no ^{1}H T_2 selection). (c) ^{1}H T_2 relaxation curves for the interfacial component and core crystallites. 208

6.15 Investigation of the interfacial domain in PE-M b.q. using the combined ^{1}H spin-diffusion-^{13}C T_1 selection technique with ^{13}C detection (Fig.6.1.c). For each t_m two spectra were acquired: ^{13}C T_1 filtered crystalline spectrum (t_{f1} = 3s) and the reference spectrum (t_{f1} = 10 ms). The difference (non-crystalline) spectrum was obtained by subtraction of the crystalline from the reference spectrum, without a scaling factor. The region 28.5-31.8 ppm in the non-crystalline spectrum corresponds to the disordered non-trans interface, the region 31.8-34.5 ppm – to the all-trans interfacial domain. (a) Dependence of the lineshape of the difference spectra on t_m. (b) Dependence of the normalized integral intensity on t_m 209

6.16 Proposed morphological structure of semi-crystalline ethylene co-polymers (branched units not shown). 210

CHAPTER 1

REVIEW OF MORPHOLOGICAL AND RHEOLOGICAL STUDIES OF ETHYLENE–α–OLEFIN COPOLYMERS FOCUSING ON BRANCHING DISTRIBUTION-PROPERTIES RELATIONSHIP

1.1 Background and motivation

Polyolefins play an important role in our industrial society. Worldwide more than 40 million tons of polyethylene, polypropylene, and copolymers are produced per year – most by the Ziegler-Natta process. This accounts for more than 40 % of the whole production of plastics. The recently commercialized metallocene process for the synthesis of polyolefins has higher throughput than the traditional Ziegler-Natta polymerization and allows for better control of product composition.

The metallocene process allows for the synthesis of ethylene–α–olefin copolymers linear low density polyethylenes, (LLDPEs) inaccessible by the traditional Ziegler-Natta synthesis. On the other hand, significant structural differences exist between novel metallocene and conventional Ziegler-Natta LLDPEs. While intramolecular distributions of branched α-olefin units in both, metallocene and conventional ethylene–α–olefin copolymers, obey Bernoullian statistics,[1-5] intermolecular composition distributions in these systems are drastically different.[5-7] Conventional LLDPEs are highly heterogeneous copolymers with significant contents of both highly and low-branched molecules. In contrast, in metallocene systems α-olefin units are statistically distributed among the polymer chains.[5,6] Obviously, for the optimization of the

processability and performance of novel LLDPEs it is necessary to know how the branching distribution affects the properties of LLDPEs in the liquid and in the solid state. However, while it is known, that the distribution of branched units may have a significant effect on crystallization behavior and morphology in LLDPEs,[8-11] the molecular factors governing the relationship between branching distribution and properties in LLDPEs are not fully understood.

The goal of this investigation is to determine the effect of branching distribution on the crystallization kinetics, on the viscoelastic properties of LLDPEs in the melt and during crystallization, and on the morphology and molecular mobility in the solid state. This investigation consists of two parts. The first part is a melt and melt-crystallization study, where the structure and viscoelastic properties of LLDPE in the molten state and during crystallization are investigated. The second part is a solid-state study, dealing with the morphology and molecular mobility in solid LLDPEs. In both parts, the effects of branching distribution were elucidated through the systematic analysis of metallocene and Ziegler-Natta LLDPEs samples, whose molecular structure known in detail.

The major purpose of the melt investigation is the understanding of structural factors, controlling viscoelastic behavior of LLDPEs undergoing melt-solid transition during the isothermal and non-isothermal crystallization. In this work, the rheological properties of crystallizing LLDPEs are monitored by dynamic and steady shear techniques, crystallization kinetics is determined in parallel DSC experiments. It is known that the melt-solid transition in

crystallizing polymers can be treated as physical gelation, so the analysis of the rheological data is performed within the framework of the rheological theory of gelation, developed by Winter et al.[12-15]

It is shown that the critical crystallinity (ϕ_{cr}) for the melt-solid transition is similar in the metallocene and Ziegler-Natta copolymers ($1.5 < \phi_{cr} < 5\%$ w/w). However, Ziegler-Natta LLDPE has a higher crystallization rate and a narrower solidification interval than metallocene LLDPE. This observation is related to the significant content of almost linear chains in the heterogeneous Ziegler-Natta copolymer. It is shown that stable near-critical physical gels, whose crystallinity remains in the vicinity of ϕ_{cr} on the timescale of hours can be prepared from LLDPEs using step-crystallization and partial melting temperature programs developed in this study. Viscoelastic properties of stable critical and near-critical gels are characterized by dynamic and steady-shear rheological techniques. The crystallinity and chain conformation in stable physical gels, prepared from the metallocene LLDPEs are determined by Raman spectroscopy. The molecular model describing the relationship between branching distribution and non-isothermal crystallization behavior in LLDPEs was proposed based on the results obtained in this investigation.

LLDPE morphology was investigated by solid-state NMR, combined with WAXS (wide angle X-ray scattering), DSC (differential scanning calorimetry), and TEM (transmission electron microscopy). The NMR techniques,[16] used in this work allow the discrimination of morphological domains, based on the molecular mobility and NMR relaxation rates, thus

enabling the researcher to target different morphological areas directly, rather than to rely on line-fitting procedures.

The major emphasis in the solid-state investigation is the analysis of the relationship between branching distribution, crystallite thickness distribution and molecular mobility in the crystalline and amorphous domains of LLDPEs. The crystallite thickness distribution controls the molecular mobility in the crystalline domains and influences such important macroscopic properties of solid LLDPEs as creep, crack resistance and toughness.[17-20] Thus the ability to determine and control the crystallite thickness distribution is critical for the optimization of performance in solid LLDPEs. A simple, direct non-destructive solid state NMR technique for the determination of the lamellar thickness distribution in ethylene copolymers was developed and applied during this study.[21] The validity of this novel NMR technique was proven by comparing the results obtained with crystallite thickness distributions, measured by TEM and Raman techniques.[21] The structure of the interfacial region between the crystalline and amorphous domains in LLDPEs was studied by ^{1}H spin-diffusion, relaxation and ^{13}C spectroscopy. It was proven that the crystalline-amorphous interface in ethylene–α–olefin copolymers is formed by all-trans yet partially mobile chains, protruding from the crystalline into the amorphous region. A novel solid state NMR technique, CODEX[22] was applied for studying the local chain conformation near branch in LLDPE crystallites, in combination with 2-D exchange MAS NMR and ^{13}C T_1 and T_2 selection methods. The effect of branch length and branching distribution on morphological partitioning and

local mobility of branched units was characterized using ^{13}C T_1 and T_2 selection techniques.

With the aid of metallocene catalysts, the structure of the plastics synthesized can be controlled for the first time within wide limits, creating a new class of LLDPEs. However, significant differences in molecular structure between conventional and novel copolymers can result in unexpected property changes, and not necessarily in the desired direction. This investigation sheds light on the structural characteristics of novel and LLDPEs, and how they affect their performance and processability. The outcome of this research will allow future researchers to optimize ethylene–α–olefin copolymers for the desired applications.

1.2 Metallocene and Ziegler-Natta catalysis for synthesis of LLDPEs

A Ziegler-Natta catalyst is formed by a series of heterogeneous reactions of alkylates of aluminum with complexes of transition metals (such as Zr).[23]

$$TiCl_4 + AlR_3 \rightarrow TiCl_3R + AlR_2Cl$$

$$TiCl_4 + AlR_2Cl \rightarrow TiCl_3R + AlRCl_2$$

$$TiCl_3R + AlR_3 \rightarrow TiCl_2R_2 + AlR\,Cl_2$$

$$TiCl_3R \rightarrow TiCl_3 + R^*$$

$$TiCl_3 + AlR_3 \rightarrow TiCl_2R + AlR_2Cl$$

The novel metallocene catalyst is synthesized by homogeneous reaction of complexes of transition metals with methylaluminoxane[5] (Fig.1.1) Conventional Ziegler-Natta catalysts are generally polymorphous solids on whose surface relatively non-uniform catalytic action takes place. In contrast to that, metallocene systems, either in solution or supported, can be considered as single-site catalysts.

Because of the heterogeneous nature of the catalyst, conventional ethylene–α–olefin copolymers prepared through Ziegler-Natta process (ZLLDPE), have highly non-uniform intermolecular composition distribution and broad distribution of molecular weights (M_w/M_n = 3-5) .[5,23] In conventional LLDPEs, the low-molecular weight sub-fraction is enriched by branched units, while the high-molecular weight fraction contains relatively few branched units. On the other hand, in metallocene LLDPEs the intermolecular composition distribution is rather narrow; branched (α-olefin) units are statistically distributed among polymer chains.[5,10,24] Molecular weight distribution is also narrower for metallocene systems[5]: M_w/M_n = 2-3. The intramolecular composition distribution (i.e. distribution of branched units along the polymer chain) to a good approximation can be considered random for both Ziegler-Natta and metallocene copolymers.[1-5,23, 25]

1.3 Branching and crystallization rates in LLDPEs

Virtually all types of industrial processing of LLDPEs involve melting and crystallization. Thus understanding the effect of the branching distribution on the crystallization rate is of primary importance for predicting LLDPE behavior during processing. Theoretical and experimental aspects of polymer crystallization have been the subject of numerous books and review articles.[26-33] However, crystallization behavior of branched molecules is still not completely understood.

Analysis of the crystallization kinetics of commercial LLDPEs is greatly hindered due to their blend-like character. Indeed, both metallocene and Ziegler-Natta LLDPEs can be described as blends of statistical copolymers with varying branching. Highly branched molecules can't accommodate crystalline stems, formed by long linear segments. As a result, upon crystallization molecules tend to separate based on the branching content. The fractionation process tends to reinforce the separation of spherulitic crystallization into two processes: primary crystallization of dominant lamellae, forming the skeletal framework of spherulites and secondary crystallization within spherulites.[28-35] The primary lamellae are mostly formed by molecules with low branching content, while secondary crystallization primarily arises from more branched molecules.[34-35] The bulk crystallization kinetics of LLDPEs includes a variety of processes: primary nucleation, growth of primary lamellae and in-filling. In principle, each

of these processes can be influenced by the branching content, so the effect of branching on the bulk crystallization rate is more complicated than its influence on the rate of crystallite growth. However, the results obtained by Lambert and Phillips[34-35] by studying narrow-distributed ethylene–octene fractions indicate that for the early stages of crystallization at low supercooling $(T_{cr} > 110\,^{o}C)$ the effect of branching on the overall crystallization kinetics in LLDPEs is determined by its influence on the crystal growth rate.

According to the widely accepted Laurizen-Hoffman (LH) theory, the rate of the isothermal growth G for a polymer crystal is given by eq.1.1[26-33]

$$G_i = G_0 \exp\left[-\frac{U^*}{R(T - T_\infty)}\right] \exp\left[\frac{K_g}{T\Delta Tf}\right] \qquad (1.1)$$

Here i = I, II or III qualifies the crystal growth regime and the undercoling ΔT = T_m -T_{exp} which is the difference between the equilibrium melting temperature T_m and the crystallization temperature T_{exp}. The pre-exponential factor G_0 has a very weak temperature dependence and may be considered as constant.

The first exponential term accounts for the temperature dependence of the segmental transport across the liquid/solid interface, whereas the second exponential term describes the driving force for the crystal growth as expressed under the assumption of a coherent secondary nucleation process. U^* is the activation energy for the segmental transport and $T\infty$ is the temperature below which molecular motion, necessary for the transport of segments across the liquid-solid interface, becomes infinitely slow. $T\infty$ is usually taken as $T_g - 30$ K. When isothermal crystallization is studied far above the glass transition (as is the

case for crystallization of LLDPEs at low supercooling) the exact values of T_∞ and U^* and even the functional form of the first term do not affect in any significant way the crystal growth rate[26] .

At low supercooling, the crystal growth is controlled by a process of coherent secondary nucleation where the nucleation constant $K_{g(i)}$ is given by

$$K_g(i) = \frac{2ib_0\sigma\sigma_e T_m}{f\,k\Delta H} \qquad (1.2)$$

Here i has a value of 1 for regime II and a value of 2 for regimes I and III, b_0 is the thickness of a monomolecular layer in the direction normal to the growth plane, σ is the lateral crystal/melt interfacial energy, σ_e is the fold surface free energy, k is Boltzmann's constant, ΔH is the enthalpy of fusion of a perfect crystal at its equilibrium melting temperature, and f- is a correction factor used to compensate for changes in ΔH with temperature.

The different regimes may be envisioned as resulting from the relative rates of two competing processes: secondary nucleation and surface spreading. If the rate of deposition of secondary nuclei is i and the rate of surface spreading is g, then if expressed in units of area covered per unit time, the regimes correspond to the following conditions:

regime I: $i << g$

regime II: $i \approx g$

regime III: $i > g$

The introduction of branched units influences both the rates of nucleation (presence of non-crystallizable units hinders nucleation) and surface spreading

(branched units slow down the reptation). On the other hand, *g* is more sensitive to the molecular mobility than *i*. Thus *g* greatly decreases when the molecular weight exceeds the reptation threshold. Exclusion of branched units to the folds changes the packing of crystalline chains in the lamellae, thus affecting the surface energy σ_e. The overall crystallization regime for branched polymers results from the balance of the described factors.

The data obtained by Lambert et.al.[34-35] show that both crystal growth rate and bulk crystallization rate decrease drastically with the increase in branching content. For low molecular weight fractions of branched PE (M_W = 18-25 kg/mol) crystallization occurs in regimes I and II, while for higher M_w (M_W = 104-175 kg/mol) regimes II and III were observed.

Alizadeh et al.[36] investigated isothermal and non-isothermal crystallization of ethylene–octene copolymers over a broad temperature range. Based on the analysis of crystallization kinetics determined by DSC and considering the final morphology of crystallized copolymers they proposed that below a characteristic crystallization temperature T* the mechanism of LLDPE crystallization undergoes a drastic change. According to Alizadeh et al., crystallization above T* results in the formation of lamellar structures, while crystallization below T* causes the formation of very small fringed-micellar-type crystallites. The value of T* depends on copolymer composition. So far this hypothesis has not been tested by the structural investigation *in situ*.

1.4 Structural development during crystallization of HDPE and LLDPE

Akpalu et al[37] studied isothermal crystallization of slightly branched LLDPE (0.21 % mol C-8) using time-resolved light scattering and time-resolved simultaneous WAXS and SAXS techniques[37]. According to this work the SAXS pattern appears before crystallinity becomes detectable by WAXS. This indicates that at the early stages of crystallization the framework of spherulites is being formed by rather disordered structures. These structures are enriched in longer methylene sequences. As crystallization proceeds, the degree of order in the initially formed structures increases; eventually they transform to mature primary lamellae. The secondary crystallization occurs when more branched chains crystallize in "liquid pockets " between stacks of primary lamellae.

Bark et.al[38] studied crystallization of HDPE by time-resolved simultaneous WAXS and SAXS. Similar to the results of Akpalu,[37] it was shown that crystallization of HDPE can be described as a two-stage process. During the primary crystallization, thicker lamellae form the framework of spherulites. During the secondary stage, after spherulites fill the volume, further crystallization occurs in liquid pockets inside existing spherulites. Time evolution of WAXS and SAXS patterns indicates that initially formed structures have a low degree of order. As the crystallization proceeds, the degree of order increases. The results of time-resolved SAXS investigation by Sasaki et al.[39] also indicate that disordered structures formed during the early

stages of isothermal crystallization of HDPEs and LLDPEs evolve into mature lamellae as crystallization proceeds.

Song et al.[40-41] applied time-resolved SAXS for the investigation of crystallization behavior in 50/50 blends of HDPE with LDPE. It was shown that HDPE and LDPEs form separate lamellar bundles. The HDPE component in the blend investigated dominates the crystallization process at early stages of crystallization, forming the framework of the spherulitic structure.

1.5 Possibility of liquid-liquid phase separation in LLDPE melts

The blend-like character of LLDPEs implies the possibility of liquid-liquid phase separation in these copolymers. The occurrence of liquid-liquid phase separation in LLDPE melts would have a great impact on the melt rheology, crystallization behavior and solid-state morphology of these widely used polymers. Because of that, the melt phase composition of LLDPEs and HDPE-LLDPE blends was the subject of extensive investigation during the recent years.[42-51]

Hill et al.[42-44] proposed that the heterogeneous solid-state morphology observed in LLDPEs and LLDPE:HDPE blends is indicative of liquid-liquid phase separation in the melt above the melting temperature of HDPE. Obviously, it is not the only possible explanation available. The separation between linear and branched chains may occur during crystallization.

More convincing data were obtained by Alamo et al.[46-48] and Wignall et al.,[49-50] who investigated heterogeneous LLDPEs and HDPE-LLDPE blends,

both in the melt at 160 °C and in the solid state using SANS (small-angle neutron scattering) technique.

It was shown that a highly branched fraction having a content of branched units exceeding 5 % mol. forms a dispersed phase[48] in the melt. However, even for highly heterogeneous LLDPEs the estimated content of the dispersed phase was rather low (2% vol).[48] Also, the molecular masses of polymers used in these SANS experiments were rather high (i.e. $M_{w\ HDPE-D}$ = 140 kg/mol), so hydrogen-deuterium isotope effects cannot be excluded as the driving force behind the observed liquid-liquid phase separation phenomena.[48] Thus, one canexpect that in non-deuterated LLDPEs the content of dispersed phase will be even below 2% vol.

As mentioned above, during time-resolved SAXS/WAXS investigations of crystallizing HDPEs and LLDPEs the SAXS pattern appears before the emergence of Bragg peaks at wide angles[36-37]. Ryan et al.[50] interpreted these observations by proposing the occurrence of liquid-liquid phase separation during the early stages of crystallization. According to Ryan, the liquid-liquid phase separation below T_m results in the appearance of a metastable "ordered melt" predominantly formed by polymer chains in all-trans conformation, but lacking the long-range order present in crystallites. During the later stages of crystallization this "ordered melt" would transform into crystallites. So far the existence of such a "ordered melt" has not been proven by any l technique that is sensitive to the local chain conformation, such as NMR or Raman spectroscopy.

1.6 Effect of the catalyst type on the rheological properties of LLDPE and HDPE in the melt

Gabriel et al.[52] investigated melts of homogeneous and heterogeneous LLDPEs by shear creep recovery measurements. It was shown that in contrast to metallocene systems for Ziegler-Natta LLDPEs the temperature dependence of recoverable shear compliance does not obey the time-temperature superposition principle. This deviation was interpreted as the evidence of liquid-liquid phase separation occurring in melts of heterogeneous LLDPEs. Based on the magnitude of deviation the content of dispersed phase was estimated as 2% vol., which is consistent with the value proposed by Wignal et al. [48]

According to Vega et al.,[53] viscosity and flow activation energy are higher for metallocene HDPEs than for their Ziegler-Natta analogs having similar average molecular weight. Also the dependence of the viscosity on the molecular weight is steeper for metallocene HDPEs. These observations were related to narrow molecular weight distributions and the total absence of long branches in metallocene system.[53]

1.7 Avrami parameters for the crystallization of HDPE

The early stages of isothermal crystallization of HDPE conform to the Avrami equation [54,55]

$$(W_L/W_0) = exp(-zt^n) \qquad (1.3)$$

where W_L is the weight fraction of the liquid polymer remaining after time t, W_0 – the weight fraction of the crystalline polymer at infinite time. n and z are constants at constant temperature.

Both z and n are indicative of the crystallization mechanism. For non-seeded melt-crystallization of HDPE the values of n are usually in the range 2-4.[54,55]

Interesting results were obtained in partial melting experiments, where a variety of HDPEs were crystallized after being partially molten below the main melting point and subsequently re-crystallized in the presence of the unmolten material[55]. Values of the Avrami exponent n_{pm} observed for partially molten samples were far lower $(1.35 < n_{pm} < 1.58)$ than for the isothermal crystallization of the same materials $(2.97 < n < 3.87)$. According to Banks et al.[55] the observed decrease in the apparent values of n is consistent with the residual crystallites acting as seeds for consequent crystallization.

This result can be of interest for the analysis of crystallization kinetics of commercial LLDPEs containing a range of fractions with different equilibrium melting temperatures and crystallization rates.[5,25,34,35]

1.8 Rheological models for the description of liquid-to solid transition induced by crystallization

The transformation from a liquid to a solid state induced by crystallization can be considered as physical gelation, where connectivity is provided by crystalline regions acting as the thermoreversible bonds. The liquid-

solid transition (gel point) occurs when the first molecular cluster has grown to infinite size i.e. to the size of sample.[12-15,56]

The approach of the gel point by the gelling system has typically been recognized by a zero-shear viscosity η_0 which increases during cross-linking until it diverges at the gel point. Beyond the gel point the material can be characterized by its growing equilibrium modulus, G_e, which is zero before and at the gel point. It was shown that both in chemical and in physical gelation the gel point has its own distinctive rheological properties, which can be characterized by slow power-law dynamics. This expresses itself in a self-similar relaxation modulus:[13-15]

$$G = -S_c t^{-n_c} \quad \text{for} \quad \lambda_0 < t < \infty \tag{1.4}$$

The gel stiffness, S_c [Pa s^n], and the critical relaxation exponent n_c are rheological material parameters; n_c can adopt values $0 < n_c < 1$. Higher values of S_c correspond to stiffer gels, smaller n_c correspond to higher cross-linking density.[14,56] The self-similar relaxation occurs in the terminal zone at long times, $\lambda_0 < t < \infty$. The lower limiting relaxation time λ_0 characterizes the crossover to the entanglement relaxation or glass transition. The self-similar relaxation behavior can also be expressed by a power law relaxation time spectrum.

$$H(\lambda) = \frac{S_c \lambda^{-n_c}}{\Gamma(n)} \text{ ; for } \lambda_0 < \lambda < \infty \quad (\Gamma(y) \text{ is the gamma function}) \tag{1.5}$$

The self-similar relaxation results in power-law dynamic moduli

$$G'(\omega) = S_c\ \Gamma(1-n_c)\ \cos(n_c\pi/2)\ \omega^{n_c} \quad \text{for } \omega < 1/\lambda_0 \qquad (1.6)$$

$$G''(\omega) = S_c\ \Gamma(1-n_c)\ \sin(n_c\pi/2)\ \omega^{n_c}$$

and a constant loss angle $\delta = \pi n_c / 2$ at low frequencies.

It can be seen that at the gel point *tan* δ in the low frequency region becomes frequency independent (plateau region), which can be used as the basis for gel point detection. The parameters S_c and n_c can be directly calculated from G' and G'' at the gel point . It is interesting to note that for the isothermal crystallization of highly branched ethylene–butene co-polymer the degree of bulk crystallinity at the gel point does not exceed 3 % w/w.[13]

Boutahar et al.[57] studied isothermal crystallization of HDPE using DSC, light microscopy and oscillation shear techniques. Crystallization kinetics measured by DSC was correlated with the time dependence of the storage modulus G'. It was proposed that at early stages of crystallization, the polyethylene melt can be treated as a suspension of colloidal particles in a liquid viscoelastic matrix, where crystallites act as filling agents.[57]

According to ref.[57] the low-frequency storage modulus of a crystallizing melt can be related to the bulk crystallinity $\phi(t)$ by a simple equation

$$\phi(t) = \left(\frac{G'(\phi) - G'(0)}{G'_\infty} \right)^{1/3} \qquad (1.7)$$

where $G'(0)$ is the storage modulus of a fluid matrix and G'_∞ the final storage modulus measured after complete crystallization ($\phi = 0.84$).

This relationship implies that the functional form of $G'(\phi)$ dependence is the same for all ϕ, which is not necessarily correct. Indeed, the primary crystallites are being formed during the growth of spherulites, while the secondary crystallization occurs inside supramolecular structures. Thus the formation of the same amount of primary and secondary crystallites would have different effects on rheological properties.

Teh et al.[58] described the crystallinity dependence of the elastic shear modulus using the Kerner-Halpin equation developed for the description of dispersions in the form

$$G/G_l = (1+AB\phi)/(1-B\Phi\phi) \qquad (1.8)$$

where G_l is the shear modulus of the melt, A and B are functions of the Poisson ratio of the spherulites, and Φ is maximum packing fraction of the solid melt.

For the crystallizing melt the physical meaning of the fitting parameters A, B and Φ is not clearly defined. Based on the similarity between crystallization kinetics and the time dependence of the storage modulus, it was proposed that the rate of the storage modulus increase corresponds to the rate of secondary nucleation.[58] The validity of that approach requires further proof.

Jackson et al.[59,60] investigated the temperature dependence of the equilibrium shear modulus of polymethylene and its branched copolymers. Polymethylene is structurally identical to HDPE, its copolymers are analogs of LLDPE, but in contrast to polyethylene these polymers were synthesized by decomposition of diazoalkyl compounds. Considering crystalline domains as

rigid cross-links, the temperature dependence of the shear modulus in the vicinity of the melting point was estimated using the theory of rubber elasticity:

$$G = kT(\nu^c/N_a)/V_u \qquad (1.9)$$

where ν^c is the number of crystalline chain sequences, calculated based on the thermodynamic theory of co- polymer melting[59], N_a the Avogadro number, and V_u is the molar volume of methylene segment .[59]

Values of the shear modulus, calculated from Eq.(1.9) are at least two orders of magnitude lower than experimentally determined. The difference between predicted and experimentally determined values of G can be related to the propagation of the crystalline order into the amorphous domain, interaction between crystallites, and effects of the crystalline-amorphous interface and the crystallite's ability to act both as cross-links and fillers.

1.9 The effect of branch content on LLDPE morphology

The influence of branching on the LLDPE morphology was the subject of extensive theoretical and experimental investigations.[8-11,59-73] Here the most important aspects of the branching-morphology relationship directly related to the subject of the current investigation will be briefly reviewed.

1.9. 1 Melting temperatures

The majority of researchers agree that branched units longer than methyl are excluded from the crystalline phase [8,60]. Thus for branched ethylene copolymers other than ethylene–propene the melting behavior has to be independent of the type of branched unit. For random copolymers under the stipulation that only crystalline and amorphous phases are present and the crystalline phase remains pure, the equilibrium melting temperature can be expressed as

$$\frac{1}{T_m} - \frac{1}{T_m^0} = -\frac{R}{\Delta H_u} \ln(x) \qquad (1.13)$$

Here x is the content of branched units, T_m is the equilibrium melting temperature of LLDPE, $T_m{}^0$ the equilibrium melting temperature of the infinite HDPE crystal, and ΔH_u the enthalpy of melting for HDPE.[59-61] It can be seen that for low branching x, Eq.1.1.3 implies a linear decrease of the equilibrium melting temperature with branching.

Because of kinetic restrains, real polymers can not achieve the structural conditions stipulated by the equilibrium requirements. As a result experimentally observed melting temperatures of random copolymers $T_{m.exp.}$ are systematically lower, than those predicted by Eq.(1.13). However, the analysis of the melting behavior of melt-quenched LLDPEs having narrow composition distributions proved that for branching contents x ranging from 0 to 8 % mol. the melting temperature $T_{m.exp}$ appears to linearly decrease with branching. The data from co-monomers varying from butene to octene fall onto the same curve,

which is consistent with the exclusion of branched units. However the slope in the $T_{m,exp}(x)$ dependence is steeper than predicted by Eq. 1.13.[8,9,36,62] Melting temperatures observed for ethylene–propene copolymers are consistently higher than in other copolymers, indicating accommodation of methyl group within the crystalline lattice.[63,64]

In commercial LLDPEs, the type of composition distribution greatly affects the melting behavior. Melting temperatures of Ziegler-Natta LLDPEs were shown to be higher than in metallocene analogs having similar overall branching[19]. In contrast to data presented by Alamo and Alizadeh,[8,9,36] Kim et al.[19] demonstrated that in commercial copolymers hexyl branches cause stronger depression of the melting point than ethyl or butyl sidechains. This phenomenon was related to a stronger perturbation of crystalline order by larger branches. On the other hand, the observed difference in the melting behavior may be caused by the difference in the intermolecular branching distributions between the octene copolymers studied and the rest of the samples, investigated by Kim.

1.9.2 Lattice structure

HDPE and ethylene–α–olefin copolymers containing less than 8 % mol. of branched units form the orthorhombic crystalline lattice when melt-crystallized at ambient pressure.[8,63-69] WAXS data reported by many research groups prove that in comparison to HDPEs the crystalline lattice in LLDPEs expands in both *a* and *b* directions.[66-69] The lattice expansion was observed for the variety of sidechains, ranging from propyl to n-decanyl.[66-69] Initially, these

phenomena were thought to be related to the inclusion of branched units into the crystalline lattice.[66-67] However the inclusion of branches longer than methyl appears to be inconsistent with solid-state NMR data[70] and results of the thermodynamic analysis.[71] In addition, the lattice expansion was observed not only in LLDPEs but also in samples of HDPE, both solution and melt-crystallized, and in *n*-alkanes [72-73]. Moreover, it was shown that in many cases the degree of lattice expansion is reciprocally proportional to the lamellar thickness.[68-69] Thus, the lattice expansion in LLDPEs is related to the reduction in crystallite thickness due to branching rather than to the inclusion of branched units. According to Bunn,[71] because of reduced crystallite thickness lateral cell dimensions can be altered by the local stress exerted at the base planes.

The increase in the branching content above 10 % mol. may lead to the decrease in the lattice symmetry. WAXS patterns indicate the presence of both orthorhombic and monoclinic crystallites in a melt-crystallized ethylene–butene copolymer, containing 12% mol. branched units.[74]

1.9.3 Crystallinity

The degree of crystallinity *(ϕ)* in LLDPEs depends on the branching *x* and molecular weight.[8] It is not significantly influenced by the chemical nature of the comonomers. Indeed, for all monomers other than propene the $\phi(x)$ data fall to the same curve.[8,75,76] Levels of crystallinity for ethylene–propene copolymers are consistently higher than for their equally branched analogs, which is consistent with inclusion of methyl units into the crystalline phase.[8,63,76]

The effect of branching on crystallinity is quite strong. For instance, for M_w = 90 kg/mol the degree of crystallinity drops from 50 to 7 % w/w as the branch content increases from 0.5% mol. to 6 % mol.[8,62,76] For fixed branch content, an increase in the molar mass causes substantial decrease in crystallinity: in LLDPE, containing 2.3 % mol of branched units the increase in M_w from 10 to100 kg/mol causes a crystallinity reduction from 50 to 40 % vol.[76]

1.9.4 Lamellar structure

LLDPEs containing up to 4 % of branched units form lamellar crystals during melt-crystallization. For low co-unit contents (below 1 % mol.) straight, well-defined lamellae are formed, while for higher branching lamellae are smaller and curved. The crystalline lamellar thickness in LLDPEs (determined by TEM, SAXS and Raman spectroscopy) rapidly decreases with increased branching.[8, 62,76] For fixed branch content, the crystallite thickness decreases with the increase in molar mass, the observed variation in crystallite thickness is in good agreement with the decrease of the melting temperature with molar mass. Using a series of quenched narrow distributed LLDPEs with branch length varying from 2 to 6 carbons it was shown that the lamellar thickness is not affected by the chemical nature of the sidechains.[8,62,76]

As branching increases from 3 to 6 % mol., bundle-like crystals appear along the lamellar structures. Highly-branched copolymers containing more than 8 % mol branched units form only bundled crystals.[7,10,77]

1.9.5 Interfacial structure

Flory et al.[78] pointed out that a demarcation between the ordered crystalline region and the disordered liquid-like region could not be sharply defined in a semicrystalline polymer. The dissipation of order must be gradual. Consequently an interfacial region develops that involves partially ordered sequence of chain units.

The interfacial content in polyethylene and ethylene copolymers was evaluated by Raman spectroscopy and SAXS techniques.[8,62,76,79,80] It was shown that the interfacial content is greatly influenced by the thermal history, branching and molar mass. For instance, for the series of quenched ethylene–hexene copolymers with M_w = 90 kg/mol the overall fraction of interfacial region increases from 0.1 to 0.18 as branching increases from 1 to 4 % mol.[8,76] This increase in the interfacial content may be related to the reduction of the crystallite thickness by increased branching. The interfacial content also increases with molar mass. For quenched ethylene-hexene copolymers the increase in M_w from 100 to 400 kg/mol results in the interfacial content increase from 0.12 to 0.16.[8,76] However, significant scattering of the experimental data does not allow to determine the relationship between the nature of sidechains and the interfacial structure.

It should be noted that SAXS and Raman techniques do not allow for the direct observation of the interfacial region. In SAXS the interfacial content is determined from an analysis of the density correlation function.[81] The

interpretation of SAXS data heavily relies on assumed morphological models.[81] Because of low contrast and the broad crystallite thickness distribution in LLDPEs, SAXS pattern may not even contain a distinct peak. Thus, precision of SAXS measurements in LLDPEs is rather low. In Raman spectroscopy, the interfacial content is determined as the difference between unity and combined mass fractions of crystalline and amorphous phase.[8,76,83,84] This procedure involves the subtraction of values of similar magnitude, i.e. it is intrinsically prone to errors. Besides, for LLDPEs the assignment of Raman peaks to crystalline and amorphous domains remains the subject of controversy.[82-84] More reliable information about the interface structure can be obtained by solid-state NMR techniques. Application of NMR techniques for the investigations of phase composition in LLDPEs will be reviewed later in this chapter.

1.9.6 Supramolecular structure

A variety of supramolecular structures have been observed in solid polyethylene and ethylene–α–olefin copolymers. For instance, in addition to mature spherulites, immature asymmetric spherulite structures and rod-like aggregates were detected in samples of linear polyethylene, crystallized in different thermal regimes [7,8,10,85,86] In some cases, LLDPE samples have a random morphology without detectable supramolecular structures.[86] The type of supramolecular structures formed in LLDPE can be influenced by crystallization regime, branching, and molecular weight. Low molecular weight and low branching favor the formation of well-defined spherulites. As branching

increases, the maximal molecular mass within which spherulites can be formed decreases markedly.

Spherulites are more likely to be formed during isothermal crystallization. In quenched systems, the variety of morphological forms including distorted spherulites, thin rods and rod-like aggregates are routinely observed.[85,86]

Bensason et al. studied the branching dependence of the morphology in metallocene LLDPEs.[7] According to the classification system proposed by Bensason[7] the morphology of homogeneous LLDPEs fall into four categories. Type IV corresponds to very low branched (0-1 % mol), high-density (0.96-0.93 g/cm^3) systems. LLDPE IV forms lamellar crystals and well-defined spherulites. Copolymers type III (branching 1-3% mol, density 0.93-0.9 g/cm^3) have less perfect lamellae and can also form spherulites. LLDPE II has a lower density (0.9-0.89 g/cm^3) and higher branching (4-8% mol). This type of copolymers has a mixed morphology, consisting of lamellae and bundle-like crystals and is unlikely to form spherulites. Type I copolymers have densities below 0.89 also, branching above 8% mol. and predominantly form bundled crystals. Spherulite structures have not been observed in highly branched copolymers.[7]

1.10 Investigation of LLDPE morphology by solid-state NMR

High resolution ^{13}C NMR spectra of solid ethylene copolymers can be acquired using the traditional techniques of solid-state NMR such as fast spinning of sample around an axis that forms the magic angle (54.74°) with the direction of the external magnetic field, and heteronuclear dipolar decoupling by continuous irradiation on the proton resonance frequency. This magic-angle spinning (MAS) in combination with the dipolar decoupling allows to eliminate anisotropic broadening effectively and to obtain structural information contained in isotropic chemical shifts.[16]

Advanced solid-state NMR techniques allow for the discrimination of morphological domains based on the segmental mobility. These methods give the researcher a unique opportunity to selectively excite magnetization in the morphological regions of interest without the interference of other domains. Moreover, the selection can be fine-tuned. For instance, the solid-state NMR technique can be used for the selective observation of sub-domains of different mobility within the amorphous region. In this study solid-state NMR is utilized as the major experimental tool, so the previous applications of the solid state-NMR for the investigation of LLDPE are reviewed separately and in more detail than other structural techniques.

1.10.1 Phase composition

Based on the result of theoretical analysis[78,87] as well as Raman and SAXS[8,79-85] investigations, it was proposed that developed interfacial regions exists in polyethylene and ethylene copolymers. However neither Raman nor SAXS techniques allow for the direct observation of signals related to the interfacial domain. In contrast to that, the solid-state NMR may provide the direct information about the interfacial region.

In the crystalline phase, the polymer chains exist in all-trans planar zig-zag conformations, while in the disordered amorphous domain both trans- and gauche chain conformations are present. Because of the gamma-gauche effect, the difference in average chain conformation results in a difference in the ^{13}C isotropic chemical shift for the backbone methylene units in crystalline and amorphous domains. As a result, crystalline and amorphous

Signals in the methylene region (28-34 ppm) can be resolved in a ^{13}C spectrum under magic angle spinning (MAS) (Fig.1.2).[16]

The use of selection ("filtering") techniques allows for the observation of signals from methylene units, located in sub-domains of different mobility within amorphous and crystalline morphological regions. Thus, details of the morphological structure can be determined from the analysis of the methylene region in high-resolution ^{13}C NMR spectra with a precision inaccessible by other techniques. The currently applied approach for the analysis of phase composition by solid-state NMR includes three major steps: (1) A fully relaxed DP(direct polarization)/MAS spectrum representing combined signals from all

morphological domains is acquired. (2) Separate spectra representing morphological regions of different mobility are acquired using filtering techniques. The molecular mobility in different morphological domains is characterized using selection and NMR relaxation techniques. The chemical shifts corresponding to signals from crystalline, amorphous and interfacial domains are determined based on the results of selection experiments. (3) The overall phase composition is determined by fitting the experimental spectra, acquired in (1) and (2) by Gaussian or Lorentzian lineshapes, centered at chemical shift values corresponding to signals from crystalline, amorphous and interfacial domains, as assigned in (2).

Kitamaru et al.[88] investigated the molar mass dependence of the phase composition in hydrogenated polybutadienes of different molecular weights, containing 2.2 % mol. of ethyl branches. Hydrogenated polybutadiene can be considered as an analog of LLDPE, having narrow molecular weight and composition distributions.

"Crystalline" spectra, containing only the signal from the crystalline domain, were acquired using the CPT_1 filtering technique, that suppresses magnetization from mobile domain, having short $^{13}C\ T_1$. "Non-crystalline" spectra were acquired using $^{13}C\ T_1$ selection (modified DP/MAS saturation-recovery technique). This method allows for the suppression of magnetization from rigid domains based on $^{13}C\ T_1$ selection. Sub-domains of different mobility within the non-crystalline domain were detected using combined saturation-recovery and $^{13}C\ T_2$ filtering technique. Application of this technique allows

distinguish contributions from regions having similar ^{13}C T_1, yet different ^{13}C T_2 relaxation times.

Kitamaru et al.[88] showed that the non-crystalline signal contains contributions from two components, having different chemical shift (30 and 30.5 ppm). Both components have similar ^{13}C T_1 (0.16 s), but different T_2 relaxation rates (400 μs and 25 μs respectively). The resonance at 30 ppm was assigned to the signal from liquid-like amorphous phase with random chain conformation and rubber-like mobility. The component at 30.5 ppm was assigned to the more rigid crystalline-amorphous interface.

The relative contents of each non-crystalline sub-phase were determined by fitting of fully relaxed and non-crystalline spectra by superposition of Lorentzian lineshapes. The results of the lineshape analysis for the non-crystalline signal are shown at (Fig.1.3). It can be seen that amorphous and interfacial signals were not completely resolved.

Results received indicate that the molar mass increase from 16 to 420 kg/mol causes the mass fraction of the amorphous (rubbery) domain to increase from 0.43 to 0.68, the interface content remains constant (0.18). While the results obtained by Kitamaru[88] agree with the Raman spectroscopy data[62] available for similar samples, the fitting of unresolved lines by a distribution of lineshapes can't be considered a highly reliable procedure. Indeed, the signals from the interfacial and amorphous domains may be inhomogeneously broadened, so the corresponding lineshapes may be different from both Lorenzian and Gaussian.

Using similar NMR techniques Kitamaru et al.[89] characterized the molecular weight dependence of phase structure in HDPE. It was found that for low molecular weights (M_w <30 kg/mol) the content of rubbery phase is very low. However, with the increase in M_w the rubbery component appears. An increase in M_w from 10 to 3000 kg/mol causes the weight fraction of the interfacial component to increase from 0.06 to 0.16 while the fraction of the rubbery phase increases from 0.06 to 0.2.

Kuwabara et al.[90] investigated the influence of branching distribution and thermal history on phase structure of LLDPEs using solid-state NMR, DSC and TEM. Metallocene and Ziegler-Natta LLDPEs used by Kuwabara[90] had almost identical overall branch content (~1.9 % mol) and similar molar mass (M_w ~ 100 kg/mol), which allows to elucidate the morphological effect of the branching distribution. The effect of thermal history was evaluated by comparing the isothermally crystallized and quenched samples. The NMR pulse programs used by Kuwabara[90] and the approach to the analysis of NMR data were similar to those applied by by Kitamaru et.al .[88-89] The phase compositions were determined by fitting the lineshape of a fully relaxed single-pulse ^{13}C spectrum by three Lorentzian lineshapes, which were assigned to the crystalline, amorphous (rubbery) and interfacial domains. It was found that metallocene samples have a lower crystallinity and higher contents of both interfacial and rubbery components than Ziegler-Natta LLDPEs with similar thermal histories. A decrease in the crystalline content due to quenching was detected in all tested copolymers. The mass fraction of the interfacial domain ranged from 0.38

(isothermally crystallized Ziegler-Natta LLDPE) to 0.44 (quenched metallocene LLDPE), dcpending on the thermal history of samples. Contents of the rubbery phase varied from 0.09 (quenched Ziegler-Natta LLDPE) to 0.13 (quenched metallocenc LLDPE). The lamellar thickness, determined by TEM and melting temperatures determined by DSC were lower for metallocene than for Ziegler-Natta copolymers, with similar thermal histories.

Thc difference between phase compositions in metallocene and Ziegler-Natta samples, detected by Kuwabara[90] is rather subtle. While the results reported seem to make sense in the general context of the information available about composition-morphology relationships in LLDPEs,[8,76] it is not clear if the accuracy of the of the fitting procedure is sufficient for the precise determination of the effects of thermal history and branching distribution on phase composition. Also it should be noted that the "interfacial" contents reported by Kitamaru et al.[88] and Kuwabara et al.[90] are so large that it suggests that data treatment procedure used in the ref.[88-90] include into the interfacial domain parts of what is usually considered amorphous.

The process of the equilibration of spatially inhomogeneous longitudial magnetization under the influence of homonuclear dipolar couplings is called spin-diffusion.[16,91] ^{1}H spin diffusion can be applied for the direct determination of mutual spatial location of morphological domains. For instance, $^{1}H\ T_{1\rho}$ selection allows to dcstroy magnetization in mobile domains, with short $^{1}H\ T_{1\rho}$, so only the crystalline domain remains magnetized. During the equilibration of the resulting non-equilibrium magnetization by ^{1}H spin diffusion magnetization

initially spreads to the areas, located in close proximity to the crystalline region, i.e. to the interfacial domain. It takes more time for the magnetization to reach the core of the amorphous region.[16,91] Thus, by varying the time for spin diffusion the (mixing time t_m) it is possible to restore magnetization selectively within a certain distance from the initially magnetized morphological domain. Crystalline and amorphous signals in ^1H spin-diffusion experiments can be resolved using ^{13}C detection under MAS conditions.

Kimura et al.[92] applied a spin-diffusion technique with ^1H $T_{1\rho}$ selection for the investigation of the interfacial structure in HDPE. It was shown that in HDPE the morphological domain located between crystalline and amorphous regions indeed contributes to the intensity of methylene signal at 30.5-31 ppm. However this conclusion was based on a lineshape analysis of the crystalline signal, rather than on the direct observation of the signal from the interfacial region.

Obviously, the lineshape analysis of unresolved lines is the major source of the controversy in the interpretation of the NMR data. For instance, the chain conformation and the degree of order in the interfacial domain can't be determined without resolving the interfacial signal. Thus, the development of improved "filtering" pulse programs resulting in the efficient resolution of the amorphous and interfacial signals is highly desirable.

1.10.2 Solid-state NMR analysis of morphologieal partitioning of branehed units in LLDPEs

Due to differences in isotropie ehemical shifts the signals of the ehain ends, methyl and methylene segments belonging to branehed units ean be resolved from the backbone methylene signals in ^{13}C MAS spectra.[93-96] The analysis of morphologieal partitioning of branehed units is based on the applieation of filtering teehniques that enable the researeher to selectively observe signals from the branehed units embedded in different morphological domains.[95,97-99]

VanderHart and Perez[97,98] studied partitioning of branehed units in ethylene–butene and ethylene–propene copolymers using a variety of CP(eross-polarization) techniques under MAS eonditions. In CP NMR magnetization is transferred from ^{1}H to ^{13}C nuelei by the heteronuelear dipolar coupling in the presence of suitably matched radio-frequency irradiation at both resonance frequencies. CP produces more intense signals than direct ^{13}C polarization teehnique, which is a significant advantage for the investigation of braneh sites in LLDPEs, where the overall branching is low. However, the strength of the dipolar eoupling and therefore the efficiency of the magnetization transfer is affeeted by the local molceular mobility, so the peak intensities in the CP spectrum may not reflect the true sample composition.[16]

Three types of spectra were acquired: CP MAS, $^{1}H\ T_{1\rho}$ filtered CP MAS and $^{1}H\ T_{2}$ filtered CP MAS. The CP MAS spectrum (cross-polarization time 1 ms) contains signals from both mobile (amorphous) and rigid (crystalline)

domains. $^{1}H\ T_{1\rho}$ filtering allows to observe selectively crystalline signals by suppressing signals from the amorphous domain, which have a short $^{1}H\ T_{1\rho}$. The $^{1}H\ T_{2}$ filtering method creates the opportunity for the selective observation of signal from the mobile domains, where $^{1}H\ T_{2}$ is relatively long. In order to quantify branching partitioning CP efficiency for all branched units was evaluated by comparing the CP and ^{13}C direct polarization spectra, recorded with short recycle delay (5s).

The data obtained were interpreted in the framework of two-phase morphological model (i.e. the existence of separate interfacial domain was ignored). No evidences of inclusion of branches other than methyl into the crystalline domains was found.[97-98] It was estimated that for both ethylene–butene and ethylene–propene copolymers as much as 50-75 % of methyl chain ends and 42-63 % of vinyl chain ends were included into the crystalline domain. For the ethylene–propene co-polymer 21-27% of methyl branches is included into the crystalline domain.

Perez et al.[99] studied the effect of thermal history on the partitioning of branched units in ethylene–butene co-polymer using CP-MAS technique. The CP efficiency is higher for the crystalline domain, so the use of a short CP time (t_{cp}= 0.2 ms) sufficiently reduces the intensity of the amorphous signal. According to Perez[99] as much as 9% of ethyl branches may be included into the crystalline domain. The influence of thermal history on branching partitioning was found to be insignificant. It should be noted that for the interfacial region, the CP efficiency can be rather high, so the signal from the branch unit

embedded into the interfacial region may contribute to the spectrum acquired with $t_{cp}= 0.2\ ms$.

McFaddin et al.[100] studied morphological partitioning of branched units in copolymers of deuterated ethylene with protonated 1-alkenes ranging from propene to 1-octadecene. In such systems it is possible to observe selectively only signals corresponding to branched units without the interference of deuterated backbone methylenes. Based on $^{13}C\ T_1$ relaxation behavior of branched units, it was concluded that for all investigated copolymers the branched units are located in the same mobile (amorphous) phase.

Kuwabara et al.[90] determined the partitioning of butyl branches in metallocene and Ziegler-Natta ethylene–hexene copolymers using $^{1}H\ T_{1\rho}$ selection and $^{13}C\ T_2$ relaxation measurements. Received results were interpreted in the framework of a three-phase model. According to Kuwabara[90] butyl branches arc completely excluded from the crystalline domain, the mass fractions of branched units for the interfacial and amorphous regions are 0.63 and 0.37, respectively. No marked difference in the morphological partitioning of branches in metallocene and Ziegler-Natta polymers was detected.

The approach for the determination of branch partitioning used in the articles rcviewed[97-100] seems reasonable; however, the factors reducing the accuracy of proposed techniques are worth mentioning. The application of CP techniques for quantitative measurements requires exact knowledge of CP efficiencies for various branch sites, which is not always possible. For instance, the relaxation behavior and mobility of methyl end-groups can be different from

the rest of branch carbons. Filtering techniques decrease the signal intensity, so the signal-to noise ratio in the "filtered" spectra can be rather poor, especially for the systems having a low branch content. Signals from branches incorporated into the crystallite and interface region as defects can be inhomogeneously broadened, which also reduces the accuracy of quantitative morphological analysis.

1.11 Motivation for the thesis work

Understanding of the structural and rheological effects of branching distribution is made paramount by the recent developments in catalyst technology. Yet in spite of significant amount of information about LLDPEs available in the literature, not enough of the systematic studies connecting branching distribution with properties of LLDPEs have been performed.

On the other hand, many aspects of LLDPE structure can now be studied in a great detail. Powerful techniques and approaches for the characterization of molecular structure, morphology and rheological properties of LLDPEs are currently available. This creates an exciting opportunity to perform research, which will answer a number of questions important from both the scientific and the technological point of view.

1.12 References

1. Hsieh, E. T.; Randall, J. C."Ethylene-1-Butene Copolymers. 1. Comonomer Sequence Distribution." *Macromolecules*, **15**, 253 (1982).

2. Hsieh, E. T.; Randall, J. C."Monomer Sequence Distributions in Ethylene-1-Hexene Copolymers." *Macromolecules*, **15**, 1402 (1982).

3. Kimura, K.; Yuasa, S.; Maru, Y."Carbon-13 nuclear magnetic resonance study of ethylene-1-octene and ethylene-4-methyl-1-pentene copolymers." *Polymer*, **25**, 441 (1984).

4. Kimura, K.; Shigemura, T.; Yuasa, S."Characterization of Ethylene-1-Butene Copolymer by Differential Scanning Calorimetry and ^{13}C-NMR Spectroscopy." *J.Appl.Polym.Sci.*, **29**, 3161 (1984).

5. Kaminsky, W."New polymers by metallocene catalysis." *Macromol. Chem.Phys.*, **197**, 3907 (1996).

6. Gelfer, M. Y.; Winter, H. H."Effect of branch distribution on rheology of LLDPE during early stages of crystallization." *Macromolecules*, **32**, 8974 (1999)

7. Bensason, S.; Minick, J.; Moet, A.; Chum, S.; Hiltner, A.; Baer, E."Classification of Homogeneous Ethylene-Octene Copolymers Based on Comonomer Content." *J. Polym.Sci., B: Polym.Phys.*, **34**, 1301 (1996).

8. Alamo, R. G.; Mandelkern, L."The crystallization behavior of random copolymers of ethylene." *Thermochimica Acta*, **238**, 155 (1994).

9. Alamo, R.; Domszy, R.; Mandelkern, L."Thermodynamic and Structural Properties of Copolymers of Ethylene." *J. Phys Chem*, **88**, 6587 (1984).

10. Mathot, V. B. F. Structure, crystallization and melting of linear, branched and copolymerized polyethylenes as revealed by fractionation methods and DSC. In *New Advances in Polyolefins;* Chung, T. C. Ed.; Plenum Press: NY, 1993; 121.

11. Kim, M. H.; Phillips, P. J."Nonisothermal Melting and Crystallization Studies of Homogeneous Ethylene/a-olefin Random Copolymers." *Journal Applied Polymer Science*, **70**, 1893 (1998).

12. Pogodina, N. V.; Winter, H. H."Polypropylene crystallization as a physical gelation process." *Macromolecules*, **31**, 8164 (1998).

13. Horst, R. H.; Winter, H. H."Stable critical gels of a crystallizing copolymer of ethcne and 1-butcne." *Macromolecules*, **33**, 130 (2000).

14. Schwittay, C.; M.Mours; Winter, H. H."RheologicalnExprcssion of Physical Gclation in Polymcrs." *Faraday Discussions*, **101**, 93 (1995).

15. Winter, H. H.; Mours, M."Rheology of Polymers ncar Liquid-Solid Transitions." *Advances in Polymer Science*, **134**, 166 (1997).

16. Schmidt-Rohr, K.; Spicss, H. W. *Multidimensional Solid-State NMR of Polymers*; Acad.Press: NY, 1994.

17. Popli, R.; L.Mandelkern."Influence of Structural and Morphological Factors on the Mcchanical Properties of the Polyethylenes." *J. Polymer Science B; Polymer Physics*, **25**, 441 (1987).

18. Hu, W.-G.; Bocffel, C.; Schmidt-Rohr, K."Chain Flips in Polycthylcne Crystallitcs and Fibers Charactcrized by Dipolar ^{13}C NMR." *Macromolecules*, **32**, 1611 (1999).

19. Kim, Y.-M.; Park, J.-K."Effect of Short Chain Branching on the Blown Film Propcrtics of Linear Low Density Polyethylene." *Journal of Applied Polymer Science*, **61**, 2315 (1996).

20. Hosoda, S.; Uemura, A."Effcct of the Structural Distribution on the Mcchanical Propertics of Linear Low-Density Polyethylenes." *Polymer Journal*, **24**, 939 (1992).

21. Gelfer, M.Y.; Beyer, F.; Gido, S. P. ; Alamo, R. ; Schmidt-Rohr, K. "Polyethylene Crystallite Thickness Distribution from ^{1}H NMR Relaxation, Calibratcd by Electron Microscopy and Raman LAM. " Submittcd to *Macromolecules*

22. deAzevedo, E. R.; Hu, W.-G.; Bonagamba, T. J.; K.Schmidt-Rohr."Centerband-Only detcction of Exchangc: Efficicnt Analysis of Dynamics in solids by NMR." *JACS*, **121**, 8411 (1999).

23. Odian, G. G. *Principles of polymerization*; McGraw-Hill: Ncw York, 1970.

24. Mathot, V. B. F.; Pijpers, M. F. J."Molecular Structurc, Mclting Bchavior, and Crystallinity of 1-Octene Bascd Vcry Low Density Polycthylcnes (VLDPEs) as Studicd by Fractionation and Hcat Capacity Mcasurcments with DSC." *J.Appl.Polym.Sci*, **39**, 979 (1990).

25. Hlatky, G. G."Metallocene catalysts for olefin polymerization - Annual review for 1996." *Coordination Chemistry Reviews*, **181**, 243 (1999).

26. Phillips, P. J."Polymer Crystals." *Rep.Prog.Phys.*, **53**, 549 (1990).

27. Huang, J.; Prasad, A.; Marand, H."Study of the temperature dependence of isothermal spherulitic growth rate data for poly(pivalactone) in blends with poly(vinylidene fluoride): a link between coherent secondary nucleatio theory and mixing thermodynamics." *Polymer*, **35**, 1896 (1984).

28. Armistead, K.; G.Goldbeck-Wood."Polymer Crystallization Theories." *Advances in Polymer Science*, **100**, 223 (1992).

29. Wunderlich, B. *Macromolecular physics*; Academic Press: New York, 1973-80; Vol. 2.

30. Sperling, L. H. *Introduction to physical polymer science*; Wiley: New York, 1986.

31. Strobl, G. R. *Physics of Polymers*; Springer-Verlag: Berlin, 1996.

32. Point, J. J."New Approach to the Mechanism of Oligomer Crystallization." *J. Chem. Soc. Faraday Trans.*, **91**, 2565 (1995).

33. Mandelkern, L. *Crystallization of Pollymers*; McGraw-Hill: NY, 1964.

34. Lambert, W. S.; Phillips, P. J."Crystallization kinetics of fractions of branched polyethylenes .2. Effect of molecular weight." *Polymer*, **3**, 3585 (1996).

35. Lambert, W. S.; Phillips, P. J."Crystallization kineticsof low-molecular weight fractions of branched polyethylenes." *Macromolecules*, **27**, 3537 (1994).

36. Alizadeh, A.; Richardson, L.; Xu, J.; McCartney, S.; Marand, H."Influence of Structural and Topological Constraints on the Crystallization and Melting Behavior of Polymers. 1.Ethylene/1-Octene Copolymers." *Macromolecules*, **32**, 6221 (1999).

37. Akpalu, Y.; Kielhorn, L.; Hsiao, B. S.; Stein, R. S.; Russell, T. P.; VanEgmond, J.; Muthukumar, M."Structure development during crystallization of homogeneous copolymers of ethene and 1-octene: Time-resolved synchrotron X-ray and SALS measurements." *Macromolecules*, **32**, 765 (1999).

38. Bark, M.; Zachmann, H. G.; Alamo, R.; Mandelkern, L."Investigations of the crystallization of polyethylene by means of simultaneous small-angle and wide-angle X-ray scattering." *Makromol. Chem.*, **193**, 2363 (1992).

39. Sasaki, S.; Tashiro, K.; Kobayashi, M.; Izumi, Y.; Kobayashi, K."Microscopically viewed structural change of PE during the isothermal crystallization from the melt - II. Conformational ordering and lamellar formation mechanism derived from the coupled interpretation of time-resolved SAXS and FTIR data." *Polymer*, **40**, 7125 (1999).

40. Song, H. H.; Stein, R. S.; Wu, D.--. Q.; Ree, M.; Phillips, J. C.; LeGrand, A.; Chu, B."Time-Resolved SAXS on Crystallization of a Low Density Polyethylene/High-Density Polyethylene Polymer Blend." *Macromolecules*, **21**, 1180 (1988).

41. Song, H. H.; Wu, D.--. Q.; Chu, B.; Satkowski, M.; Ree, M.; Stein, R. S.; Phillips, J. C."Time-Resolved Small-Angle X-ray Scattering of a High Density Polyethylene/Low density Polyethylene Blend." (1990).

42. Hill, M. J.; Barham, P. J.; Keller, A."Phase segregation in blends of linear with branched polyethylene: the effect of varying the molecular weight of the linear polymer." *Polymer*, **33**, 2530 (1992).

43. Hill, M. J.; Barham, P. J."Morphology maps of binary blends of copolymers produced using the metallocene catalyst process." *Polymer*, **41**, 1621 (2000).

44. Hill, M. J.; Barham, P. J."Liquid-liquid phase separation in blends containing copolymers produced using metallocene catalysts." *Polymer*, **38**, 5595 (1997).

45. Hill, M. J.; Morgan, R. L.; Barham, P. J." Minimum branch content for detection of liquid-liquid phase separation , using indirect techniques, in blends of polyethylene with ethylene-octene and ethylene-butene copolymers." *Polymer*, **38**, 3003 (1997).

46. Alamo, R. G.; Graessley, W. W.; Krishnamoorti, R.; Loshe, D. J.; Londono, J. D.; L.Mandelkern; Stehling, F. C.; Wignall, G. D."Small Angle Neutron Scattering Investigations of Melt Miscibility and Phase Segregation in Blends of Linear and Branched Polyethylenes as a Function of the Branch Content." *Macromolecules*, **30**, 561 (1997).

47. Alamo, R. G.; Londono, J. D.; Mandelkern, L.; Stehling, F. C.; Wignall, G. D."Phase-Behavior of Blends of Linear and Branched Polyethylenes in the Molten and Solid States by Small-Angle Neutron-Scattering." *Macromolecules*, **27**, 411 (1994).

48. Wignall, G. D.; Alamo, R. G.; Londono, J. D.; Mandelkern, L.; Stehling, F. C."Small-Angle Neutron Scattering Investigations of Liquid-Liquid Phase Separation in Heterogeneous Linear Low-Density Polyethylene." *Macromolecules*, **29**, 5332 (1996).

49. Wignall, G. D.; Alamo, R. G.; Londono, J. D.; Mandelkern, L.; Kim, M. H.; Lin, J. S.; Brown, G. M."Morphology of blends of linear and short-chain branched polyethylenes in the solid state by small-angle neutron and X-ray scattering, differential scanning calorimetry, and transmission electron microscopy." *Macromolecules*, **33**, 551 (2000).

50. Wignall, G. D.; Londono, J. D.; Lin, J. S.; Alamo, R. G.; Galante, M. J.; Mandelkern, L."Mrphology of Blends of Linear and Long-Chain Branched Polyethylenes in the Solid State-a Study by SANS,SAXS, and DSC." *Macromolecules*, **28**, 3156 (1995).

51. Ryan, A. J.; Fairclough, J. P. A.; Terrill, N. J.; Olmstead, P. D.; Poon, W. C. K."A scattering study of nucleation phenomena in polymer crystallisation." *Faraday Discussions*, **112**, 13 (1999).

52. Gabriel, C.; Kaschta, J."Comparison of different shear rheometers with regard to creep and creep recovery measurements." *Rheologica Acta*, **37**, 358 (1998).

53. Vega, J. F.; MunozEscalona, A.; Santamaria, A.; Munoz, M. E.; Lafuente, P."Comparison of the rheological properties of metallocene-catalyzed and conventional high-density polyethylenes." *Macromolecules*, **29**, 960 (1996).

54. Mandelkern, L.; Alamo, R. G. Crystallization Kinetics. In *Physical Properties of Polymers Handbook;* Mark, E. J. Ed.; American Institute of Physics: Woodbury, NY, 1996; p. 417.

55. Banks, W.; Gordon, M.; Sharples, A."The Crystallization of Polyethylene after Partial Melting." *Polymer*, **4**, 289 (1963).

56. Hess, W.; Vilgis, T. A.; Winter, H. H."Dynamic Critical Behavior during Chemical Gelation and Vulcanization." *Macromolecules*, **21**, 2536 (1998).

57. Boutahar, K.; Carrot, C.; Guillet, J."Crystallization of Polyolefins from Rheological Measurements-Relation between the transformed fraction and dynamic moduli." *Macromolecules*, **31**, 1921 (1998).

58. Teh, J. W.; Blom, H. P.; Rudin, A."A Study on the Crystallization Behavior of Polypropylene, Polyethylene and their Blends by Dynamic-Mechanical and Thermal Methods." *Polymer*, **35**, 1680 (1994).

59. Jackson, J. B.; Flory, P. J.; Chaing, R.; Richardson, M. J."Shear modulus in Relation to Crystallinity in Polymethylene and its copolymers." *Polymer*, **4**, 237 (1963).

60. Richardson, M. J.; Flory, P. J.; Jackson, J. B."Crystallization and Melting of Copolymers of Polyethylene." *Polymer*, **4**, 221 (1963).

61. Flory, P.J. "Thermodynamics of Crystallization in High Polymers. IV. A Theory of Crystalline States and Fusion in Polymers, Copolymers, and Their Mixtures with Diluents. " *J.Chem.Phys.*,**17**,223(1947)

62. Alamo, R. G.; Chan, E. K. M.; Mandelkern, L."Influence of Molecular Weight on the Melting and Phase Structure of Random Copolymers of Ethylene." *Macromolecules*, **25**, 6381 (1992).

63. Shirayama, K.; Kita, S.-I.; Watabe, H."Effects of branching on Some Properties of Ethylene/a-olefin copolymers." *Makromol.Chem*, **151**, 97 (1972).

64. Baker, C. H.; Mandelkern, L."The Crystallization and Melting of Copolymers II-Variations in Unit-cell Dimensions in Polymethylene Copolymers." *Polymer*, **7**, 71 (1966).

65. Bassett, D. C. *Principles of Polymer Morphology*; Cambridge University Press: Oxford, 1981.

66. Salazar, J. M. D.; Calleja, F. B."Influence of chain defects on the crystallization of polyethylene with reference to crystal size and perfection." *Journal of Crystal Growth*, **48**, 243 (1979).

67. Hosoda, S.; Nomura, H.; Gotoh, Y.; Kihara, H."Degree of branch inclusion into the lamellar crystal for various ethylene /α-olefin copolymes." *Polymer*, **31**, 1999 (1990).

68. Howard, P. R.; Crist, B."Unit Cell Dimensions in Model Ethylene-Butene-1 Copolymers." *J.Polym.Sci.,B:Polym.Phys*, **27**, 2269 (1989).

69. Vonk, C. G.; Pijpers, A. P."An X-ray Diffraction Study of Nonlinear Polyethylene.I. Room-Temperature Observations." *J.Polym.Sci.,Polym.Phys,Ed.*, **23**, 2517 (1985).

70. VanderHart, D. L.; Perez, E."A ^{13}C NMR Method for Determining the Partitioning of End Groups and Side Branches between the Crystalline and Noncrystalline Regions in Polyethylene." *Macromolecules*, **19**, 1902 (1986).

71. Bunn, C. W.; Renffew, A.; Morgan, P. . In *Polyethylene;* Illife Ed.: London, 1975.

72. Seguella, R.; F.Rietsch."On the Isomorphism of Ethylene/α-olefin Copolymers." *J.Polym.Sci.,Polym.Lett.,*, **45**, 4175 (1974).

73. Davis, G. T.; Weeks, J. J.; Martin, G. M.; Eby, R. K."Cell Dimensions of hydrocarbon crystals: Surface effects." *J.Appl.Phys.*, **45** (1974).

74. Horst,R.; Winter,H.H. *Macromolecules* In Print

75. Strobl, G. R.; Hagedorn, W."Raman Spectroscopic Method for Determining Crystallinity of Polyethylene." *J.Polym.Sci: Polym.Phys*, **16**, 1181 (1978).

76. Alamo, R. G.; Viers, B. D.; Mandelkern, L."Phase Structure of Random Ethylene Copolymers: A Study of Counit Content and Molecular Weight as Independent Variables." *Macromolecules*, **26**, 5740 (1993).

77. Mathot, V. B. F.; Pijpers, M. F. J."Molecular Structure, Melting Behavior, and Crystallinity of 1-Octene Based Very Low Density Polyethylenes (VLDPEs) as Studied by Fractionation and Heat Capacity Measurements with DSC." *J.Appl.Polym.Sci*, **39**, 979 (1990).

78. Flory, P. J.; Yoon, D. Y.; Dill, K. A."The Interphase in Lamellar Semicrystalline Polymers." *Macromolecules*, **17**, 862 (1984).

79. Stribeck, N.; Alamo, R. G.; Mandelkern, L.; Zachmann, H. G."Study of the Phase Structure of Linear polyethylene by Means of Small-Angle X-ray Scattering and Raman Spectroscopy." *Macromolecules*, **28**, 5029 (1995).

80. Mandelkern, L."The Relation between Structure and Properties of Crystalline polymers." *Polymer Journal*, **17**, 337 (1985).

81. Balta-Calleja, F. J.; Vonk, C. G. *X-ray scattering of synthetic polymers*; Elsevier: NY, 1989.

82. Naylor, C. C.; Meier, R. J.; Kip, B. J.; Williams, K. P. J.; Mason, S. M.; Conroy, N.; Gerrard, D. L."Raman Spectroscopy Employed for the Determination of the Intermediate Phase in Polyethylene." *Macromolecules*, **28**, 2969 (1995).

83. Mandelkern, L.; Alamo, R. G.; M.A.Kennedy."Interphase Thickness of Linear Polyethylene." *Macromolecules*, **23**, 4721 (1990).

84. Mandelkern, L.; Alamo, R. G.; M.A.Kennedy."Comments on Paper "Raman Spectroscopy Employed for the Determination of the Intermediate Phase in Polyethylene"." *Macromolecules*, **28**, 2988 (1995).

85. Maxfield, J.; Mandelkern, L."Crystallinity, Supermolecular Structure, and Thermodynamic Properties of Linear Polyethylene Fractions." *Macromolecules*, **10**, 1141 (1977).

86. Mandelkern, L.; M.Glotin; Benson, R. A."Supermolecular Structure and Thermodynamic Properties of Linear and Branched Polyethylenes under Rapid Crystallization Conditions." *Macromolecules*, **14**, 22 (1981).

87. Kumar, S. K.; Yoon, D. Y."Lattice Model for Crystal-Amorphous Interphases in Lamellar Semicrystalline Polymers: Effects of Tight-Fold Energy and Chain." *Macromolecules*, **22**, 3458 (1989).

88. Kitamaru, R.; Horii, F.; Murayama, K."Phase Structure of Lamellar Crystalline Polyethylene by Solid-State High-Resolution ^{13}C NMR: detection of the Crystalline-Amorphous Interphase." *Macromolecules*, **19** (1986).

89. Kitamaru, R.; Nakaoki, T.; Alamo, R. G.; Mandelkern, L."A Carbon-13 NMR Study of the Phase Structure of Semicrystalline Polymeers: Hydrogenated Polybutadiene." *Macromolecules*, **29**, 6847 (1996).

90. Kuwabara, K.; Kaji, H.; Horii, F.; Bassett, D. C.; Olley, R. H."Solid - State 13C NMR Analyses of the Crystalline-Noncrystalline Structure for Metallocene-Catalyzed Linear Low-Density Polyethylene." *Macromolecules*, **30**, 7516 (1997).

91. Cheung, T. T. P.; Gerstein, B. C."^{1}H nuclear magnetic resonance studies of domain structures in polymers." *J.Appl.Phys.*, **52**, 5517 (1981).

92. Kimura, T.; Neki, K.; Tamura, N.; Horii, F.; Nakagawa, M.; Odani, H."High-resolution solid-state ^{13}C nuclear magnetic resonance study of the combined process of 1H spin diffusion and 1H spin-lattice relaxation in semicrystalline polymers." *Polymer*, **33**, 493 (1992).

93. Kimura, K.; Yuasa, S.; Maru, Y."Carbon-13 nuclear magnetic resonance study of ethylene-1-octene and ethylene-4-methyl-1-pentene copolymers." *Polymer*, **25**, 441 (1984).

94. Usami, T.; Takayama, S."Fine-Branching Structure in High-pressure, Low-Density Polyethylenes by 50.10-MHz ^{13}C NMR Analysis." *Macromolecules*, **17**, 1756 (1984).

95. Gillet, S.; Delpuech, J.-J."Optimum Conditions for Nondestructive Quantitative Analysis by Carbon-13 NMR." *Journal of Magnetic Resonance*, **38**, 443 (1980).

96. Axelson, D. E.; Levy, G. C.; Mandelkern, L."A Quantitative Analysis of low-Density (Branched) Polyethylenes by Carbon-13 Fourier Transform Nuclear Magnetic Resonance at 67.9 MHz." *Macromolecules*, **12**, 41 (1979).

97. Perez, E.; Vanderhart, D. L."Morphological Partitioning of Chain Ends and Methyl Branches in Melt-crystallized Polyethylene by ^{13}C-NMR." *J. Polym. Sci.: Part B: Polym.Phys.*, **25**, 1637 (1987).

98. VanderHart, D. L.; Perez, E."A ^{13}C NMR Method for Determining the Partitioning of End Groups and Side Branches between the Crystalline and Noncrystalline Regions in Polyethylene." *Macromolecules*, **19**, 1902 (1986).

99. Perez, E.; Bello, A.; Perena, J. M.; Benavente, R.; Martinez, M. C.; Aguilar, C."Solid-state nuclear magnetic resonance study of linear-low density polyethylenes: 1. Ethylene-1-butene copolymers." *Polymer*, **30**, 1508 (1989).

100. McFaddin, D. C.; Russell, K. E.; Kelusky, E. C."^{13}C nmr solid-state studies of relaxation behavior of branches in homogeneous 1-alkene-ethylene copolymers." *Polymer Communications*, **27**, 204 (1986).

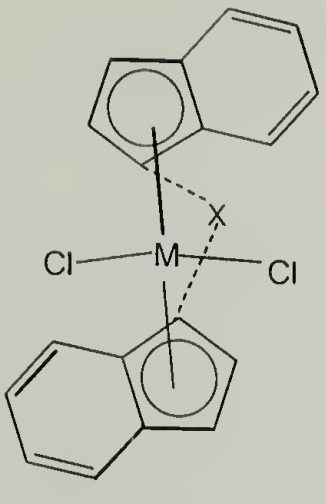

M = Zr, Hf
X = C_2H_4, Me_2Si

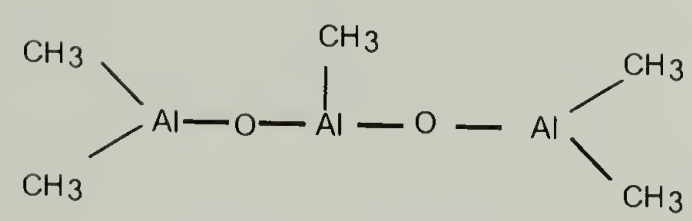

Methylaluminoxane (MAO)

L_2ZrCl_2 + MAO $\longrightarrow$

$\longrightarrow$ $L_2Zr(CH_3)Cl$ * MAO $\rightleftharpoons$ $[L_2Zr(CH_3)]^+$ $[MAO\text{-}Cl]^-$

Fig.1.1 Synthesis of a metallocene catalyst; he cation form $[L_2Zr(CH_3)]^+$ is catalytically active

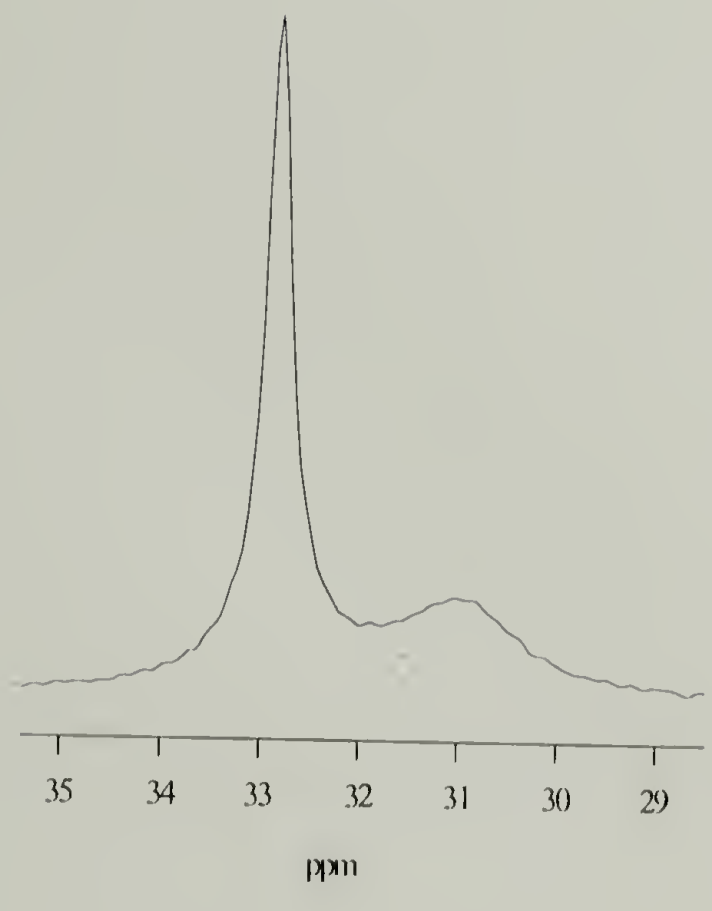

Fig.1.2 Methylene region of the ^{13}C CP MAS spectrum of Ziegler-Natta LLDPE. The narrow signal at 32.8 ppm corresponds to all-trans chains in the crystalline domain . The broad signal at 31 ppm corresponds to chains in the amorphous phase, having mixed trans and gauche conformations

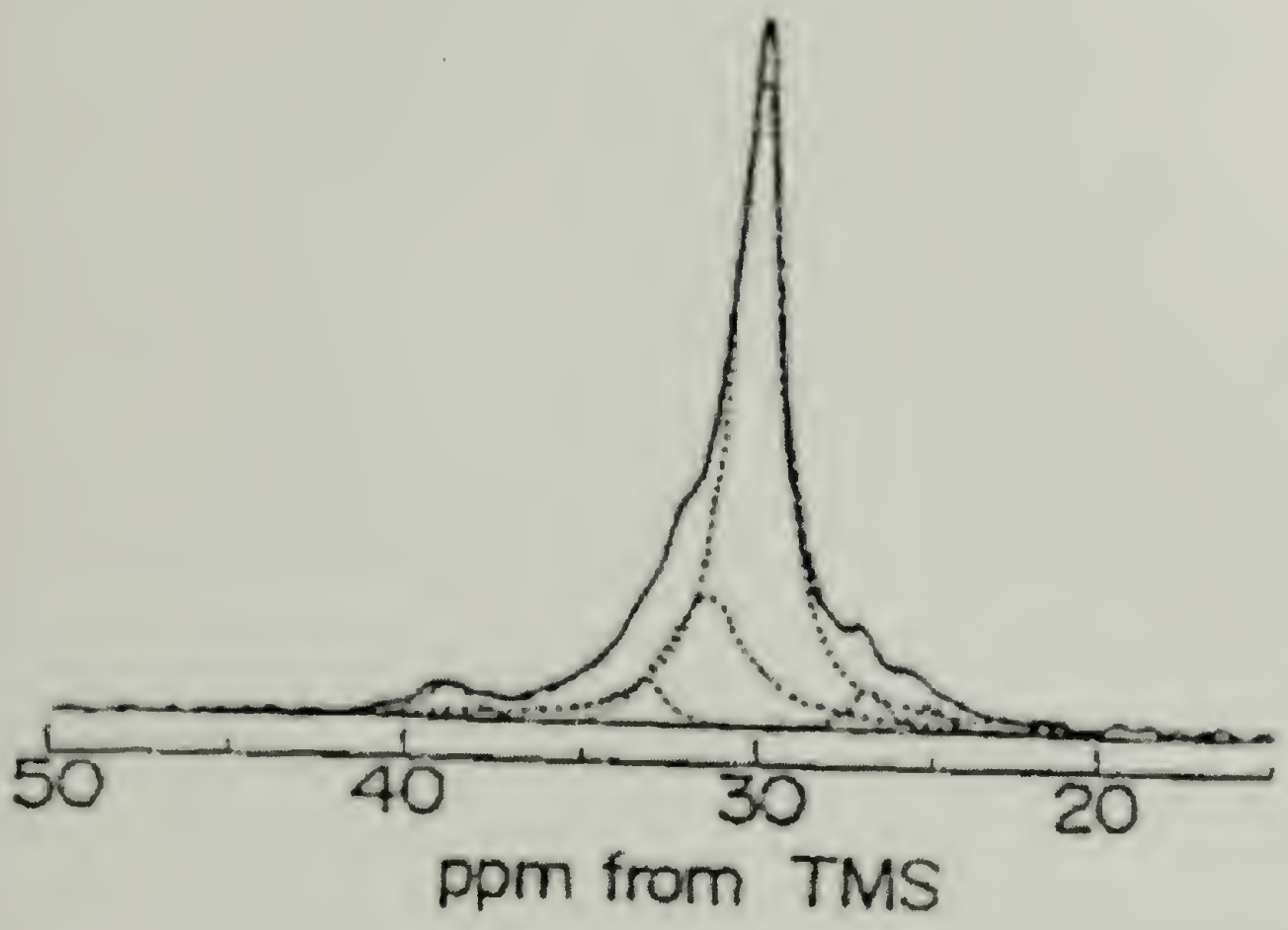

Fig.1.3 Lineshape analysis of the non-crystalline spectrum of hydrogenated polybutadiene. (Mw = 420 kg/mol); Dotted curves at 30.5 ppm represent Lorentzians for the "rubbery phase" and "interfacial domain". Lorentzians centered at 39, 34, 28 and 26 ppm are sidechain signals (From Kitamaru et al. 1996 [88])

CHAPTER 2

BASIC CHARACTERISTICS OF MATERIALS, USED IN THIS INVESTIGATION

2.1 Properties of HDPEs and LLDPEs under investigation

The major purpose of this investigation is to determine the relationship between branching distribution, crystallization behavior and solid-state properties of LLDPEs. Therefore the exact knowledge of composition distribution in tested LLDPEs is paramount for the success of this investigation. The bulk of experimental work was performed using metallocene (PE-M) and Ziegler-Natta LLDPEs (PE-ZN), manufactured by Exxon. These samples were characterized by TREF at Exxon, so corresponding branching distributions for these copolymers were known in a great detail (Fig.2.1). It can be seen that the intermolecular branching distribution of PE-M is typical for homogeneous metallocene systems, while PE-ZN is representative of Ziegler-Natta co-polymers.[1,2]

Morphological properties of ethylene co-polymers[3,4] are greatly influenced by the thermal history, so LLDPE samples were subjected to various types of the thermal treatment. One sample, PE-M b.i. (bulk isothermally crystallized), was produced by melting of the PE-M material for 10 min at 160°C, isothermal melt-crystallization at 119°C for 30 hours, and subsequent rapid quenching to –2°C. The same polymer was also rapidly quenched from the melt at 160°C to –2°C (PE-M b.q.). A sample of PE-ZN, PE-ZN b.i., was obtained by isothermal melt-crystallization at 127°C for 30 hours and rapid

quenching to -2°C. PE-ZN b.q. was obtained by quenching from the melt at 160°C to -2°C. The same polymers in the form of approximately 75-μm thick blown films were also used as received from Exxon (PE-M film and PE-ZN film).

Four high-density polyethylenes (HDPEs) were included into this study for the comparison purposes. Metallocene high-density polyethylene, HDPE-Mi, an experimental sample custom-synthesized by Exxon, was prepared by isothermal crystallization at 130 °C for 30 hours and quenching to –2°C. Ziegler-Natta HDPE-ZNi (commercially produced by Exxon) was isothermally crystallized at 127 °C for 9 hours before quenching to –2°C. Two HDPE fractions kindly provided by Alamo were investigated: Sample HDPE-NBS1484 is a narrow fraction obtained from NIST.[5] The sample was melted at 160 °C for 15 min and crystallized at 125 °C for 3 hours. The crystallization was halted by quenching in ice water. The second HDPE fraction was obtained from the Societe des Petroles D'Aquitane (S.N.P.A.).[6] It was dissolved in p-xylene (4 wt/v%) at 110°C and rapidly crystallized at 24 °C. The solution crystals were washed with methanol and dried in vacuum to constant weight. This solution-crystallized sample is denoted as HDPE-S. An ethene-propene co-polymer PE-PrL, with 10% of propene units ^{13}C labeled at the α-site, was custom-synthesized by Exxon using a metallocene catalyst. in this co-polymer are labeled ^{13}C. This PE-PrL sample was rapidly quenched from the melt from 160 to -2 °C.

2.2 References

1. Mathot, V. B. F. Structure, crystallization and melting of linear, branched and copolymerized polyethylenes as revealed by fractionation methods and DSC. In *New Advances in Polyolefins;* Chung, T. C. Ed.; Plenum Press: NY, 1993; pp. 121.

2. Kaminsky, W."New polymers by metallocene catalysis." *Macromol. Chem.Phys.*, **197**, 3907 (1996).

3. Bassett, D. C. *Principles of Polymer Morphology*; Cambridge University Press: Oxford, 1981.

4. Mandelkern, L.; M.Glotin; Benson, R. A."Supermolecular Structure and Thermodynamic Properties of Linear and Branched Polyethylenes under Rapid Crystallization Conditions." *Macromolecules*, **14**, 22 (1981).

5. Stribeck, N.; Alamo, R. G.; Mandelkern, L.; Zachmann, H. G."Study of the Phase Structure of Linear polyethylene by Means of Small-Angle X-ray Scattering and Raman Spectroscopy." *Macromolecules*, **28**, 5029 (1995).

6. Alamo, R.; Mandelkern, L."Origins of Endothermic Peaks in Differential Scanning Calorimetry." *J. Polym Sci. B. Polym. Phys*, **24**, 2087 (1986).

Table 2.1. Characteristics of the investigated ethylene-α-olefin copolymers

Polymer & Method of Synthesis		Content of Branched units	Molecular Weight	Thermal History
PE-ZN Ziegler-Natta process	PE-ZN b.i. bulk isotherm. crystallized	3.8 % mol C-6	M_W –115278 g/mol M_W/M_n=3.96	isotherm. melt-crystallized at 127 °C (30 hrs.)
	PE-ZN b.q. bulk quenched.			melt-quenched from 160 °C, 50 °C/min
	PE-ZN film			blown film
PE-M Metallocene process	PE-M b.i. bulk isotherm. crystallized	2.6%mol C-6	M_W –106749 g/mol M_W/M_n=2.39	Isothermally melt - crystallized at 119 °C (30 hrs.)
	PE-M b.q. bulk quenched			melt-quenched from 160°C, 50°C/min
	PE-M film			blown film
HDPE - NBS1484 fraction	bulk isothermally crystallized	0	M_w= 119,600 g/mol M_W/M_n=1.19	isotherm. melt-crystallized. at 127 °C (3hrs)
HDPE-S fraction	solution crystallized	0	M_w= 166,000 g/mol M_W/M_n=1.11	cryst. from a 4% solution. in xylene
HDPE-ZNi Ziegler-Natta process	bulk isotherm. crystallized	0	M_w~80,000 g/mol	isotherm. melt-crystallized at 127 °C (9 hrs)
HDPE-Mi Metallocene process	bulk isotherm. crystallized	0	M_w~110,000 g/mol	isotherm. melt-crystallized. at 130 °C (30 hrs)
PE-PrL Metallocene process, ^{13}C labeled 10% α-site C-3	~1% mol C-3;			melt-quenched from 160°C, 50°C/min

LLDPE C-6

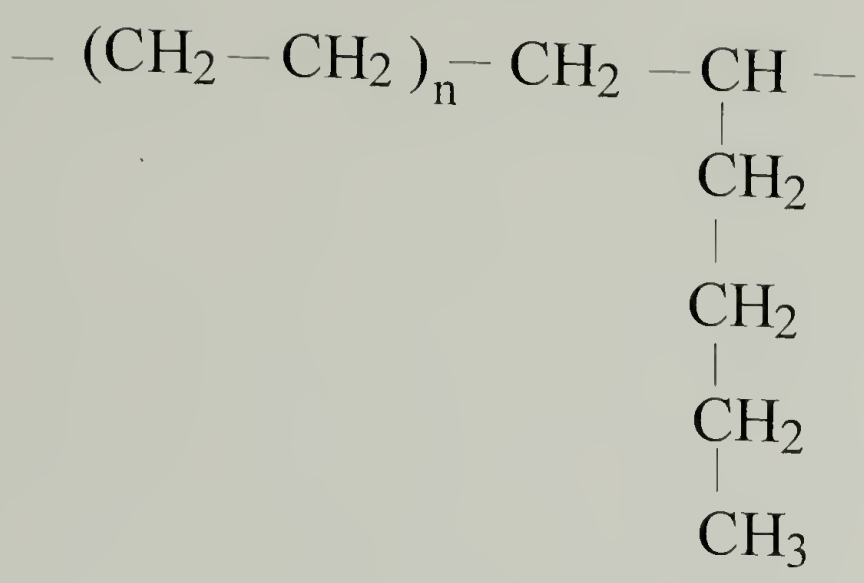

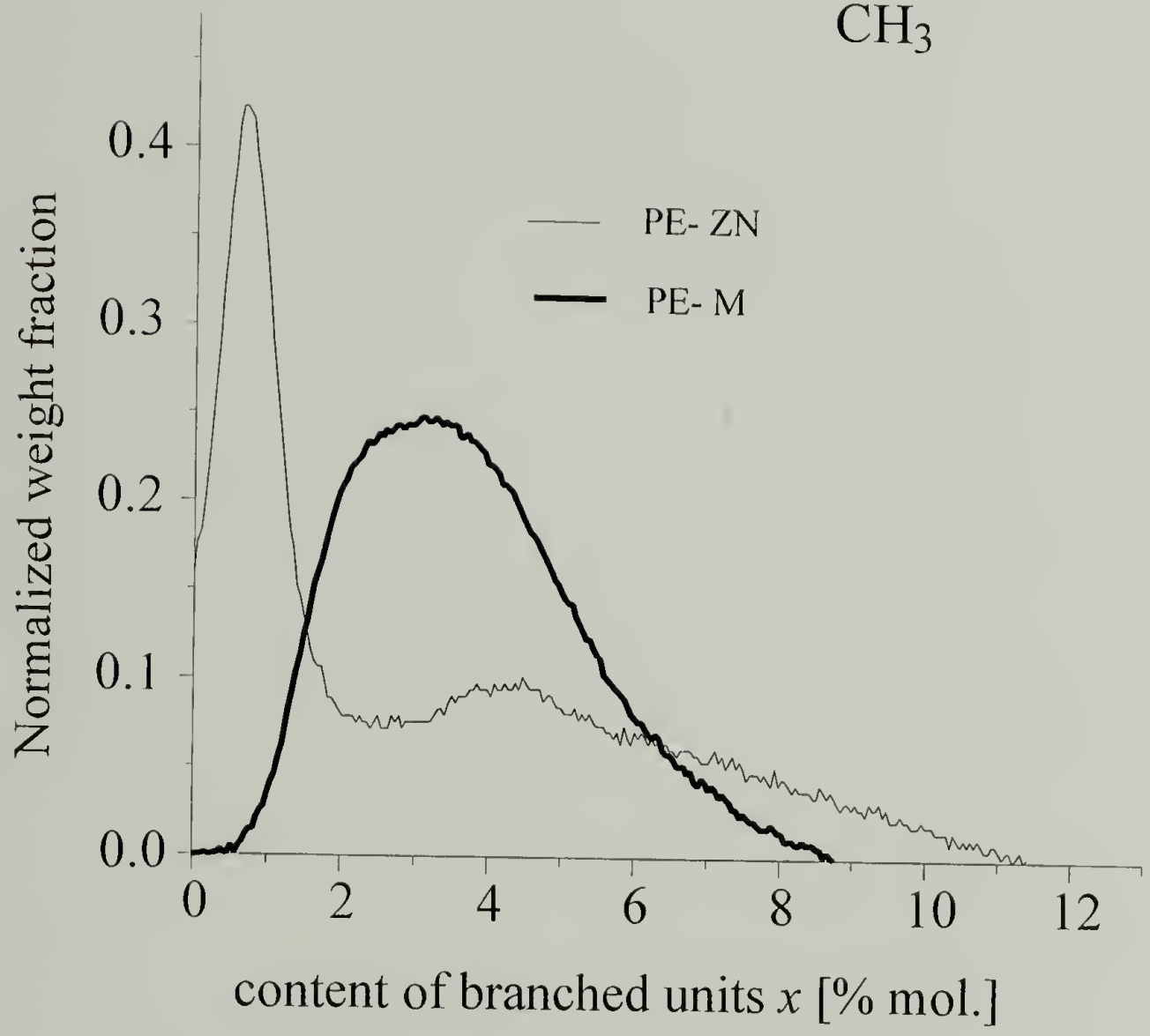

Figure 2.1 Intermolecular branching distributions in ethylene-hexene co-polymers PE-M and PE-ZN as determined by TREF (Temperature Raising Elution Fractionation) at Exxon.

CHAPTER 3

EFFECT OF BRANCHING DISTRIBUTION ON EVOLUTION OF VISCOELASTIC PROPERTIES OF LLDPES DURING ISOTHERMAL AND NON-ISOTHERMAL CRYSTALLIZATION AND PARTIAL MELTING

3.1 Abstract

The effect of branching distribution on crystallization kinetics and evolution of linear viscoelastic properties during isothermal and non-isothermal crystallization of ethylene-hexene co-polymers manufactured by metallocene (PE-M) and Ziegler-Natta (PE-ZN) processes was studied. HDPE and HDPE-LLDPE blends were included in the study for comparison purposes.

The evolution of rheological properties of crystallizing melt during the early stages of crystallization was correlated with crystallization kinetics, measured by DSC. It was shown that the melt-solid transition during physical gelation in LLDPEs occurs at very low crystallinity (ϕ<0.04). Three periods of structure development during the early stages of LLDPE crystallization were described: the initial structure formation (0<ϕ< 0.005), the development of the physical network (0.002<ϕ<ϕ_{gel}), the tightening of the physical network (ϕ>ϕ_{gel}). The strong effect of thermal history on crystallization behavior and the broad temperature range of liquid-solid transition observed in metallocene LLDPE were related to the homogeneous branching distribution in that co-polymer. Temperature protocols for the preparation of stable critical gels from ethylene co-polymers using step-crystallization and partial melting are described.

3.2 Introduction

This chapter is devoted to the analysis of the relationship between the branching distribution in LLDPEs and its viscoelastic behavior during melting and crystallization. Special emphasis is made on the polymer properties in the vicinity of the melt-solid transition. Melting and melt-crystallization are the critical stages of LLDPE processing. While it is known that melting temperatures and equilibrium crystallinity in LLDPEs may be strongly influenced by branching distribution,[1-6] many aspects of the relationship between branching distribution, crystallization and melting behavior are not fully understood.

It is known that liquid-solid transformation in crystallizing polymers can be considered physical gelation, where connectivity is provided by the crystalline regions acting as physical cross-links. The liquid-solid transition (gel point) in a solidifying system is defined by the appearance of sample spanning connectivity. The material at the gel point (critical gel) expresses itself with a characteristic self-similar relaxation pattern, which can be reliably detected using dynamic rheometry. This creates an opportunity for the analysis of the viscoelastic behavior of crystallizing LLDPEs in the framework of the rheological theory of gelation.[7-12]

In order to obtain comprehensive information about the relationship between composition and solidification behavior in LLDPEs crystallization and

melting experiments were performed using a variety of temperature protoeols. All tested LLDPE samples were eharaeterized by Temperature Raising Elution Fraetionation (TREF), so the eorresponding branehing distributions are known in a great detail. Metalloeene (HDPE-M) and Ziegler-Natta(HDPE-ZN) HDPEs and HDPE-LLDPE blends were ineluded into this study for eomparison purposes.

The researeh eonsists of five parts: (1) Investigation of the rheologieal properties of LLDPE **melts** above T_m using dynamie and steady-shear rheometry. (2) Analysis of phase eomposition of LLDPE **melts**. In this part the possibility of liquid-liquid phase separation in LLDPE melts was explored using statie ^{13}C NMR teehnique. (3) Investigation of the **isothermal crystallization** behavior. The isothermal erystallization kineties, determined by DSC were eorrelated with the evolution of dynamie viseoelastie properties of LLDPEs. The effeet of branehing distribution on the erystallization kineties and on the erystallinity dependenee of the viseoelastie properties was determined. (4) Investigation of the solidifieation behavior during **non-isothermal crystallization** (eooling ramp). This seetion deseribes the effeet of branehing distribution on the evolution of viseoelastie properties during non-isothermal erystallization of LLDPEs (5) Preparation and eharaeterization of **stable critical gels**. It was shown that the stable eritieal and near-eritieal gels, whose viseoelastie properties remain eonstant on the timeseale of hours, ean be prepared from LLDPEs using step-erystallization and partial melting proeedures.

Rheological properties of stable critical gels were determined using dynamic and steady-shear techniques. Local molecular conformation and crystallinity in stable critical gels, prepared from metallocene LLDPEs were characterized by Raman spectroscopy.

Based on the results, obtained in this work, a model explaining the effect of molecular structure on the crystallization kinetics and viscoelastic behavior of LLDPEs during the isothermal and non-isothermal crystallization was proposed. The outcome of this investigation can be used for the optimization of LLDPE processability through the modification of intermolecular branching distribution by blending or by the modification of catalyst.

3.3 Background information

3.3.1 Factors, controlling the lineshape in static ^{13}C NMR spectra of LLDPEs

Gamma-Gauche Effect The conformational change of the isotropic chemical shift for the methylene groups in aliphatic structures is called γ-gauche effect.[13] The γ (third-neighbour) position from the $^{13}CH_2$ group under consideration is at the end of the β-γ bond which can be trans- or gauche to the ^{13}C-α bond. For a gauche conformation, the signal is shifted upfield by about 5 ppm compared to the trans- conformation. In a linear chain, there are two γ positions, so that shifts by about 10 ppm or more can occur. So the isotropic chemical shift for the methylene group is indicative of trans-gauche ratio in the chain, i.e. of the average chain conformation of the polyethylene backbone.

Anisotropic Broadening In the ^{13}C static spectra in the absence of heteronuclear decoupling the linewidth of the methylene signal is predominantly determined by the ansiotropic broadening due to the heteronuclear dipolar coupling and chemical shift anisotropy.[13] The extent of the broadening is greatly affected by the local molecular mobility. The linewidth for the signals corresponding to the rigid (crystalline) domains with strong dipolar coupling may reach hundreds of ppm. In contrast, in the mobile (non-crystalline) domains the anisotropic effects are weakened by the motional averaging, so non-crystalline signal may be hundreds times more narrow than the crystalline one. As the result the lineshape of the methylene signal (29-34 ppm) in the static ^{13}C spectrum is determined by the contributions from the mobile domains. The location of the peak maximum depends on the average chain conformation in the mobile phase. Thus simultaneous presence of several mobile phases, having different average chain conformations will manifest itself by the splitting of the methylene signal.

3.3.2 Physical gelation by crystallization

It was proven that the rheological theory of gelation adequately describes liquid-solid transitions in flexible-chain polymers induced by crystallization or melting.[11, 14,15]

Short overview of the rheological theory of gelation is presented in the introduction (Chapter 1.8).

While the evolution of the rheological properties of crystallizing polymers is consistent with the physical gelation process, the morphological structure of physical gels in the vicinity of the gel point is not understood in a great detail. One of the most important aspects of physical gelation is the nature of thermo-reversible structures, acting as physical cross-links. For the isothermal crystallization of flexible chain polymers, such as isotactic polypropylene or highly branched ethylene-butene co-polymer the degree of bulk crystallinity at a gel point does not exceed 3 % w/w.[14,15] Low crystallinity at the gel point indicates that connectivity can not be provided by the direct contact of crystallites. The alternative explanation includes network formation by random connection of tie molecules by the crystalline domains. Indeed, it is known[17] that the same polymer chain can go through several amorphous and crystalline regions. Thus crystalline regions can be presented as cross-links, linking together several neighboring chains. This mechanism of physical cross-linking corresponds to the network formation in chemical gelation.

3.4 Experimental

3.4.1 Materials

Branching content, branching distributions and molar mass parameters of the samples under investigation are described in Chapter 2. (Table 2.1., Fig 2.1). The composition distribution for PE-M is typical for metallocene LLDPEs, while the composition distribution of PE-ZN is representative of Ziegler-Natta

systems.[1] Branching distribution, for PE-M and PE-ZN determined by TREF are presented at Fig.2.1. Ziegler-Natta HDPE (HDPE-ZN), commercially manufactured by Exxon and metallocene HDPE (HDPE-M) custom-manufactured by Exxon were tested for comparison purposes in order to elucidate the effect of branching and molecular weight distribution on rheology and crystallization behavior of ethylene co-polymers. LLDPE:HDPE blends were prepared by melt-blending PE-M and HDPE-ZN at 180 °C using a Brabender extruder.

3.4.2 NMR

Static ^{13}C NMR spectra were obtained with a Bruker MSL-300 spectrometer. A ^{13}C resonance frequency of 75.5 MHz frequency was employed.

3.4.3 DSC

Isothermal crystallization kinetics in LLDPEs was measured using a Perkin-Elmer DSC-7 calorimeter.

3.4.4 Rheomery

Oscillatory shear measurements were performed on a strain controlled rheometer ARES LS 3 manufactured by Rheometric Scientific. Steady-shear experiments were performed at stress-controlled rheometer "StressTech"

manufactured by Viscotech. All rheological experiments were done with 25 mm parallel plates.

The frequency range 0.1-100 rad/s. was used in the dynamic experiments. While this frequency range covers sufficiently low frequencies allowing for the observation of the characteristic rheological patterns of critical gels, the measuring time for a single data point was short enough, so that the rheological properties of crystallizing sample did not undergo significant change during the individual measurements. A small strain amplitude of $\gamma_a = 0.01\text{-}0.03$ was chosen in order to ensure minimal influence of imposed strain on the crystallization process.

Steady shear experiments include shear rate sweep, yield stress measurements using logarithmic stress sweep mode and creep test at constant stress τ_{cr} =12 kPa.

Thermal programs, utilized in rheological and DSC experiments are presented in Fig.3.1a-d. Non-isothermal crystallization experiments (Fig.3.1b.) were performed at low cooling rate (4°C/hr) to allow for data acquisition at low frequencies. Step-crystallization and partial melting temperature programs (Fig.3.1c.-d.) were designed for the preparation of stable physical gels from LLDPEs. During step crystallization procedure the sample was held at 160 °C for 10 min. to erase the effect of prior thermal history, then rapidly cooled to 140 °C. After that, it was slowly (4°C/min) cooled to the temperature of the first isothermal step T_1, held for 300 min, then cooled to the lower temperature T_2.

Isothermal annealing for 300 min was repeated at lower temperatures $T_3, \ldots T_i$.. During the partial melting (Fig.3.1d.), the sample was slowly heated from 25 °C to the temperature of the first isothermal step T_1, then held isothermally for 300 min. The annealing process is repeated at higher temperatures T_2, $T_3 \ldots T_i$. To ensure reproducibility, all samples used in partial melting experiments were prepared under identical conditions: by slow (1°C/min) cooling from 160 to 25 °C. Temperature increments of 1[°C] $(T_{i+1}-T_i)$ were used in partial melting and step crystallization experiments.

3.4.5. FT Raman measurements

The Raman investigation was performed by A. Heintz. Fourier transform Raman spectra were recorded on a Bruker FRA 106 spectrometer equipped with a Nd:Yag laser (1.064 μm). The excitation/collection geometry was 180° and spectral resolution was maintained at 4 cm^{-1}. Laser power at the sample was 200 mW, and 1024 scans were signal averaged. The temperature program used in the Raman experiments duplicates those described above for partial melting and was carried out inside the spectrometer under N_2. The sample was packed into a glass capillary and heated by a cell attached to an Omega proportional controller. The temperature was calibrated to the melting point of benzoic acid and was stable to ±0.5 °C. Heating due to the laser was negligible at temperatures above 50 °C.

Curve fitting procedures were employed to calculate the degree of crystallinity using the Bruker Opus software package. A baseline was drawn

from 1600-960 and then the spectra were normalized to the total integrated intensity of the CH_2 twisting region. Band widths and shapes were fixed according to the literature.[16] The Levenberg-Marquardt algorithm was used to fit the intensities and positions. To ensure compatibility of temperature scale in Raman and rheological experiments temperature controllers were calibrated using benzoic acid standard.

3.5. Experimental results and discussions

3.5.1 Absence of liquid-liquid phase separation during isothermal melt-crystallization of LLDPEs

Because of the intermolecular composition heterogeneity LLDPEs can be considered as the blends of statistic co-polymers with varying co-monomer content. Both theoretical predictions and experimental observations prove the possibility of phase separation in the blends of statistic copolymers.[18,19]

The occurrence of liquid-liquid phase separation in LLDPE melts would affect both the rheology and the crystallization kinetics in these co-polymers. Thus the knowledge of phase composition in the melt is necessary for the correct analysis of factors, controlling various aspects of crystallization behavior in these systems.

Based on the results of SANS Alamo et al.[20] and Wignal et.al.[21] proposed that liquid-liquid phase separation can occur in highly heterogeneous LLDPEs above the melting point. In that case a fraction of the highly branched chains (containing more than 5% mol. of branched units) can phase separate from the

lightly branched majority. Because of significantly higher averagc branching the average chain conformation may be different in the dispersed phasc than in the rest of thc melt.

Another proposed mcchanism for liquid-liquid phase separation includes the formation of "ordered melt" below $T_{m.}$[22] According to that scenario at the initial stage of polyethylene crystallization liquid-liquid phase separation occurs when the "ordered melt" phase separates from regular disordered melt. Thc ordered melt is rather mobile, it lucks the long-range order, present in crystallites, yet it is predominantly formed by linear chain segments in all-trans conformation, similar to the crystalline phase in HDPE. In contrast, the trans:gauche ratio in the regular (disordered) melt is determined by the thermal equilibrium.

Obviously, both mechanisms of phase separation result in the formation of two mobilc phases, having different average chain conformations. Due to γ-gauche effect conformation differcnce will result in the diffcrent isotropic ^{13}C chemical shift for the methylene signals, corresponding to different mobile phases.[13] Thus liquid-liquid phase separation will manifest itself by splitting of methylene signal in static ^{13}C spectrum.

^{13}C spectra, recorded during the isothermal crystallization of PE-M and PE-ZN are presented at Fig. 3.2 While the methylene signal becomcs more broad as crystallization proceeds, the line splitting did not occur. The observed increase in linewidths with the progress of crystallization can be relatcd to the

decrease in the overall mobility resulting from the development of the crystalline phase. Thus, the extent of liquid-liquid phase separation during isothermal crystallization of LLDPEs is insignificant, the content of hetero-phase is below the sensitivity limit of the NMR technique (5% vol).

3.5.2 Melt rheology

Dynamic and steady-shear rheological properties of LLDPEs and HDPEs above the melting temperature are presented at Fig 3.3. *G'* and *G''* values are similar for PE-M and PE-ZN having similar weight-average molecular weight. In all tested samples the slope in $G'(\omega)$ and $tan\ \delta(\omega)$ dependencies deviates from values predicted by the Rouse theory [23,24] which indicates that experimentally tested frequency range only partially overlaps with "terminal zone". Because of lower average molecular weight values of *G'* and steady shear viscosity η are lower for HDPE-ZN than for the rest of the polymers under investigation.

The flow activation energy E_α is slightly lower in tested Ziegler-Natta polymers than in metallocene systems (Table 3.1). In steady shear rate-sweep experiments the onset of power-law behavior occurred at lower shear rates, the values of power exponent *n* were lower in Ziegler-Natta systems than in metallocene analogs. The values of power exponent *n*, observed in metallocene systems exceed 1, which is unusually high. This can be related to the onset of

slip at high shear rates $\dot{\gamma}$ >20 s^{-1}. Detailed diseussion of power-law behavior in polymers ean be found in the monograph by Larson.[25]

The observed differenee in the melt rheology ean be related to broader moleeular weight distribution [26-27] in Ziegler-Natta polymers. The experimental results suggest that the rheologieal properties of tested LLDPE melts are eontrolled by the moleeular weight distributions rather than by distribution of branehed units.

3.5.3 Isothermal erystallization

Crystallization kineties in LLDPEs was determined using DSC teehnique. Kinetie eurves $\phi(t)$ for the isothermal erystallization of PE-ZN and PE-M are presented at Fig.3.4 In spite of higher overall branehing, PE-ZN crystallizes faster and at higher temperatures than PE-M. Effeetive values of the Avrami exponent n, determined for LLDPEs are signifieantly lower $(1<n<2)$ than the values for HDPEs deseribed in literature $(2<n<3)$.[28] We propose that the observed phenomena may be related to the eomposition heterogeneity of LLDPEs. Indeed, both metalloeene and eonventional LLDPEs ean be deseribed as blends of fraetions with varying branehing eontent. The rate of the isothermal erystallization is signifieantly higher for low-branehed ehains,[29-30] thus higher bulk erystallization rate in PE-ZN may result from a signifieant eontent of low-branehed moleeules in that eo-polymer. Crystallites formed by almost linear moleeules may aet as nueleating agents for more branehed ehains. Aeeording to

Banks et al.[31] values of the Avrami exponent n $(1<n<1.5)$, determined during erystallization of HDPE melt in the presenee of HDPE erystallites, acting as nueleating agents are suffieiently lower than values of n measured during the isothermal melt-erystallization of identieal HDPE samples ($2<n<3$).

The gel point (t_{gel}) in tested samples was deteeted by the first appearanee of the maximum in $tan\ \delta\ (\omega)$ dependenee. The eorresponding eritieal erystallinity, $\phi_{gel}=\phi\ (t_{gel})$, was determined by eomparing rheologieal patterns with kinetie eurves $\phi(t)$, measured by DSC. The values of viseoelastie parameters of the eritieal gel S_C and n_C and the degree of erystallinity at the gel point ϕ_{gel} are quite similar in metalloeene and eonventional eo-polymers (Fig. 3.5). However the dependeneies of gel time t_{gel}, S_C and n_C on erystallization temperature are steeper for PE-ZN than for PE-M, indieating a narrower solidifieation interval in the isothermal erystallization of PE-ZN (Fig.3.5). In order to determine the relationships between erystallinity ϕ and the viseoelastie properties of erystallizing polymers the isothermal erystallization kineties $\phi(t)$, measured by DSC was eompared with time evolutions of viseoelastie properties $G'(t)$ and $tan\ \delta(t)$ independently determined under identieal eonditions by the oseillatory shear teehnique. $G'(\phi)$ and $tan\ \delta\ (\phi)$ dependeneies (Fig.3.6) were derived by plotting values of G' and $tan\ \delta$ versus the degree of crystallinity, eorresponding to the same experimental time. While experimentally determined erystallinity values $\phi(t)$ were used, eorresponding values of viseoelastie

functions were obtained by the interpolation of discrete experimental data sets $G'(t)$ and $tan\ \delta(t)$ by fourth order polynomials.

Observed changes of slope in $G'(\phi)$ and $tan\ \delta(\phi)$ dependencies (Fig. 3.6) indicate that the structure development at early stages of crystallization can be separated at three periods: the primary strueture formation ($0<\phi<0.002$), the formation of the physical network ($0.002<\phi<\phi_{gel}$), the tightening of the physieal network ($\phi>\phi_{gel}$). (Fig.3.6). Even if DSC-crystallinity remains very low during the primary strueture formation, the viseoelastic properties undergo signifieant change during that period. This observation parallels the results of real-time scattering experiments, when the formation of low-ordered structures during the early stages of erystallization of HDPEs and LLDPEs, was deteeted by SAXS before the development of WAXS detectable crystallinity.[32] The shapes of $G'(\phi)$ and $tan\ \delta(\phi)$ dependencies are distinetly different in PE-M and PE-ZN, whieh indieates the struetural difference in corresponding physieal gels. At the present time the morphology of physieal gels in the vicinity of gel point is not known in a great detail, nor the relationship between the morphology and mechanieal properties of physical gels is well understood. However it can be proposed that the difference in the eharaeter of $G'(\phi)$ and $tan\ \delta(\phi)$ dependencies ean be related to the different types of supermoleeular struetures formed during the early stages of crystallization of PE-ZN and PE-M. Indeed, it is known that the presence of branched units hinders formation of well-defined spherulites.[33,34]

Almost linear chains, present in PE-ZN ean form relatively large spherulites. In eontrast, in PE-M all ehains eontain branehed units, so supermoleeular struetures formed in PE-M will be small and poorly defined.[33-35]

3.5.4 Non-isothermal erystallization (eooling ramp)

The industrial proeessing of thermoplastie polymers predominantly oeeurs under non-isothermal eonditions, so the understanding of the relationships between moleeular strueture and non-isothermal solidifieation behavior of LLDPEs is of great praetieal importanee. Evolution of viseoelastie properties of PE-M, PE-ZN and HDPE-ZN during slow (4°C/hr) non-isothermal erystallization was investigated by the oseillatory shear teehnique (Fig. 3.7.) Melt-solid transition in non-isothermal erystallization was deteeted by the steep inerease in G' and simultaneous drop in $tan\ \delta$. The value of the slope in $G'(T)$ dependenee in the vieinity of melt-solid transition was used as the measure of transition widths, the larger slope eorresponding to the narrower transition interval.

As eompared to PE-ZN, PE-M has a lower eontent of branehed units and a narrower intermoleeular branehing distribution. However, liquid-solid transition during non-isothermal erystallization of PE-M oeeurs at lower temperature and over a broader temperature range than in Ziegler-Natta system. (Fig.3.7 a-b). The steepest transition at highest temperature was observed in linear polymer HDPE-ZN (Fig.3.7e).

The relative width of the solidification interval at higher cooling rates (120-300 °C/hr) was evaluated based on the width of DSC thermograms, recorded during cooling ramp. In parallel to the rheological data DSC results (Fig.3.8) indicate broader melting interval and lower transition temperature for PE-M copolymer. Both DSC and rheological results strongly suggest that the presence of sufficient fraction of molecules with low content of branched units (x<0.75 % mol) rather than the overall widths of branching distribution determines the solidification behavior during non-isothermal crystallization of ethylene co-polymers. In order to test this hypothesis we studied non-isothermal crystallization of HDPE-ZN:PE-M blends. Results obtained are presented at Fig.3.9. While the increase in HDPE-ZN content in the blend from 10 to 50 [% w/w] enhances overall composition heterogeneity, it also causes the narrowing of the solidification interval. For instance, the solidification interval for PE-ZN is as narrow as for HDPE-ZN:PE-M blend containing 25%[w/w] of HDPE-ZN. The overall branching is almost twice as high in PE-ZN as in the blend (3.8 % mol vs. 1.95 % mol), however the content of low-branched chains (0<x<0.75% mol) is quite similar in these systems (24%mol. vs.25 % mol). These observations indicate that the rheological behavior in the vicinity of liquid-solid transition is indeed determined by the content of linear and almost linear molecules, rather than by the overall branching.

3.5.5 Step-crystallization procedure

Physical gels formed during the isothermal crystallization of LLDPEs are transient formations. Their structure and properties constantly change as crystallization proceeds. It hinders the application of structural methods and steady-shear rheological techniques traditionally applied for the characterization of physical gels[36]. However, in this study we developed the thermal programs for the preparation of stable gels, whose crystallinity ϕ remains in the vicinity of ϕ_{cr} for period of time, sufficient for the structural characterization.

The proposed step-crystallization protocol (Fig 3.1c) allows to change crystallinity in controlled increments. Indeed, the presence of ethyl branches limits the maximal lamellar thickness in LLDPE crystallites.[33,37,38] As the result during the isothermal step at the highest temperature T_1 only the longest linear segments, able to form relatively thick lamellae, will crystallize. During the next cooling step at lower temperature the amount of chains, involved in the crystallization process increases, resulting in the increase in crystallinity. The extent of the crystallinity change $\Delta\phi = \phi_{i+1}-\phi_i$ between two isothermal step depends on the temperature difference $(T_{i+1}-T_i)$. Obviously $\Delta\phi$ can be made rather small.

The evolution of dynamic viscoelastic properties of PE-M, PE-ZN and HDPE-ZN during step-crystallization is presented at Fig.3.10 It can be seen that the branching distribution greatly affects the solidification behavior of ethylene co-polymers during step-crystallization. PE-M rapidly equilibrates during the

isothermal step, its properties remain stable for hours. The metallocene system forms the stable critical gel during the isothermal step at 119.5 °C. In contrast, viscoelastic properties of PE-ZN and HDPE-ZN did not equilibrate during the isothermal annealing steps, but continued to evolve similar to the isothermal crystallization behavior. The comparison of results of isothermal and step-crystallization experiments (Fig.3.10-3.11) reveals that in all tested systems the physical gels, formed in the process of the isothermal crystallization are stiffer than those obtained by step-crystallization process. The most pronounced effect of the thermal history on the solidification behavior was observed in PE-M. On the other hand, in HDPE-ZN viscoelastic properties of physical gels, prepared using isothermal and step-crystallization temperature programs are quite similar.(Fig.3.10-3.11.).

The time dependence of crystallinity $\phi(t)$ during step-crystallization of PE-M was measured using DSC.(Fig.3.12) Obtained results prove that step-cooling procedure allows to slow down the progress of crystallization in PE-M, so that the crystallinity remains in the vicinity of critical point on the timescale of hours.

Drastic decrease in the crystallization rate, observed in the step-cooling procedure may be caused by the change in the nucleation mechanism. The rapid quenching to the experimental temperature, applied in isothermal crystallization process favors homogeneous nucleation. In contrast, during step-crystallization the undercooling is very low throughout the whole process, which favors the

heterogeneous nucleation mechanism.[17] However, while the change in the nucleation mechanism explains the decrease in the crystallization rate, observed both in PE-M and PE-ZN (Fig.3.11-12) it can not account for the strong correlation between branching distribution and the effect of thermal history on the crystallization behavior.

We propose that drastic difference between non-isothermal solidification behavior of LLDPE-M and LLDPE-ZN is related to the difference in intermolecular branching distributions. Indeed, Ziegler-Natt LLDPE contains significant amounts of both almost linear (1% mol<x) and highly branched (x>5% mol) chains. Assuming random distribution of branched units along the polymer backbone the sequence probability distribution can be easily calculated Fig.3.13.[37,38] The results of statistic analysis indicate that the content of short methylene sequences in almost linear chains is very low, the content of long linear segments in highly branched molecules is also rather small. Thus in Ziegler-Natta LLDPE long and short methylene sequences predominantly belongs to different molecules. In contrast, PE-M can be presented as the blend of branched chains with average branching gradually changing in the vicinity of x_{avg} (2.6 % mol). In that case the same molecule contains comparable amount of shorter and longer methylene sequences. It means that both short and long methylene sequences are covalently bound in homogeneous LLDPE. During the step-crystallization longer linear segments are able to crystallize at higher temperatures while shorter linear sequences remain in the amorphous domain. In

metallocene co-polymers where the branching distribution is homogeneous, long and short methylene segments can be found within the same chains (Fig. 3.13, 3.14). Therefore, in PE-M the crystallites formed by the crystallization of long linear segments are covalently bound to the parts of molecules, remaining in the amorphous domain. The presence of the crystalline "anchors" reduces the molecular mobility of shorter linear segments, obstructing their access to the nucleation centers. Thus even if the crystallization of these segments is thermodynamically allowed, it would be kinetically hindered for steric reasons. In contrast, during the isothermal crystallization all crystallites are formed simultaneously, so both long and short linear segments have equal access to the nucleation centers. In highly heterogeneous PE-ZN almost linear molecules are enriched by long linear segments, while shorter linear segments are predominantly confined to highly branched molecules. As the result the crystallites, formed by long methylene squences, located in chains with low average branching do not affect the behavior of more branched molecules enriched by the shorter methylene segments. In HDPE, where crystallization is not hindered by the presence of branched units the effect of thermal history on the crystallization behavior is minimal.

The results of the melt investigation indicate that experimentally accessible frequency range only partially overlaps the terminal zone. In principle it may result in delay in the detection of gel point in the case when plateau region appears at very low frequencies, which can not be experimentally

observed. In order to prove that the appearance of a "plateau" pattern in *tan δ* (ω) dependence is indicative of the formation of physical network the stable critieal and near-critical gels, prepared from PE-M by step-crystallization proeedure were investigated using ereep technique and yield stress measurements. The analysis of the dynamie rheological patterns recorded during step-erystallization of PE-M proved that the critieal gel is formed at 119.5 °C. Gels prepared below 119.5 °C exhibit solid-like dynamie viseoelastic properties at low stress. Yield stress measurements demonstrate the onset of the yield stress oecurring in the vieinity of gel point, whieh is eonsistent with the development of eonnectivity. (Fig.3.15a) Zero-shear rate viseosity diverges for materials, having non-zero yield stress τ_Y. However, the viseosity of the structured fluid ean be measured using ereep technique. If ereep stress τ_{cr} exceeds τ_Y the structures break allowing the fluid to flow, in that ease ereep viseosity η_c ean be determined from the creep data. The temperature dependenee of the ereep viseosity at τ_{cr} = 12 [kPa] is presented at Fig.3.15 b It should be noted that the shear rate during the ereep experiments did not exeeed 1/s.

Signifieant inerease in the flow aetivation energy, observed in the vieinity of gel point is also eonsistent with the onset of the strueture formation. The value of flow aetivation energy at high temperatures $(T > T_{gel})$ determined from creep viscosities is slightly below than the value, measured in dynamie experiments. This differenee ean be eaused by the breaking of molceular clusters under the influence of shear field.

Observed good agreement between the results of dynamic and steady-shear measurements prove that the dynamic rheological technique indeed can be used for the detection of physical gelation in crystallizing LLDPEs.

3.5.6 Partial melting procedure

Another approach for the preparation of stable critical gel utilizes the step-like heating protocol for the partial melting (Fig.3.1d). In that case, the thinnest lamellae, whose T_m is below T_1, melt during the heating ramp and isothermal annealing at T_1. Thicker crystallites, having higher melting temperature persist after the equilibration at T_1. Then, after the process is repeated during the next isothermal steps at T_i all crystallites with melting temperature below T_i will be destroyed. Thus, the step-like partial melting procedure allows to decrease the crystallinity in fixed increments. As in the step-crystallization experiment, the system's viscoelastic properties can be monitored *in situ* by the oscillatory shear technique. The partial melting program includes only heating steps, so it can be reliably implemented in the measurement cell of spectroscopic devices.

The evolution of the viscoelastic properties of PE-M and PE-ZN during partial melting is presented at Fig.3.16. It can be seen that partial melting procedure allows to prepare stable critical gels both from metallocene and from Ziegler-Natta LLDPEs. By performing the rheological and Raman spectroscopic experiments in parallel it is possible to find the relationship between

crystallinity, local chain conformation and viscoelastic properties of physical gels in the vicinity of the gel point

Information regarding the chain packing and chain conformation can be derived from the Raman spectral region from 1600 to 150 cm^{-1}. In particular, the band at 1416 cm^{-1} arises from orthorombic crystal field splitting, and those at 1060 cm^{-1} and 1130 cm^{-1} are characteristic of long trans sequences. Both regions have been used to determine the degree of crystallinity in polyethylene samples.[13,39-43] Strobl et al.[39,40] calculated the degree of crystallinity by dividing the intensity of the 1416 cm^{-1} band by the total CH_2 twisting intensity and comparing with the value obtained for a completely crystalline sample. Naylor et al., instead, used the ratio of the 1060 cm^{-1} skeletal stretch to the CH_2 twist.[43] The two methods are in good agreement for calculating the degree of crystallinity of HDPE. In contrast, for LLDPE, crystallinity based on the intensity at 1416 cm^{-1} is usually below the one derived from the 1060 cm^{-1} band.[43]

Raman spectra, recorded during partial melting of LLDPE-M are presented inFig.3.17 The temperature dependence of crystallinity, calculated from Raman data is presented at at Fig. 3.18. It can be seen that the crystallinity at the gel point is rather low. Above 120 °C, the band at 1416 cm^{-1} virtually disappeared, indicating the absence of orthorombic crystal field splitting. Yet the crystallinity determined from the overall intensity at 1060 cm^{-1} corresponds to 5 ± 3 % [w/w], which is consistent with the critical crystallinity detected in isothermal and step-crystallization experiments.

Results of the Raman investigation suggest that in the physical gels near the critical point distorted orthorombic crystallites act as physical cross-links. These crystallites are formed by trans-segments. However due to the thermal expansion the interchain distance in the unit cell is large enough to eliminate the crystalline field splitting. While this explanation is consistent with the rheological results further investigations will be required in order to define the factors contributing to the relationship between morphology and mechanical properties of LLDPEs.

3.6 Conclusions

The effect of branching distribution on the rheological properties of LLDPEs in the melt and during isothermal and non-isothermal crystallization was studied by using steady- and oscillatory shear rheometry. Crystallinity and local chain conformation in LLDPE near liquid-solid transition was determined by Raman spectroscopy technique.

It was shown that rheological properties in the melt are predominantly determined by the molecular weight distribution, rather than by branching. In contrast, the type of branching distribution has a profound effect on the crystallization behavior of LLDPEs. While the overall branching is significantly lower and the branching distribution is more narrow in PE-M, its melting temperature is lower and the solidification intervals determined in a variety of cooling regimes are broader for this co-polymer than for its conventional analog

PE-ZN. The narrow solidification interval observed in the highly heterogeneous co-polymer PE-ZN results from the significant content of almost linear chains. In contrast, the homogencous co-polymer PE-M contains a variety of crystallizable sub-fractions with gradually varying branching, contributing to the overall solidification process; this results in the broad solidification range. In the metallocene system longer and shorter linear segments belong to the same chains. During non-isothermal crystallization of metallocene LLDPEs the crystallites formed at higher temperatures are covalently bound with non-crystallized chain segments, decreasing their mobility and affecting their crystallization rate. On the other hand in heterogeneous ZN co-polymers the chains, having low branch content are enriched by long linear segments, while shorter linear segments are predominantly confined to highly branched molecules. As a result, crystallites formed at higher temperatures by long linear segments do not have a significant effect on the crystallization behavior of shorter linear sequences. Thus, the effect of the thermal history on the crystallization behavior is more pronounced in PE-M than in its conventional analog.

The ability to predict the solidification behavior of LLDPEs based on their composition can be extremely useful for the optimization of industrial processes. Indeed, co-polymers and blends of co-polymers with desired rheological properties both in the melt and during crystallization may be produced by blending or by varying the catalyst. These materials will deform

and solidify in a desired way under the influence of stress, strain and temperature fields occurring during processing.

3.7 References

1. Gelfer, M. Y.; Winter, H. H."Effect of branching distribution on rheology of LLDPE during early stages of crystallization." *Macromolecules*, **32**, 8974 (1999).

2. Kim, M. H.; Phillips, P. J.; Lin, J. S."The equilibrium melting points of random ethylene-octene copolymers: A test of Flory and Sanchez-Eby theories." *J.Polym.Sci B Polymer Physics*, **38**, 154 (2000).

3. Wagner, J.; Abu-Iqyas, S.; Monar, K.; Phillips, P. J."Crystallization of ethylene-octene copolymers at high cooling rates." *Polymer*, **40**, 4717 (1999).

4. Kim, M. H.; Phillips, P. J."Nonisothermal Melting and Crystallization Studies of Homogeneous Ethylene/a-olefin Random Copolymers." *Journal Applied Polymer Science*, **70**, 1893 (1998).

5. Alamo, R.; Domszy, R.; Mandelkern, L."Thermodynamic and Structural Properties of Copolymers of Ethylene." *J. Phys Chem*, **88**, 6587 (1984).

6. Alamo, R. G.; Mandelkern, L."The crystallization behavior of random copolymers of ethylene." *Thermochimica Acta*, **238**, 155 (1994).

7. Hess, W.; Vilgis, T. A.; Winter, H. H."Dynamic Critical Behavior during Chemical Gelation and Vulcanization." *Macromolecules*, **21**, 2536 (1988).

8. Chambon, F.; Winter, H. H."Stopping of Crosslinking Reaction in a PDMS Polymer at the Gel Point." *Polymer Bull.*, **13**, 499 (1985).

9. Winter, H. H.; Chambom, F."Analysis of Linear Viscoelasticity of a Crosslinking Polymer at the Gel Poin." *Journal of Rheology*, **30**, 376 (1986).

10. Chambon, F.; Winter, H. H."Linear Viscoelasticity at the Gel Point of a Crosslinking PDMS with Imbalanced Stochiometry." *Journal of Rheology*, **31**, 683 (1987).

11. Schwittay, C.; M.Mours; Winter, H. H."RheologicalnExpression of Physical Gelation in Polymers." *Faraday Discussions*, **101**, 93 (1995).

12. Nijenhuis, K.; Winter, H. H."Mechanical Properties at the Gel Point of a Crystallizing Poly(vinyl chloride) Solution." *Macromolecules*, **22**, 411 (1989).

13. Schmidt-Rohr, K. ; Spiess, H.W. *Multidimentional Solid-State NMR and Polymers;* Acad. Press: NY, 1994.

14. Pogodina, N. V.; Winter, H. H."Polypropylene crystallization as a physical gelation process." *Macromolecules*, **31**, 8164 (1998).

15. Horst, R. H.; Winter, H. H."Stable critical gels of a crystallizing copolymer of ethene and 1-butene." *Macromolecules*, **33**, 130 (2000).

16. Rull, F.; Prieto, A. C.; Casado, D. M.; Sobron, F.; Edwards, H. G. M."Estimation of Crystallinity in Polyethylene by Raman-Spectroscopy." *J. Raman. Spec.*, **24**, 545 (1993).

17. Young R.J.; Lovell P.A. *Introduction to Polymers*; Chapman&Hall: NY 1991, p.284.

18. Kuchanov, S. I.; Panyukov, S. V."Molecular theory of solutions and blends of heteropolymers. I. Thermodynamics of amorphous multicomponent polymer systems." *J.Polym.Sci.,B:Polym. Phys.*, **36**, 937 (1998).

19. Krause, S. In *Polymer Blends;* Paul, D. R.; Newman, S. Eds.; Acad.Press: NY, 1978; Vol. 1; pp. 16-114.

20. Alamo, R. G.; Graessley, W. W.; Krishnamoorti, R.; Loshe, D. J.; Londono, J. D.; L.Mandelkern; Stehling, F. C.; Wignall, G. D."Small Angle Neutron Scattering Investigations of Melt Miscibility and Phase Segregation in Blends of Linear and Branched Polyethylenes as a Function of the Branch Content." *Macromolecules*, **30**, 561 (1997).

21. Wignall, G. D.; Alamo, R. G.; Londono, J. D.; Mandelkern, L.; Stehling, F. C."Small-Angle Neutron Scattering Investigations of Liquid-Liquid Phase Separation in Heterogeneous Linear Low-Density Polyethylene." *Macromolecules*, **29**, 5332 (1996).

22. Ryan, A. J.; Fairclough, J. P. A.; Terrill, N. J.; Olmstead, P. D.; Poon, W. C. K."A scattering study of nucleation phenomena in polymer crystallisation." *Faraday Disc.*, **112**, 13 (1999).

23. Rouse, P. E."A Theory of the Linear Viscoelastic Properties of Dilute Solutions of Coiling Polymers." *J.Chem.Phys.*, **21**, 1272 (1953).

24. Doi, M.; Edvards, S.F. *The Theory of Polymer Dynamics*; Clarendon Press:Oxford 1995.

25. Larson, R. G. *The Structure and Rheology of Complex Fluids*; Oxford Univ. Prcss: NY, 1999.

26. Wasserman, S. H.; Graesslcy, W. W."Effcets of Polydispcrsity on linear viseoelastieity in entangled polymer melts." *polymer Engineering and Science*, **36**, 543 (1992).

27. Wasscrman, S. H.; Gracssley, W. W."Predietion of linear viseoelastic responee of cntangled polyolefin melts from molccular weight distribution." *polymer Engineering and Science*, **36**, 852 (1996).

28. Mandelkern, L.; Alamo, R.G. In *Physical Properties of Polymers Handbook*; By Mark, E.J., Ed.; American Institute of Physics: Woodbridge NY 1996, p. 417.

29. Lambcrt, W. S.; Phillips, P. J."Crystallization kincties of fractions of branehcd polycthylcncs .2. Effect of molecular weight." *Polymer*, **3**, 3585 (1996).

30. Lambert, W. S.; Phillips, P. J."Crystallization kineticsof low-molccular weight fractions of branched polycthylenes." *Macromolecules*, **27**, 3537 (1994).

31. Banks, W.; Gordon, M.; Sharples, A."The Crystallization of Polyethylcnc aftcr Partial Mclting." *Polymer*, **4**, 289 (1963).

32. Akpalu, Y.; Kielhorn, L.; Hsiao, B. S.; Stein, R. S.; Russell, T. P.; VanEgmond, J.; Muthukumar, M."Structure developmcnt during crystallization of homogcneous copolymers of cthene and 1-octene: Timc-resolvcd synehrotron X-ray and SALS mcasurements." *Macromolecules*, **32**, 765 (1999).

33. Mandelkcrn, L.; M.Glotin; Benson, R. A."Supermolceular Structure and Thcrmodynamic Properties of Linear and Branched Polyethylenes undcr Rapid Crystallization Conditions." *Macromolecules*, **14**, 22 (1981).

34. Alamo, R. G.; Mandclkcrn, L."Thc crystallization bchavior of random copolymcrs of cthylcne." *Thermochimica Acta*, **238**, 155 (1994).

35. Bensason, S.; Miniek, J.; Moet, A.; Chum, S.; Hiltner, A.; Baer, E."Classifieation of Homogeneous Ethylcnc-Octcne Copolymcrs Based on Comonomer Content." *J. Polym.Sci., B: Polym.Phys.*, **34**, 1301 (1996).

36. Djabourov, M."Gelation-A Reviow." *Polymer International*, **25**, 135 (1991).

37. Riehardson, M. J.; Flory, P. J.; Jaekson, J. B."Crystallization and Melting of Copolymers of Polyethylene." *Polymer*, **4**, 221 (1963).

38. Flory, P. J."Theory of Crystallization in Copolymers." *Trans Far Soc.*, **51**, 848 (1955).

39. Strobl, G. R.; Hagedorn, W."Raman Speetroseopie Method for Determining Crystallinity of Polyethylene." *J.Polym.Sci: Polym.Phys*, **16**, 1181 (1978).

40. Mutter, R.; W.Stille; G.Strobl."Transition Regions and Surfaee Melting in Partially Crystalline Polyethylene-a Raman-Speetroseopie Study." *J.Polym.Sci.,B:Polym.Phys*, **31** (1993).

41. Mandelkern, L.; Alamo, R. G.; M.A.Kennedy."Comments on Paper "Raman Speetroseopy Employed for the Determination of the Intermediate Phase in Polyethylene"." *Macromolecules*, **28**, 2988 (1995).

42. Rodrigues-Cabello, J. C.; Martin-Monge, J.; Lagaron, J. M.; Pastor, J. M."Determination of the eontent of extended ehain segments in isotropie and uniaxially stretehed polyethylenes by Raman speetroseopy." *Macromolecular Chemistry and Physics*, **199**, 2767 (1998).

43. Naylor, C. C.; Meier, R. J.; Kip, B. J.; Williams, K. P. J.; Mason, S. M.; Conroy, N.; Gerrard, D. L."Raman Speetroseopy Employed for the Determination of the Intermediate Phase in Polyethylene." *Macromolecules*, **28**, 2969 (1995).

Table 3.1 Rheological characteristics of the investigated ethylene α-olefin copolymers

Polymer	Flow Activation Energy E_α [kJ/mol]	Power exponent n In the viscosity dependence on shear rate (160 °C)	Slope $\frac{\partial \ln G'}{\partial \ln \omega}$ $(10^{-2}<\omega<10^{0})$
PE-ZN	25	1.16	1.12
PE-M	27	1.72	1.3
HDPE-ZN	23	0.96	1.16
HDPE-M	24	0.95	1.15

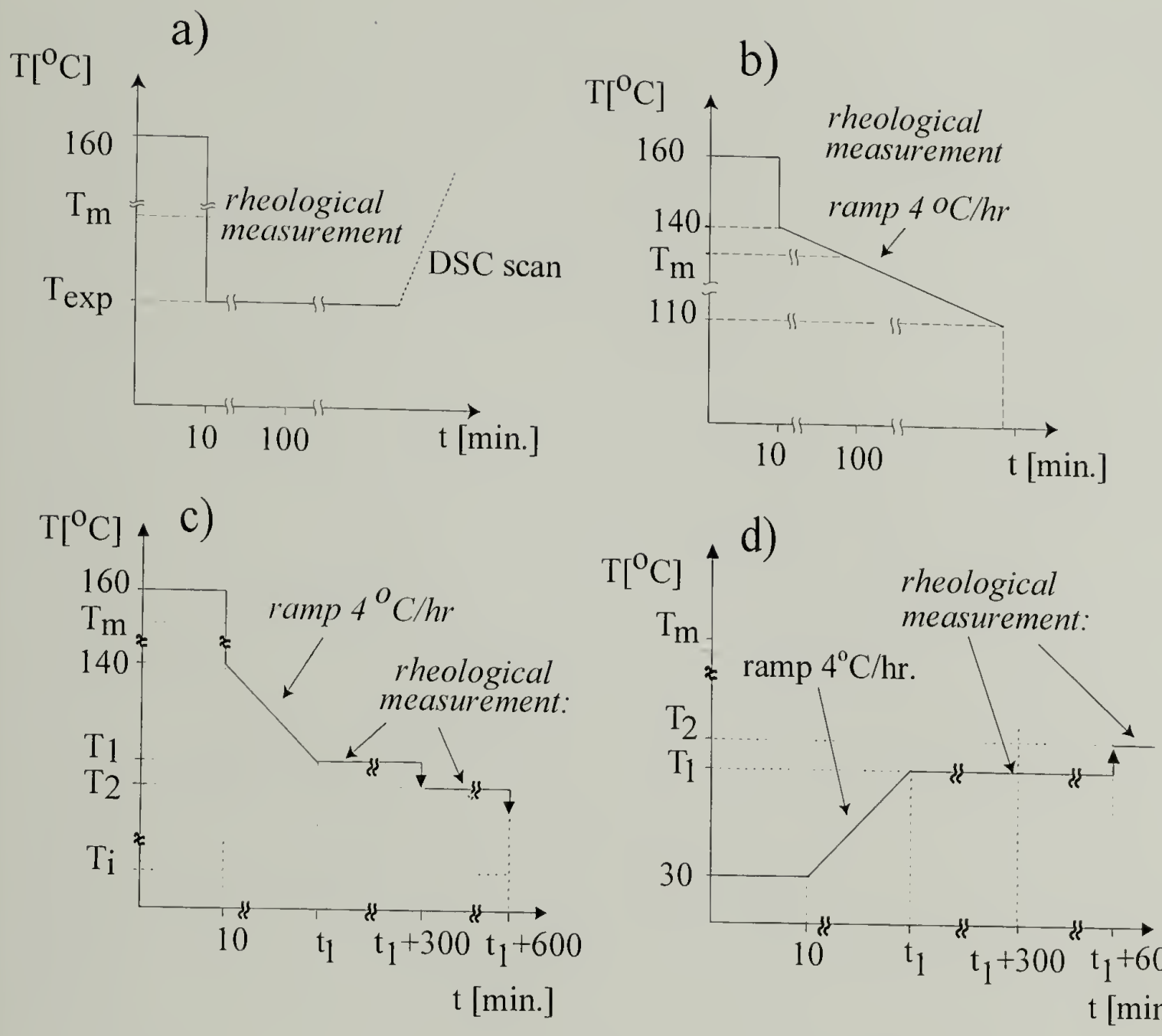

Figure 3.1 Isothermal and non-isothermal temperature programs utilized in rheological and DSC experiments: (a) isothermal crystallization; (b)non-isothermal crystallization; (c) step-crystallization; (d) partial melting; the samples for partial melting were slowly cooled from 160 °C to 130 °C with a cooling rate of 1 °C/min.

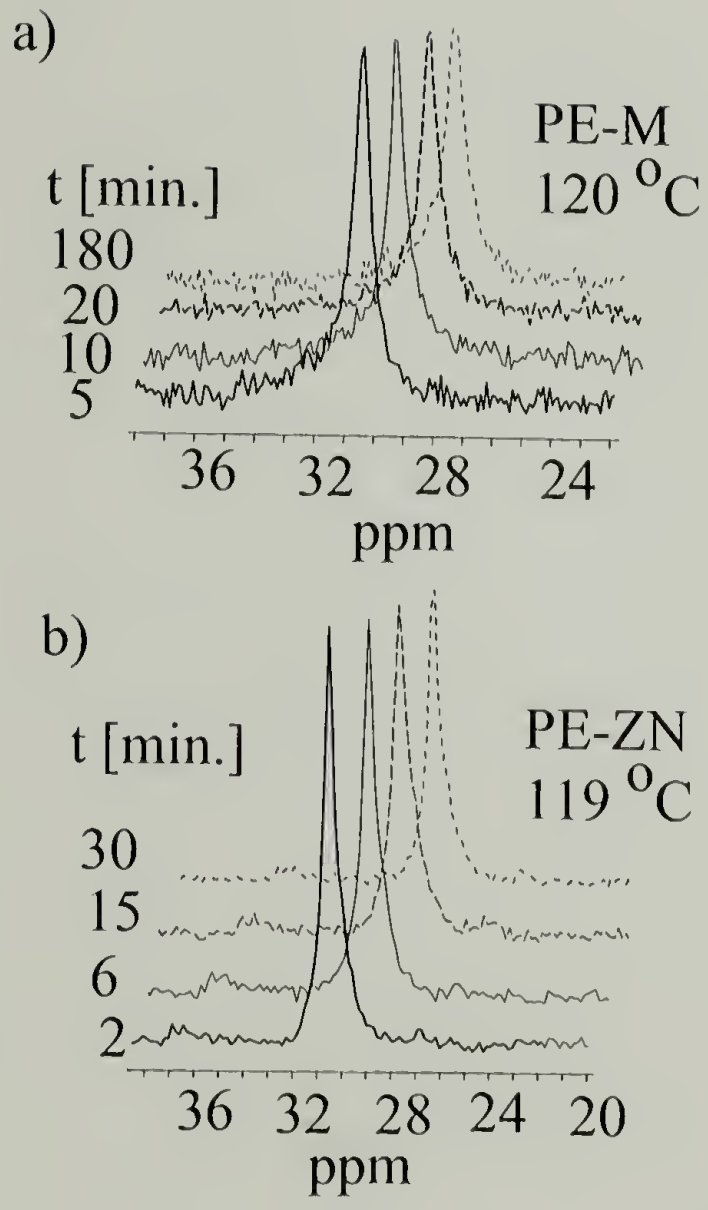

Figure 3.2 Static ^{13}C direct polarization spectra, acquired during isothermal crystallization of LLDPEs (plots have been offset to show details of time evolution).

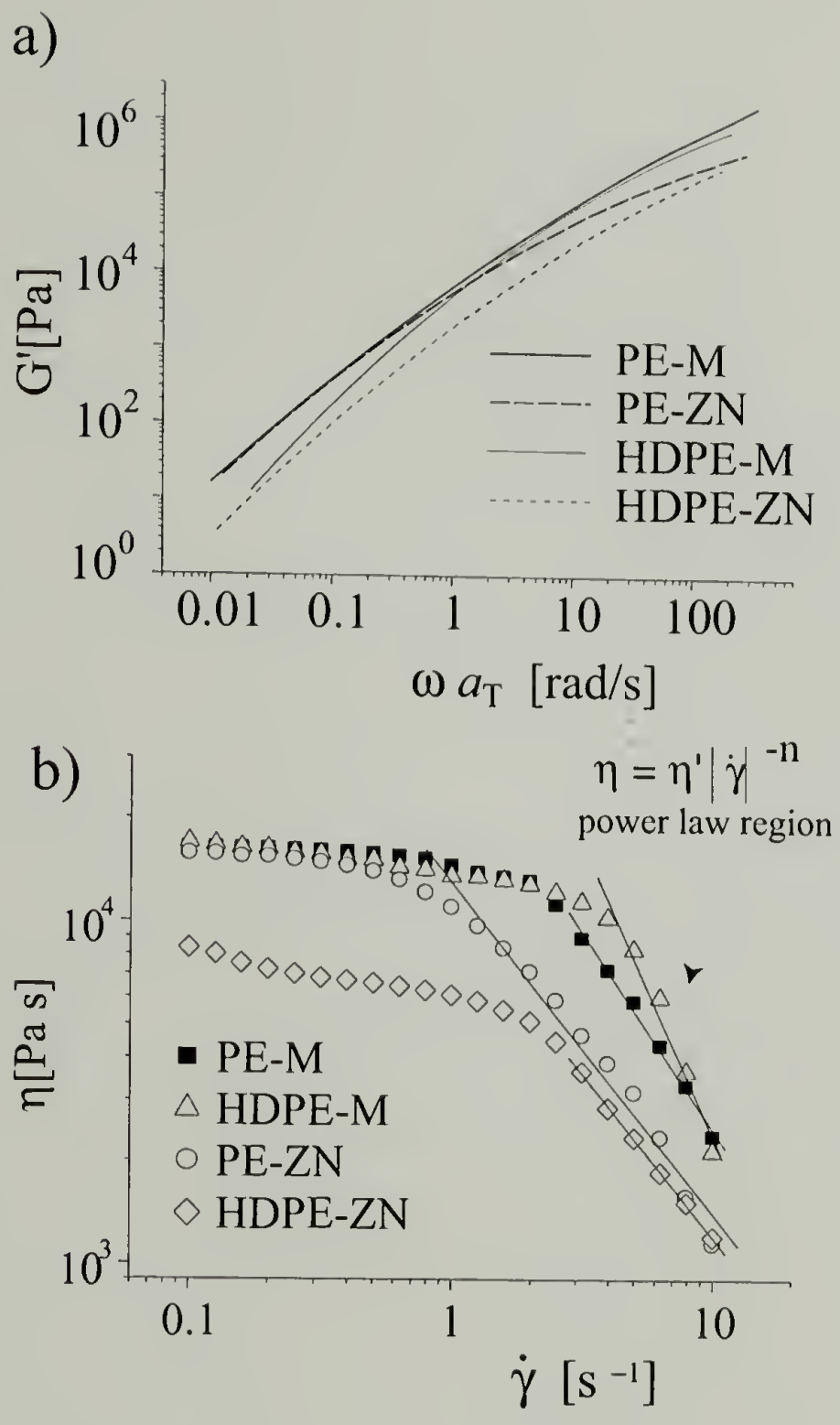

Figure 3.3 (a) frequency dependence of the storage modulus for ethylene co-polymers. T_{ref}=140 °C; a_T : logarithmic shift factor (b) the shear rate dependence of the steady shear viscosity for ethylene co-polymers T = 160 °C.

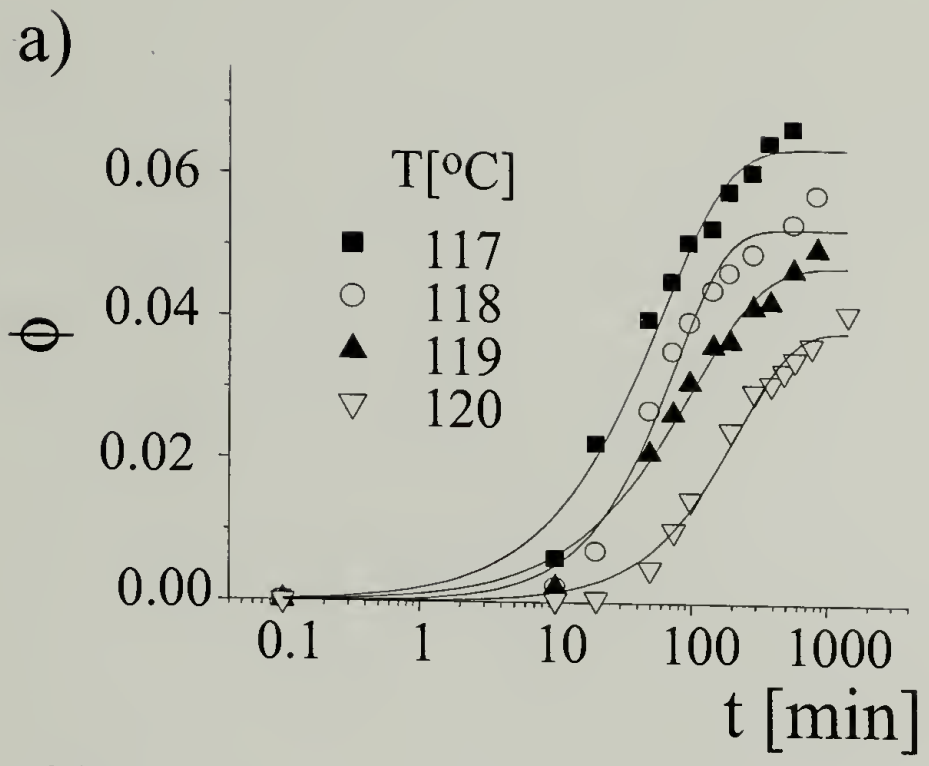

Figure 3.4 Isothermal crystallization kinetics for LLDPEs (by DSC); symbols : experimental data; lines: Avrami fit. (a)PE-M; (b) PE-ZN.

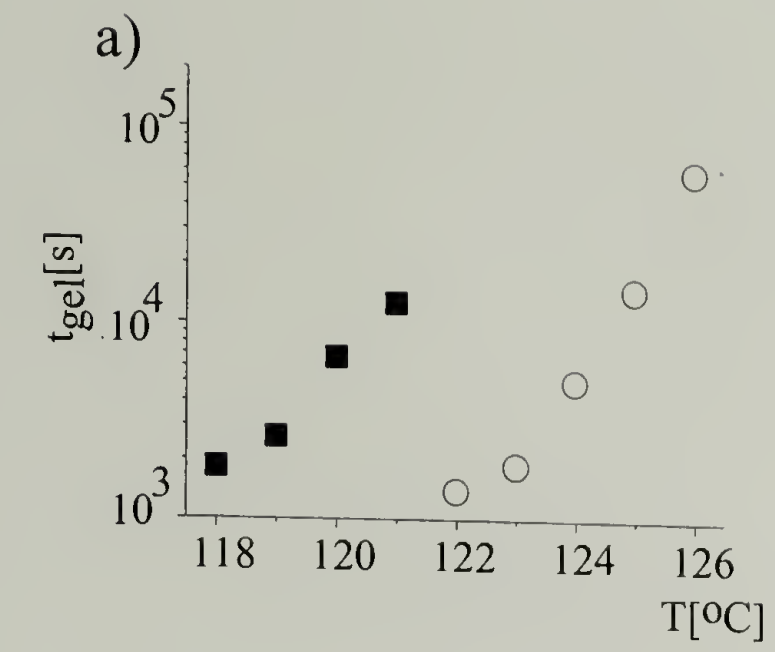

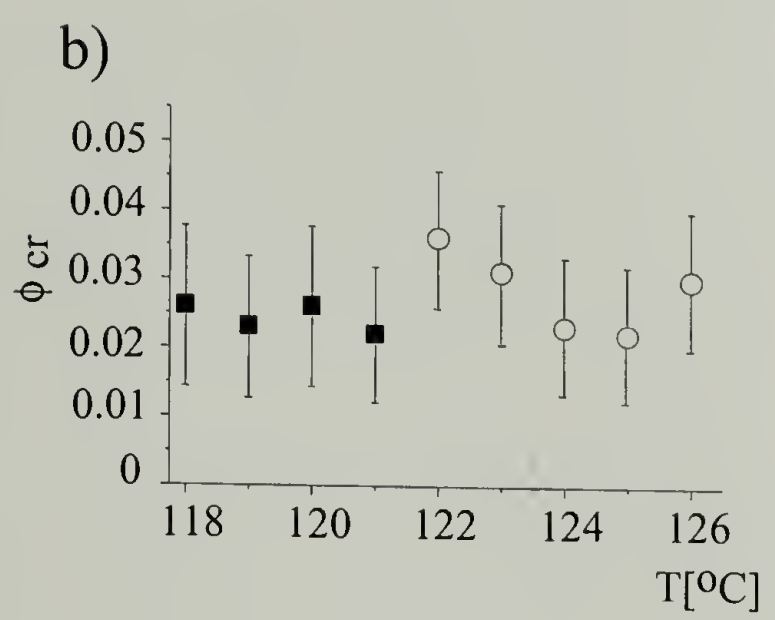

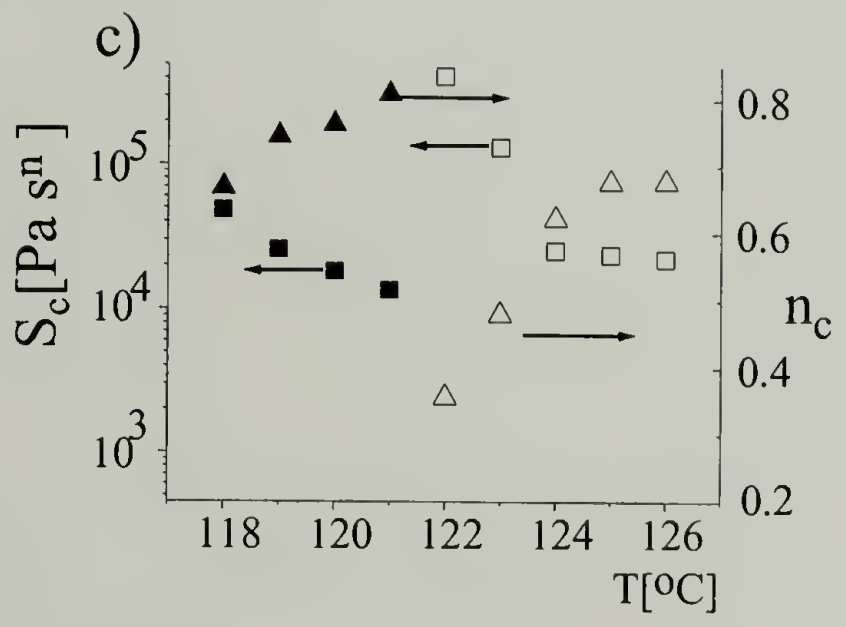

Figure 3.5 Dependence of the viscoelastic properties of critical gel on the crystallization temperature ; solid symbol: PE-M; open symbol: PE-ZN: (a) gel time; (b) crystallinity at gel point; (c) gel stiffness S_c and relaxation exponent n_c.

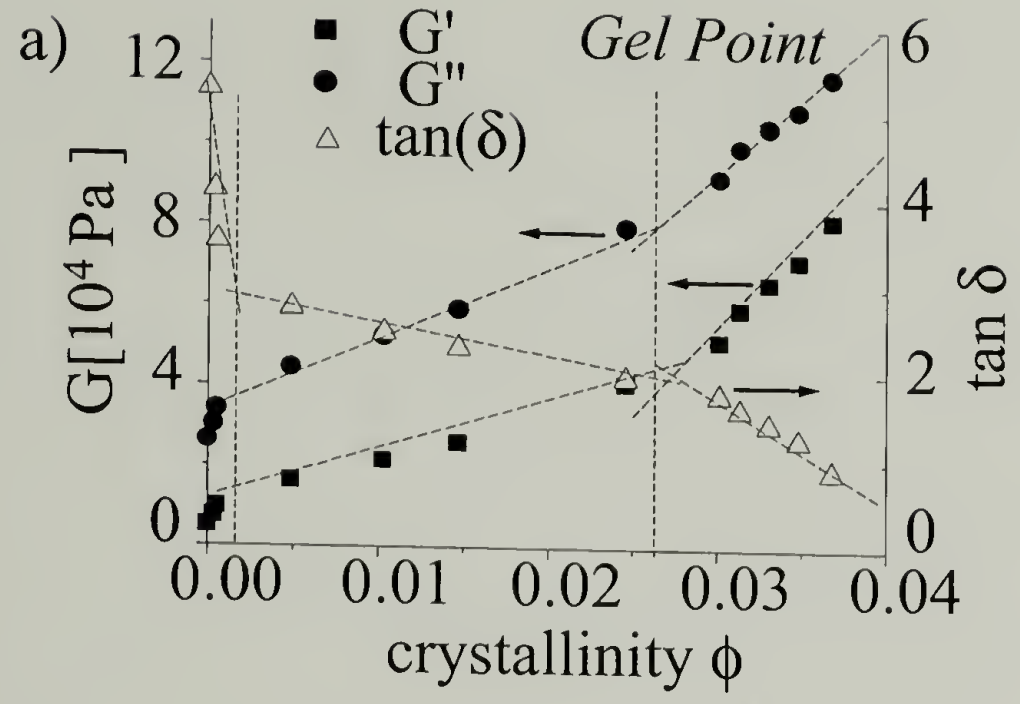

Figure 3.6 Crystallinity dependence of dynamic viscoelastic properties of LLDPEs during the isothermal crystallization (ω=[1 rad/s]); (a) PE-M; (b) PE-ZN

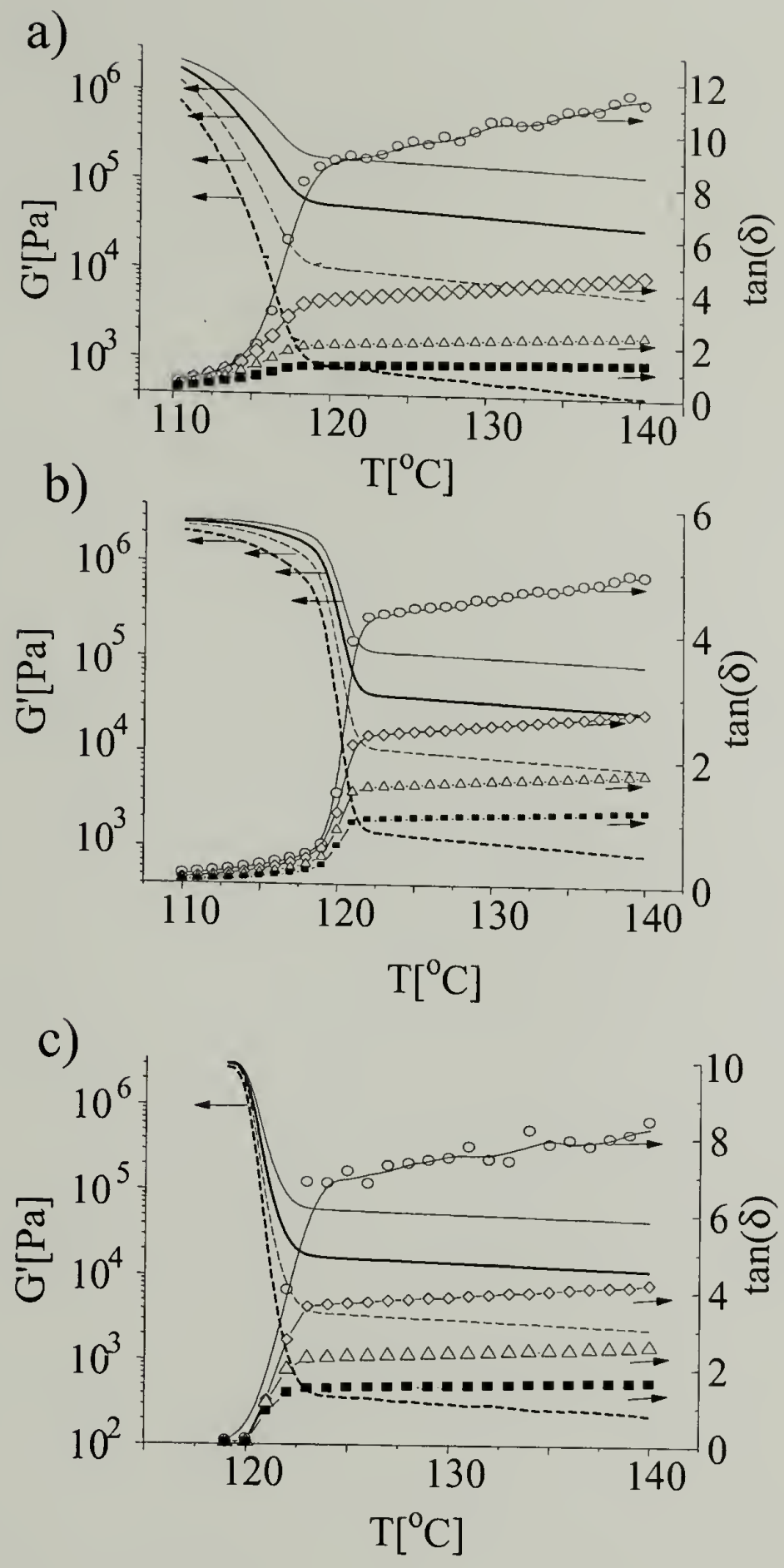

Figure 3.7 Temperature dependence of dynamic viscoelastic properties of LLDPEs during non-isothermal crystallization (cooling ramp 4 °C/hr); lines -*G′* symbols-*tan* δ
ω= 0.2 [rad/s]: ----- ○ ; 1.26 : ----- ◇ ; 5: —— △;
and 20 rad/s: —— ■ .
The samples are: (a) PE-M; (b) PE-ZN; (c) HDPE-ZN

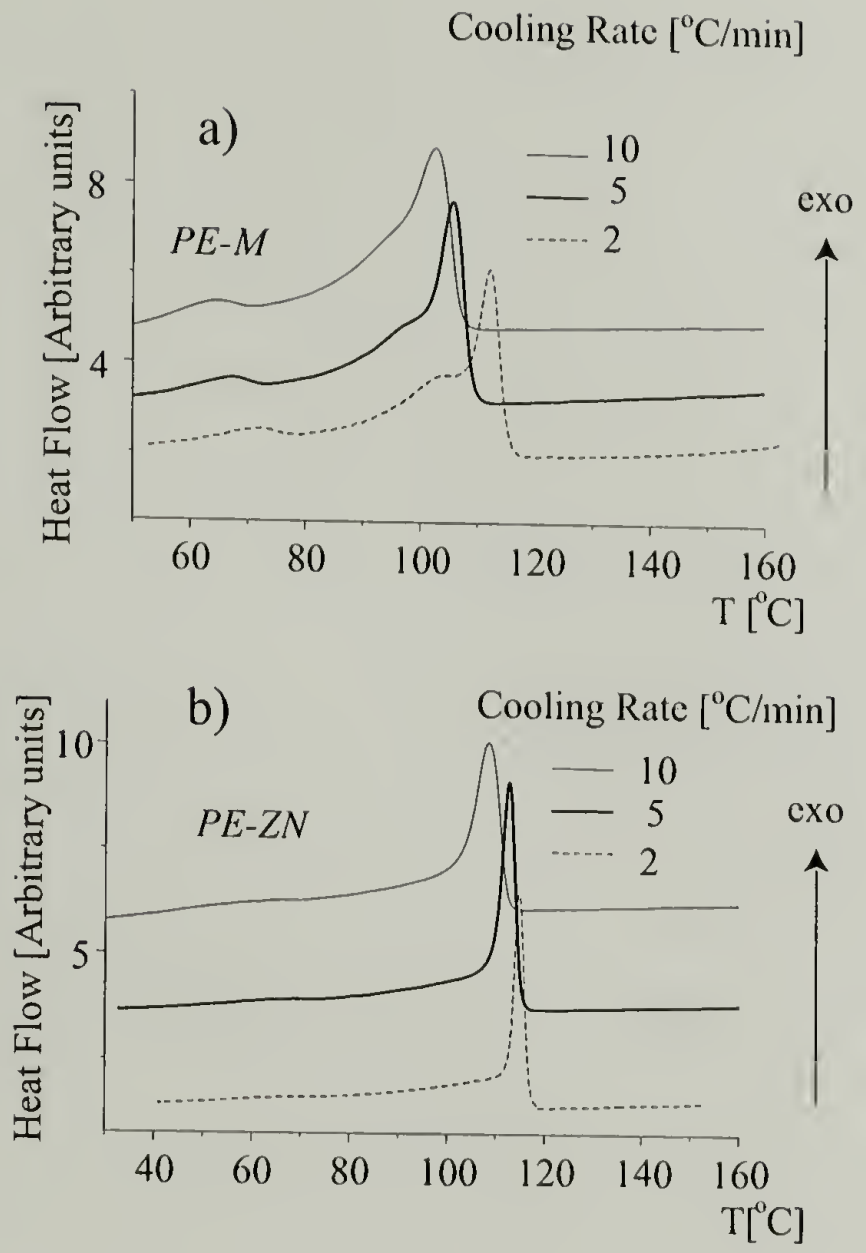

Figure 3.8 DSC exotherms acquired during nonisothermal crystallization of LLDPEs. (a) PE-M; (b) PE-ZN.

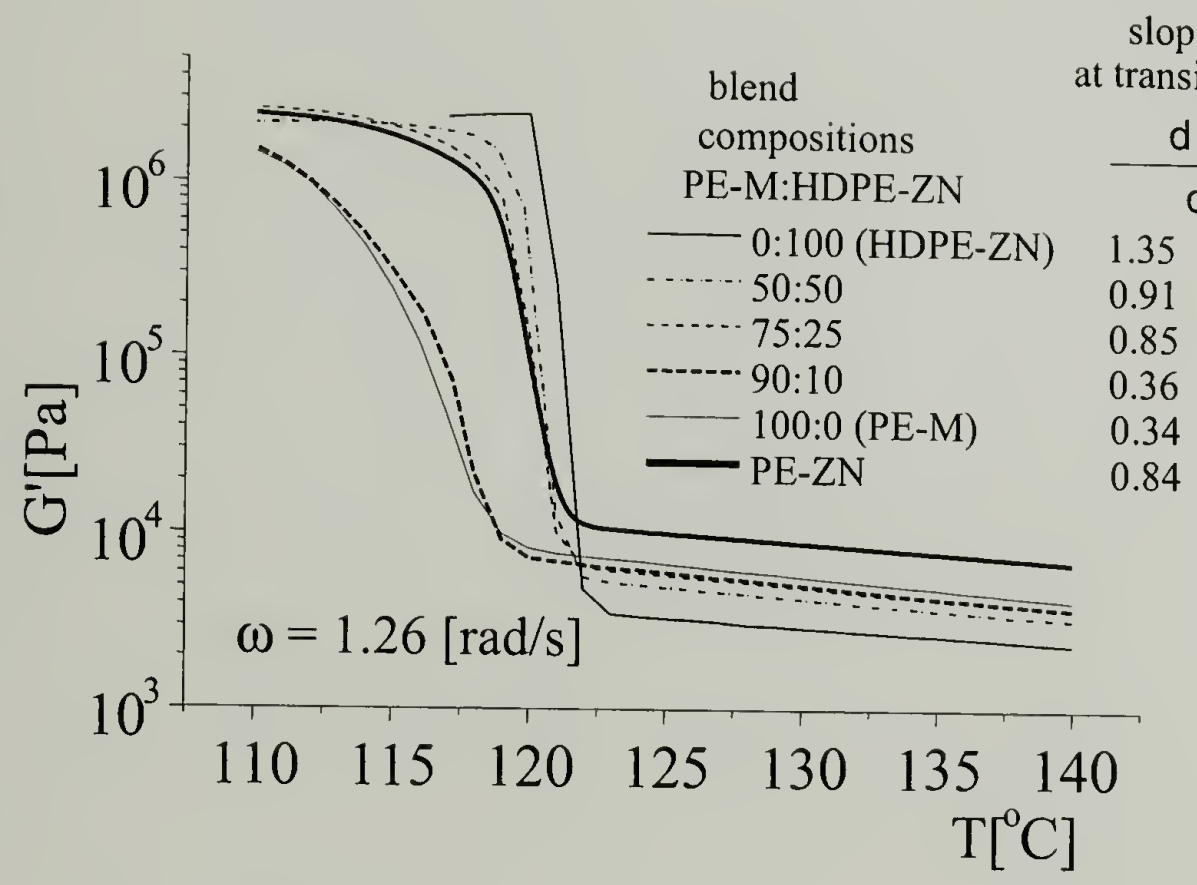

Figure 3.9 Temperature dependence of storage modulus *G'(T)* during non-isothermal crystallization in PE-M:HDPE-ZN blends.

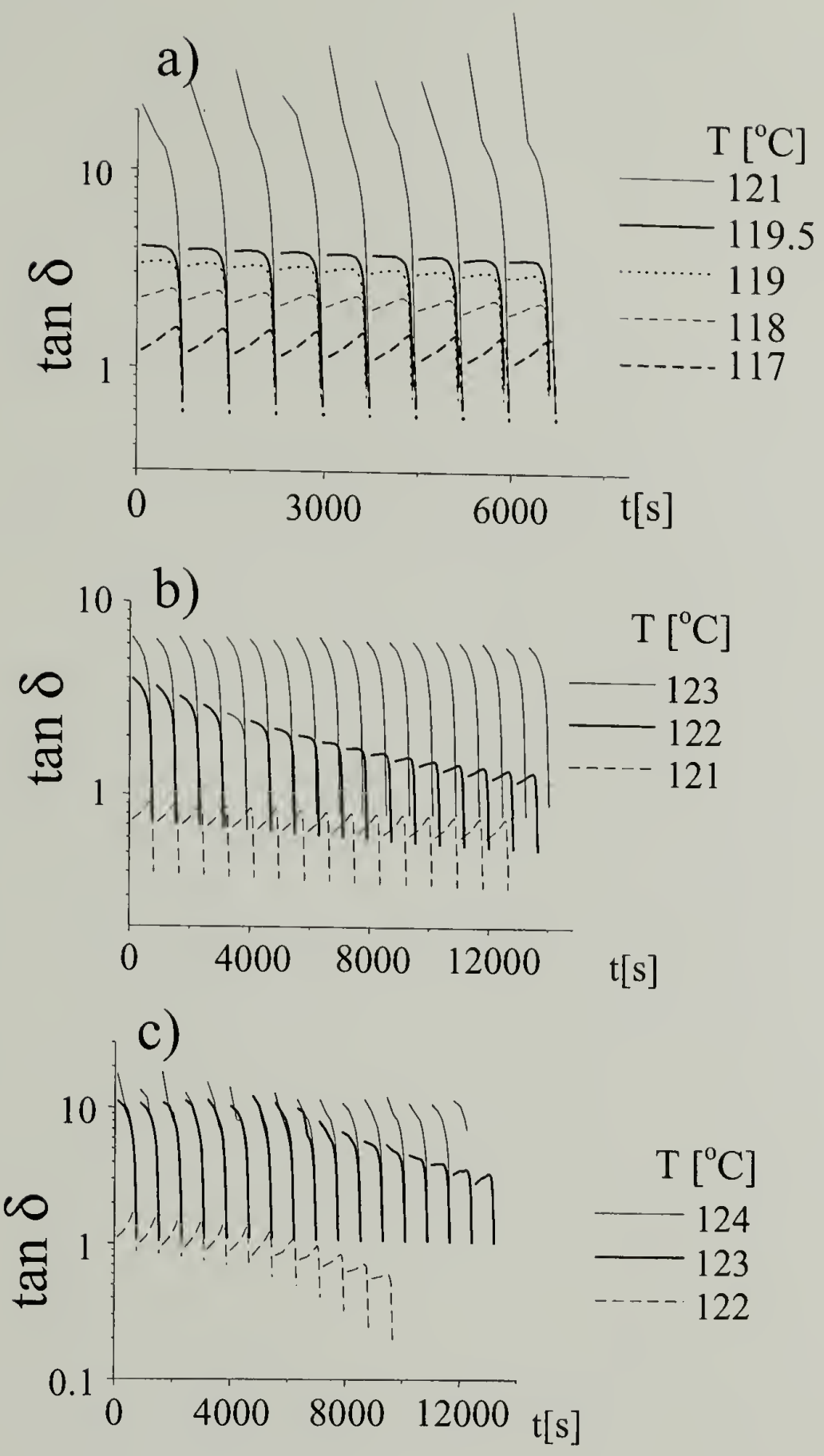

Figure 3.10 Rheological patterns of physical gels prepared by step-crystallization (time evolution of viscoelastic properties during the isothermal steps) (a) PE-M; (b) PE-ZN; (c)HDPE-ZN.

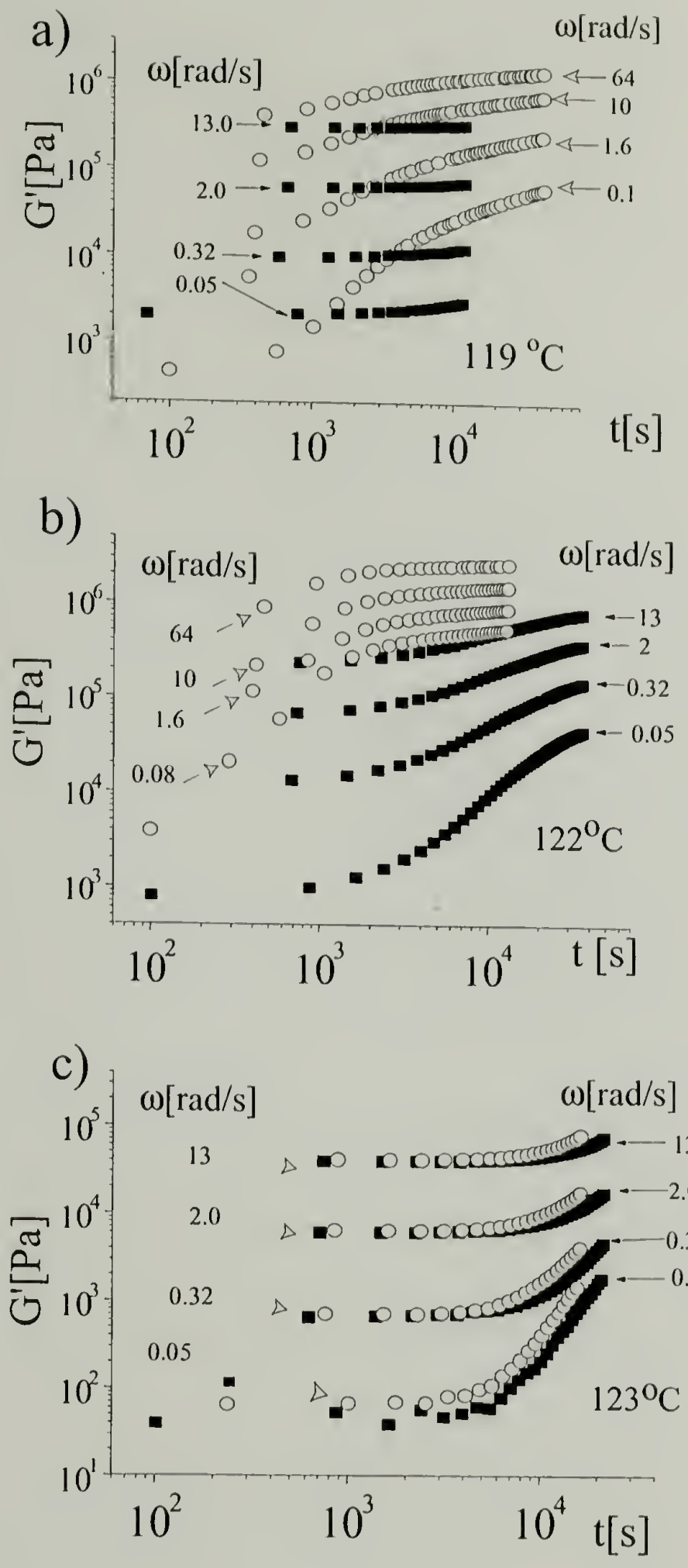

Figure 3.11 Time evolution of storage modulus during the isothermal and step - crystallization; open symbols: isothermal crystallization; solid symbols: step-crystallization.
(a) PE-M ; (b) PE-ZN; (c) HDPE-ZN.

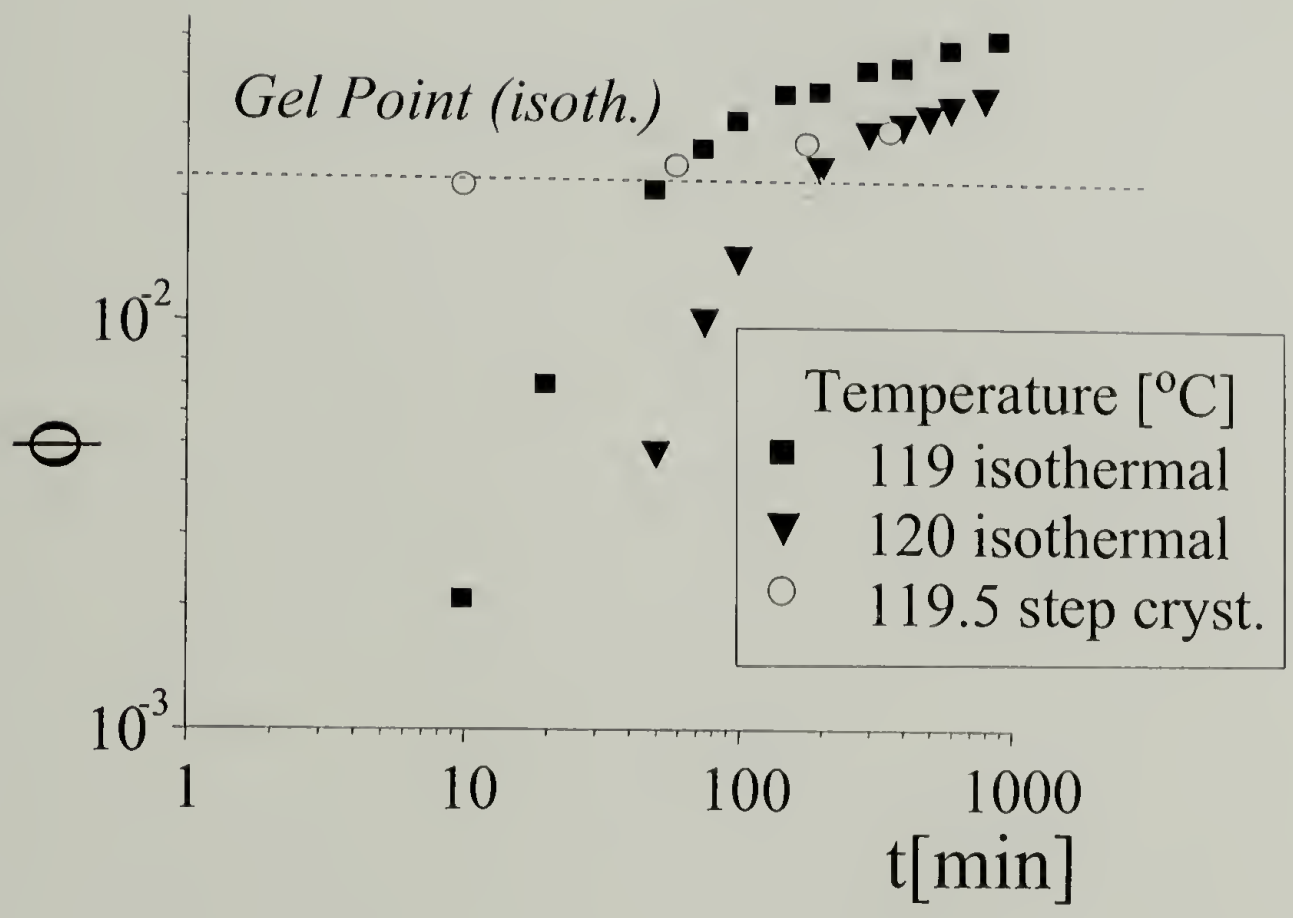

Figure 3.12 Crystallization kinetics for isothermal and step-crystallization of PE-M. For step-crystallization the duration of the final isothermal step at 119.5 [°C] was used as the crystallization time

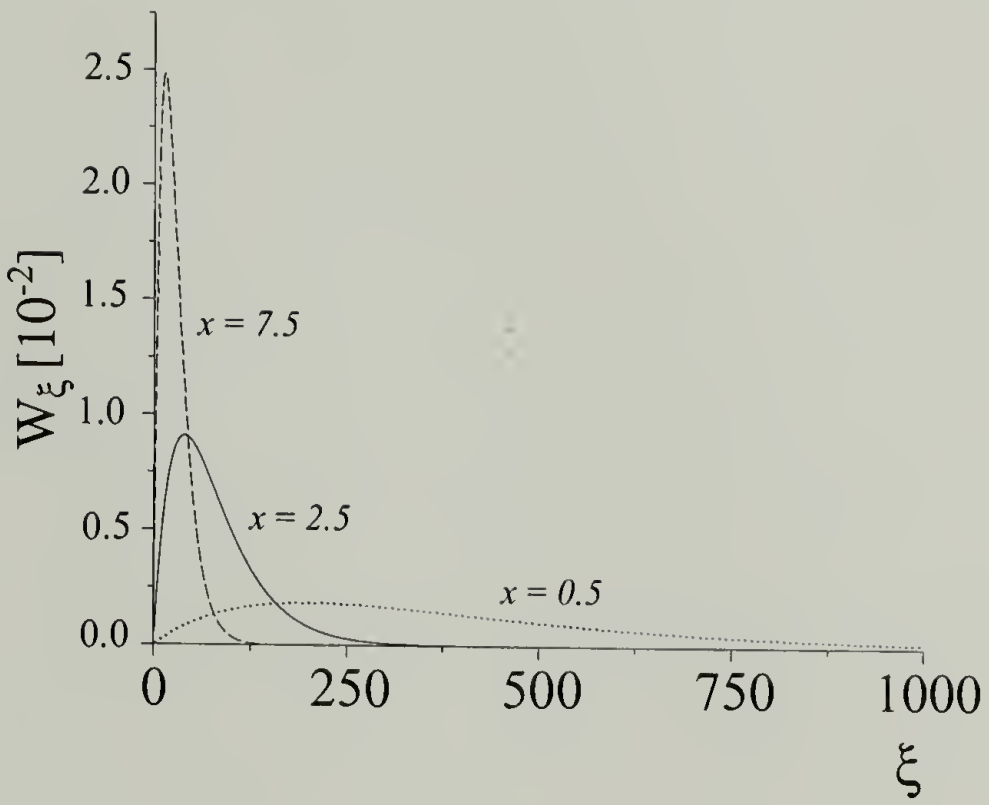

Fig. 3.13 Sequence probability distributions for the random co-polymers having different average branching x [%mol]; ξ- number of consecutive methylene units in a sequence;
W_ξ-weight fraction of a sequence, containing ξ units; $W_\xi = \xi(1-p)^2 p^\xi$;

here $p=\left(\frac{100\% - x}{100\ \%}\right)$ the probability for the methylene group to be succeeded by another methylene group.

$$T_o > T_m > T_1 > T_2$$

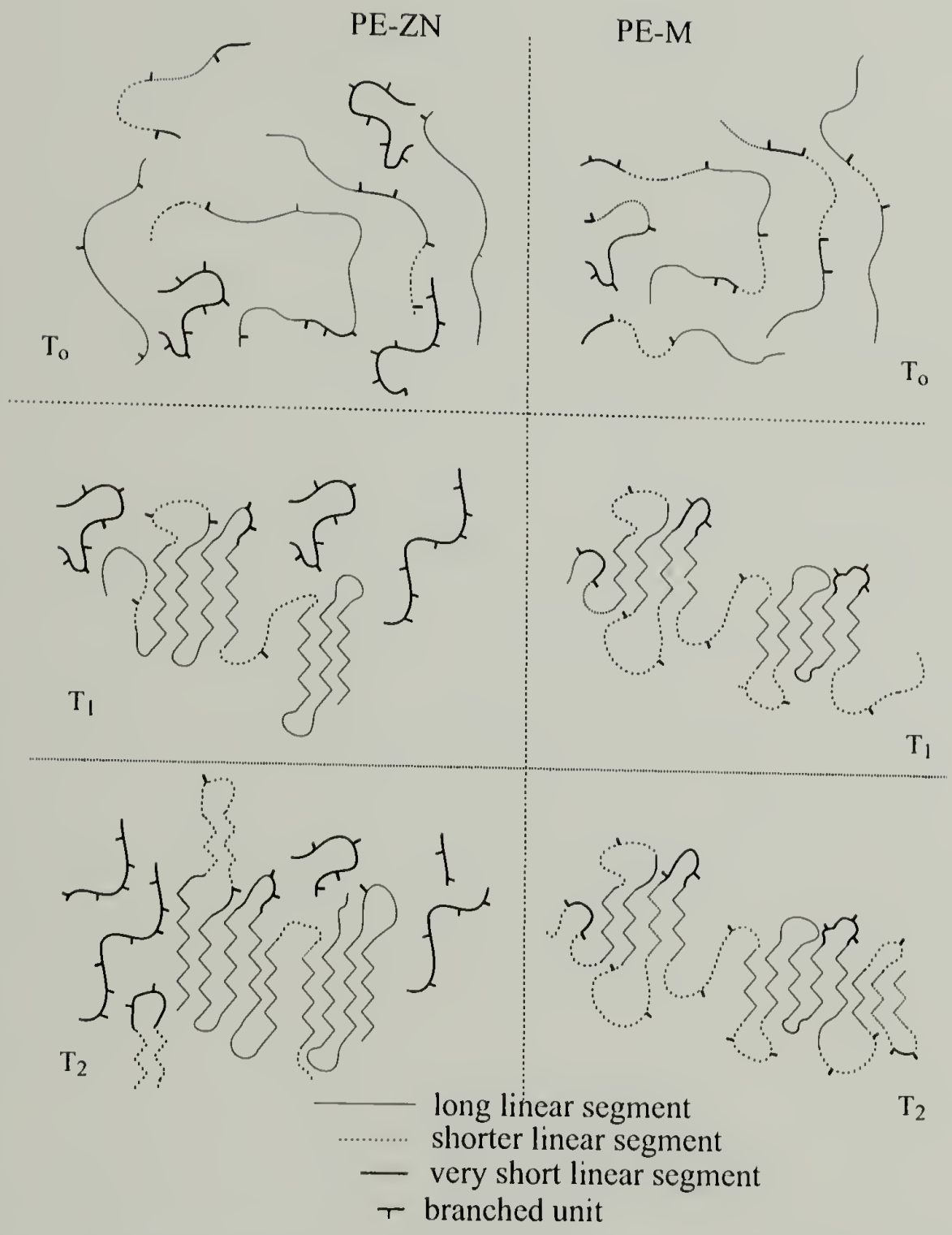

Figure 3.14 Structural model describing behavior of metallocene and Ziegler -Natta LLDPEs during step-crystallization.
In PE-M longer and shorter linear sequences belong to the same molecules i.e. they are covalently bound. During step-crystallization the crystallization of long methylene sequences decreases the molecular mobility and hinders crystallization of short sequences; in PE-ZN longer and shorter linear segments form separate crystallites, so their mutual influence is minimal.

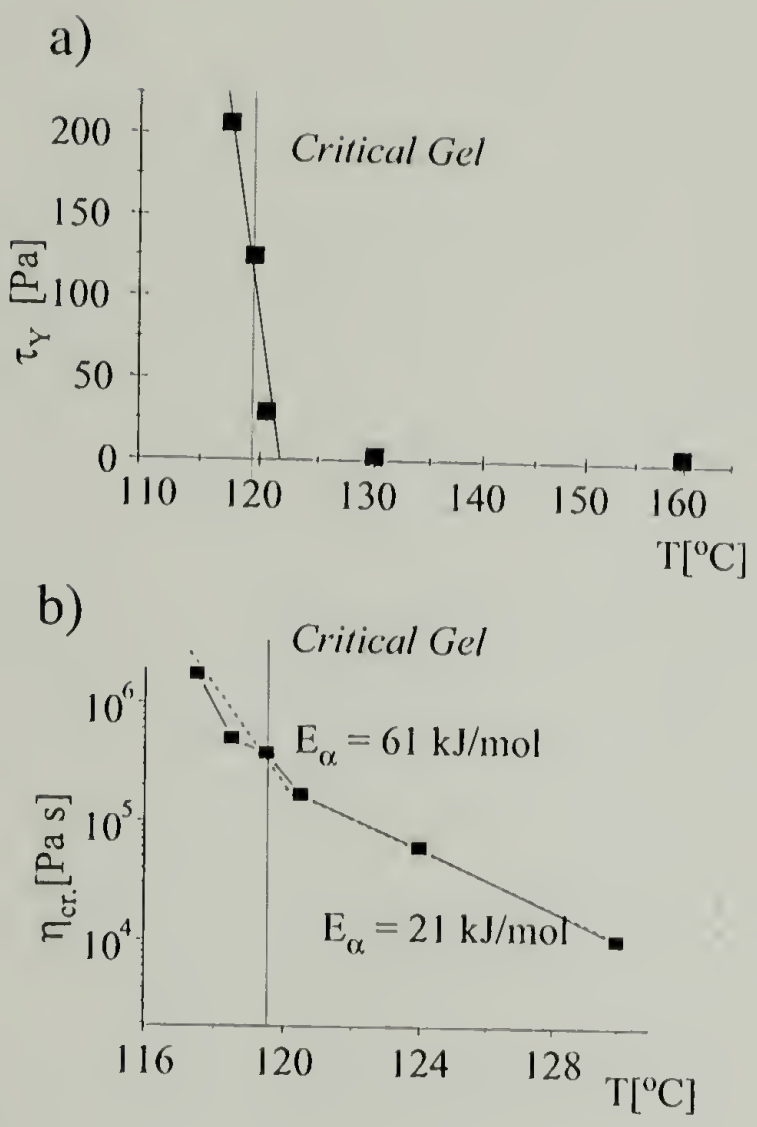

Figure 3.15 Steady-Shear properties of critical gels formed during step-crystallization of PE-M. (a) temperature dependence of yield stress τ_Y; (b) temperature dependence of the creep viscosity η_{cr} (measured at τ_{cr} = 12 kPa). E_α -flow activation energy

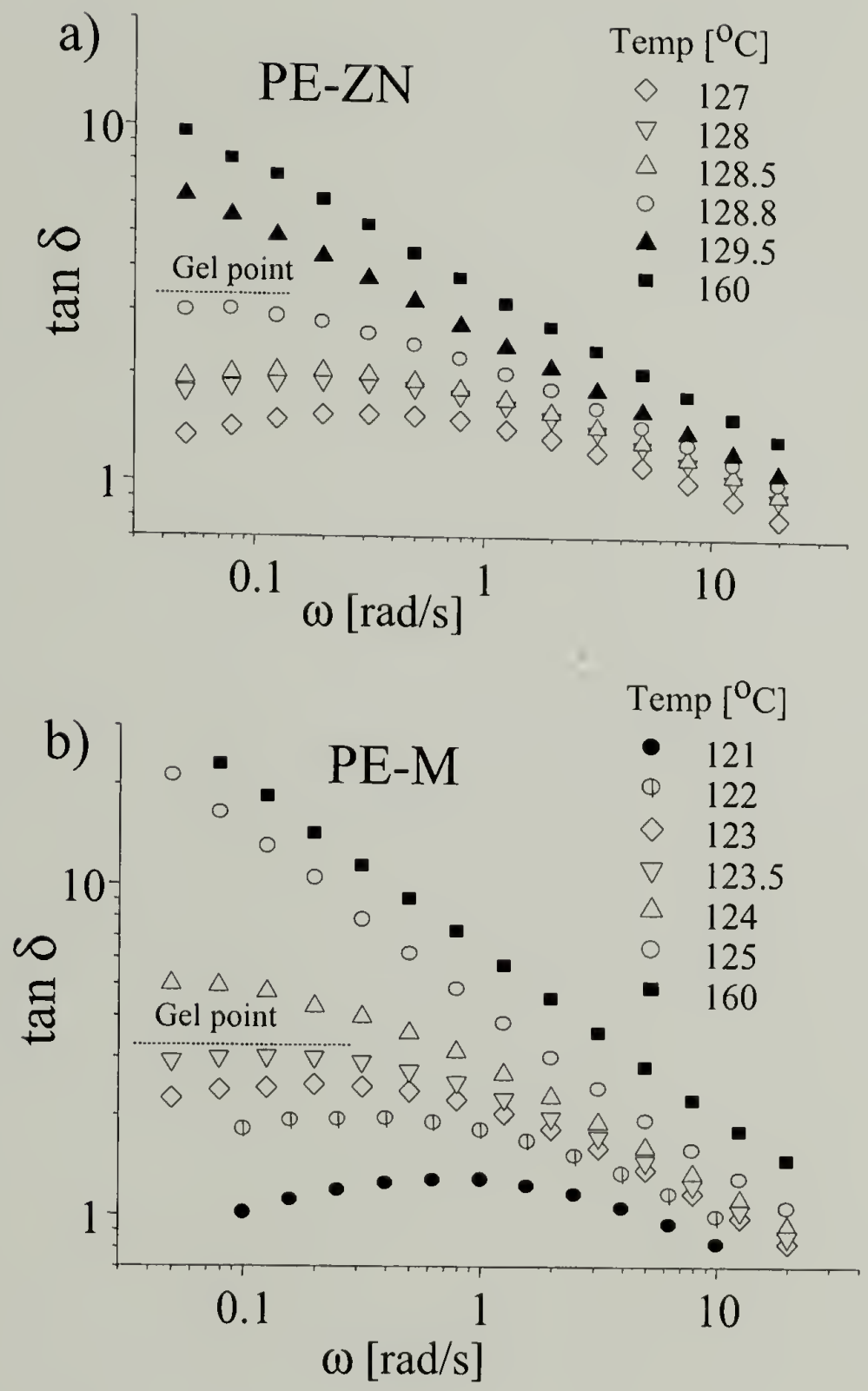

Figure 3.16 Dynamic viscoelastic properties of stable physical gels formed during partial melting of LLDPEs.
(a) PE-ZN ; (b) PE-M

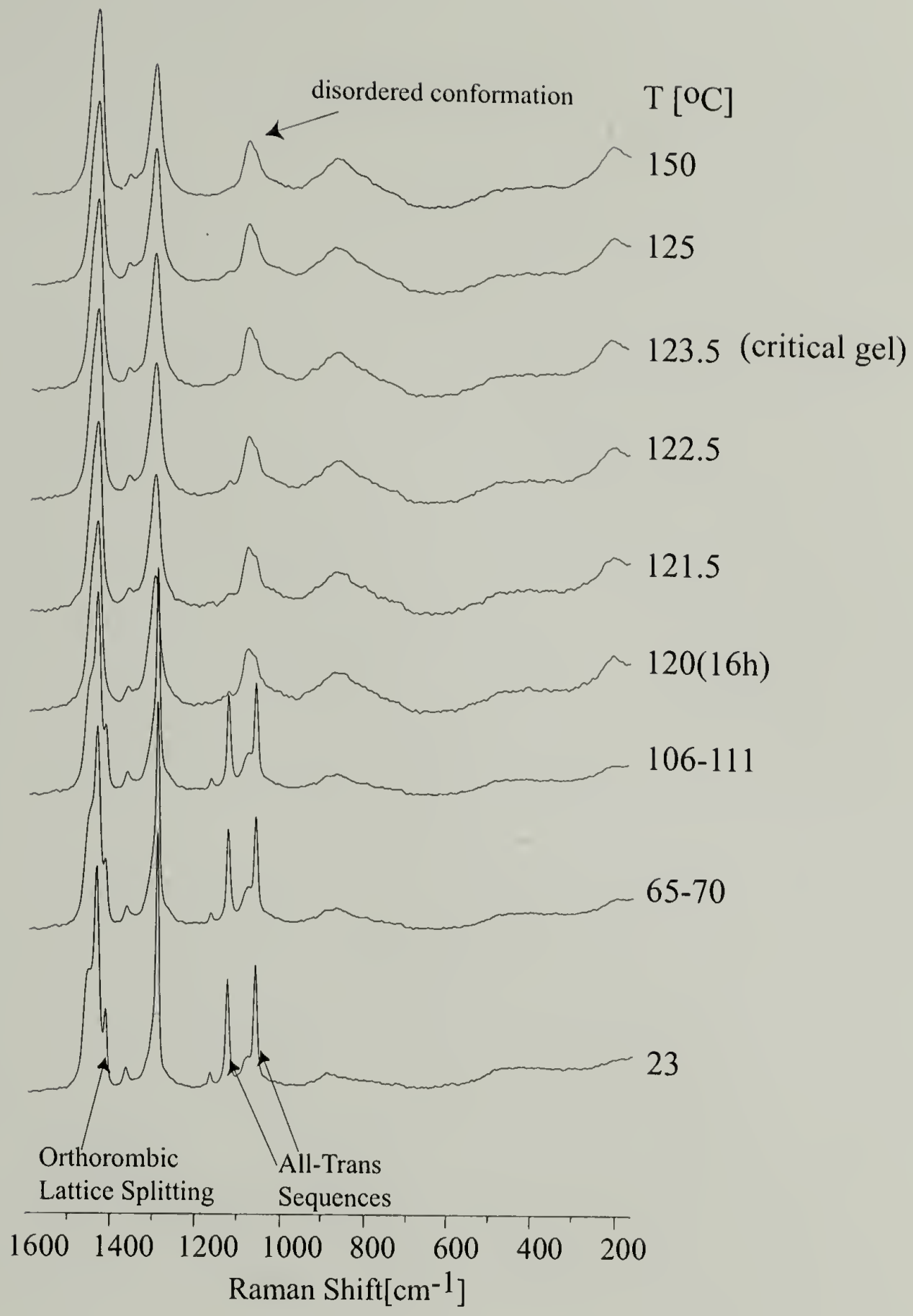

Figure 3.17 Raman spectra acquired during partial melting of PE-M

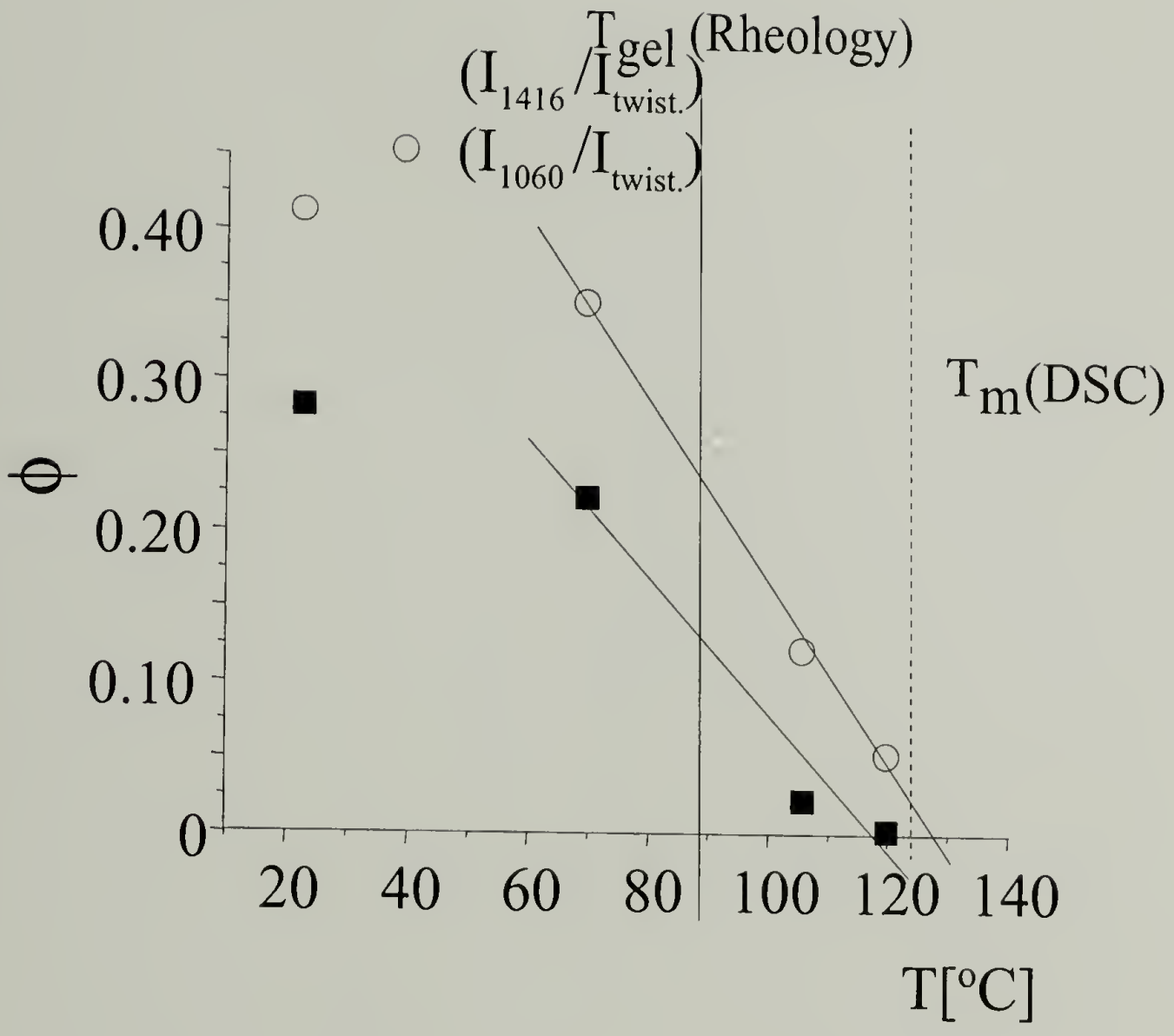

Figure 3.18 Temperature dependence of the Raman Crystallinity during partial melting of PE-M determined based on the intensity ratio of the 1416 cm^{-1} band to the overall intensity of CH_2 twisting signal[47] - ■ and from the the intensity ratio for 1060 cm^{-1} band[50] - ○

CHAPTER 4

DETERMINATION OF THE CRYSTALLITE-THICKNESS DISTRIBUTION IN POLYETHYLENES FROM ^{1}H NMR ROTATING FRAME RELAXATION

4.1 Abstract

The crystallite thickness distribution in linear low-density polyethylenes (LLDPEs) and high-density polyethylenes (HDPEs) can be determined sensitively and conveniently from nuclear magnetic resonance (NMR) ^1H $T_{1\rho}$ relaxation times, due to the strong thickness-dependence of the rate of the 180° – flip motion in the crystallites. This $T_{1\rho}$ relaxation time — thickness relation has been calibrated by comparison with transmission electron micrographs for the LLDPEs, and with Raman scattering for a melt and solution-crystallized HDPE. The non-exponentiality of the NMR $T_{1\rho}$ decay is shown experimentally to be due to a distribution of crystallite thicknesses, with the widest distribution for isothermally crystallized Ziegler-Natta LLDPE and the narrowest for quenched metallocene LLDPE, in good agreement with the electron micrographs. The average crystallite thickness from the TEM-calibrated NMR data correlate well with those estimated from melting temperatures in differential scanning calorimetry. Compared to other techniques, the NMR experiments provide a more reliably volume-averaged thickness distribution. By a $T_{1\rho}$-selection — spin diffusion — $T_{1\rho}$-measurement technique, spin diffusion effects are shown to be negligible on the relevant 30-ms time scale.

4.2 Introduction

It is known that in branched ethylene co-polymers overall branching has a profound influence on the crystallite thickness.[1] Hence, it can be proposed that the lamellar thickness in LLDPEs will be also sensitive to the branch distribution. The crystallite thickness in ethylene co-polymers and its distribution are the fundamental parameters of the morphology of these polymers affecting macroscopic properties such as creep rates or moduli. Thus the effect of the branch distribution on the macroscopic properties of solid LLDPEs will be strongly correlated with its influence on the lamellar thickness. Obviously, a reliable determination of crystallite thickness distribution is an essential part of this investigation, aimed at the analysis of the relationship between composition distribution and properties of LLDPEs.

Current techniques for the determination of lamellar thickness distribution include electron microscopy, small-angle X-ray scattering (SAXS) and Raman spectroscopy. Microscopy provides direct visualization of polymer morphology, but the sample has to be stained or etched in order to achieve contrast between amorphous and crystalline domains. It is not always possible to find a proper etching reagent, the staining procedure is labor-intense and can result in artifacts, absolute calibrations in scanning electron microscopy (SEM) and transmission electron microscopy (TEM) are demanding, and accurate volume averaging can be challenging. High-quality small-angle X-ray scattering (SAXS) data give the density autocorrelation function that reflects the

morphology, including the crystallite thickness. However, in systems with wide thickness distributions the scattering pattern may not even contain a distinct peak before Lorentz correction. Additionally, in LLDPEs the contrast is rather low, so the data processing requires smoothing, approximation techniques and the use of assumed morphological models.[2] The longitudinal acoustic mode (LAM) observed in Raman scattering at low frequencies measures the length of the straight chain stems. This technique tends to underestimate the width of the distribution, and cannot be applied reliably for broad distributions.[3-6] Besides, the application of the Raman (LAM) technique requires knowledge of the Young's elastic modulus in the chain direction. Although this value is well known for linear polyethylene crystals, the Young's modulus of micelle-type crystallites, as those formed from random ethylene copolymers with a relatively high concentration of comonomer is subject to uncertainties.[7]

In principle, the crystallite thickness distribution can also be obtained from the distribution of melting temperatures of a DSC melting endotherm following the Gibbs-Thomson equation.[8-9] However, the method is valid only if reorganization or superheating does not occur during the melting scan and if the value of crystalline basal free energy is known.[10] Moreover, this DSC method is not applicable to random copolymers in which the comonomer unit is not crystallizable, such as LLDPE.[10] Copolymer melting is affected by the concentration of non-crystallizable comonomer in the melt as well as by the lamellar thickness. However, the melt composition in copolymer with non-equilibrium crystallinity is unknown which makes determination of the correct

distribution from DSC impossible. In view of these limitations, we applied the DSC technique only for the evaluation of average lamellar thicknesses.

In this work, we describe a simple solid-state NMR technique for determining the lamellar thickness distribution, applicable for polyethylene and ethylene copolymers. The method is based on the correlation between the crystallite thickness and the $^{1}H\ T_{??}$ relaxation time in the crystalline domains of polyethylene and ethylene copolymers, which is caused by the thickness dependence of the rate of the 180° chain flips that drive the $^{1}H\ T_{??}$ relaxation in polyethylene.[11] It is shown that the clearly non-exponential character of the relaxation curves is related to the variation of the lamellar thickness throughout the sample, rather than to the contribution of the crystalline-amorphous interface or crystalline defects. Spin-diffusion effects[12-15] are insignificant on the relevant 30-ms time scale.

The relaxation-rate-lamellar thickness distribution relationship is calibrated using TEM thickness-distribution data of LLDPE materials and Raman LAM of solution- and melt-crystallized HDPE fractions. As a result, a straightforward algorithm for the determination of the lamellar thickness distribution in PEs from $^{1}H\ T_{1\rho}$ relaxation data is obtained.

4.3 Experimental

4.3.1 Materials and sample preparations

Preparation of samples, used in this investigation is described in the Chapter 2. Information about molecular structure and thermal histories of materials, used in this investigation was summarized in Table 2.1

4.3.2 DSC

The average lamellar thickness was evaluated based on DSC melting peaks using the Gibbs-Thomson relation:

$$T_m = T_m^0\left(1 - \frac{2\sigma_{ec}}{\Delta H_u L}\right)$$

Melting thermograms were recorded with a DSC-8 (TA Instruments). The following parameters were used: heat of fusion $\Delta H_u = 2.8*10^9$ erg/cm^3, infinite-crystal thickness melting point $T_m^0 =$ 418.7 K, and surface energy $\sigma_{ec} = 92.0$ erg/cm^2 .[17-18]

The applicability of the Gibbs-Thomson relation between melting temperature and lamellar thickness for polyethylene and ethylene co-polymers is controversial.[6-7,10,18] According to extensive studies by Bassett et al.,[18] the lamellar thickness in HDPEs can be reliably correlated with the melting temperature measured by DSC. In contrast, Alamo et al.[6,10] argue that while in branched co-polymers the position of the maximum in endothermic peak represents a meaningful melting temperature, strong re-crystallization effects in

HDPE may result in a significant change in the lamellar thickness during the DSC experiment. Thus, the measured value of T_m would not correspond to the original crystallite thickness. While the exact shape of the lamellar thickness distribution cannot be precisely determined from the shape of melting peaks, in this work, we assume that the melting temperature determined by DSC may be applied for the evaluation of the average lamellar thickness in LLDPEs and HDPEs.

Since the melting peaks in LLDPEs are rather broad, we defined the maximum in the melting peaks recorded at 10 K/min as the melting temperature T_m.[6] In case of bimodal melting curves, the higher-temperature maximum was used. Error bars are used to take into account the width of the melting peaks. In order to compensate for overheating effects observed in HDPEs, melting temperatures for these systems were determined by extrapolation of heating rate dependencies of T_m to zero heating rate.

4.3.3 TEM

TEM investigation was performed by Dr. R. Bayer and Prof. S. Gido.(UMASS, PSE).

All samples were prepared for transmission electron microscopy (TEM) following the methods described by Brown and Butler.[19] Using a Leica Ultracut UCT microtome, equipped with a Leica EM FCS cryogenic sample chamber, the samples were first microtomed at -150°C with a fresh glass knife to produce a smooth surface for staining. The samples were then stained in RuO_4 vapor for 2

hours and then allowed to degas overnight in a fume hood. Thin sections approximately 500 Å thick were then microtomed using a Diatome diamond knife at room temperature. TEM was performed using a JEOL 100 CX TEM operated at 100 kV accelerating voltage. Micrographs were collected for a range of magnifications depending on lamellar size and density.

To determine the lamellar thickness distribution, several prints of each sample were made at significant enlargements. A grid of lines approximately 2 cm apart was drawn on each print so that each cell of the grid covered approximately 0.1 micron^2. Using calipers, lamellar thickness was measured for each lamella within each square in the grid. The area of the lamella measured was marked so that no lamella within a single square of the grid was counted twice. Measurements were made for all lamellae in each square of the grid of a given print.

Two methods were used to calibrate the magnification of the lamellar size measurements. First, prints of a replica calibration grid having 2160 lines/mm were made at the same enlargement as those used for measurement purposes. From these prints, the magnification of the photographic enlargement was calculated. Second, microspheres of polystyrene with a mean diameter of 91 nm and known size distribution were placed on the samples via dilute aqueous solution. Measurements of these spheres, visible in the prints of the lamellar morphology, were then used to provide a second, independent measurement of the magnification. The two methods gave magnifications

which were within 10% of one another. The calibration by the microspheres was chosen as representative of the true magnification.

4.3.4 Raman LAM

Raman data were provided by Prof. R.Alamo (Florida State University) Low frequency Raman spectra were obtained at ambient temperature in a SPEX 1403 double monochromator spectrometer. The excitation source was provided by an argon ion laser (λ =514.5 nm) operating with an effective power at the sample of ~ 100 mW. The procedures for converting the raw data into an ordered chain length distribution have been previously described.[3-5] The value of Young's modulus in the chain direction used in the analysis was $2.9 * 10^{12}$ dyn/cm^2.

Thickness distributions derived from Raman and SAXS analysis of HDPE-NBS1484[4] showed the best agreement if the chain tilt with respect to the lamellar normal was assumed to be small ($< 20°$). In this work, we also used this assumption in the comparison of the Raman and NMR results on HDPE-NBS1484 and HDPE-S.

4.3.5 NMR

^1H $T_{1\rho}$ relaxation was measured on a Bruker MSL 300 spectrometer, at a ^{13}C frequency of 75.5 MHz and a ^1H frequency of 300.1 MHz. The simple pulse sequence of the ^1H spin-lock MAS experiment with ^{13}C detection is shown in Fig. 4.1a. The spin-lock field strength was 71 ± 5 kHz. As demonstrated in Fig. 4.2, signals of the all-trans crystalline and partly gauche amorphous chains are resolved in the ^{13}C MAS spectrum, so that relaxation rates in these domains can

be determined independently. The height rather than the area of the all-trans peak is measured, since broad interfacial components contribute significantly to the peak area, but not much to its height. Therefore, the relaxation rate of the crystallite core is reflected better by the peak height than by the area.

^1H $T_{1\rho}$ selection with spin diffusion and $T_{1\rho}$ measurement. The pulse sequence presented at Fig. 4.1b allows us to assess the extent to which spin diffusion between amorphous and crystalline regions affects the $T_{1\rho}$ relaxation times. It can also be used to evaluate the distance between thick and thin crystallites. Magnetization in fast-relaxing domains with short ^1H $T_{1\rho}$ (amorphous domains and thin crystallites) relaxes during the filter spin lock time t_f, so only thick crystallites, where ^1H $T_{1\rho}$ relaxation is relatively slow, remain magnetized. The resulting spatially inhomogeneous magnetization is partially equilibrated by ^1H spin-diffusion during the mixing time t_m. By varying t_m it is possible to restore magnetization within a certain distance from the thicker crystallites. For instance, t_m = 100 ms corresponds to the equilibration of magnetization on the length scale of 10 nm. After this filtering and equilibration, a ^1H $T_{1\rho}$ relaxation curve is measured by varying the second spin-lock time t. If the $T_{1\rho}$ relaxation behavior were affected by spin diffusion, the t-dependence should change with the distribution of magnetization around the crystallites produced by spin diffusion during t_m. If the spin diffusion explanation holds, after equilibration over the relevant morphological regions (e.g. the interface and one amorphous layer) the relaxation curve without selection should be recovered.

If the distance between fast and slow-relaxing crystalline domains is less than 10 nm, the normalized relaxation curve *(I/I_{max} vs. t)* recorded after t_m = 100 ms will be identical to the relaxation curve recorded in the absence of $T_{1\rho}$ selection.

4.4 Results and Discussion

In this section it will be shown that $T_{1\rho}$ relaxation is sensitive to PE structure. It will be explained that $T_{1\rho}$ depends on the crystallite thickness via chain flip motions. The crystallite thickness distributions in selected samples will be measured by TEM. $T_{1\rho}$-distributions will be extracted from the relaxation curves, and from these data the crystalline-thickness dependence of $T_{1\rho}$ will be determined empirically. Comparison with Raman LAM and DSC will be used to further confirm the validity of the approach.

4.4.1. Sensitivity of $T_{1\rho}$ relaxation to PE structure

^{1}H $T_{1\rho}$ relaxation in the crystalline domains of polyethylenes is strongly affected by sample composition and thermal history. Figure 4.2(a) shows striking differences both in terms of the average relaxation time and the nonexponentiality, even for the same material with different thermal histories, and between samples of similar crystallinity but different branch distribution. Fast and almost mono-exponential relaxation in PE-M film contrasts with slower and less exponential relaxation in PE-ZN film of similar crystallinity, and even

slower and more non-exponential relaxation in bulk isothermally crystallized PE-ZN (PE-ZN b.i.).

Similar differences in relaxation behavior are observed among HDPEs, see Fig. 4.2(b). While isothermally crystallized HDPE-Mi shows very slow relaxation with a time constant of at least 200 ms, HDPE-S exhibits relaxation on a 60-ms time scale. In HDPE-NBS1484, the relaxation is strongly non-exponential, with a fast initial decay and a major slow component.

4.4.2. Mechanism of crystallite-thickness dependence of $T_{1\rho}$

The differences in $T_{1\rho}$ relaxation rates and curve shapes are ultimately due to differences in crystallite thicknesses and their distributions, according to the following mechanism: As demonstrated in reference,[11] the crystallite $^{1}H\ T_{1\rho}$ relaxation in polyethylene is driven by 180° chain flips in the crystallites. It has been shown by dielectric relaxation[20] that the rate $k = 1/2\tau_c$ of these flips depends strongly on the lamellar thickness. For instance, the dielectric loss maximum at 70°C shifts from $3*10^3$ /s at a thickness of 10 nm to 10^5/s at 5 nm. This dependence of the flip rate on the crystallite thickness results in the strong thickness dependence of the flip-motion-driven relaxation rate $k_\rho = 1/T_{1\rho}$. Thus, the $T_{1\rho}$ relaxation times and their distribution can be directly linked to the crystallite thickness distribution. It creates an opportunity to determine the lamellar thickness distribution in LLDPEs from $^{1}H\ T_{1\rho}$ relaxation data.

4.4.3. Crystallite thickness distributions from TEM

To confirm and calibrate the dependence of $T_{1\rho}$ on the crystallite thickness L, an independent determination of the crystallite thicknesses is required. The crystallite thickness distribution was characterized in PE-ZN b.i., PE-ZN film, and PE-M film by TEM after vapor-phase ruthenium oxide staining of the amorphous domains in LLDPEs as described above.[19] Figure 4.3a shows micrographs of two of the samples. The number-averaged lamellar thickness distribution P(L) was determined from TEM micrographs by counting the frequency of different lamellar thicknesses within the field of observation. The resulting distributions are plotted in Fig. 4. The data show significant polydispersity in the lamellar thicknesses (Fig. 4.3a, 4.4). The broadest distribution of lamellar thicknesses was observed for isothermally crystallized PE-ZN b.i. and the narrowest for the PE-M film.

4.4.4. Fitting procedures to determine $p(T_{1\rho})$.

To determine the relation between the crystallite-thickness distributions from TEM and the $T_{1\rho}$ relaxation, the $T_{1\rho}$ distribution $p(T_{1\rho})$ has to be extracted from the relaxation curve $I(t)$, to which it is related by a simple superposition formula

$$I(t)=\int_{T_{1\rho}\min}^{\infty} p(T_{1\rho})\, e^{-t/T_{1\rho}}\, d(T_{1\rho}) \qquad (4.1)$$

Note that the lower limit of the integral is not zero, but the minimum $T_{1\rho}$ relaxation time, which for 180° flips in PE is ~ 1 ms. Extraction of $p(T_{1\rho})$ from $I(t)$ requires a Laplace transformation or equivalent procedure. Since long (>50 ms) periods of spin-lock irradiation can damage the NMR equipment, $I(t)$ is often not measured to complete relaxation, which prevents the application of various Laplace-transformation procedures. We avoided numerical instabilities and overinterpretation of the data by using simple two- or three-parameter fit functions for $I(t)$ or $p(T_{??})$. It is found that not all of these functions provide perfect fits to $I(t)$; this provides valuable indications of the true shape of the distribution function $p(T_{1\rho})$. Two types of fit functions were used: A Gaussian distribution for $p(T_{1\rho})$, and a stretched exponential for $I(t)$.

The Gaussian distribution of relaxation times, with a position parameter and a width parameter, was used to calculate fit curves to $I(t)$ according to Eq.(1) and the least-squares fit to the experimental $I(t)$ was determined:

$$I_N(t) \leftarrow \frac{1}{\sigma\sqrt{2\pi}} \int_0^\infty \exp\left(-\frac{t}{\tau}\right) \exp\left(-\left(\frac{\tau-\tau_o}{\sqrt{2\sigma}}\right)^2\right) d\tau \qquad (4.2)$$

The stretched exponential or Kohlrausch-Williams-Watts (KWW) function[21]

$$I_N(t) \leftarrow e^{-\left(\frac{t}{t_{WW}}\right)^{\beta_{WW}}} \qquad (4.3)$$

is widely used for the characterization of nonexponential relaxation processes.[21] It is also a two-parameter function. The β-parameter, $1 > \beta > 0$, characterizes the deviation from single-exponential behavior. The time parameter τ_{ww} is related to the average relaxation time by $T_{1\rho\,avg} = (\tau_{ww}/\beta)\Gamma(1/\beta)$, where Γ denotes the Γ-function. The corresponding distribution of relaxation times $p_{KWW}(T_{1\rho})$ is given by the following series expansion[21]

$$p_{kww}(T_{1\rho}) = -\frac{\tau_{ww}}{\pi T_{1\rho}^{\,2}} \sum_{k=0}^{\infty} \frac{(-1)^k}{k!} (\sin \pi\beta_{ww} k + 1) \left(\frac{T_{1\rho}}{\tau_{ww}} \right)^{\beta_{ww} k + 1} \qquad (4.4)$$

Larger values of β correspond to narrower distributions of relaxation times; for $\beta = 1$, the relaxation curve is a single exponential and the distribution function a single peak at τ_{ww}, $p_{KWW}(T_{1\rho}) = \delta(T_{1\rho} - \tau_{ww})$

In Figure 4.5, the quality of the Gaussian and KWW fits is compared for the most non-exponential I(t) function found experimentally, that of PE-ZN b.i. It is found that the Williams-Watts function provides a significantly better fit to the experimental data than does the Gaussian distribution. The corresponding distributions $p(T_{1\rho})$ are shown at the right. Note that the upturn of $p_{KWW}(T_{1\rho})$ at small $T_{1\rho}$ is not unphysical. It is the result of a "bunching up" of intensity due to the minimum of the $T_{1\rho}(L)$ curve (see below); near that minimum, a wide range

of L values produce nearly the same $T_{??}$ value. Without it, the fast initial decay of the experimental *I(t)* curve is not reproduced correctly.

Gaussian and KWW distributions $p(T_{1\rho})$ for the three samples are shown in Fig 4.4b,c. The results are consistent in terms of distribution widths and positions. For instance, both fitting procedures yield the broadest distribution of relaxation times for PE-ZN b.i. and the narrowest for PE-M film.

In Fig. 4.4, the $p(T_{1\rho})$ are also compared with the *p(L)* distributions from TEM. Both the averages and the widths of the $p(T_{1\rho})$ and *p(L)* curves match qualitatively.

4.4.5 Empirical $T_{1\rho}(L)$ curve

The qualitative agreement between ^1H $T_{1\rho}$ and lamellar thickness distributions, Fig. 4.4 a-c, confirms that there is a simple correlation between $T_{1\rho}$ and L. We determined an empirical calibration curve $T_{1\rho}(L)$ by plotting the mean value of $T_{1\rho}$ determined from the Williams-Watts fit of the experimental $T_{1\rho}$ decay curve, against the mean lamellar thickness (L_{avg}), determined by TEM. In a previous study of a poly(ethylene-vinylacetate) copolymer (PE/VA), we found that a lamellar thickness of 4.9 nm corresponds to a relaxation time of 1.5 ms; this point was also added to the calibration curve. The final calibration curve is taken to be a smooth curve guided by the experimental points,

$$T_{1\rho}(L) = 5.4 - 2.7\,L + 0.4\,L^2 \qquad (4.5)$$

as presented in Fig. 4.6. The curve cannot be linear in L, since $T_{1\rho}$ must exhibit a minimum of ~ 1 ms. As required, Eq. (5) produces a minimum value of 0.84 ms. It occurs when the jump rate is equal to the Larmor frequency of the spin lock field B_1, i.e. when $k = \gamma B_1$, where γ is the magnetogyric ratio. At both higher and lower jump rates, the relaxation is slower.

At long $T_{1\rho}$ values, e.g. for HDPE-NBS1484, it might seem surprising that values of up 200 ms can be derived from measurements with a maximum spin lock time of only 30 ms. Note that the error bars on *I(t)* are so small that it is possible to measure $T_{1\rho}$ values of up to 200 ms reliably if *I(t)* is a single-exponential. What is unknown is whether even longer relaxation times and corresponding larger domain sizes are present.

4.4.6 *V(L)* from TEM and NMR

Using the simple relation between $T_{1\rho}$ and L of Eq.(5), the distributions $p(T_{1\rho})$ can be converted into volume fractions *V(L)* of crystallites with thickness L. The volume fraction is the relevant quantity, since the NMR signal is proportional to the mass or volume of the crystallites. ased on the "differential conservation of the integral"

$$V(L)\, dL = p(T_{1\rho})\, dT_{1\rho}$$

the conversion is calculated as

$$V(L) = p(T_{1\rho}(L))\frac{d(T_{1\rho}(L))}{dL} \qquad (4.6)$$

To compare with the TEM data, these also have to be converted into volume fractions. The thicker the crystallites, the larger their contribution in terms of the volume fraction. Thus, we have

$$V(L) = c\,L\,p_{TEM}(L) \qquad (4.7)$$

where c is a normalization factor with units of an area. This simple relation assumes that the lateral width of lamellar segments counted in the micrographs is independent of the crystallite thickness.

Figure 4.7 compares the resulting NMR- and TEM-derived distributions $V(L)$ for the three LLDPE materials. The agreement of the average-thickness values is expected since these were inputs into the empirical $T_{1\rho}(L)$ curve, but the good match of the widths is an independent confirmation of the validity of the approach.

Figure 4.8 shows the $T_{1\rho}$ relaxation curves and derived $V(L)$ distributions for the four HDPEs. For sample HDPE-NBS1484, Fig. 4.8(c), a bimodal distribution gives a slightly better fit of the data than does the stretched-exponential relaxation function. Such a bimodal distribution is also suggested by DSC, where a major, relatively sharp high-temperature melting peak and a smaller (~ 8%), low-T_m shoulder are observed. In addition, a previous SAXS

analysis of this sample[4] produced a bimodal distribution similar to the one in Fig. 4.8(c).

It might be surprising that a relatively broad distribution is obtained for the solution-crystallized fraction HDPE-S, Fig. 4.8(d). While it is partially reassuring that a Raman study of this material also showed a distribution width of ~ 2 nm,[5] this still less than the NMR-derived distribution. Potentially, tight loops hinder the flips of some of the chain stems and thus lead to a wider distribution of $T_{1\rho}$ relaxation times that is not related to a crystallite-thickness distribution.

Due to the relatively long relaxation times and resulting incomplete relaxation within 30 ms, the uncertainties in the *V(L)* distributions derived from $T_{1\rho}$ NMR for the HDPE samples are larger than for the distributions of the LLDPEs in Fig. 4.7. In particular, the width of the distributions at larger L values may be estimated incorrectly; usually, it will tend to be underestimated since a non-exponential slow-down of the relaxation at longer times cannot be anticipated from the short-time data.

4.4.7 Summary of calculation procedure

The procedure for calibrating the dependence of the ^1H $T_{1\rho}$ relaxation time on the crystallite thickness included five major steps:

(a) ^1H $T_{1\rho}$ relaxation curves *I(t)* of the crystallite cores were measured by solid-state NMR under MAS.

b) The distribution of relaxation times $p(T_{1\rho})$ was determined by a stretched-exponential fit to the experimental $I(t)$ data, followed by Laplace transformation. (Eq. 1a-1c).

c) Distributions of lamellar thicknesses $V(L)$ were independently determined by TEM for samples also characterized by NMR.

d) A calibration curve $T_{1\rho}(L)$ was calculated based on the resulting dependence of the average $T_{1\rho}$ on the average lamellar thickness.

e) The volume-averaged lamellar thickness distribution $V(L)$ was calculated from $p(T_{1\rho}(L))$.

It is important to note that in future applications of the technique, only the three relatively simple steps a), b), and e) are required, since the $T_{1\rho}(L)$ curve can be taken from this work.

4.4.8 Comparison of lamellar thicknesses from DSC, Raman LAM, TEM, and NMR

Figure 4.9 shows DSC traces of several of the materials studied. Figure 4.10 compares the average crystallite thicknesses determined from NMR $T_{1\rho}$ relaxation with those obtained from TEM, Raman LAM, and DSC as discussed in the Experimental section. For the DSC data, the error bars reflect the width of the melting range. The agreement for the wide variety of samples is very satisfactory.

4.4.9 Relaxation by chain flips vs. spin diffusion

In order to understand the advantages and limitations of the $T_{1\rho}$ -based crystallite-thickness distribution measurement in polyethylenes, it is desirable to determine the physical origin of processes causing the morphology-relaxation rate relationship. As mentioned above, crystallite-thickness dependent molecular motions in the crystallites[11] that drive ^{1}H $T_{1\rho}$ relaxation can fully account for the observed behavior. However, an alternative explanation of morphology-relaxation rate dependence, in terms of ^{1}H spin diffusion, was proposed by Packer et al.[12-14] According to this view, the $T_{1\rho}$ relaxation rate in semi-crystalline polymers is controlled by ^{1}H spin-diffusion, which leads to exchange of magnetization between crystalline lamellae and surrounding amorphous domains. Since the spin diffusion is not faster than the shortest $T_{1\rho}$ relaxation time in the system, non-exponential $T_{1\rho}$ relaxation curves would result even for a uniform crystallite thickness. According to the model of refs.[12-14] the intrinsic relaxation rate is identical for all crystalline domains, but for thicker crystallites equilibration by spin diffusion takes a longer time, resulting in a longer effective relaxation time. Contributions from the crystalline-amorphous interface and defects in the crystalline phase could also be invoked as reasons for non-exponential relaxation in the crystalline phase. [22-23]

It is reassuring to recognize that according to all theories proposed, thinner crystallites result in faster $T_{1\rho}$ relaxation. Only the interpretation of the details of the nonexponential function $I(t)$ will be different.

We estimate that spin diffusion effects become important only after ~ 30 ms, as shown in ref.[11] The effective spin diffusin time is $t_{sd} = (t_m - T_{1\rho a})/2$,[15] where wc have taken into account the scaling of the dipolar couplings to –1/2 by the spin locking field; $T_{1\rho a}$ is the (intrinsic) relaxation time in the amorphous regions. For thick crystallites, spin-diffusing magnetization is slow to traverse a significant fraction of the crystallites within $t_{sd} < 12$ ms, the value corresponding to $t_m < 30$ *ms*. For thin crystallites, the $T_{1\rho}$ relaxation times in the crystalline and the amorphous regions are quite similar, so that a gradient of magnetization that can drive spin diffusion is built up only after long spin-lock times, when the relaxation has already proceeded significantly. In addition, since we measure the peak height, we are detecting predominantly the signal from the core of the crystallites, which is least affected by spin diffusion. Direct experimental proof for the insignificance of spin diffusion effects is given in the next section.

4.4.10 $T_{1\rho}$ selection experiments with spin diffusion and $T_{1\rho}$ measurement

To prove that spin diffusion is unimportant for the $T_{1\rho}$ data shown, we introduced the experiment sketched in Fig. 4.1(b). It consists of a ^1H $T_{1\rho}$ filter, spin diffusion during t_m, followed by a $T_{1\rho}$ measurement. The experimental results for PE-ZN b.i. and PE-M film with a filter time of $t_f = 10$ ms are presented at Fig. 4.11.

First of all, after a short t_m, i.e. immediately after depletion of the magnetization in the non-crystalline regions by the $T_{1\rho}$ filter, spin diffusion during the spin lock into the depleted noncrystalline regions would quickly decrease the magnetization in the crystallites. This should lead to a faster initial decay than without selection. The experiment, however, shows a much slower initial decay after the filtering.

Further, it can be seen that on the time scale of 20 ms, the effect of proton spin-diffusion is insignificant. The time scale of the $T_{1\rho}$ experiment is 1/2 30 ms = 15 ms. Thus, spin-diffusion cannot have a considerable effect on the shape of the relaxation curve. Moreover, even after t_m = *100* ms, spin-diffusion does not change the relaxation behavior in bulk isothermally crystallized PE-ZN, and does not lead to full equilibration in PE-M film, see Fig. 4.11.

More specifically, the spin diffusion during t_m changes the distribution of magnetization in the interfacial and amorphous regions. At short mixing times, i.e. immediately after the $T_{1\rho}$ filter, the magnetization is confined to the cores of the crystallites, while after mixing times of 20 and 100 ms it has diffused into the interfacial and amorphous domains. The change in the magnetization distribution will lead to a change in the spin diffusion behavior during the spin lock after t_m. The mixing-time independence of the shape of the $T_{1\rho}$ relaxation curve of PE-ZN b.i. after the $T_{1\rho}$ filter shows that spin diffusion effects are insignificant, i.e. the $T_{1\rho}$ relaxation is independent of the spin diffusion to the amorphous or interfacial layers.

The data presented in Fig. 4.11 also show that within 100 ms, the spin-diffusing magnetization of the selected slow-relaxing thick crystallites does not reach the fast-relaxing thin crystallites. This means that the distance between thick and thin crystalline domains exceeds 10 nm in PE-ZN b.i. In contrast, in PE-M film the faster-relaxing, thinner crystallites are near the selected thick ones. Thus, this experiment can provide interesting information on the proximity of crystallites of different thicknesses.

In summary, the experimental data for the double $T_{1\rho}$ experiment with spin diffusion show that the nonexponentiality in $^{1}H\ T_{1\rho}$ relaxation is not caused significantly by the crystalline-amorphous interface, by spin-diffusion between crystalline and neighboring amorphous domains, or contributions of crystalline defects. This confirms that the major reason for the morphology-relaxation rate correlation in LLDPEs and HDPEs is the thickness dependence of the chain-flip rate in the crystallites. In addition, spin diffusion at the longest spin-lock times would not distort the determination of the thickness distribution significantly, since the thickness dependence of the spin diffusion and $T_{1\rho}$ relaxation effects is similar.

4.4.11 Perspective

$^{1}H\ T_{1\rho}$ measurements are easy to perform with good signal-to-noise ratios, and reproducibility is rarely an issue. Based on the $T_{1\rho}$ decay times of the experimental $I(t)$ curves and the $T_{1\rho}(L)$ calibration curve of Fig. 4.6, a crude determination of the average crystallite thickness is possible without involved

calculations. The strong dependence of $T_{1\rho}$ on L provides excellent thickness resolution: For instance, $T_{1\rho}$ = 17 ms corresponds to L = 10 nm, and $T_{1\rho}$ = 50 ms to L = 15 nm. Information on the width of the distribution is directly obtained from the curvature of *log(I(t))*, i.e. the degree of nonexponentiality of *I(t)*. The procedures for detailed calculations of the *p(L)* distribution are simple and quite straightforward. In the future, more complex algorithms such as least-squares fits with logarithmically spaced positive coefficients and a penalty against ruggedness can also be implemented.[24-25] The ^{1}H $T_{1\rho}$ NMR experiment is non-destructive; the sample can also be used in other experiments.

Based on our results and literature data,[11] we conclude that the method is suitable for a broad range of ethylene copolymers. A limiting criterion may the absence of specific interactions, such as hydrogen bonding between different chains, so the rate of molecular motion in the crystallites depends predominantly on the lamellar thickness. A new $T_{1\rho}(L)$ calibration may have to be performed only if the comonomers have strong interactions. Otherwise, the calibration curve presented in Fig. 4.6 may be used for various LLDPEs and HDPEs.

For a detailed determination of crystallite thickness distributions, it is best to combine the NMR method presented here with electron microscopy or Raman LAM. The main advantage of the NMR technique is the reliable volume-average of the thickness distribution even for broad distributions.

4.5 Conclusions

A simple yet effective solid-state NMR technique allowing for the determination of the lamellar thickness distribution in polyethylenes from $^{1}H\ T_{1\rho}$ relaxation data has been developed and tested on a series of samples of metallocene and Ziegler-Natta LLDPEs with different thermal histories, as well as several HDPEs. The dependence of the $T_{1\rho}$ relaxation time on the lamellar thickness in LLDPEs is caused by the strong crystallite-thickness dependence of the rate of 180° chain flips in the crystallites that drive the $^{1}H\ T_{1\rho}$ relaxation in LLDPEs. The distributions of $T_{1\rho}$ relaxation times $p(T_{1\rho})$ determined by stretched exponential fitting of the experimental $^{1}H\ T_{1\rho}$ relaxation curves show good qualitative agreement with the corresponding distributions of crystallite thicknesses in the LLDPE samples determined by TEM. From these data, an empirical calibration curve $T_{1\rho}(L)$ was determined. The validity of the technique has been confirmed by comparison with Raman and DSC data. Using a new $^{1}H\ T_{1\rho}$ selection technique, it was proven that the non-exponential character of $T_{1\rho}$ relaxation in LLDPEs is caused predominantly by variations in the lamellar thickness, while contributions from crystalline defects and spin-diffusion are insignificant on the time scale of the experiment. The method can be applied to commercial polyethylenes without chemical modification or isotope enrichment. It is complementary to electron microscopy and small-angle scattering by providing a particularly reliable average over the whole sample.

4.6 References

1. Alamo, R. G.; Mandelkern, L."The crystallization behavior of random copolymers of ethylene." *Thermochimica Acta*, **238**, 155 (1994).

2. Balta-Calleja, F.J.; Wonk, C.G. *X-ray Scattering of Synthetic Polymers*; Elsevier: NY, 1989.

3. Snyder, R. G.; Krause, S. J.; Scherer, J. R."Determination of the Distribution of Straight-Chain Segment Lengths in Crystalline Polyethylene from the Raman Lam-1 Band." *J. Polym. Sci.,Polym.Phys. Edn.*, **16**, 1593 (1978).

4. Snyder, R. G.; Scherer, J. R."Interpretation of Longitudial-Acoustical Mode Spectra of Polymers." *J.Polym.Sci.,Polym.Phys*, **18**, 421 (1980).

5. Stribeck, N.; Alamo, R. G.; Mandelkern, L.; Zachmann, H. G."Study of the Phase Structure of Linear polyethylene by Means of Small-Angle X-ray Scattering and Raman Spectroscopy." *Macromolecules*, **28**, 5029 (1995).

6. Alamo, R.; Mandelkern, L."Origins of Endothermic Peaks in Differential Scanning Calorimetry." *J.Polymer Science B:Polymer Phys.*, **24**, 2087 (1986).

7. Alamo, R. G.; Chan, E. K. M.; Mandelkern, L."Influence of Molecular Weight on the Melting and Phase Structure of Random Copolymers of Ethylene." *Macromolecules*, **25**, 6381 (1992)

8. Gibbs, J.W. *The Scientific Work of J. Williard Gibbs*; V.I. Longmans Green: NY, 1906.

9. Thomson, J.J. *Applications of Dynamics*; Macmillan: London, 1988.

10. Lu, L.; Alamo, R. G.; Mandelkern, L."Lamellar Thickness Distributions in Linear Polyethylene and Ethylene Copolymers." *Macromolecules*, **27**, 6571 (1994).

11. Hu, W. G.; Boeffel, C.; Schmidt-Rohr, K."Chain Flips in Polyethylene Crystallites and Fibers Characterized by Dipolar ^{13}C NMR." *Macromolecules*, **32**, 1611 (1999).

12. Colquhoun, I. J.; Packer, K. J."Nuclear Magnetic Resonance in Solid Ethylene/α-Olefin Copolymers: Relaxation, Spin-diffusion and Lamellar Widths." *British Polymer Journal*, **19**, 151 (1987).

13. Packer, K. J.; Pope, J. M.; Yeung, R. R.; Cudby, M. E. A."The Effect of Morphology on ^{1}H NMR Spectra and Relaxation in Semicrystalline Polyolefins." *J. Polym.Sci: Polym. Phys.*, **22**, 589 (1984).

14. Cudby, M. E. A.; Packer, K. J.; Hendra, P. J."Proton n.m.r. spin-lattice relaxation in the rotating frame and the thickness of the crystalline lamellae in some polyethylenes." *Polymer Communications*, **25**, 303 (1984).

15. Cheung, T. T. P.; Gerstein, B. C."^{1}H nuclear magnetic resonance studies of domain structures in polymers." *J.Appl.Phys.*, **52**, 5517 (1981).

16. Gelfer, M. Y.; Winter, H. H."Effect of branch distribution on rheology of LLDPE during early stages of crystallization." *Macromolecules*, **32**, 8974 (1999).

17. Mandelkern, L.; Alamo, R.G. In *Physical Properties of Polymers Handbook*, Mark, E.J., Ed. American Institute of Physics: Woodbury, NY, 1996 pp. 123-124.

18. Bassett, D. C.; Hodge, A. M."On the morphology of melt-crystallized polyethylene II. Lamellae and their crystallization conditions." *Proc.Roy.Soc.*, **A377**, 39 (1981).

19. Brown, G. M.; Butler, J. H."New method for the characterization of domain morphology of polymer blends using ruthenium tetroxide staining and low voltage scanning electron microscopy (LVSEM)." *Polymer*, **38**, 3937 (1997).

20. Ashcraft, C. R.; Boyd, R. H."A Dielectric Study of Molecular Relaxation in Oxidized and Chlorinated Polyethylenes." *Journal of Polymer Science: Polymer Physics*, **14**, 2153 (1976).

21. Lindsey, C. P.; Patterson, G. D."Detailed Comparison of the Williams-Watts and Cole-Davidson functions." *J.Chem.Phys*, **73**, 3348 (1980).

22. Axelson, D. E."Crystalline Order in Polyethylene: A ^{13}C NMR CP/MAS Solid-State T_1 study." *J. Polym. Sci: Polym.Phys.*, **20**, 1427 (1982).

23. Axelson, D. E.; Mandelkern, L.; Popli, R.; Mathieu, P."Carbon-13 NMR of Polyethylenes: Correlation of the Crystalline Component T1 with Structure." *J. Polym.Sci: Polym. Phys*, **21**, 2139 (1983).

24. Whittall, K. P."Innvestigation of Analysis Techniques for Complicated NMR Relaxation Data." *J. Magnetic Resonance*, **95**, 221 (1991).

25. Whittall, K. P.; Mackay, A. L."Quantitative Interpretation of NMR Relaxation Data." *J. Magn.Reson.*, **84**, 134 (1989).

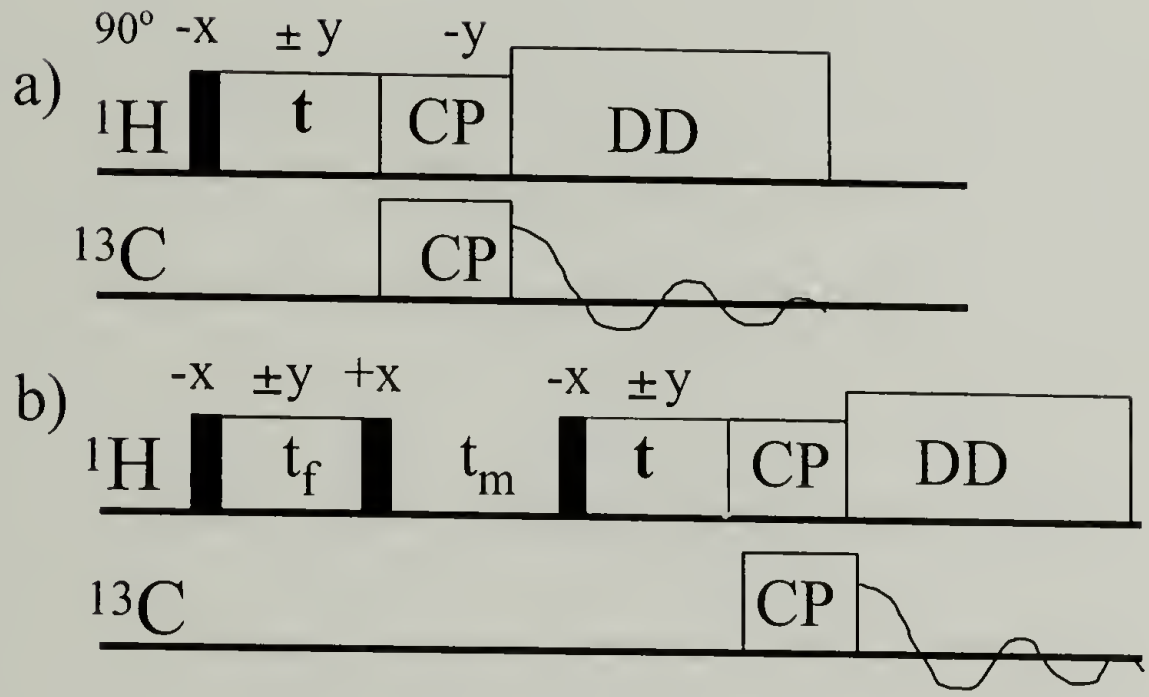

Figure 4.1. NMR pulse sequences used in this work.
(a) Standard ^{1}H $T_{1\rho}$ experiment
with ^{13}C detection. (b) Selection of long $T_{1\rho}$ components,
spin diffusion during t_m, and subsequent ^{1}H $T_{1\rho}$
measurement with ^{13}C detection.

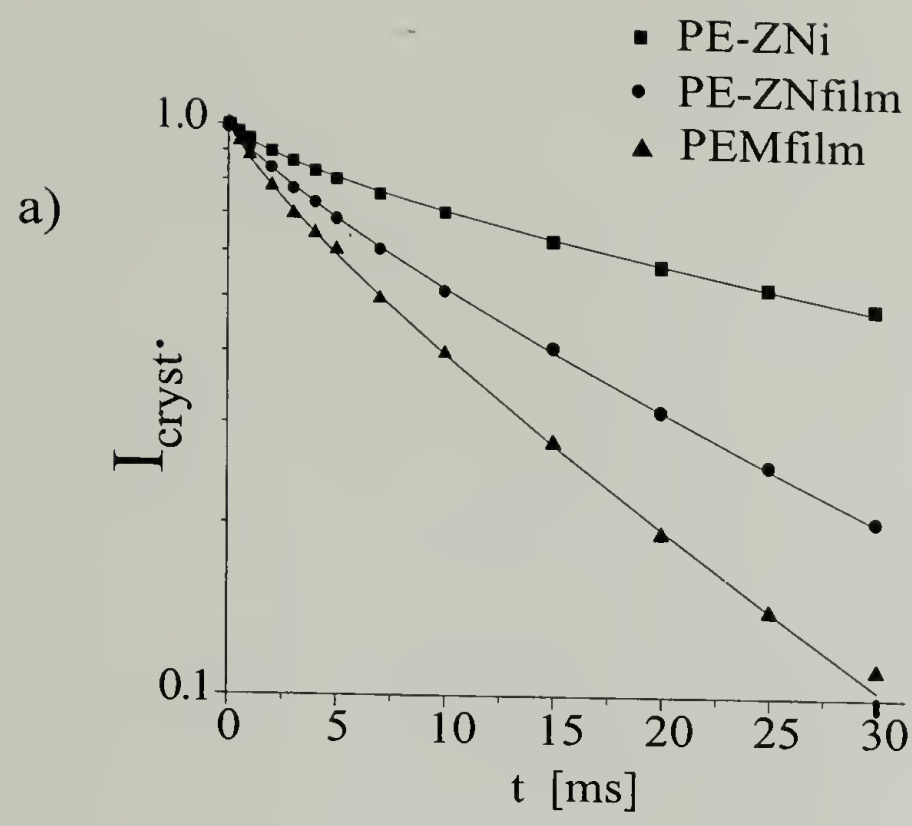

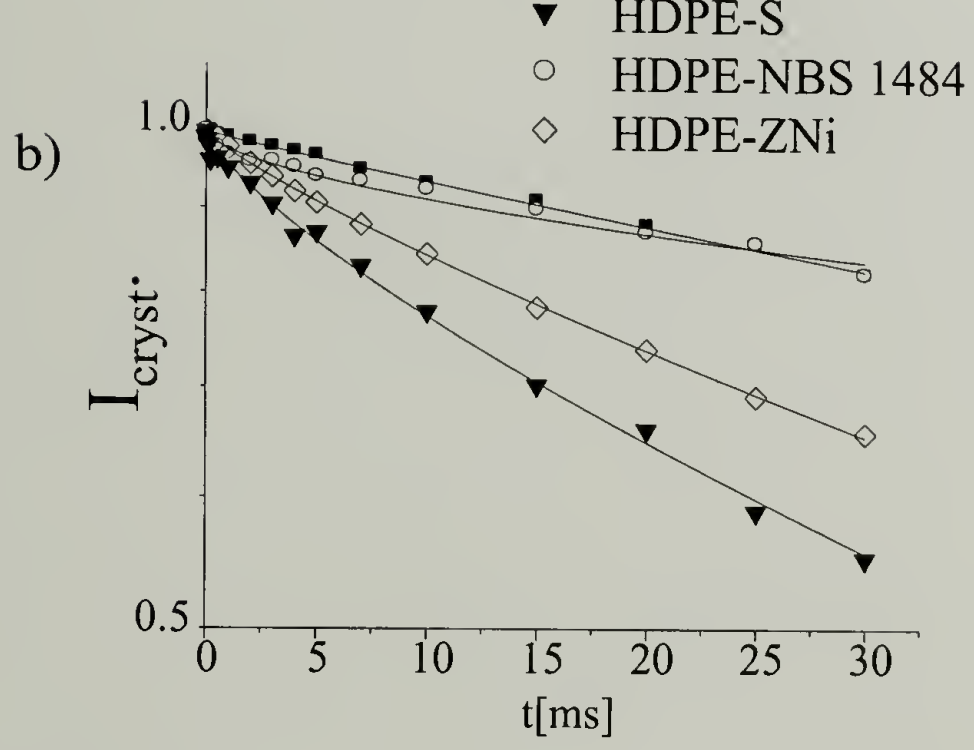

Figure 4.2. $T_{1\rho}$ relaxation curves I(t) obtained by plotting the peak height of the all-trans peak at 32.8 ppm as a function of the spin-lock time t. (a) I(t) for LLDPEs. The strong effect of thermal history observed for the PE-ZN material, isothermally crystallized (PE-ZN b.i.) and as a quenched film (PE-ZN film), is striking. (b) I(t) curves for four HDPE: HDPE-Mi ; HDPE-NBS1484 ; HDPE-S.

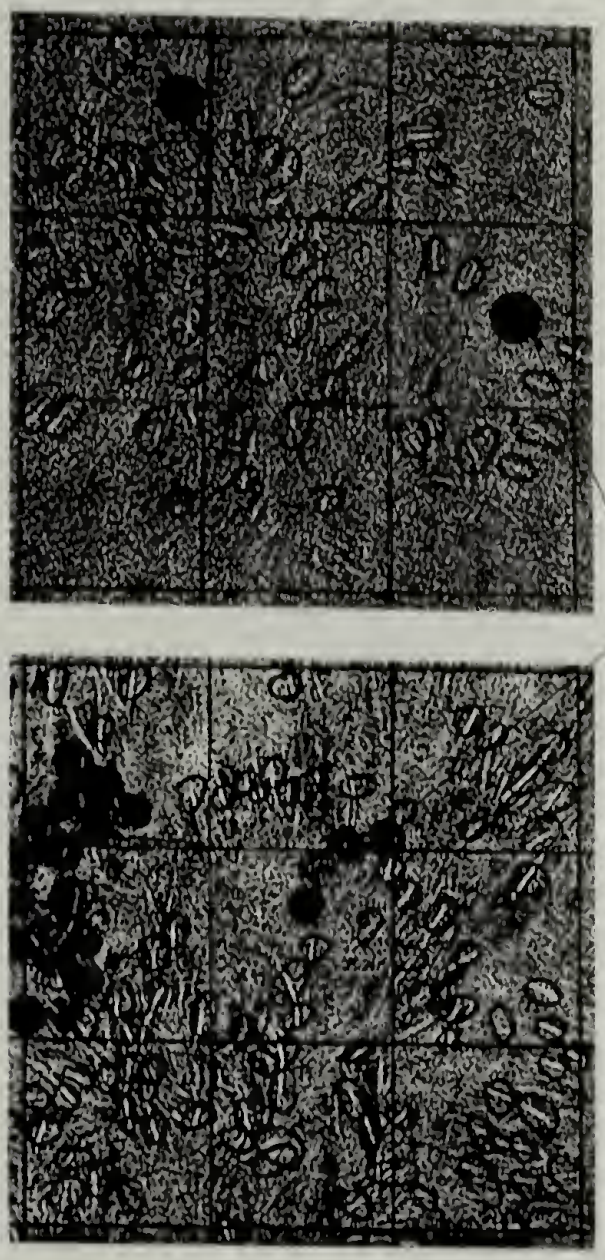

Figure 4.3 Micrographs (partial views) with circles indicating sampling of lamellae for thickness measurements.

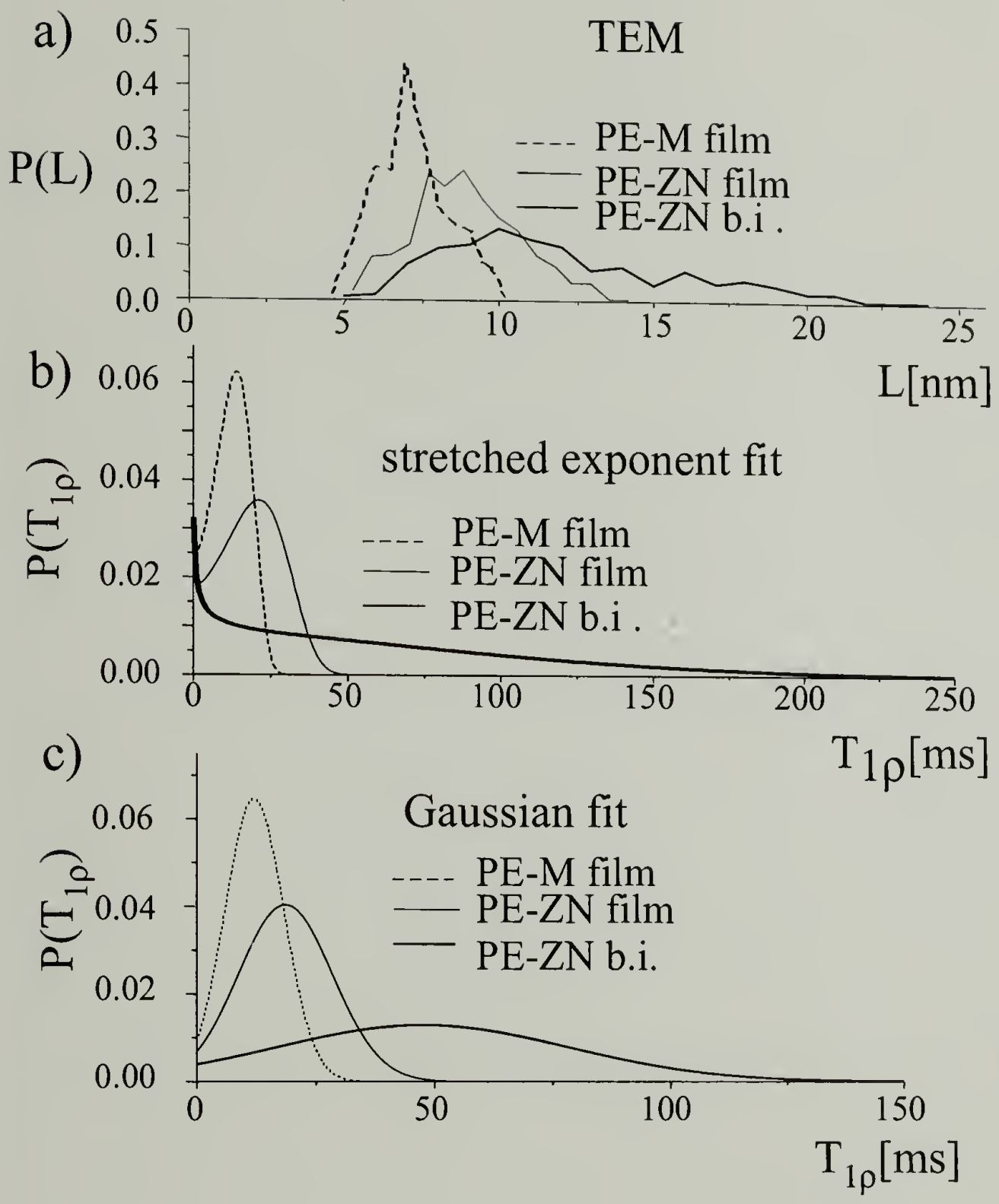

Figure 4.4 (a) Lamellar thickness distribution p (L) determined by TEM. (b) Distribution of relaxationtimes p ($T_{1\rho}$) determined by Williams-Watts fitting of ^1H $T_{1\rho}$ relaxation curves. (c) Distribution of relaxation times p ($T_{1\rho}$) determined by Gaussian fitting of ^1H $T_{1\rho}$ relaxation curves. The good qualitative agreement between p ($T_{1\rho}$) and p (L) indicates a simple $T_{1\rho}$ (L) correlation.

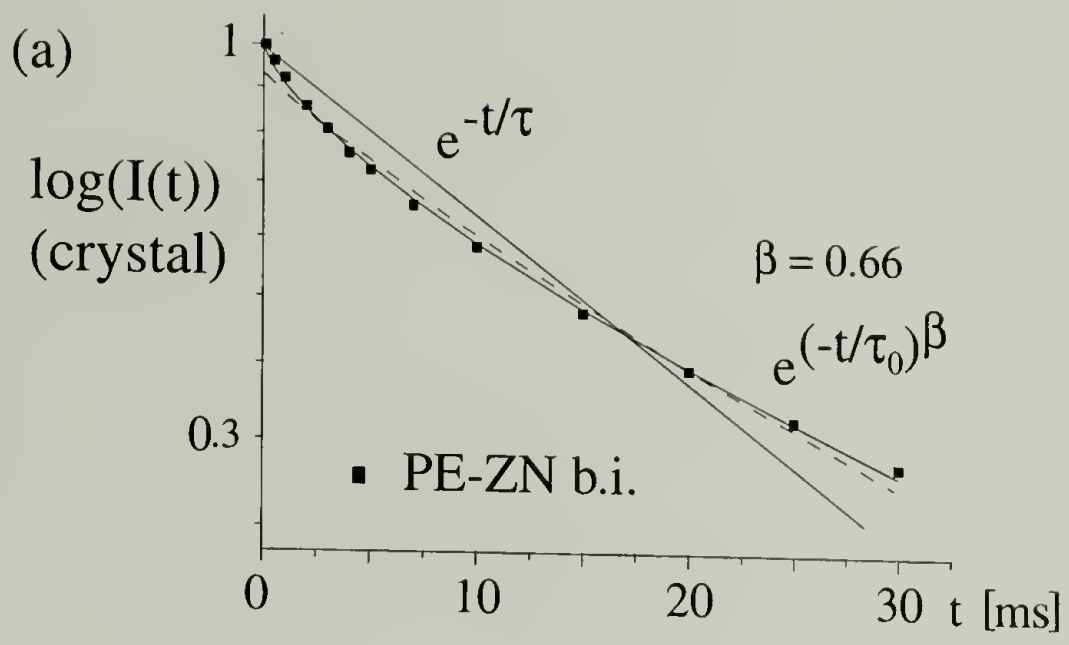

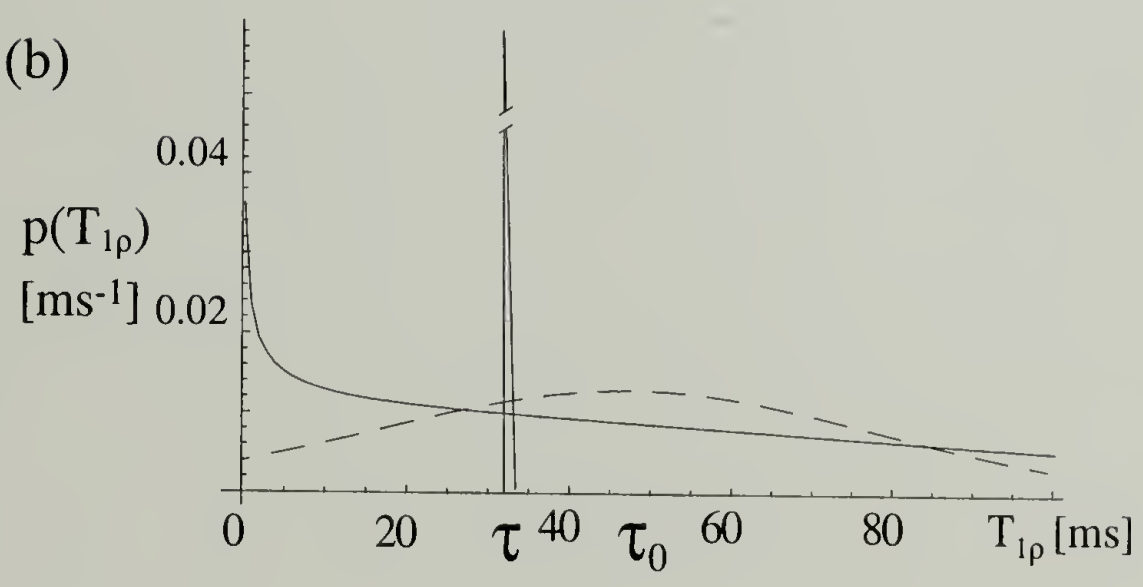

Figure 4.5. (a) $T_{1\rho}$ decay data (squares) for PE-ZN b.i., showing pronouncedly nonexponential behavior, with single-exponential fit (straight line), Gaussian distribution fit (dashed curve), and stretched-exponential fit (full curve). The stretched-exponential provides clearly the best fit. (b) Corresponding distributions of relaxation times for the Williams-Watts fit (solid line), the Gaussian distribution fit (dashed line), and the single-exponential fit (delta-function).

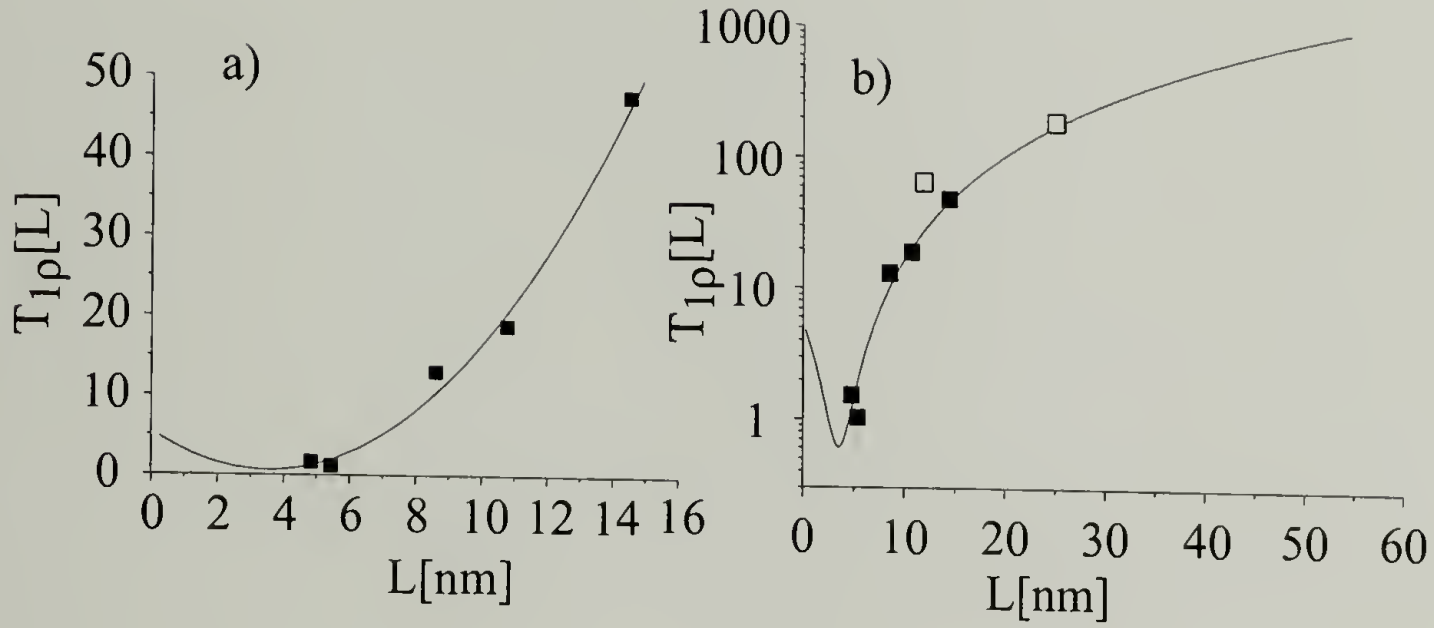

Figure 4.6. Empirical calibration curve for converting $T_{1\rho}$ times to crystallite thicknesses The points indicate average $T_{1\rho}$ and L values of the samples measured by both NMR and TEM. (a) Linear $T_{1\rho}$ scale. (b) Logarithmic $T_{1\rho}$ scale. Filled symbols : TEM data; open symbols: Raman data.

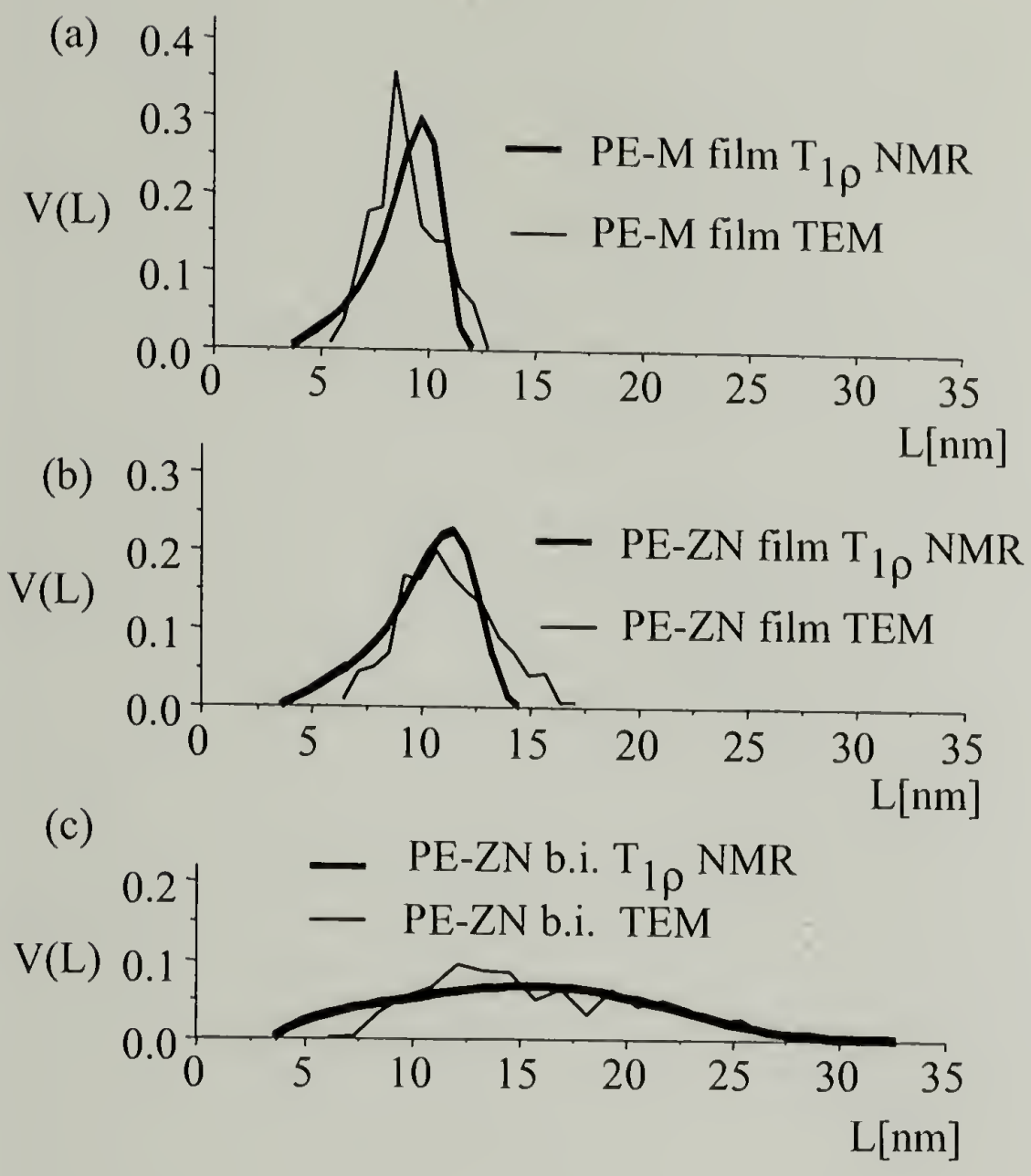

Figure 4.7. Comparison of thickness distributions V(L) of LLDPEs as determined by NMR and by TEM: (a) PE-M film; (b) PE-ZN film; (c) PE-ZN b.i. (bulk. isothermally crystallized).

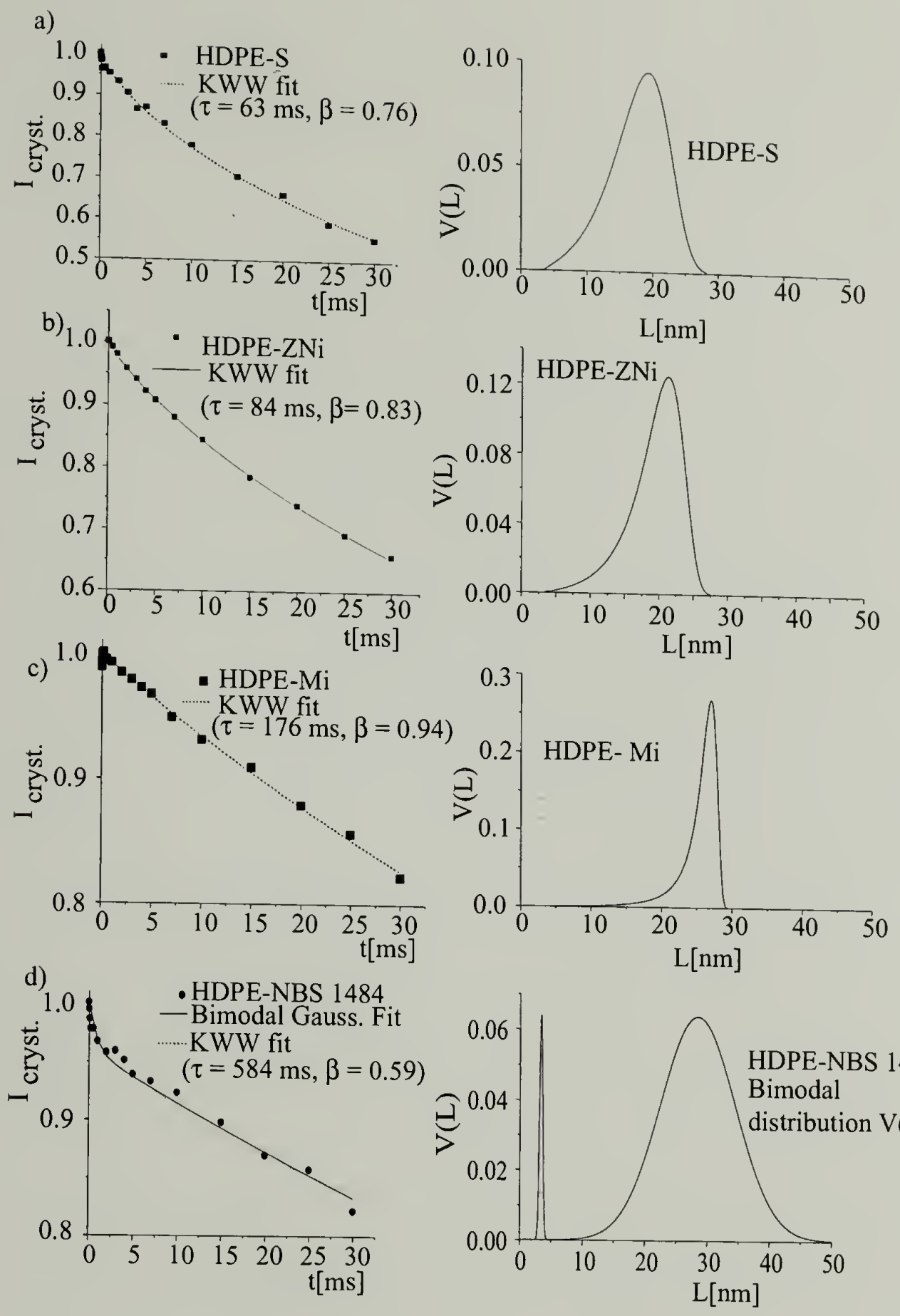

Figure 4.8. $T_{1\rho}$-relaxation curves I(t) and corresponding thickness distributions V(L): (a) solution crystallized HDPE-S. (b) isothermally melt-crystallized Ziegler-Natta HDPE ZNi
(c) Isothermally melt-crystallized metallocene HDPE-Mi;
(d) isothermally melt-crystallized HDPE-NBS1484; the bimodal distribution shown on the right with 4% of small crystallites gives better fit than the KWW function (stretched exponential).

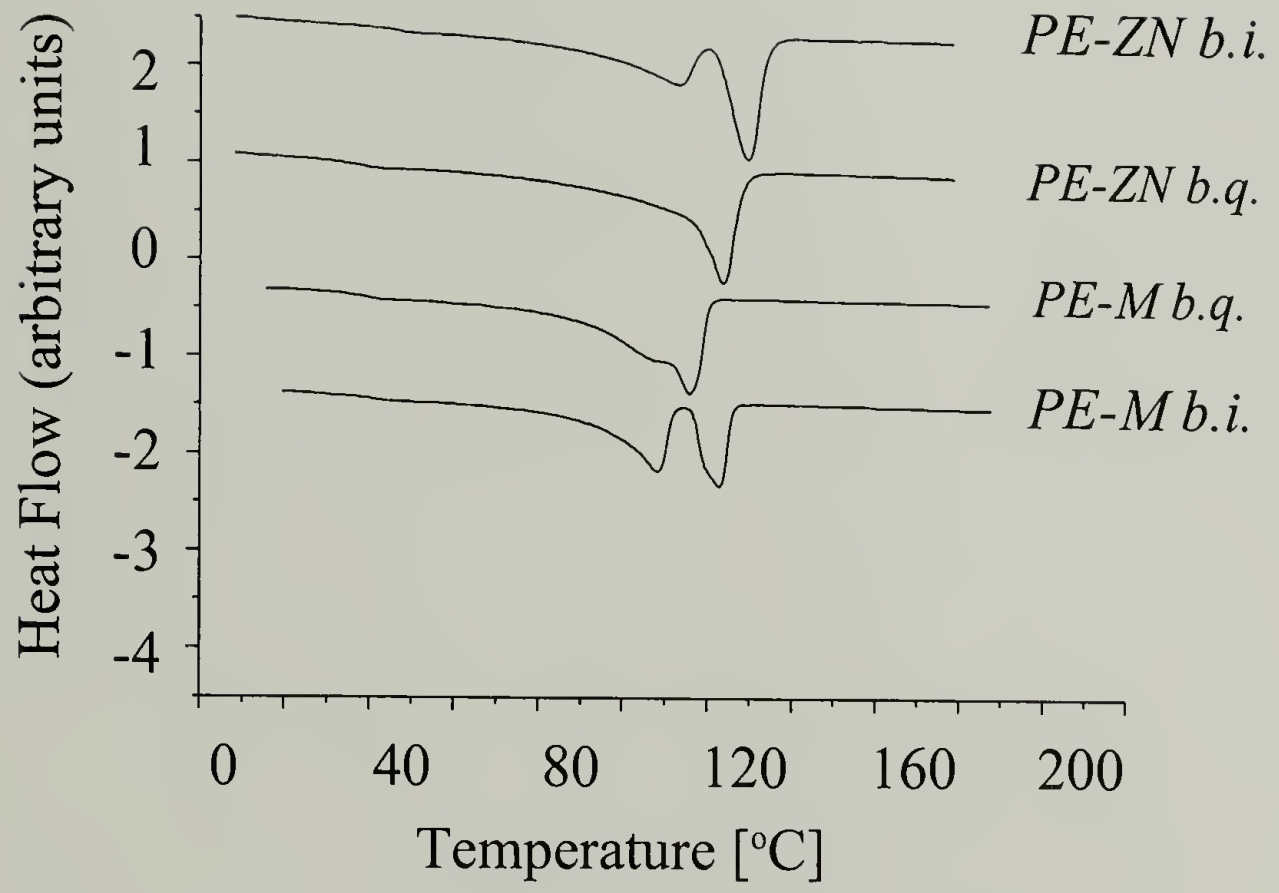

Figure 4.9. DSC melting curves for several LLDPE samples used in this study. The DSC lamellar thicknesses were estimated from the maxima in the melting curves, using the Gibbs-Thomson relation.

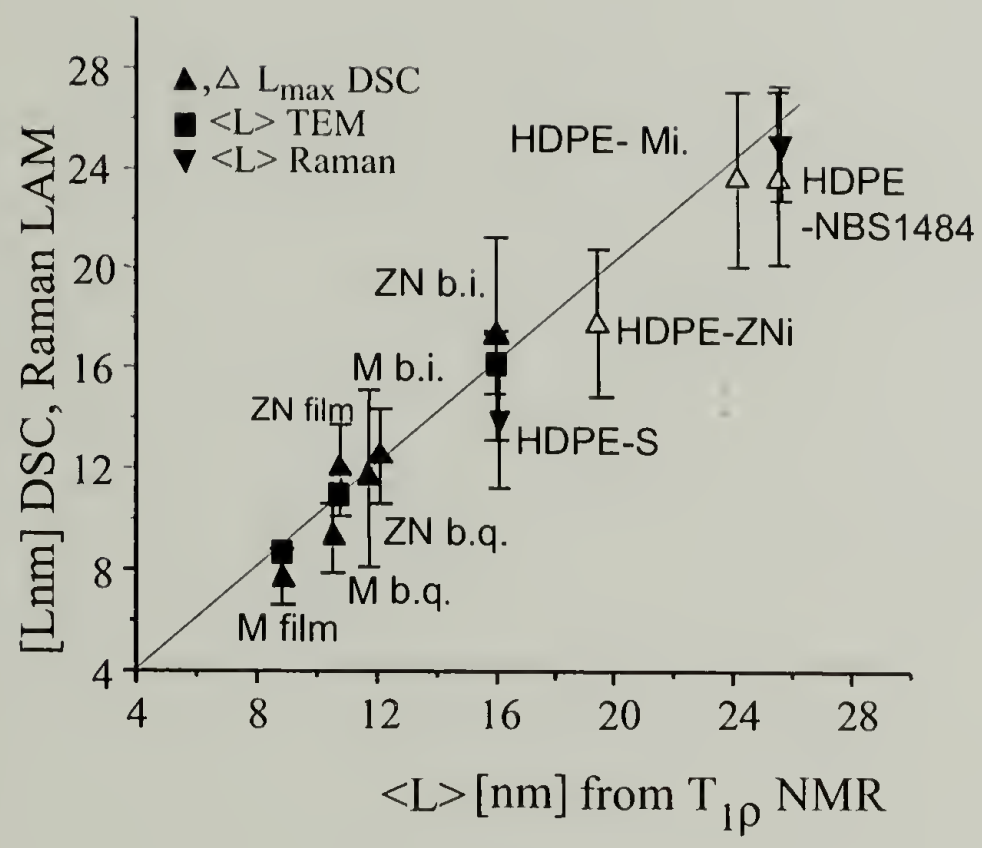

Figure 4.10. Comparison of lamellar thicknesses determined by NMR (x-axis) with those from DSC, Raman LAM, and TEM (vertical axis). Open symbols: HDPEs, for which the interpretation of the relationship between lamellar thickness and melting temperature is controversial.

a)

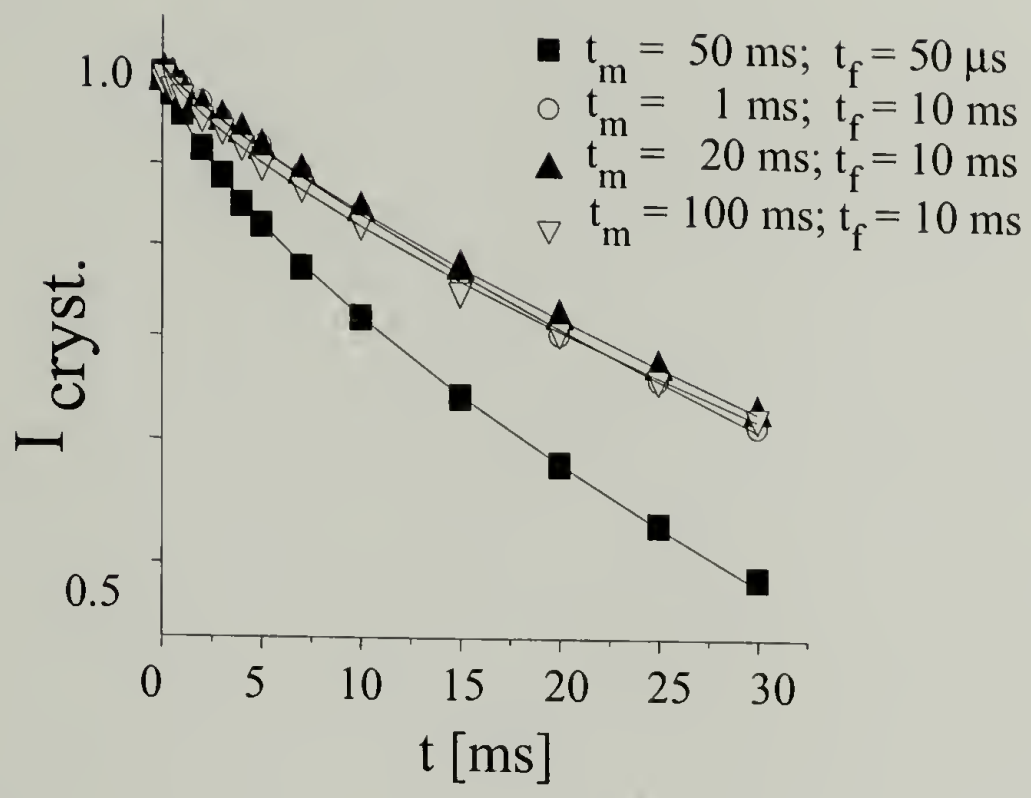

b)

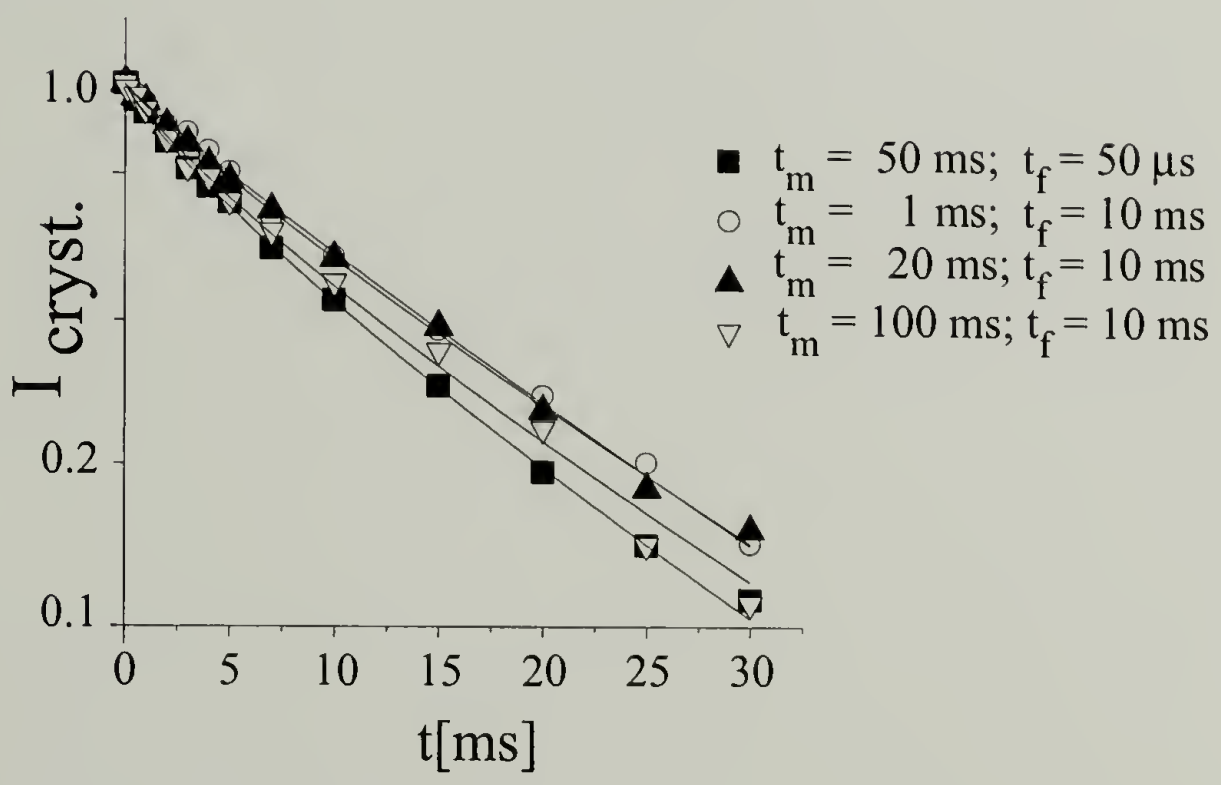

Figure 4.11. $T_{1\rho}$ selection, spin-diffusion during tm and $T_{1\rho}$ measurement for (a) PE-ZN b.i., (b) PE-M film. For each sample, the curve without selection is compared with curves after 30-ms spin lock selection and mixing times of 1 ms, 20 ms, and 100 ms. The invariance of the PE-ZN b.i. curves to mixing time shows that spin diffusion and the resulting magnetization distribution ution do no affect the decay under spin lock; this means that it is not significantly affected by spin diffusion.

CHAPTER 5

EFFECTS OF THE BRANCHING DISTRIBUTION ON LOCAL MORPHOLOGY AND MOLECULAR MOBILITY IN LLDPES AS CHARACTERIZED BY SOLID-STATE NMR

5.1 Abstract

For semi-crystalline ethylene-α-olefin co-polymers (LLDPEs) produced by the metallocene or Ziegler-Natta processes, the influence of the composition distribution and thermal history on the morphology and molecular mobility in the crystalline and amorphous domains was determined using solid-state NMR. While the investigated metallocene LLDPE (PE-M) contains fewer branched units (2.6 % mol C-6) and possesses narrower composition distribution than its Ziegler-Natta analog (PE-ZN; 3.8% mol C-6), the metallocene co-polymer has thinner crystalline and amorphous domains, a higher rate of chain diffusion between amorphous and crystalline regions, and lower molecular mobility in the amorphous regions than a conventional (Ziegler-Natta) LLDPE with similar thermal history. A morphological model relating the observed differences to the branching distributions in these LLDPEs was proposed. It was shown that in heterogeneous PE-ZN, the crystalline domains are predominantly formed by almost linear chains, forming thick lamellae, while the amorphous regions are enriched by highly branched molecules. The small amount of covalent bonds between the crystalline and amorphous domains results in high molecular mobility in the amorphous regions. In contrast, in homogeneously branched PE-

ZN crystalline and amorphous regions are formed by the segments, belonging to same molecules. The presence of branched units in all chains limits the lamellar thickness in PE-M. The numerous covalent links between crystalline and amorphous regions reduce the amorphous mobility in the metallocene co-polymer.

5.2 Introduction

It is known that in LLDPEs, differences in intramolecular branching distribution may result in drastically different morphologies, even in systems with similar overall branching.[1-3] Still, the molecular mechanism behind the relationship of the branching distribution with the morphology is not fully understood.

In this chapter, the effects of the composition distribution and thermal history on morphology and molecular mobility in the crystalline and amorphous domains of LLDPEs will be analyzed using solid-state NMR techniques. The molecular mobility in the crystalline and amorphous domains will be characterized by a combination of static ^{1}H, *CP MAS* and relaxation techniques. The lamellar thickness distributions in the investigated co-polymers will be determined by a novel solid-state NMR method, that we have developed.[4-5] The results obtained will be independently confirmed by *CP*, ^{1}H spin-diffusion and $^{13}C\ T_1$ relaxation measurements.

The solid-state NMR techniques used in this investigation allow for the reliable determination of morphologieal parameters and molccular characteristics of LLDPEs from thc expcrimcntal data without fitting of unrcsolvcd signals and application of assumed morphological models. All LLDPE samples uscd in this study were eharacterizcd by Tcmperaturc Raising Elution Fractionation (TREF), so their intermolecular branehing distributions arc known in grcat detail. Based on thc results obtained a morphological modcl cxplaining the effect of molecular structure on crystallite thiekncss and molceular mobility was proposed.

5.3 Baekground Information. Solid-state NMR teehniques

5.3.1 Crystallinity measurement

The degree of crystallinity was measurcd using single-pulsc ^{13}C *MAS* with proton dceoupling, by eomparing the integral intcnsities of pcaks at 32.8 ppm (the crystalline region) and 31.0 (the amorphous region) (Fig.1). The ^{13}C T_1 is far longer in the crystalline domains than in the amorphous domains of LLDPEs, on the order of hundreds of seeonds vs. seconds, respeetivcly. Thus, it is impossible to get a fully relaxed speetrum and to average enough seans for good signal-to noisc at the same timc. From another perspectivc, in a spcetrum reeorded with a shorter reeyelc delay, the noise level is low, and the amorphous signal is fully rclaxcd, but apparent intcnsities of crystallinc and amorphous signals do not reflect thc real degree of crystallinity. In a single-pulsc gatcd

decoupled spectrum, the signal from crystalline domain may be fully suppressed; however while the gated decoupling procedure does not cause significant change in the amorphous lineshape, the intensity of the amorphous signal decreases.

As shown by Hu and Schmidt-Rohr overlapping crystalline and amorphous signals in a fully relaxed ^{13}C single-pulse MAS spectrum may be resolved, based on the procedure whereby the amorphous lineshape is fitted by the lineshape of amorphous signal from the corresponding gated decoupled spectrum. The procedure is outlined below in three major steps:

1) Three spectra were recorded for each sample (Fig 1): a fully relaxed ^{13}C spectrum (recycle delay $t_0 = 5000s$) with a number of scans $NS_{sf} = 8$; a gated decoupled spectrum (recycle delay $t_0 = 5s$),with $NS_{gd} = 512$; a partially relaxed spectrum ($t_0 = 50s$) with $NS_{pr} = 128$.

The lineshape of the broad amorphous signal in the fully-relaxed single-pulse ^{13}C spectrum is obscured by noise (Fig. 5.1a), so it is difficult to use this spectrum for the fitting procedure. In the partially-relaxed single-pulse spectrum, the amorphous signal is fully relaxed, and the signal to-noise ratio is good, but the amorphous and the crystalline signals are not fully resolved. The ^{13}C single-pulse gated decoupled spectrum recorded with a recycle delay t_0 of 5s has insignificant contribution from the crystalline domain (Fig.1b), however, the intensity of the amorphous signal is reduced by the gated decoupling procedure,

thus the scaling factor needed for the fitting procedure may bc different from thc ratio of thc number of scans.

2) The correction factor $f = (NS_{gd}/NS_{pr}) / (I_{gd}/I_{pr})$ was determined by fitting the amorphous lineshape in the partially- relaxed single pulse spectrum by the gated decoupled spectrum.(Fig.5.1b). (Here I_{gd} and I_{pr} denote signal intensitics for gated decoupled and partially relaxed spectra respectively).

3) Using the corrected scaling factor $f \times (NS_{sp}/NS_{gd})$, the amorphous lineshape in the fully relaxed spectrum was fitted by the amorphous signal in the gated decoupled spectrum (Fig.5.1c) Thus amorphous and crystalline signals in the fully-relaxed spectrum were effectively resolved.

It should be noted that the described procedure did not require any specific assumption about the lineshape of the amorphous or crystalline signals.

5.3.2 Morphology and molecular mobility

Thc relative molecular mobility in the amorphous domains in LLDPEs was determined from the linewidth of the central part of static ^{1}H spectra. Narrowing of the ^{1}H signal corresponds to an increase in the molecular mobility in the given region by at least the same factor as the change in the lineshape.[7]

Due to the motional averaging of dipolar coupling, the *CP*-efficiency decreases with an increase in molecular mobility. This produces opportunity for the evaluation of the molecular mobility in the amorphous domains by

comparing relative intensities of crystalline and amorphous signals in ^{13}C direct polarization and *CP* spectra.

Other experiments which discriminate morphological domains based on the molecular mobility are *CP* T_1 filtering and gated decoupling techniques. The *CP* T_1 filter sequence (Fig 2a) allows selective observation of signal from rigid domains, where the ^{13}C T_1 is sufficiently longer than the filtering time t_f.

In polyethylene and ethylene co-polymers, the ^{13}C T_1 relaxation time increases with the increasing lamellar thickness.[8-9] The ^{13}C T_1 relaxation rate in polyethylene is controlled by chain diffusion, which equilibrates magnetization between crystalline and amorphous regions.[7-8] In turn, the rate of the 180° chain flip, which is the elementary step in chain diffusion process, greatly decreases with the increase in crystallite thickness[9,10] resulting in inverse correlation between lamellar thickness and ^{13}C T_1 relaxation rate in the crystalline domain. Therefore, in ethylene co-polymers longer ^{13}C T_1 relaxation times correspond to larger crystallite thicknesses and lower molecular mobility in the crystalline domains.[9]

The gated decoupling technique (Fig.2b) utilizes undecoupled evolution during t_f and short recycle delays (t_0 = 5s) to suppress signals from the rigid regions having long ^{13}C T_1 and strong dipolar couplings. Spectra recorded with a sufficiently long t_f contain only signals from the amorphous regions. The linewidths of the signals observed in gated decoupled spectra are indicative of

molecular mobility in the amorphous domain. An increase in molecular mobility results in a narrowing of the linewidth due to motional averaging.

Relative crystallite thicknesses were characterized by the ^{1}H spin-diffusion technique with ^{13}C detection under MAS (Fig.2c). In this experiment, the magnetization in the rigid crystalline domains was destroyed using a T_2 selection.[12,13] The spatially inhomogeneous longitudial magnetization that results is equilibrated by spin-diffusion during t_m. In the spin-diffusion experiment, magnetization is transferred to the crystalline regions from the amorphous domains; in unfiltered *CP* experiments magnetization of all morphological domains is observed simultaneously. Therefore a larger crystallite thickness corresponds to a larger difference in the intensity of crystalline signals measured in *CP* and spin-diffusion experiments if the spectra are scaled to equal heights of the amorphous peaks. ^{13}C detection allows enhanced resolution of signals from amorphous and crystalline regions.

5.3.3 $^{1}H\ T_{1\rho}$ technique for the determination of the lamellar thickness distribution

In this work we applied the novel solid-state NMR technique for the quantitative determination of volume-averaged crystallite thickness distributions in ethylene co-polymers from $^{1}H\ T_{1\rho}$ data as described in Chapter 4.[5-6] The method is based on the correlation between crystallite thicknesses and $^{1}H\ T_{1\rho}$ relaxation times in the crystalline domains of polyethylene and ethylene

copolymers, which is caused by the dependence on thickness of the 180° chain flip rate that drives $^{1}H\ T_{1\rho}$ relaxation in polyethylene.[10,11]

The $^{1}H\ T_{1\rho}$ relaxation times were determined under MAS using ^{13}C detection, so that crystalline and amorphous signals were suitably resolved. In order to confirm the method's validity, the lamellar thickness distributions measured by the novel solid-state NMR technique[5,6] were compared with results of *CP*, $^{13}C\ T_1$ relaxation, and spin-diffusion experiments.

5.4 Experimental

5.4.1. Materials

Compositions, thermal histories and branching distributions of the LLDPE samples studiedare described in chapter 2. Six LLDPE samples (Table2.1) were chosen specifically to find relationships between composition, thermal history and texture. Indeed, the composition distribution for PE-M is typical for metallocene LLDPEs, while the composition distribution of PE-ZN is representative of Ziegler-Natta systems.[14] Metallocene HDPE HDPE-M (also produced by Exxon) was tested for comparison purposes in order to elucidate the effect of branching on the morphology of LLDPEs.

5.4.2 DSC

DSC measurements were performed in *TA Instruments* DSC 2910 scanning calorimeter.

5.4.3 NMR

Solid state ^{13}C and ^{1}H *NMR* spectra were obtained with a Bruker MSL-300 spectrometer equipped with a MAS unit. A ^{13}C resonance frequency of 75.5 MHz and a ^{1}H frequency of 300 MHz were employed. In MAS experiments, 7-mm diameter rotors were used at a spinning speed of 4 kHz.

5.5 Experimental Results

Based on the greater content of branched units in PE-ZN compared to PE-M, one may expect lower crystallinity and smaller lamellar thickness in the Ziegler-Natta copolymer. However, our observations reveal a quite different picture.

5.5.1 Crystallinity and crystallite thickness distributions

The crystallinity in the studied samples was determined from ^{13}C *MAS* direct polarization spectra, using the fitting technique described above (Fig.5.1). The degree of crystallinity is quite similar in metallocene and conventional LLDPEs. Both in metallocene and conventional co-polymers the effect of thermal history on crystallinity is relatively small (Fig.5.3). The highest crystallinity was observed in isothermally crystallized samples, the lowest- in

blown films. The narrowing of crystalline signals observed in isothermally-crystallized samples (Fig 5. 4) can be related to the higher degree of order in the crystalline domains and also to the decrease in the content of crystalline-amorphous interface in these systems.

Lamellar thickness distributions determined by the $^{1}H\ T_{1\rho}$ technique are presented at Fig 5.5. Average lamellar thickness is consistently greater in Ziegler-Natta systems than in metallocene systems with similar thermal history. Crystallite thickness distributions in the bulk are broader in isothermally crystallized samples when compared to bulk-quenched samples. Indeed, the isothermal crystallization process results in the formation of thick lamellae, while thin lamellae form during the final quenching step, resulting in broad lamellar thickness distributions. The lowest average lamellar thicknesses and narrowest thickness distributions are observed in blown films. This can be attributed to more efficient quenching in thin films, as compared to bulk polymers.

Comparison of *CP* and spin-diffusion spectra (Fig.5.6) indicates that equilibration between crystalline and amorphous regions is faster in the metallocene systems than in the conventional analogs, confirming the smaller average lamellar thickness in PE-M.

$^{13}C\ T_1$ relaxation times are shorter (Table 5.1) and the content of thick, "core" crystallites with long T_1 is lower in PE-M than in PE-ZN co-polymers with analogous thermal history. (Fig.5.7). This indicates that the average

lamellar thickness is lower in metallocene co-polymers.[8,9] $^{13}C\ T_1$ relaxation rates are slower in isothermally crystallized polymers than in their quenched analogs, demonstrating a larger average crystallite thickness in isothermally crystallized systems. The fastest $^{13}C\ T_1$ relaxation was observed in blown films, indicating even thinner lamellae than in quenched bulk samples.

The absence of signals from the branched units in $CP\ T_1$ spectra even at the shortest t_f suggests that branched units are excluded from crystalline phase in all co-polymers studied. It should be noted that the content of "core crystalites" is far lower in LLDPEs than in the linear polyethylene. Indeed, in HDPE-Mi the crystalline signal intensity at t_f= 500 s is 75% of the signal intensity at t_f= 1s, whereas in isothermally crystallized PE-ZN, only 15% of the signal remains after 500 s, and in the quenched PE-M only 7%.

It can be seen that the lamellar thicknesses determined from $^1H\ T_{1\rho}$ relaxation data are in a good agreement with the results of *CP* - spin diffusion and $CP\ T_1$ experiments.

5.5.2 Molecular mobility in the amorphous domain

The central part of the static ^1H spectrum is significantly narrower in PE-ZN than in PE-M, which indicates higher mobility in the amorphous domains of the conventional LLDPEs (Fig.5.8). On the other hand, in both metallocene and conventional copolymers, the broadest ^1H signals are observed in films, and the spectra of isothermally crystallized sample are the narrowest. Therefore, the

highest molecular mobility in amorphous domains can be found in isothermally crystallized samples (Fig.5.8), while the amorphous phase in blown films is the least mobile.

Gated decoupled spectra (Fig.5.9) do not provide evidence of the inclusion of branches into the crystalline phase. Splittings of the signals of branched units corresponding to branches in the crystalline and amorphous domains were not observed. The linewidths for β and 2 - carbon ^{13}C signals in PE-M are greater than in their conventional analogs. This observation confirms that the amorphous regions are less mobile in metallocene co-polymers.

The amorphous signal in *CP* spectra of PE-M is more intense than in PE-ZN analogs with similar thermal history and crystallinity (Fig.5.3,5.10). The greater *CP* efficiency is indicative of lower molecular mobility in the amorphous domains of PE-M.

While the effect of thermal history on crystallinity in the samples studied was shown to be insignificant, the relative intensity of the amorphous signal in *CP* spectra is always lower in isothermally-crystallized samples than in quenched samples. In agreement with the results of static ^{1}H and gated decoupling experiments, this observation indicates higher molecular mobility in the amorphous domain of isothermally crystallized samples.

5.6 Discussions

The drastic differences, observed in the morphology and molecular mobility of metallocene and Ziegler-Natta LLDPEs is directly related to the difference in intramolecular branching distributions.

According to the TREF data,[14] (Fig.2.1) the branching distribution $P(x)$ in PE-ZN systems is bimodal, with relatively high fractions of both low-branched units (branching content $x < 0.5$ *% mol*) and highly branched chains (5% mol $< x <$ 12% mol). In contrast, the unimodal intermolecular branching distribution in PE-M can be described as a skewed Gaussian centered at $x_{avg} = 2.6$ % mol In metallocene co-polymer the contents of highly (x > 5% mol) and low-branched ($x < 1$ mol %) chains are low.

As a result, in PE-ZN the crystalline domains are predominantly composed of low-branched chains, forming relatively thick lamellae. At the same time, the amorphous domains in PE-ZN are enriched by highly branched co-polymer molecules, which contain only short linear segments and are predominantly excluded from the crystalline phase. Thus, the number of covalent bonds between amorphous and crystalline domains in PE-ZN is smaller, resulting in high mobility in the amorphous regions (Fig.5.11a).

In metallocene systems, sufficiently long linear segments of polymer chains form the crystalline domains, while branched segments of the same chains are confined to the amorphous region (Fig.5.11b). The presence of non-crystallizable branched segments in all chains yields limits to the lamellar

thickness in PE-M. Numerous covalent bonds between amorphous and crystalline domains of PE-M decrease the molecular mobility in the amorphous phase. Due to lower average crystallite thickness the crystalline mobility is higher in PE-M samples than in their PE-ZN analogs with similar thermal history. On the other hand, mobility in the amorphous domains is lower in the metallocene co-polymer PE-M than in its conventional analog PE-ZN (Fig.5.11).

Opposite trends in the thermal-history dependence of molecular mobility were observed for crystalline and amorphous domains. In both metallocene and Ziegler-Natta systems, the highest crystallite thickness can be observed in the isothermally-crystallized samples, which results in the lowest crystalline mobility in the isothermally crystallized materials.[3,6,7,9,10] On the other hand, the highest molecular mobility in the amorphous domains was observed in isothermally crystallized samples. Because the overall crystallinity is similar in quenched and isothermally crystallized bulk samples, thickening of crystalline domains also results in thickening of amorphous regions and reduction in the content of the crystalline-amorphous interface, as indicated by narrowing of the crystalline signal.(Fig.5.4) Thus the amorphous phase is less constrained in isothermally crystallized samples, resulting in higher molecular mobility in these materials. Combination of fast quenching and deformation results in a very constrained amorphous phase in blown films. Indeed, in spite of the lower

overall crystallinity, amorphous-phase molecular mobility is lower in films than in quenched and isothermally crystallized bulk samples.

The reason for the observed $^{13}C\ T_1$ reduction in LLDPEs as compared to HDPE is not fully understood. The decrease in T_1 may be caused by the intense chain-diffusion between the crystalline and amorphous regions in LLDPEs. However, branching should slow down this process, because branches longer than methyl can not enter the crystalline phase.[15-16] Also, it may be proposed that a dynamic equilibrium exists between the crystalline and amorphous regions of LLDPEs due to the fast motion of chains between branches, causing linear chain segments to move between crystalline and amorphous regions. Such a process can cause the equilibration of the magnetization between the amorphous and crystalline regions and a significant decrease in T_1.

5.7 Conclusions

The validity of a novel solid-state NMR technique for the determination of lamellar thickness distribution has been confirmed by comparison with independent NMR experiments.

A morphological model describing the relationship between branching distribution, crystallite thickness and molecular mobility in LLDPEs has been proposed based on the results of solid-state NMR investigation.

According to that model, in highly heterogeneous Ziegler-Natta co-polymers the crystalline domains are enriched in almost linear chains, while the amorphous domains are formed by highly branched molecules. In contrast, in homogeneous metallocene systems both crystalline and amorphous domains are formed by segments, belonging to the same chains. Consequently, in metallocene co-polymers the average thickness of crystalline and amorphous domains is lower, the rate of chain diffusion in the crystalline region is higher, and the molecular mobility in the amorphous domain is lower than in an even more branched Ziegler-Natta analog (Fig.5.11).

The influence of thermal history on the molecular mobility in the crystalline domain is predominantly determined by its effect on the lamellar thickness. In quenched samples the smaller lamellar thickness results in higher crystalline-phase mobility than in isothermally crystallized materials. On the other hand, the efficient quenching constrains the amorphous phase, so the amorphous-phase mobility in quenched samples is lower than in isothermally crystallized ones even if the crystalline mobility is higher.

The morphological structure of LLDPEs determines their mechanical properties.[17-18] Further developments of the catalyst technology will allow to reach an even higher degree of control over LLDPE compositions. Thus, the understanding of the composition-morphology relationship will become even more important for the manufacturing and formulation of polyethylene-based materials with desired properties.

5.8 References

1. Kuwabara, K.; Kaji, H.; Horii, F.; Bassett, D. C.; Olley, R. H."Solid -State ^{13}C NMR Analyses of the Crystalline-Noncrystalline Structure for Metallocene-Catalyzed Linear Low-Density Polyethylene." *Macromolecules*, **30**, 7516 (1997).

2. Kim, M. H.; Phillips, P. J."Nonisothermal Melting and Crystallization Studies of Homogeneous Ethylene/a-olefin Random Copolymers." *Journal Applied Polymer Science*, **70**, 1893 (1998).

3. Alamo, R. G.; Mandelkern, L."The crystallization behavior of random copolymers of ethylene." *Thermochimica Acta*, **238**, 155 (1994).

4. Gelfer, M.; Schmidt-Rohr, K."Investigation of Morphology and Molecular Mobility in Ethylene-Hexene Copolymers by Solid-State NMR." *Abstr. Paper.Am. Chem. Soc*, **217**, 266 (1999).

5. Gelfer, M.; Beyer, F.; Gido, S. P.; Alamo, R.; Schmidt-Rohr, K."Polyethylene Crystallite Thickness Distribution from 1H NMR Relaxation, Calibrated by Electron Microscopy and Raman LAM." *Submitted to Macromolecules*

6. Hu, W.-G.; Schmidt-Rohr, K."Characterization of ultradrawn polyethylene fibers by NMR: crystallinity, domain sizes and a highly mobile second amorphous phase." *Polymer*, **41**, 2979 (2000).

7. Schmidt-Rohr, K.; Spiess, H. W. *Multidimensional Solid-State NMR of Polymers*; Acad.Press: NY, 1994.

8. Axelson, D. E."Crystalline Order in Polyethylene: A ^{13}C NMR CP/MAS Solid-State T_1 study." *J. Polym. Sci: Polym.Phys.*, **20**, 1427 (1982).

9. Axelson, D. E.; Mandelkern, L.; Popli, R.; Mathieu, P."Carbon-13 NMR of Polyethylenes: Correlation of the Crystalline Component T1 with Structure." *J. Polym.Sci: Polym. Phys*, **21**, 2139 (1983).

10. Hu, W. G.; Boeffel, C.; Schmidt-Rohr, K."Chain Flips in Polyethylene Crystallites and Fibers Characterized by Dipolar ^{13}C NMR." *Macromolecules*, **32**, 1611 (1999).

11. Ashcraft, C. R.; Boyd, R. H."A Dielectric Study of Molecular Relaxation in Oxidized and Chlorinated Polyethylenes." *Journal of Polymer Science: Polymer Physics*, **14**, 2153 (1976).

12. Cheung, T. T. P.; Gerstein, B. C."^{1}H nuclear magnetic resonance studies of domain structures in polymers." *J.Appl.Phys.*, **52**, 5517 (1981).

13. Goldman, M.; Shen, L."Spin-Spin Relaxation in LaF_3." *Phys.Rev.*, **144**, 321 (1966).

14. Gelfer, M. Y.; Winter, H. H."Effect of branching distribution on rheology of LLDPE during early stages of crystallization." *Macromolecules*, **32**, 8974 (1999).

15. Perez, E.; Bello, A.; Perena, J. M.; Benavente, R.; Martinez, M. C.; Aguilar, C."Solid-state nuclear magnetic resonance study of linear-low density polyethylenes: 1. Ethylene-1-butene copolymers." *Polymer*, **30**, 1508 (1989).

16. Perez, E.; Vanderhart, D. L."Morphological Partitioning of Chain Ends and Methyl Branches in Melt-crystallized Polyethylene by ^{13}C-NMR." *J. Polym. Sci.: Part B: Polym.Phys.*, **25**, 1637 (1987).

17. Popli, R.; L.Mandelkern."Influence of Structural and Morphological Factors on the Mechanical Properties of the Polyethylenes." *J. Polymer Science B; Polymer Physics*, **25**, 441 (1987).

18. Kim, Y.-M.; Park, J.-K."Effect of Short Chain Branching on the Blown Film Properties of Linear Low Density Polyethylene." *Journal of Applied Polymer Science*, **61**, 2315 (1996).

Table 5.1. $^{13}C\ T_1$ relaxation times for LLDPEs and HDPE. $^{13}C\ T_1$ values calculated from the slope of the final ($t > 50$ s) part of the $I(t)$ curve

Polymer	$^{13}C\ T_1$
PE-ZN b.i.	714 s ± 35 s
PE-ZN b.q.	333 s ± 17 s
PE-ZN film	277 s ± 14 s
PE-M b.i.	476 s ± 24 s
PE-M b.q.	261 s ± 18 s
PE-M film	200 s ± 10 s
HDPE-Mi.	2500 s ± 50 s

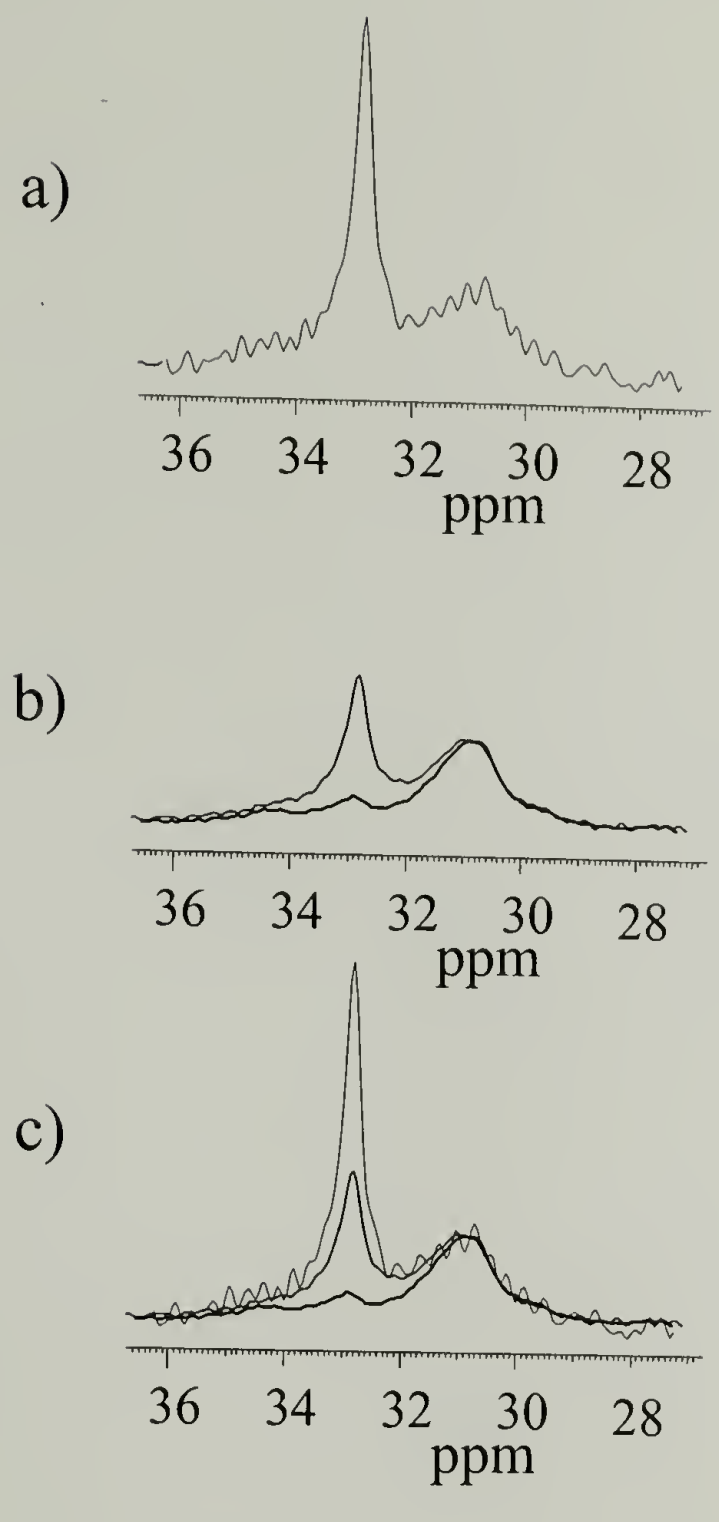

Figure 5.1 NMR technique for crystallinity measurement. LLDPE-PE-ZNq. is used as an example. a) The lineshape of the amorphous signal in the fully relaxed spectrum is obscured by noise
b) The lineshape of the amorphous signal in the partially relaxed spectrum (the recycle delay t_o = 50s) is fitted by the gated decoupled spectrum (t_o = 5s, t_f = 20 ms).
The correction factor f is determined $f = \left(\left(\frac{I_{gd}}{I_{pr}}\right)/\left(\frac{NS_{gd}}{NS_{pr}}\right)\right)$

Here I_{gd} and I_{pr} are the intensities of gated decoupled and partially relaxed spectra; NS_{gd} and NS_{pr} are corresponding numbers of scans
c) Noisy amorphous signal in fully relaxed spectrum
(t_o = 5000 s) is fitted by the lineshape of the gated decoupled spectrum, using the correction factor f determined in a). The intensity of gated decoupled spectrum is scaled $f\,(NS_{sp}/NS_{gd})$ times.

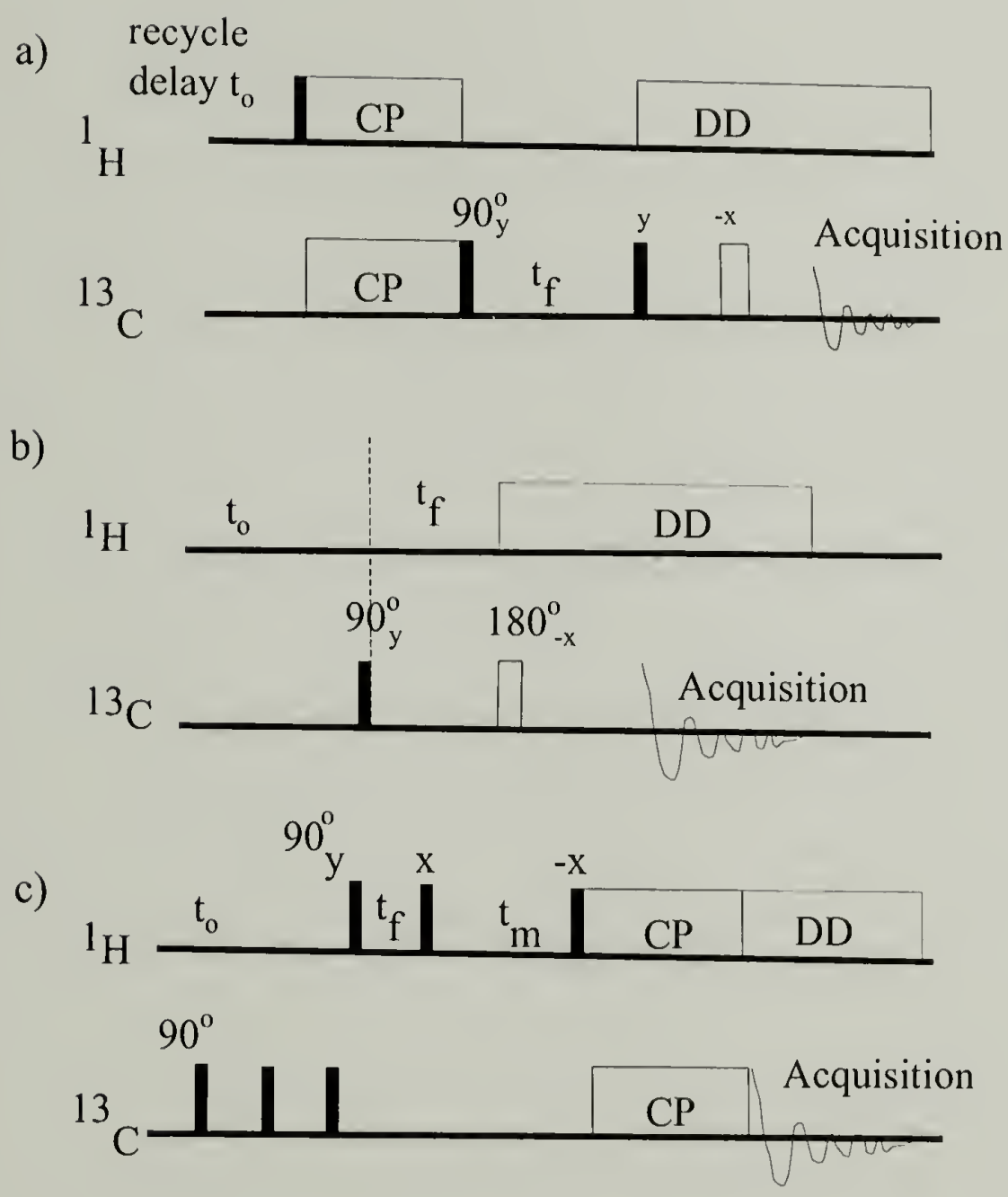

Figure 5.2 Pulse programs used in this study. 90° pulses are filled black; clear: 180° pulses, dipolar decoupling (DD), cross-polarization CP; (a) MAS CP T_1 filtering; t_f: ^{13}C T_1 filter ; (b) MAS gated decoupling; t_f: dipolar dephasing (T_2 filter); (c) ^1H spin-diffusion with ^{13}C detection; t_f: dipolar dephasing; t_m: mixing time.

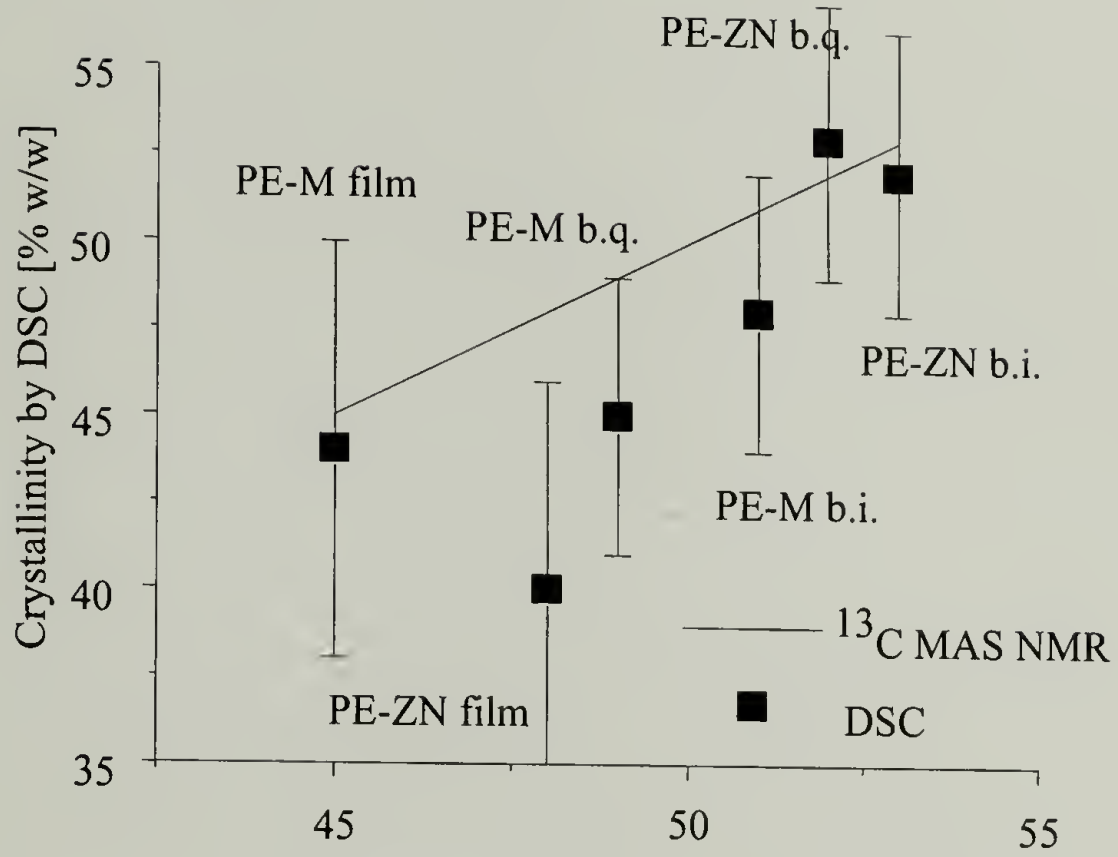

Figure 5.3 Effect of branching distribution and thermal history on crystallinity. Error margin in NMR crystallinity 3% [w/w]

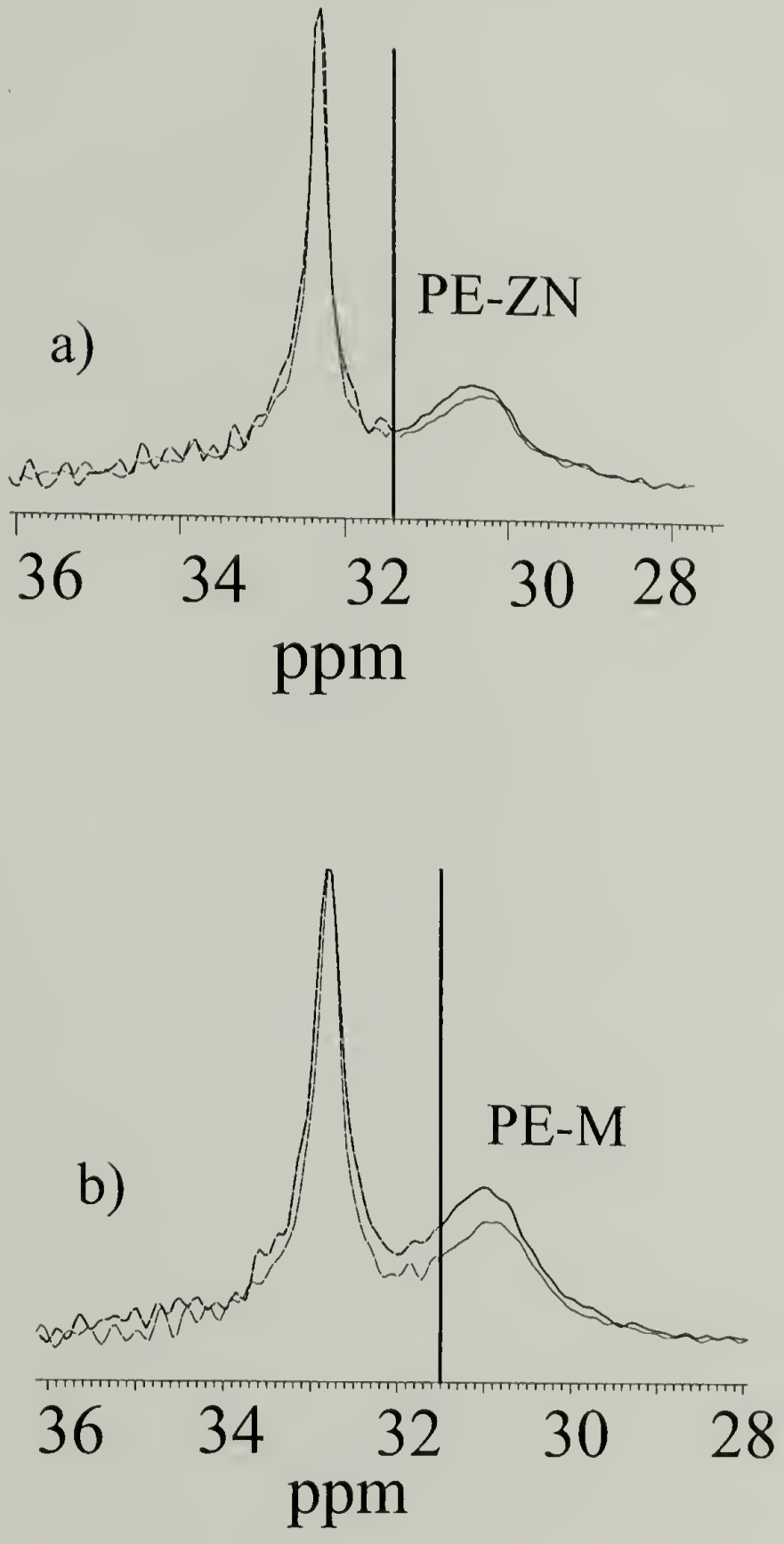

Figure 5.4 Effect of thermal history on the line shape of crystalline and amorphous signals.Heavy line: quenched sample; Thin line: isothermally crystallized sample. Crystalline peak (31.-36 ppm): from ^{13}C direct polarization experiment t_o = 5000 s Amorphous peak (28-31.5): from gated decoupled experiment t_f = 20 ms; t_o = 5s

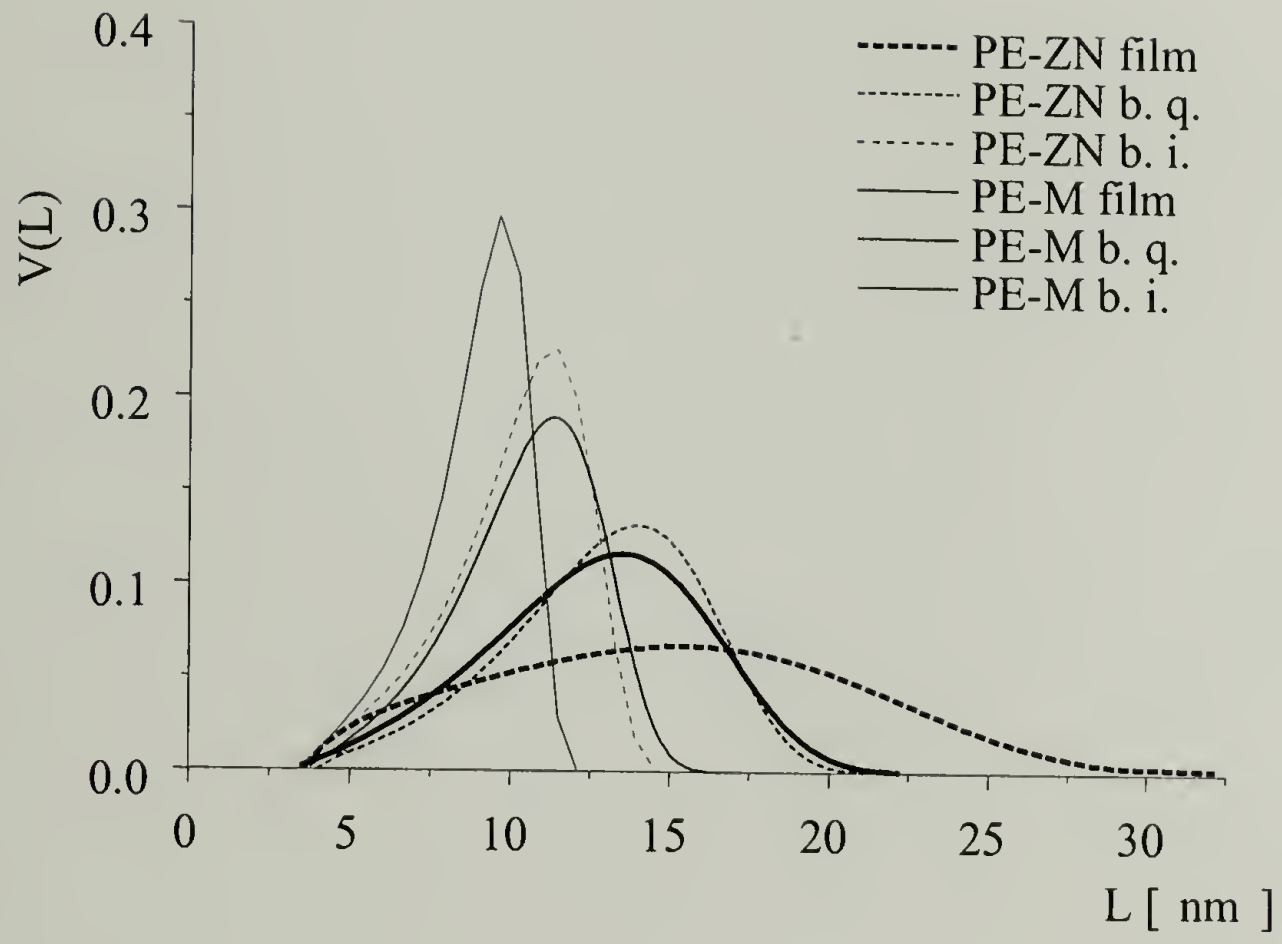

Figure 5.5 Volume-averaged lamellar thickness distributions in LLDPEs, as determined from ^{1}H $T_{1\rho}$ relaxation data.

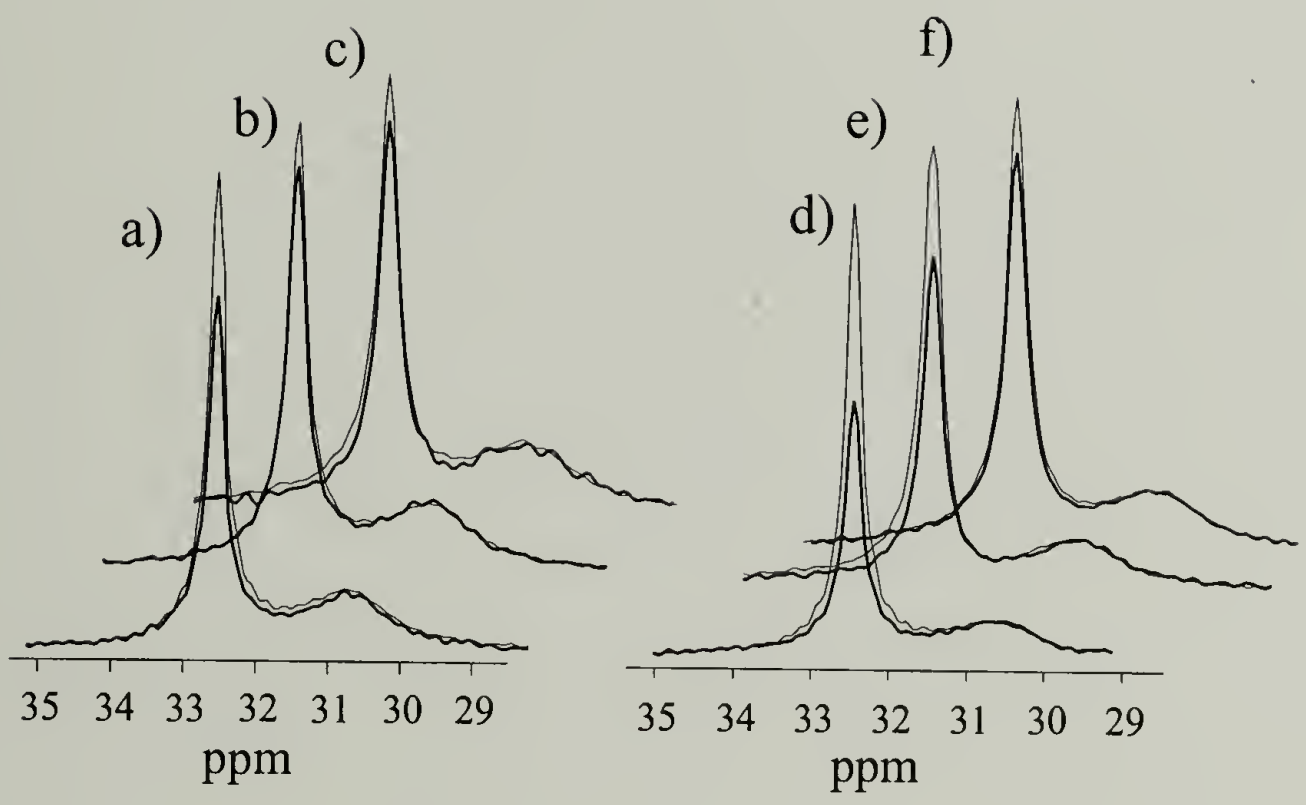

Figure 5.6 CP MAS vs. ^{1}H spin diffusion with ^{13}C detection
CP MAS; —— ^{1}H spin diffusion with ^{13}C detection,
t_m = 100m (a) PE-M b.i. ; (b) PE-M b.q. ; (c) PE-M film; (d) PE-ZN b.i.;
(e) PE-ZN b.q. ; f) PE-ZN film

I)

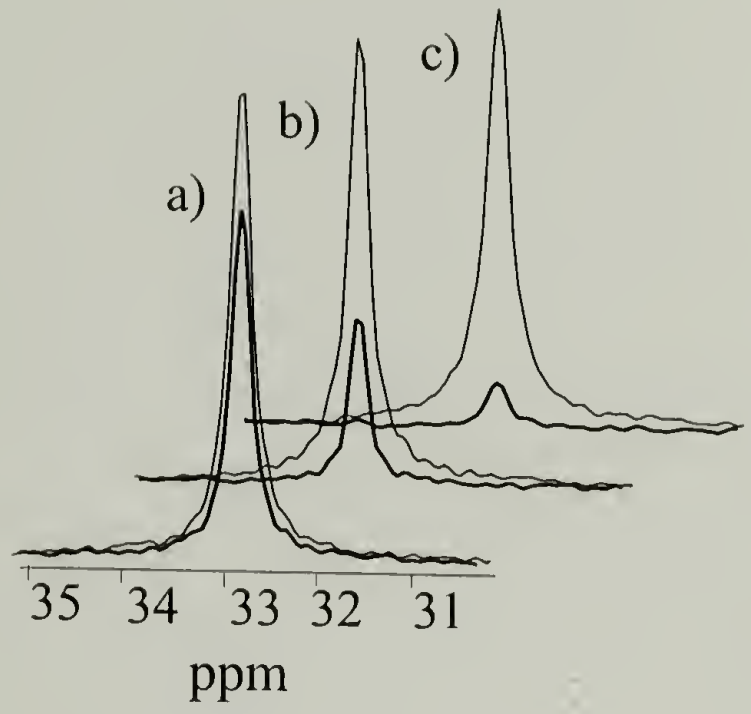

II)

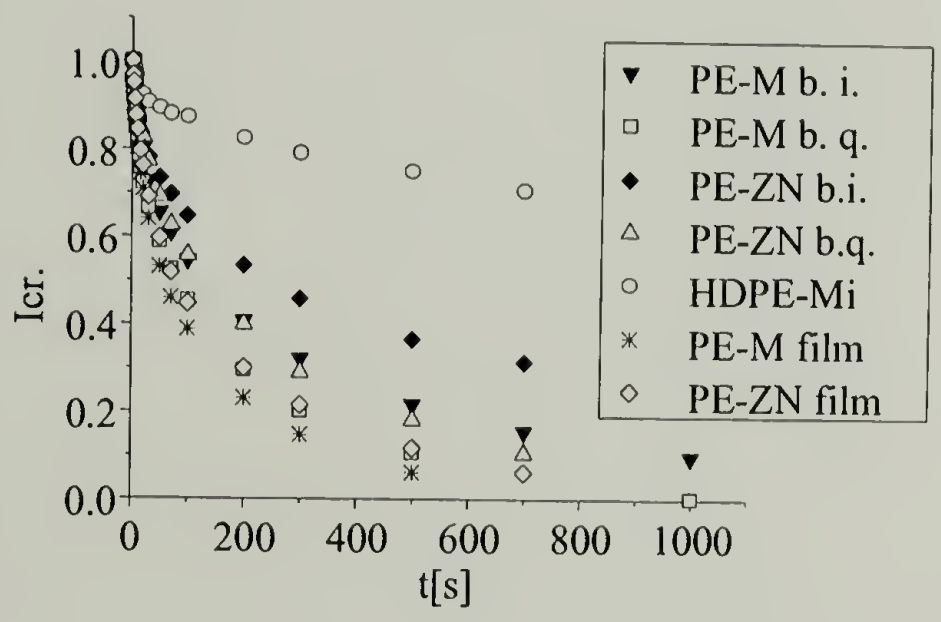

Figure 5.7. ^{13}C T_1 relaxation in ethylene co-polymers
I) MAS CP T_1 filtered spectra with ^1H decoupling
t_f = 1s; —— t_f = 500s
(a) HDPE-Mi. ; (b) PE-ZN b.i. ; c) PE-M b.q.
II) ^{13}C T_1 relaxation curves for the crystalline phase in ethylene co-polymers;

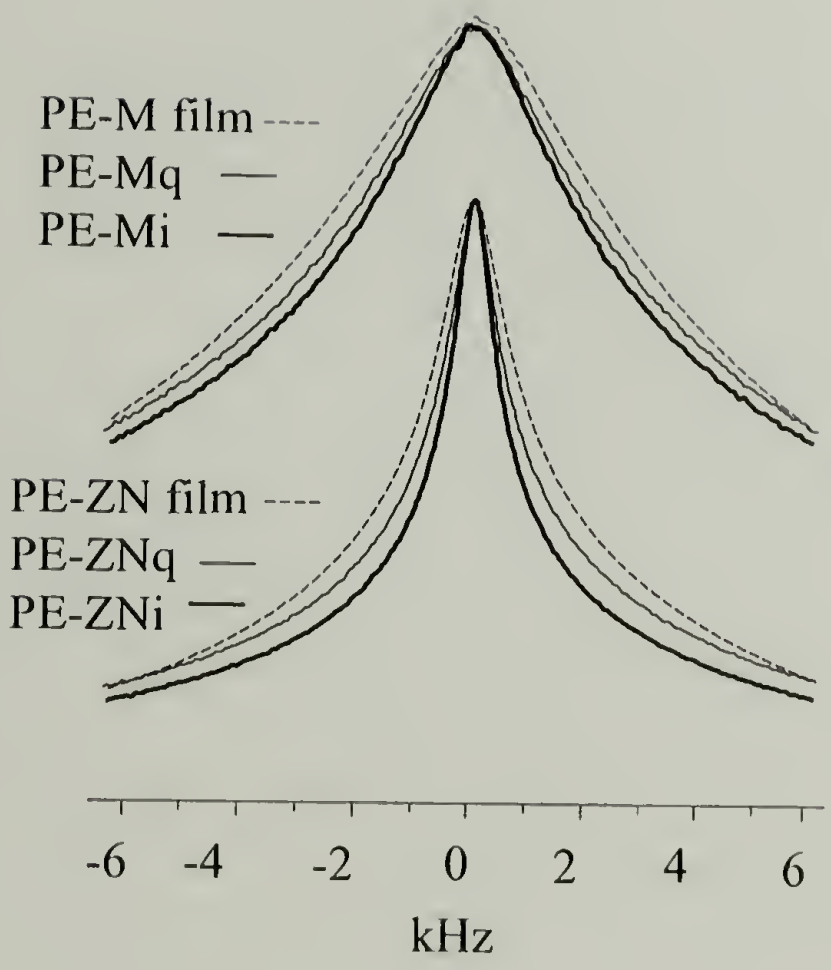

Figure 5.8 The dependence of the lineshape in static ^{1}H spectra of LLDPEs on composition and thermal history.

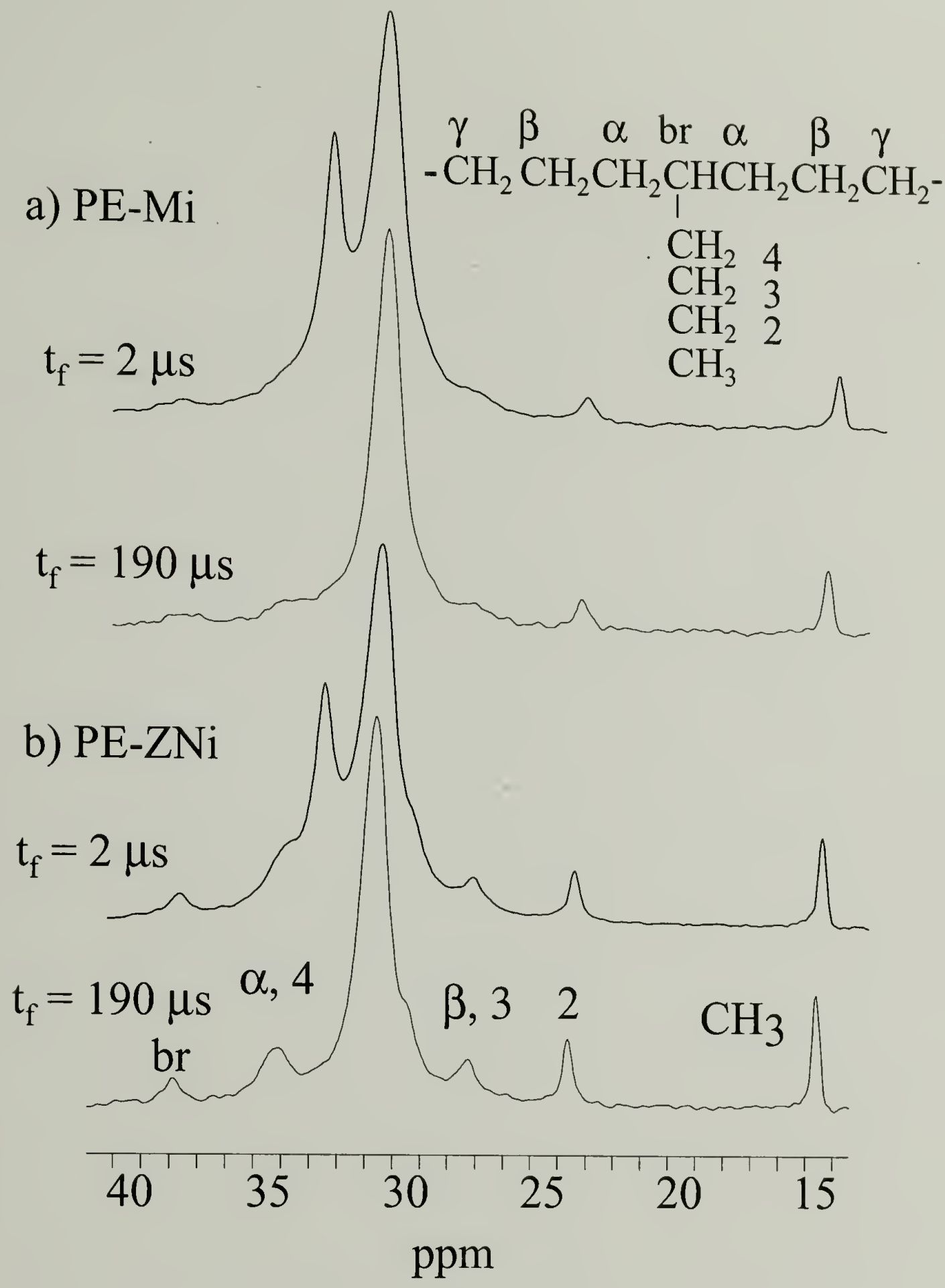

Figure 5.9 ^{13}C MAS spectra of isothermally crystallized LLDPEs after gated decoupling.

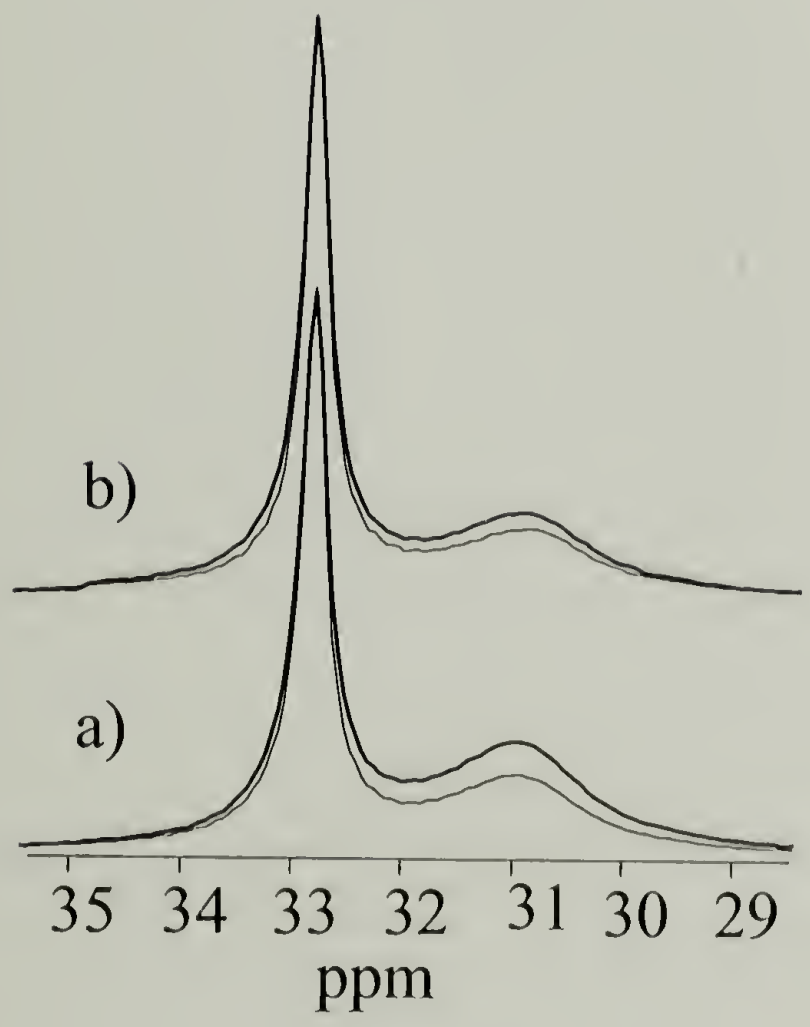

Figure 5.10 CP MAS spectra with ^{1}H decoupling
isothermally crystallized ——; quenched ——
(a) PE-M (b) PE-ZN

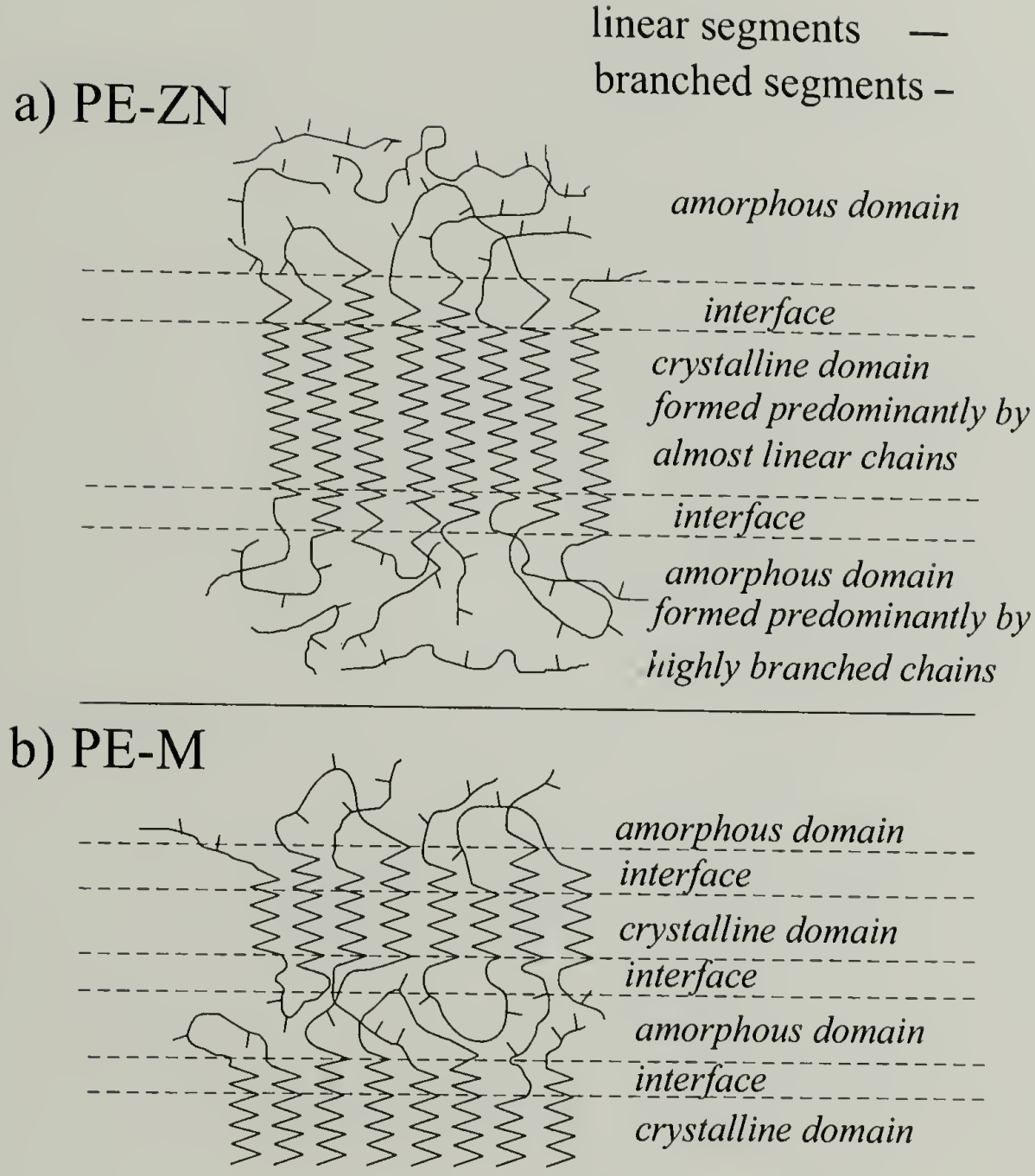

Figure 5.11 Proposed morphological structure for metallocene and Ziegler-Natta LLDPEs.

CHAPTER 6

BRANCH DEFECTS IN LLDPE CRYSTALLITES AND THE STRUCTURE OF THE INTERFACIAL DOMAIN IN LLDPEs

6.1 Abstract

The morphological partitioning of branched units, the local chain conformation in the vicinity of the crystalline defects and the structure of the crystalline-amorphous interface in LLDPEs were studied using solid-state NMR. The existence of a developed crystalline-amorphous interface formed by all-trans yet partially mobile chains was proven by spin-diffusion and relaxation techniques. The thickness of the interfacial domain was estimated as 10% of the crystallite thickness. For the ethene-propene copolymer, it was shown that up to 20% of branched units are included into the crystalline phase. The chain conformation in the vicinity of the crystalline defects, resulting from the inclusion of the methyl branches into the crystalline lattice have been studied using 2D exchange-NMR, $^{13}C\ T_1$ selection techniques, and a novel solid-state NMR technique, centerband-only detection of exchange (CODEX). Several structural models describing the crystalline branch defects were discussed. No evidence of the inclusion of branched units other than propene into the crystalline lattice was found. For a series of the ethylene-α-olefin co-polymers, the crystallite thickness and morphological partitioning of branched units determined by NMR were correlated with the lattice dimensions measured by WAXS.

6.2 Introduction

In this chapter, the application of solid-state NMR techniques for the investigation of the structure of the crystalline-amorphous interface and local chain conformation in the vicinity of the crystalline defects in LLDPEs will be described. The information about morphological partitioning of branched units obtained by NMR will be correlated with WAXS results.

Previously, the phase composition in the solid ethylene co-polymers was investigated using Raman spectroscopy, SAXS, and solid-state NMR techniques. Corresponding references were briefly reviewed in the Introduction (Chapter 1.9.5). The results of numerous theoretical and experimental investigations suggest the existence of the developed interfacial domain in the ethylene co-polymers. However, until now the information about the interfacial content and structure was derived from the analysis of unresolved lines, rather than from the direct observation of signal related to the interfacial domain.[1-10]

In this work, the structure of the crystalline-amorphous interface in LLDPEs will be characterized by spin-diffusion and relaxation techniques. The ^{1}H spin-diffusion technique with ^{13}C detection used in this study allows to select the interfacial domain based on its location between the crystalline and amorphous regions, and to observe interfacial signal without the significant interference from other morphological domains. Molecular mobility in the interfacial region will be characterized by ^{1}H spin diffusion and ^{1}H T_2 relaxation techniques. The fine structure of the interfacial domain will be studied

using ^{1}H spin-diffusion combined with a ^{13}C T_1 selection technique. This method allows to distinguish contributions from partially ordered and disordered components to the interfacial signal.

Morphological partitioning of branched units in LLDPEs was extensively studied before.[11-14] A brief review of the related literature is presented in the Introduction (Chapter 1.10.2). In this work, the distribution of branches between the crystalline and amorphous regions will be investigated using NMR selection techniques allowing for the direct observation of branched units embedded into the crystalline and amorphous domains. For the ethene-propene co-polymer (PE-PrL) the local chain conformation near the crystalline defect caused by the inclusion of the methyl branches into the crystalline phase will be investigated by solid-state NMR using 2D-exchange, ^{13}C T_1 selection, and novel CODEX techniques. Structural models describing the crystalline branch defects in ethylene- co-polymers will be discussed.

6.3 Background information. NMR techniques used in this study

6.3.1 ^{1}H spin-diffusion and combined spin-diffusion-relaxation techniques

A brief description of the spin-diffusion phenomenon has been presented in the Introduction (Chapter 1.10.1).[15,16] The ^{1}H spin-diffusion technique with ^{13}C detection applied in this work allows to select morphological domains based on their spatial location. The corresponding pulse sequence is described at Fig 6.1a. During ^{1}H T_2 filtering t_f, the magnetization in the crystalline domains

is destroyed by dipolar dephasing, so only the amorphous domains remain magnetized. The resulting spatially inhomogeneous proton magnetization equilibrates between the amorphous and crystalline domains by ^1H spin diffusion during t_m. By varying t_m it is possible to control the distance over which the equilibration of the magnetization occurs. Mixing times t_m of the order of 2-5 ms correspond to the equilibration of magnetization on a length scale of 2-4 nm, i.e. comparable to the expected thickness of the crystalline-amorphous interface. ^{13}C detection conveniently allows to resolve the signals from morphological domains having different average chain conformations. The amorphous signal is suppressed by the short CP time (28 μs) so the resonance corresponding to the crystalline-amorphous interface may be directly observed. The combined ^1H spin-diffusion - $^1H\ T_2$ relaxation technique (Fig.6.1.b) allows to study $^1H\ T_2$ relaxation behavior in the morphological domains selected by their spatial location by spin-diffusion technique.

Further discrimination of the morphological sub-domains within the interfacial region can be achieved by using $^{13}C\ T_1$ selection combined with the ^1H spin-diffusion technique. (Fig.6.1c) In this type of experiment two spectra are recorded for each mixing time t_m: A $^{13}C\ T_1$ filtered spectrum (t_f=3s) containing only the crystalline signal, and the reference spectrum (t_f=10 ms) representing all morphological domains. Both spectra are recorded with short CP (40 μs) to suppress the amorphous signal and to facilitate the observation of the interfacial region. Purely interfacial signal is obtained by subtraction of the

crystalline from the reference spectrum, without any scaling factor. Based on the known relationship between the chain conformation and ^{13}C methylene chemical shift, the interfacial signal in the range 29.0-31.8 ppm is related to the disordered non-trans interfacial component, while the resonance in the range 31.8-34.5 ppm corresponds to all-trans interfacial region.

The ^{1}H spin-diffusion techniques described above allow for the direct observation of the signal from the interfacial domain without the application of line-fitting procedures. This is a clear advantage over previously used NMR techniques [9-10] or Raman spectroscopy [1-6]

6.3.2 CODEX

The CODEX technique[17] makes it possible to study segmental reorientations with the high sensitivity and resolution of fast MAS. The pulse sequence for the CODEX experiment is shown in Fig. 6.2. For N/2 rotation periods, the spins evolve under the anisotropic chemical-shift, which is recoupled by two 180°-pulses per rotation period t_r in a spinning-speed independent fashion. Then, the magnetization is stored along the z-direction, so that it does not precess or dephase during the long mixing time t_m, which is an integer multiple of t_r. If no motions occurred during t_m, the chemical shift evolution, after a read-out pulse and another *N/2* rotation periods under the recoupled chemical-shift anisotropy, is refocused at the start of detection. If segmental reorientation did occur during t_m, the orientation-dependent

frequency has changed and the chemical-shift anisotropy is not completely refocused. The dephasing is observed with high sensitivity as a decrease in the detected line intensity. High spinning rates ν_r can be used to obtain virtually sideband-free spectra, since the dephasing is only a function of the total time Nt_r.

The often dominant signal of immobile sites can be removed by subtracting the CODEX spectrum from a reference spectrum, without an adjustable scaling factor. This reference spectrum is obtained simply by interchanging t_m and Δ in the pulse sequence of Fig. 6.2 The resulting difference spectrum is called pure exchange CODEX spectrum. During t_m and Δ, the magnetization is oriented along the z-direction and it is subject to $^{13}C\ T_1$ relaxation. Thus if the duration of the longitudinal relaxation $(t_m + \Delta)$ is sufficiently long, the amorphous magnetization may be suppressed and the resulting CODEX spectra will be representative of the crystalline region. Therefore by varying $(t_m + \Delta)$ it is possible to select the morphological domains based on $^{13}C\ T_1$ relaxation time.

The smaller the motional amplitude, the longer the time Nt_r must be to produce significant dephasing. Taking into account the size δ of the chemical-shift anisotropy, the reorientation angle can be estimated from the dependence of the intensity on δNt_r. In another series of experiments, the correlation time τ_c can be obtained as the time constant of the t_m-dependent intensity change. Information about the number M of equivalent orientational sites accessible in

the motional process and the fraction f_m of mobile segments is obtained from the final exchange intensity $I_\infty = I(t_m >> \tau_c, \delta N t_r >> 1) = f_m(M-1)/M$. *For* $f_m = 1$, the minimum I_∞ *is 1/2*, obtained for $M=2$. Generally, $I_\infty < f_m < I_\infty$.

Obviously, for the segmental motion to be detected by CODEX the segment positions before and after motion must not be NMR equivalent. For instance, a 180° flip of planar zig-zag chains in the crystalline domain exactly inverts the chemical shift tensor of the methylene segments, so the frequencies before and after flip will remain unchanged. Therefore, this kind of motion cannot be detected by CODEX. In contrast, in the vicinity of the branched units included into the crystalline region, the chain conformation may be different from planar zig-zag. Thus, the motion of the crystalline defects is observable by CODEX. As a result, a CODEX pulse sequence can be used as an effective filter allowing to suppress the backbone crystalline signal, yet to keep the signal from the crystalline defect and provide information about the local chain geometry.

6.3.3 2D exchange spectroscopy

Multidimensional exchange spectroscopy can be applied for the characterization of dynamical processes with correlation times between 10^{-5} and 10^{2} seconds. The basic principle of exchange NMR is the measurement of the NMR frequency of one the same molecular segment at two different times (before and after t_m) and the detection of slow dynamics through a change of NMR frequency. The two-dimensional spectrum $S(\omega_1, \omega_2)$ represents the

probability of finding a segment with a frequency ω_1 and, by a time interval t_m later, with frequency ω_2. Obviously in order to be detectable in the exchange spectrum the dynamic process should result in the change of the corresponding NMR frequency i.e. ω_2 and ω_2 should be different.[18]

Without any slow dynamics in the mixing time, the frequencies remain unchanged $\omega_2=\omega_1$ for all signals, so the intensity is confined to the diagonal of the (ω_1,ω_2) plane. With frequency changes during the mixing time t_m, off-diagonal signals with $\omega_2 \neq \omega_1$ appear.[18]

The pulse program for the 2D exchange experiment used in this investigation is presented at Fig.6.3. It was specifically tuned to observe slow dynamics of the propene units in the crystalline phase of PE-PrL. Indeed, a ^{13}C chemical shift filter t_f allows for selectively observation of the signal from the α-site methylene, without interference from the backbone methylene signal. In addition, a ^{13}C T_1 filter of 800 ms (t_{f1}) was used to suppress the signal from the propene units included into the amorphous phase.

6.4 Experimental

6.4.1. Materials

Compositions and thermal histories for the samples investigated are presented in Chapter 2 (Table 2.1).

6.4.2. WAXS

WAXS measurements were performed using a D500 camera equipped with a slit collimator, a standard copper K_α radiation source (λ= 0.1542 nm) and a *Ni* filter.

Orthorhombic lattice parameters *a* and *b* were calculated from the experimentally determined spacings d_{110} *and* d_{200} using the relationship

$$\frac{1}{d_{hkl}^2} = \frac{h^2}{a^2} + \frac{k^2}{b^2} + \frac{l^2}{c^2} \qquad (6.1)$$

6.4.3 NMR

Solid state ^{13}C and ^{1}H *NMR* spectra were obtained with a Bruker MSL-300 and DSX 300 spectrometers equipped with a MAS unit. A ^{13}C resonance frequency of 75.5 MHz and a ^{1}H frequency of 300 MHz were employed. In MAS experiments, 7-mm and 4-mm diameters rotors were used at spinning speeds of 4 and 5 kHz.

6.5 Experimental Results and Discussions

6.5.1 Branch partitioning in the ethene-propene co-polymers

The partitioning of the propene units in the ^{13}C labeled ethene-propene co-polymer PE-PrL was investigated using *CP* T_1 selection (Fig.5.2a in Chapter

5) and ^{13}C direct polarization techniques with a short recycle delay (2 s). *CP* T_1 filtering suppresses the amorphous signal, so the branched units included into the crystalline domain can be selectively observed. In the direct polarization spectrum recorded with short recycle delay, the signal from the crystalline domain with a long ^{13}C T_1 is suppressed. This allows for the selective observation of the signals from the branched units in the amorphous phase.

By comparing the integral intensities of the crystalline and amorphous propene signals, it was shown (Fig. 6.4) that about 20 % of the propene units are included into the crystalline phase. These observations are in good agreement with the results of Perez et al.[12-13]

6.5.2 Dependence of lattice dimensions on the crystallite thickness.

It is known that the unit cell dimensions in branched ethylene co-polymers may be larger than in HDPEs.[19-23] Factors contributing to the lattice expansion have been briefly reviewed in the Chapter 1.9.2

The results obtained in the numerous experimental and theoretic investigations indicate that in ethylene-α-olefin co-polymers only methyl branches can be included into the crystalline phase. For the larger sidebranches, the lattice cell expansion is related to the reduction of the crystallite thickness, rather than to the inclusion of the branched units into the crystalline phase.[1,19-20]

In this investigation the lattice base areas *ab* determined by WAXS for a series of LLDPE samples were correlated with the lamellar thickness, measured

using the solid-state NMR technique described in chapter 4. The results obtained are presented at the Fig.6.5. It can be seen that a reciprocal correlation indeed exists between the lamellar thickness and lattice dimensions. The lattice dimensions for ethene-propene co-polymer are distinctly larger than for the rest of co-polymers studied, which is consistent with the inclusion of methyl branches into the crystalline phase. The results of our solid-state NMR investigation (Chapter 5.5) and the literature data[10-14] indicate that the inclusion of branches other than methyl into the crystalline phase is unlikely.

6.5.3 Molecular motion and local chain conformation in the vicinity of crystalline branch defect in ethene-propene co-polymers

Based on the degree of the lattice expansion determined by WAXS combined with simulation results, Salazar et al. proposed that a fraction of the small branches can be included into the crystals in the vicinity of 2g1 kinks (gauche-trans-gauche').[23] NMR frequencies are sensitive to the local chain conformation, so the conformation of the polymer chain in the vicinity of the crystalline branch defect can be directly investigated by solid-state NMR techniques.

It is known that polyethylene chains in the crystalline domains of LLDPEs undergo 180° flips.[24] The flip motion of all-trans chains cannot be observed by CODEX. However, in the vicinity of the crystalline defects the planar zig-zag chain conformation is distorted. In that case the flip motion is detectable by CODEX technique. Information about the molecular motion in the

vicinity of crystalline defects was obtained from the t_m dependence of CODEX exchange intensity for the ^{13}C labeled propene α-site (Fig.6.6). In all CODEX measurements the amorphous contribution to the α-site signal was suppressed by a ^{13}C T_1 filter of duration $(t_m + \Delta) = 1$ s.

It can be seen that at 292 K many crystalline defects undergo motions on a 30 ms timescale. The strongly non-exponential character of the dependence of the CODEX exchange intensity on t_m suggests the co-existence of several modes of the molecular motion. The magnitude of the final exchange intensity for the α–site $I_{\alpha\infty} = 0.75$ allows to suggest that 50% of chain segments in the crystalline defect undergo two-site flips. As the temperature decreases to 262 K, the motion rate strongly decreases, which indicates that the crystalline defect motion is indeed thermally activated.

In the framework of three-bond models of the crystalline defect, which assume that the distortion of all-trans chain conformation does not spread beyond two ethylene segments adjacent to the branched unit, the local chain conformation in the vicinity of the labeled α-site can be characterized by torsional angle ψ. (Fig. 6.7 a-c). Because the amplitude of the re-orientation of the methylene segments due to the chain flips depends on ψ, the shape of CODEX buildup curves $I(N_{IF})$ for the labeled site will also depend on the torsional angle. Simulated CODEX buildup curves for 180° chain flips and various torsional angles ψ are compared with the experimental results at

Fig. 6.8. It can be seen that the experimental data are consistent only with relatively small values of ψ ($\psi = 15^{o}$).

Another source of information about the chain conformation near the crystalline defect is the chemical shift of the crystalline α-methylene site. By comparing CPT_1 and DP spectra recorded with a short recycle delay ($t_0 = 2$ s) it can be seen that the crystalline α-site resonance is shifted upfield compared to the amorphous α-site signal. (Fig.6.9) It indicates that in the vicinity of the crystalline defect, the gauche ($\psi = 60^{o}$) content is even higher than in the disordered amorphous phase. This experimental observation is consistent with gauche-trans-gauche' model of the crystalline defect proposed by Balta-Calleja et al.[24]

2D exchange spectra for the crystalline α-site of in PE-PrL are presented at Fig.6.10. Based on the shape of the 2D patterns, it can be concluded that ordered (narrow) and inhomogeneously broadened disordered components contribute to the α-site signal. The comparison of the exchange spectrum (t_m = 800 ms; Fig.6.10a) with the reference (t_m =1ms ;Fig.6.10b) reveals that the broadening caused by the exchange occurs mostly for disordered component. On the other hand, significant signal intensity is observed at 38 ppm in pure-exchange CODEX spectrum (Fig.6.6 a). It indicates that the segments, producing the narrow component in 2D exchange spectrum also undergo re-orientations. Thus, the motional rate and the geometry of the molecular motion for the ordered and disordered components may be different.

The observed experimental results suggest the complex character of morphology and molecular motion near the crystalline defect. It can be proposed that the local chain conformation near the branch included into the crystalline phase should be described by the distribution of torsional angles, rather than by a single angle ψ. Moreover, the simple three-bond model is not necessarily adequate for the description of the crystalline branch defect. Further experimental and theoretic investigations should be performed, using more advanced models that account for the distribution of chain conformations and motional modes.

6.5.4 Investigation of the structure of the crystalline-amorphous interface by spin-diffusion and relaxation techniques

The results of numerous experimental and theoretic investigations indicate the existence of a developed crystalline-amorphous interface in LLDPEs.[1-10] In contrast to previous studies, in this investigation the major emphasis is put on the application of solid-state NMR techniques that allow to resolve the interfacial signal and to characterize structure and molecular mobility in the interfacial domain without the application of line-fitting procedures.

The results of the investigation of phase structure of PE-ZN b.q. and in PE-M b.q. using ^{1}H spin-diffusion with ^{13}C detection are presented at Fig.6.11a-6.12a. Based on the ratio of integral intensities of the interfacial (t_m = 2 ms) and crystalline signals (t_m = 200 ms) the average interfacial thickness both in PE-M b.q. and in PE-ZN b.q. was evaluated as 10-15 % of the overall

thickness of the crystalline domain. (Fig. 6.11b-6.12b) The observed difference between the equilibrium signal intensities (t_m = 200 ms) for the gauche-containing fractions in PE-M b.q. and PE-ZN b.q. may be related to the different cross-polarization conditions of these samples.

The amorphous signal is suppressed by the short CP time (25 μs), so the lineshape of the interfacial signal can be directly observed in the spectra recorded with t_m = 2 and 5ms (Fig 6.13). The presence of the strong component at 32.8 ppm in the interfacial signal indicates that the interfacial domain is formed by chains in all trans-conformation. The broad lineshape of the interfacial signal at 32.8 ppm suggests that the segments forming the interfacial domain are embedded into a disordered medium.

The $^1H\ T_2$ relaxation behavior of the interfacial region in PE-ZN b.q. (Fig.6.14 a) was characterized by the combined spin-diffusion -T_2 relaxation technique described in section 6.3.1(Fig.6.1.b). For comparison purposes, the $^1H\ T_2$ relaxation behavior in the crystalline region of PE-ZN b.q. was determined using the same pulse sequence (Fig.6.1.b) with very short $^1H\ T_2$ selection time (t_f= 1μs). In that case, the crystalline magnetization is not destroyed, so the signal at 32.8 ppm (Fig. 6.14.b) corresponds to the crystalline domain. $^1H\ T_2$ for the all-trans interfacial region is 30 % longer than for the crystalline core, which proves higher mobility in the interfacial domain. (Fig.6.14 c) This observation is consistent with all-trans-segments near the interface having significant high-frequency mobility of limited amplitude.

The results of the spin-diffusion-^{13}C T_1-selection experiments are presented at Fig.6.15. It can be seen that the fastest equilibration of the magnetization occurs for the non-trans interfacial signal (29-31.8 ppm), indicating that disordered interfacial region is rather thin and it is located in close proximity to the amorphous domain. The efficient spin-diffusion in the non-trans region is consistent with relatively low molecular mobility. For the of all-trans interfacial region (31.8-34.5 ppm), the equilibration is slower, proving that this region is thicker than the non-trans (disordered) interface.

The experimental data presented indicate that the crystalline-amorphous interface in the ethylene co-polymers is predominantly formed by all-trans yet partially mobile chains. These experimental observations can be explained by proposing that the loops formed by chain segments in all-trans conformation protrude from the crystalline to the amorphous region in comb-like fashion.(Fig.6.16). The formation of rather loose loops at the crystalline-amorphous interface agrees with the results of the lattice theory calculations. According to Flory et al.[4] while 70% of chains enter the same lamellae from which they emerge, fewer than 20% of crystalline chains are engaged in adjacent folds with immediate re-entry.

6.6 Conclusions

The presence of all-trans yet partially mobile chains in the interfacial region of LLDPEs was confirmed by spin-diffusion and ^1H T_2 relaxation

techniques. Using combined a spin-diffusion-^{13}C T_1 -filtering technique, it was shown that the interfacial region contains both partially ordered all-trans and disordered trans-gauche segments. Both for metallocene and Ziegler-Natta LLDPEs the average thickness of the interfacial region was evaluated as 10-15% of the average lamellar thickness.

The morphological partitioning of branched units was studied using WAXS and solid-state NMR techniques. It was determined that 20 % of propene segments are included into the crystalline phase, while no evidence of the inclusion of butyl branches into the crystalline lattice was found. Local chain conformations and molecular motions in the vicinity of the crystalline defects were characterized using 2D exchange, ^{13}C direct polarization, CP T_1 selection, and CODEX techniques.

It was shown that crystalline defect cannot be described in a satisfactory way by a simple 3-bond model. Based on the results of 2D-exchange and CODEX experiments, it was proposed that the adequate model should account for a distribution of chain conformations and motional modes.

6.7 References

1. Alamo, R. G.; Mandelkern, L."The crystallization behavior of random copolymers of ethylene." *Thermochimica Acta*, **238**, 155 (1994).

2. Alamo, R. G.; Chan, E. K. M.; Mandelkern, L."Influence of Molecular Weight on the Melting and Phase Structure of Random Copolymers of Ethylene." *Macromolecules*, **25**, 6381 (1992).

3. Alamo, R. G.; Viers, B. D.; Mandelkern, L."Phase Structure of Random Ethylene Copolymers: A Study of Counit Content and Molecular Weight as Independent Variables." *Macromolecules*, **26**, 5740 (1993).

4. Flory, P. J.; Yoon, D. Y.; Dill, K. A."The Interphase in Lamellar Semicrystalline Polymers." *Macromolecules*, **17**, 862 (1984).

5. Stribeck, N.; Alamo, R. G.; Mandelkern, L.; Zachmann, H. G."Study of the Phase Structure of Linear polyethylene by Means of Small-Angle X-ray Scattering and Raman Spectroscopy." *Macromolecules*, **28**, 5029 (1995).

6. Naylor, C. C.; Meier, R. J.; Kip, B. J.; Williams, K. P. J.; Mason, S. M.; Conroy, N.; Gerrard, D. L."Raman Spectroscopy Employed for the Determination of the Intermediate Phase in Polyethylene." *Macromolecules*, **28**, 2969 (1995).

7. Mandelkern, L.; Alamo, R. G.; M.A.Kennedy."Interphase Thickness of Linear Polyethylene." *Macromolecules*, **23**, 4721 (1990).

8. Kumar, S. K.; Yoon, D. Y."Lattice Model for Crystal-Amorphous Interphases in Lamellar Semicrystalline Polymers: Effects of Tight-Fold Energy and Chain." *Macromolecules*, **22**, 3458 (1989).

9. Kitamaru, R.; Nakaoki, T.; Alamo, R. G.; Mandelkern, L."A Carbon-13 NMR Study of the Phase Structure of Semicrystalline Polymeers: Hydrogenated Polybutadiene." *Macromolecules*, **29**, 6847 (1996).

10. Kuwabara, K.; Kaji, H.; Horii, F.; Bassett, D. C.; Olley, R. H."Solid - State 13C NMR Analyses of the Crystalline-Noncrystalline Structure for Metallocene-Catalyzed Linear Low-Density Polyethylene." *Macromolecules*, **30**, 7516 (1997).

11. Perez, E.; Vanderhart, D. L."Morphological Partitioning of Chain Ends and Methyl Branches in Melt-crystallized Polyethylene by ^{13}C-NMR." *J. Polym. Sci.: Part B: Polym.Phys.*, **25**, 1637 (1987).

12. VanderHart, D. L.; Perez, E."A ^{13}C NMR Method for Determining the Partitioning of End Groups and Side Branches between the Crystalline and Nonerystalline Regions in Polyethylene." *Macromolecules*, **19**, 1902 (1986).

13. Perez, E.; Bello, A.; Perena, J. M.; Benavente, R.; Martinez, M. C.; Aguilar, C."Solid-state nuclear magnetic resonanee study of linear-low density polyethylenes: 1. Ethylene-1-butene copolymers." *Polymer*, **30**, 1508 (1989).

14. McFaddin, D. C.; Russell, K. E.; Kelusky, E. C."^{13}C nmr solid-state studies of relaxation behavior of branches in homogeneous 1-alkene-ethylene copolymers." *Polymer Communications*, **27**, 204 (1986).

15. Cheung, T. T. P.; Gerstein, B. C."^{1}H nuclear magnetic resonanee studies of domain structures in polymers." *J.Appl.Phys.*, **52**, 5517 (1981).

16. Goldman, M.; Shen, L."Spin-Spin Relaxation in LaF_3." *Phys.Rev.*, **144**, 321 (1966).

17. deAzevedo, E. R.; Hu, W.-G.; Bonagamba, T. J.; K.Schmidt-Rohr."Centerband-Only detection of Exchange: Efficient Analysis of Dynamies in solids by NMR." *JACS*, **121**, 8411 (1999).

18. Schmidt-Rohr, K.; Spiess, H. W. *Multidimensional Solid-State NMR of Polymers*; Acad.Press: NY, 1994.

19. Howard, P. R.; Crist, B."Unit Cell Dimensions in Model Ethylene-Butene-1 Copolymers." *J.Polym.Sci.,B:Polym.Phys*, **27**, 2269 (1989).

20. Bunn, C. W.; Renffew, A.; Morgan, P. . In *Polyethylene;* Illife Ed.: London, 1975.

21. Seguella, R.; F.Rietseh."On the Isomorphism of Ethylene/α-olefin Copolymers." *J.Polym.Sci.,Polym.Lett.,*, **45**, 4175 (1974).

22. Davis, G. T.; Weeks, J. J.; Martin, G. M.; Eby, R. K."Cell Dimensions of hydrocarbon crystals: Surface effects." *J.Appl.Phys.*, **45** (1974).

23. Salazar, J. M. D.; Calleja, F. J. B."Influence of Chain Defects on the Crystallization of Polyethylene with Reference to Crystal Size and Perfection." *J. Crystal Growth*, **48**, 283 (1979).

24. Hu, W. G.; Boeffel, C.; Schmidt-Rohr, K."Chain Flips in Polyethylene Crystallites and Fibers Characterized by Dipolar ^{13}C NMR." *Macromolecules*, **32**, 1611 (1999).

25. Schmidt-Rohr, K.; Wilhelm, M.; Spiess, H. W. "Determination of Chemical-Shift Tensor Orientation in Methylene Groups by Separated-Local-field NMR." *Magnetic Resonance in Chemistry*, **31**, 352 (1993).

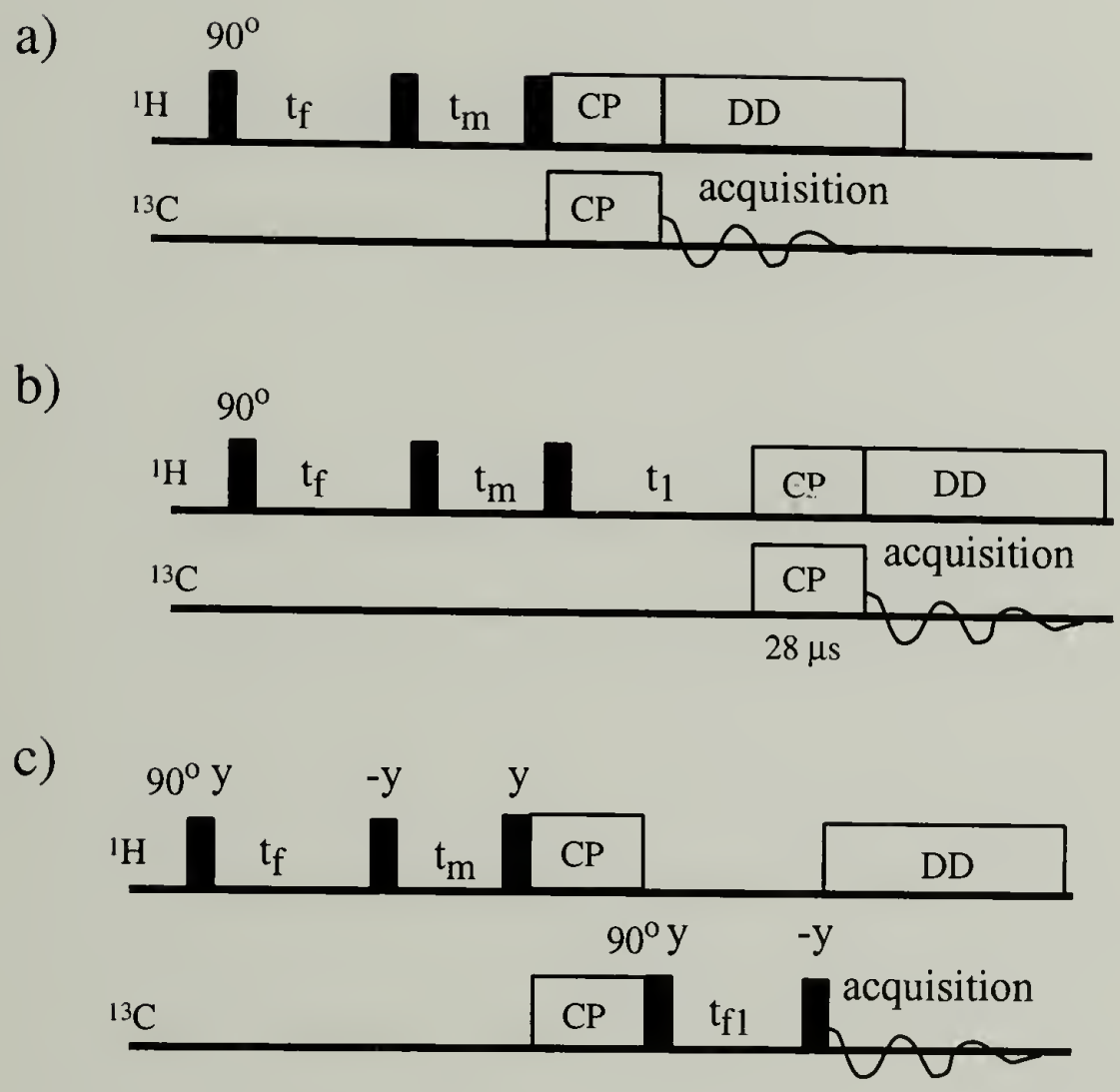

Figure 6.1 ^{1}H spin-diffusion with ^{13}C detection pulse sequences for the investigation of the phase composition in LLDPEs. 90° pulses are filled black. White: CP-cross-polarization, DD: dipolar decoupling. (a) ^{1}H spin-diffusion with ^{13}C detection; t_f -^{1}H T_2 filter (b) ^{1}H spin-diffusion combined with ^{1}H T_2 relaxation with ^{13}C detection. The ^{1}H T_2 relaxation behavior in the domains selected by tm is determined from the dependence of signal intensity on t_1 (c) ^{1}H spin-diffusion combined with ^{13}C T_1 selection with ^{13}C detection. t_{f1}: ^{13}C T_1 filter

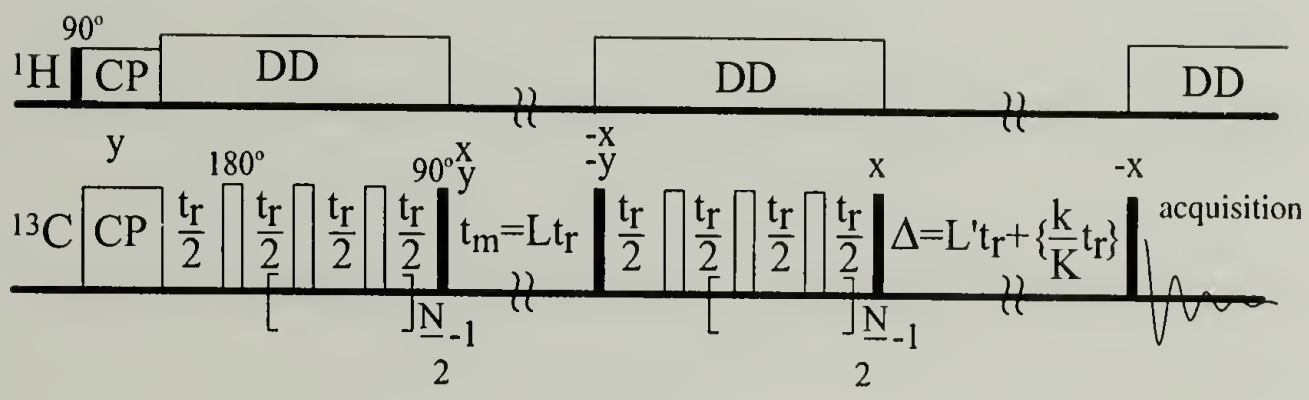

Figure 6.2 Pulse sequence for CODEX NMR: 90° pulses are filled black. White: CP-cross-polarization, DD: dipolar decoupling. t_r: rotor period. Pure-exchange spectra are obtained by measuring a reference spectrum with t_m and Δ interchanged and subtracting the CODEX spectrum from it.

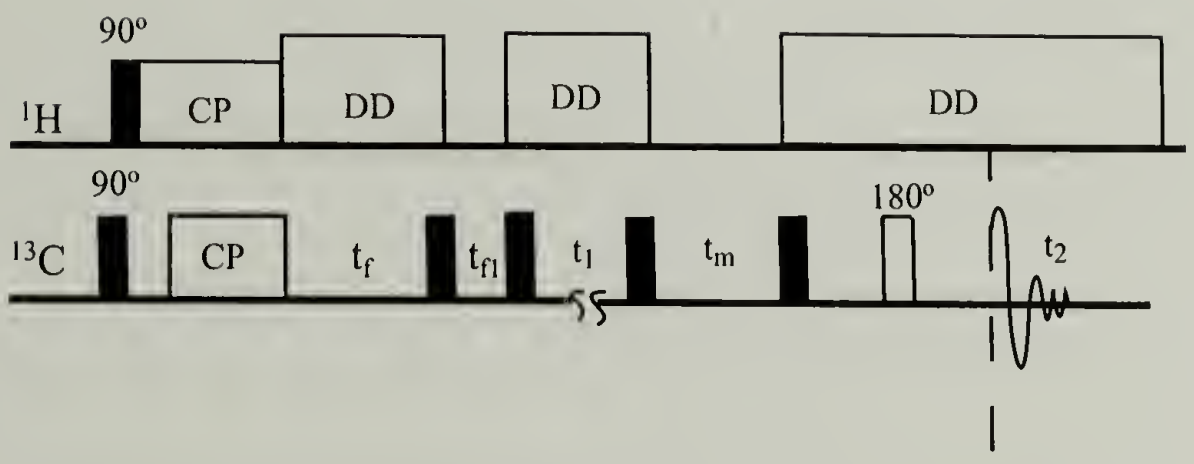

Figure 6.3 Pulse sequence for 2D exchange NMR: 90° pulses are filled black. White: CP:cross-polarization, DD: dipolar decoupling, 180° pulses. t_f: chemical shift filter, with $t_f = 1/(4\,\Delta\omega)$. Here $\Delta\omega$ is the difference between the resonance frequencies for the crystalline methylene and crystalline propene α-site; t_{f1}: ^{13}C T_1 filter

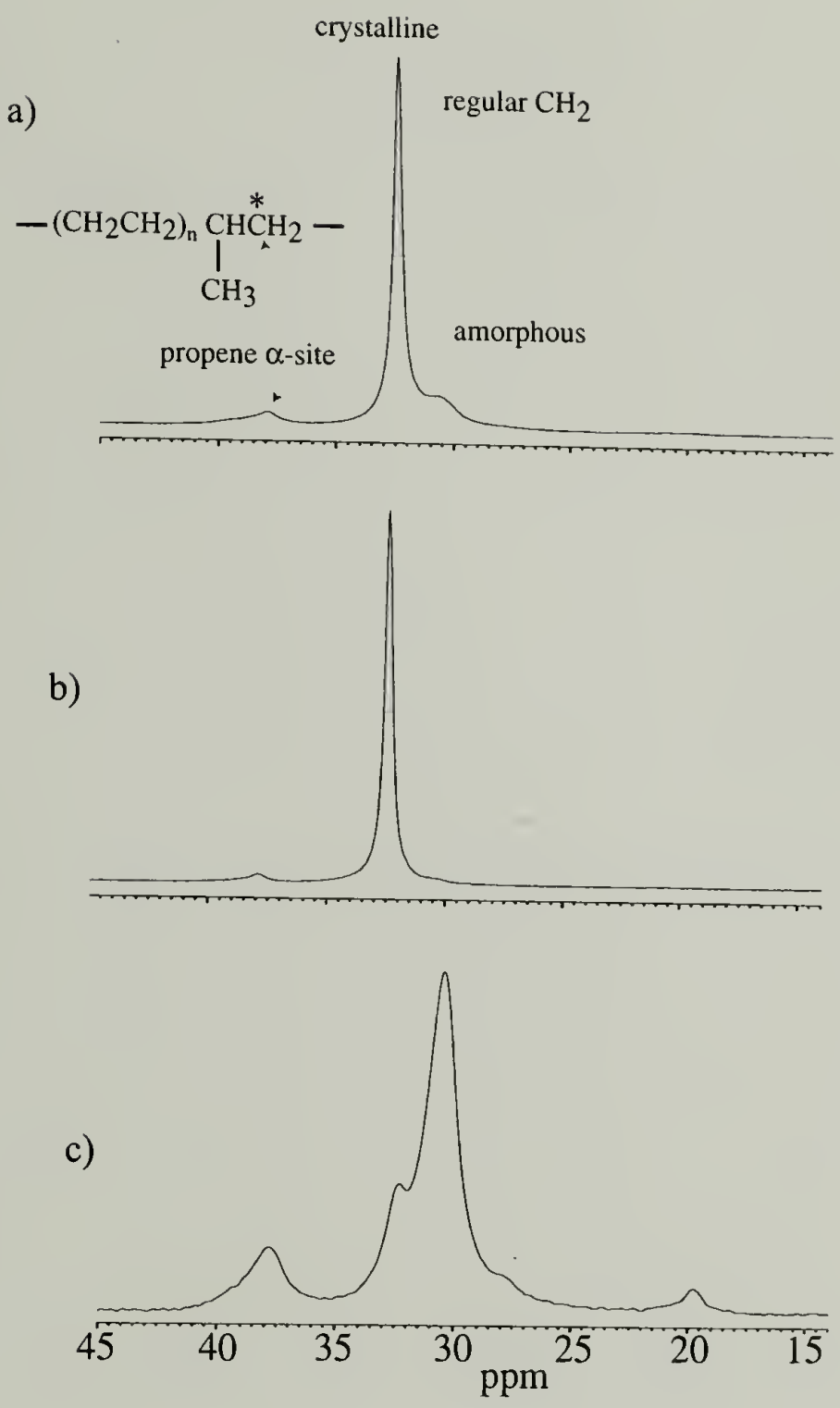

Figure 6.4 ^{13}C MAS NMR spectra of ^{13}C labeled ethene-propene co-polymer PE-PrL: (a) Cross-polarization; the overall content of propene units is ~1% mol. (b) CP/T_1 filtered spectrum with t_f = 2s; the content of the propene units in the crystalline phase is 0.46 % mol. (c) Direct polarization spectrum, with short recycle delay t_o = 2s; the content of the propene units in the amorphous phase is 2 % mol.

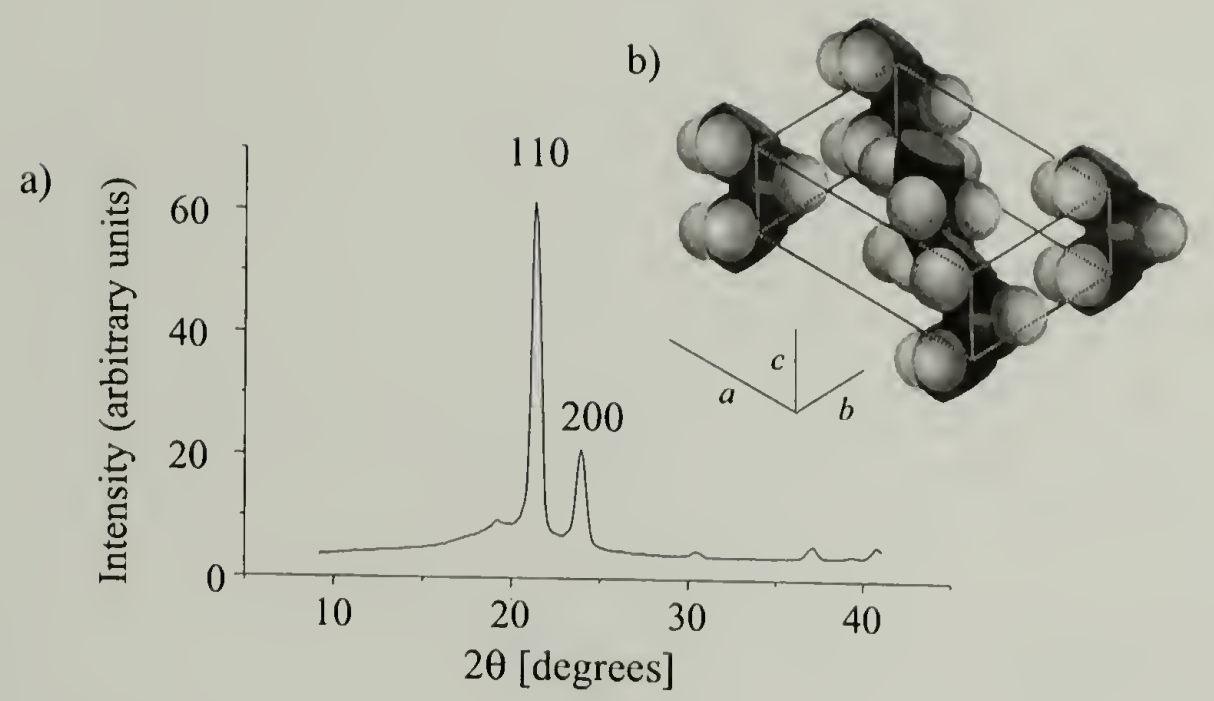

Figure 6.5 (a) WAXS pattern for PE-ZN b.q. Scattering maxima are labeled with eorresponding Bragg's indices. (b) Unit cell structure for the orthorhombie erystalline lattice. (e) Lattiee base area *ab* vs. reeiproeal erystallite thickness for the HDPE and ethylene eo-polymers;symbols: experimental data; straight line: least-squares fit of the *ab*(1/L) dependcnce ealeulated for HDPE and ethylene-hexene co-polymers (Pe-PrL excluded). The degree of lattiee expansion is distinctly higher for thc ethylene-propenc eo-polymer than for other polymers with similar lamellar thickness.

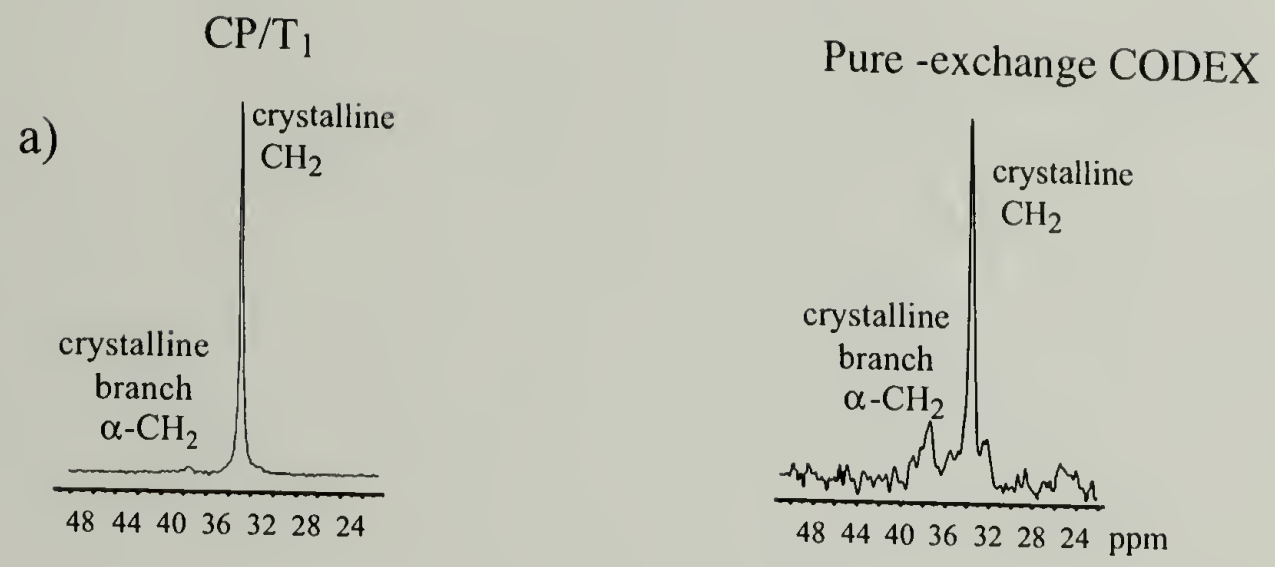

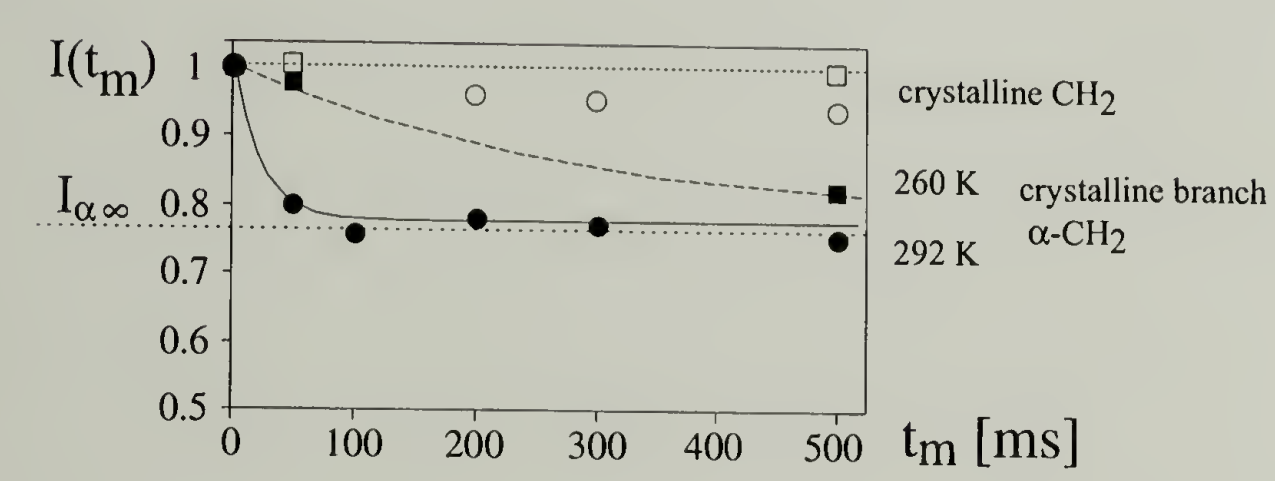

Figure 6.6 Investigation of the crystalline mobility in PE-PrL by CODEX (a) CP/T_1 filtered spectrum (t_f = 2s) vs. pure exchange- CODEX spectrum The relative intensity of the methylene backbone signal is far weaker in CODEX spectrum. (b) Normalized CODEX exchange intensities $I(t_m) = (I_{ref.} - I_{CODEX}(t_m))/I_{ref.}$) as a function of t_m for the propene α-site (solid symbols) and crystalline backbone methylene (open symbols). At 292 K many defects undergo chain flips on a 30-ms time scale.

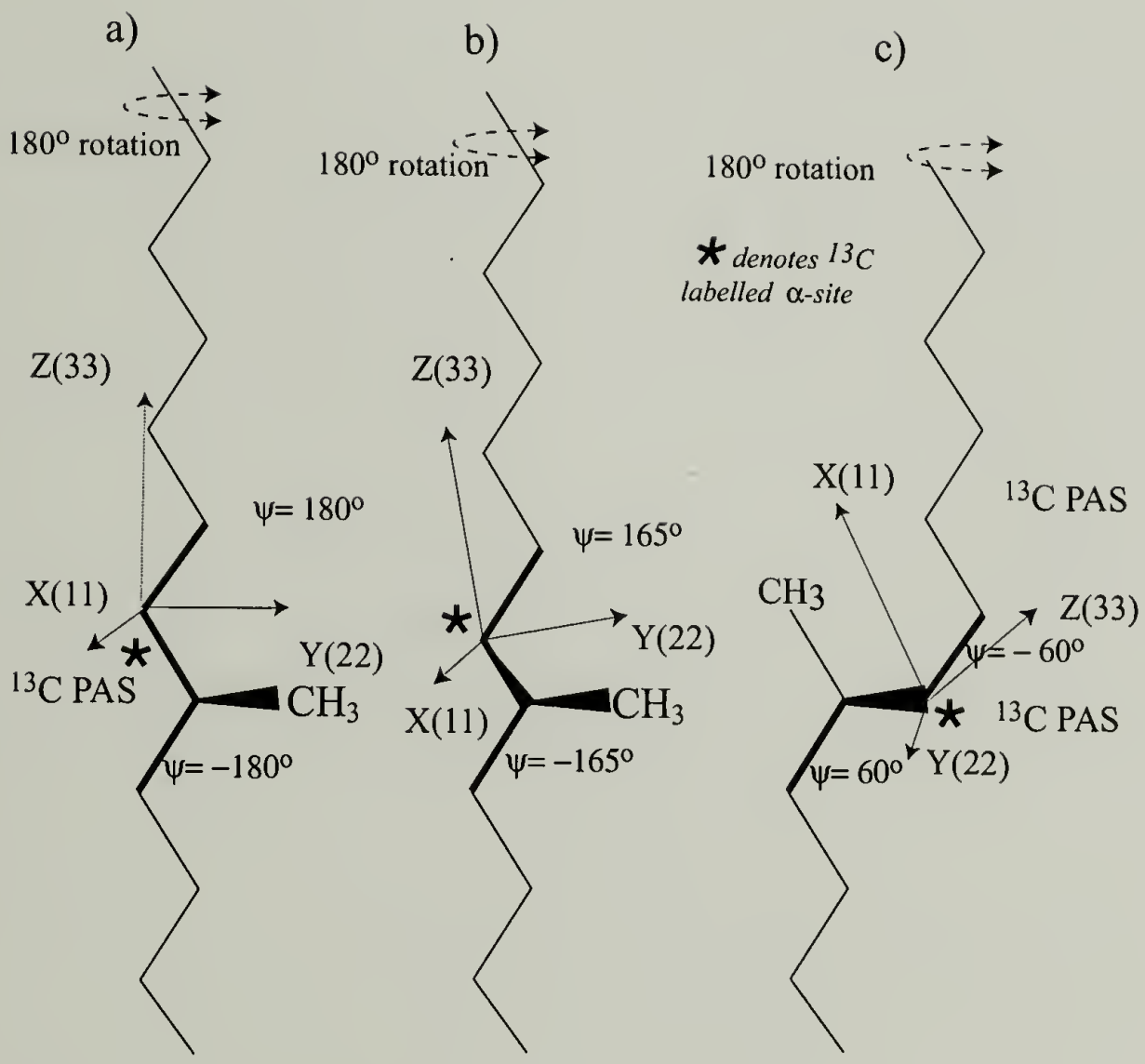

Figure 6.7. Model for the polymer chain conformation in the crystallite near a branch crystalline defect in ethylene-propene co-polymer; ψ: torsion angle; The stems on each side of the defect are parallel. The axis denotes the orientation of the principal-axes system (PAS) of the chemical shift tensor for the labeled α-methylene site. The PAS orientation in the molecular frame was drawn according to Schmidt-Rohr et al.[25]

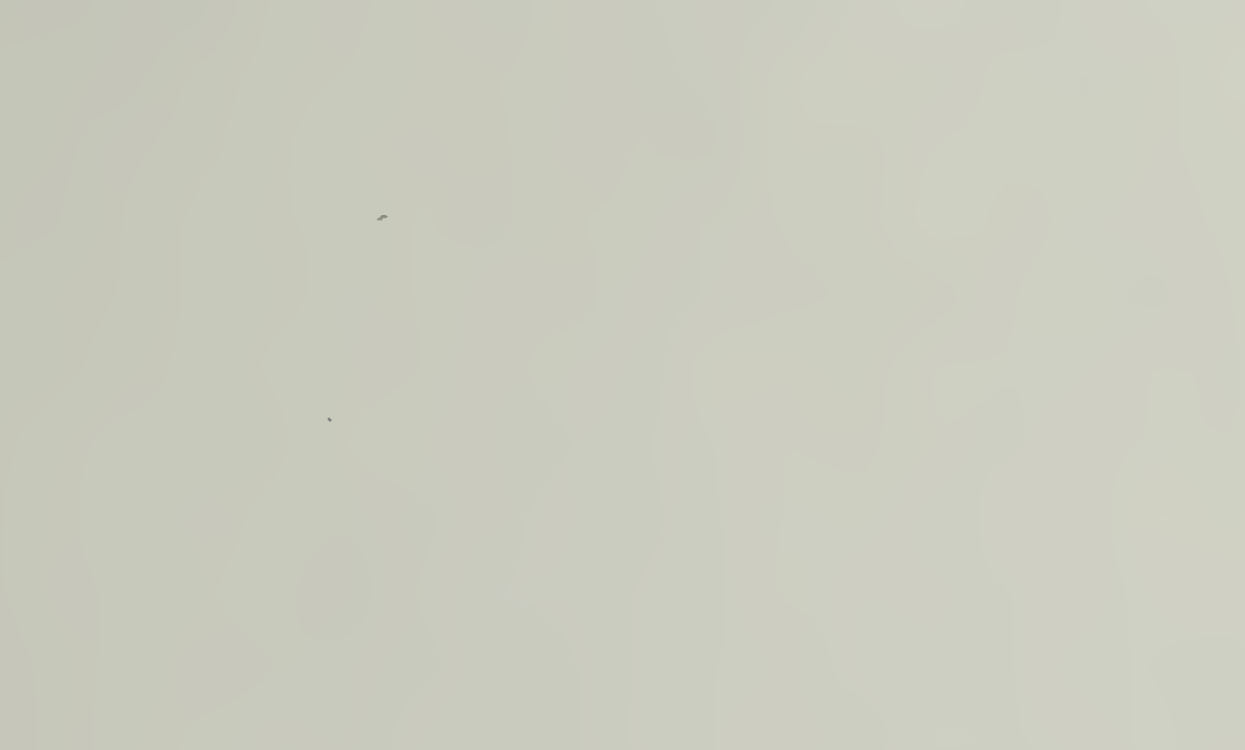

Figure 6.8. Normalized CODEX amplitude build-up for the crystalline propene α-site in PE-PrL as a function of δNt_r . Here I_α is normalized CODEX exchange intensity.The functional form of the ordinate axis $(1- I_\alpha)/4$ corresponds to 50% of crystalline defects undergoing two-site jumps.

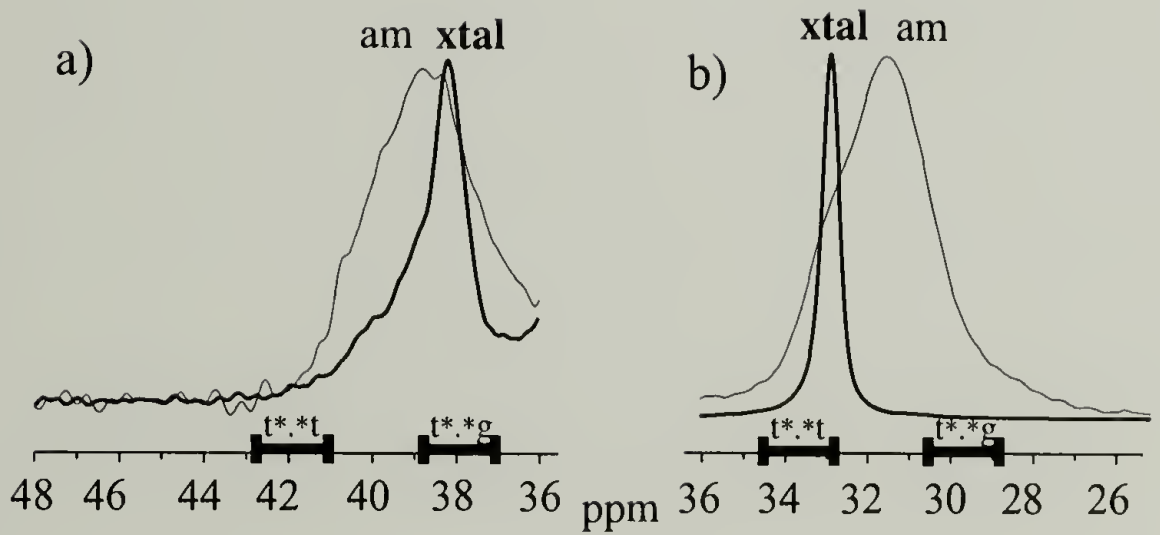

Figure 6.9 ^{13}C MAS spectra for PE-PrL, at 260 K to avoid motional broadening. —— crystalline signal CP/T_1 filtered ,t_f = 2s; —— amorphous signal; direct polarization with short recycle delay t_o =2s. (a) α-site methylene, (b) backbone methylene.The crystalline α-site signal is shifted upfield compared to the amorphous α-site resonance. Thist indicates higher gauche content in the vicinity of crystalline defects than in the disordered phase.[18]

a)

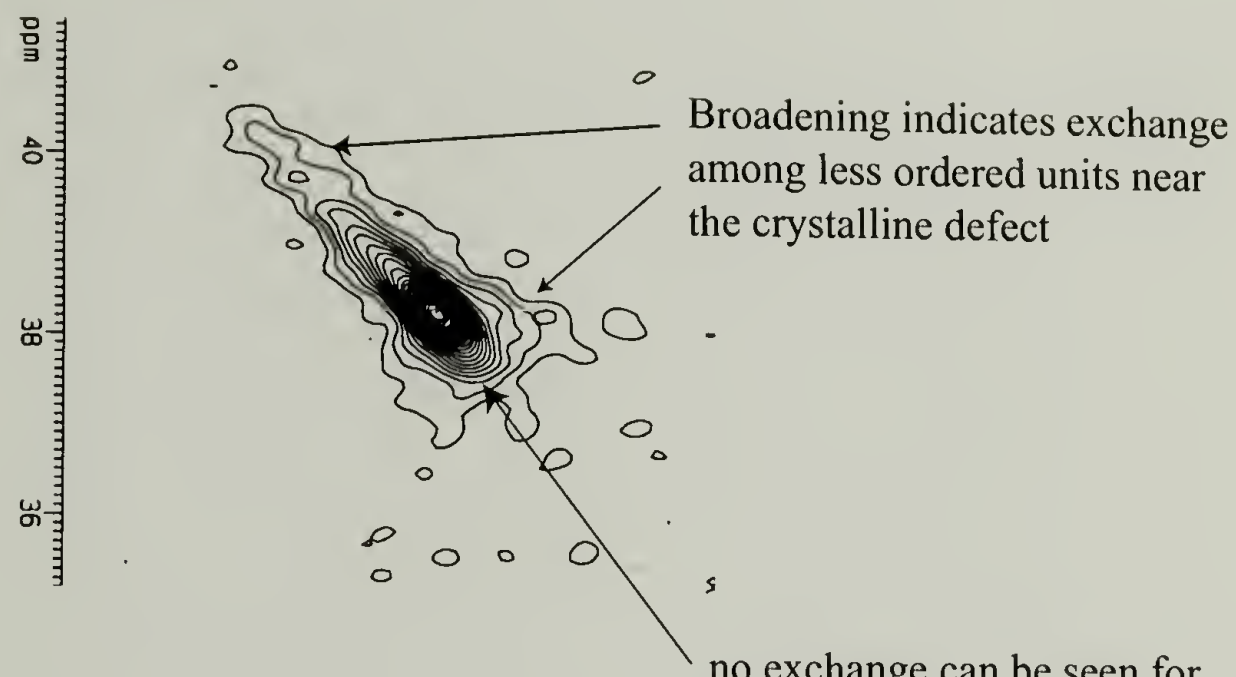

b)

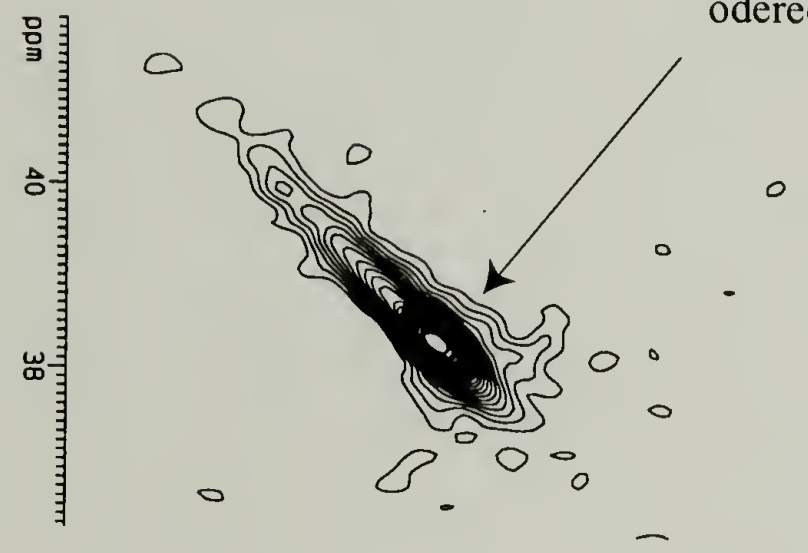

Figure 6.10 2D Exchange spectra of the crystalline α-site methylene in PE-PrL;
(a) t_m = 300 ms (b) t_m = 1 ms (reference)

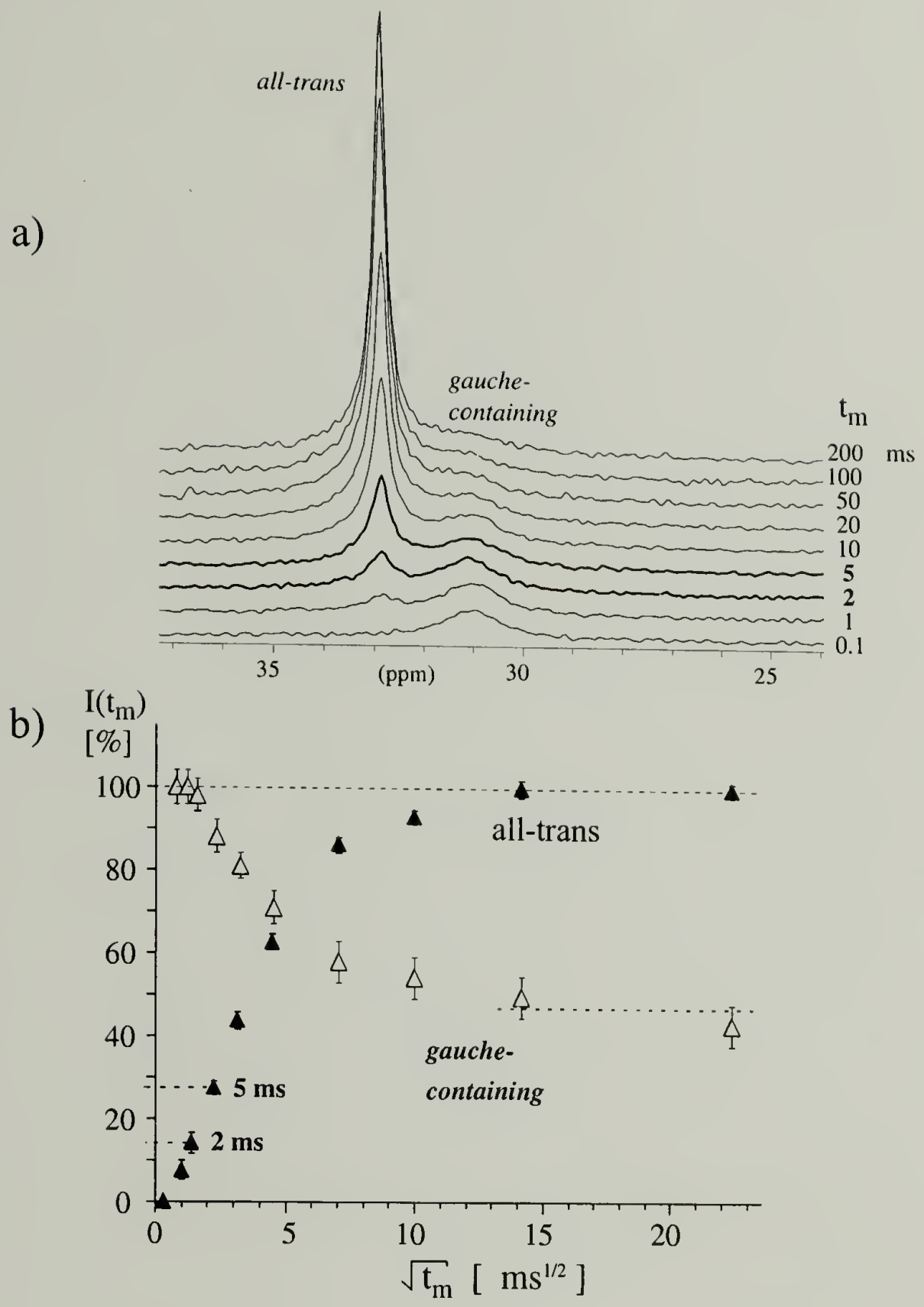

Figure 6.11 ^{1}H spin-diffusion with ^{13}C detection in PE-ZN b.q. Corresponding pulse sequence described in Fig.6.1a. t_f = 195 μs; CP =28μs. (a) Dependence ofthe ^{13}C lineshape on the mixing time t_m. t_m = 2 ms and 5 ms correspond to spin diffusion into the crystalline-amorphous interface. (b) Dependence of the normalized integral intensity of all-trans and gauche-containing components on the mixing time t_m.

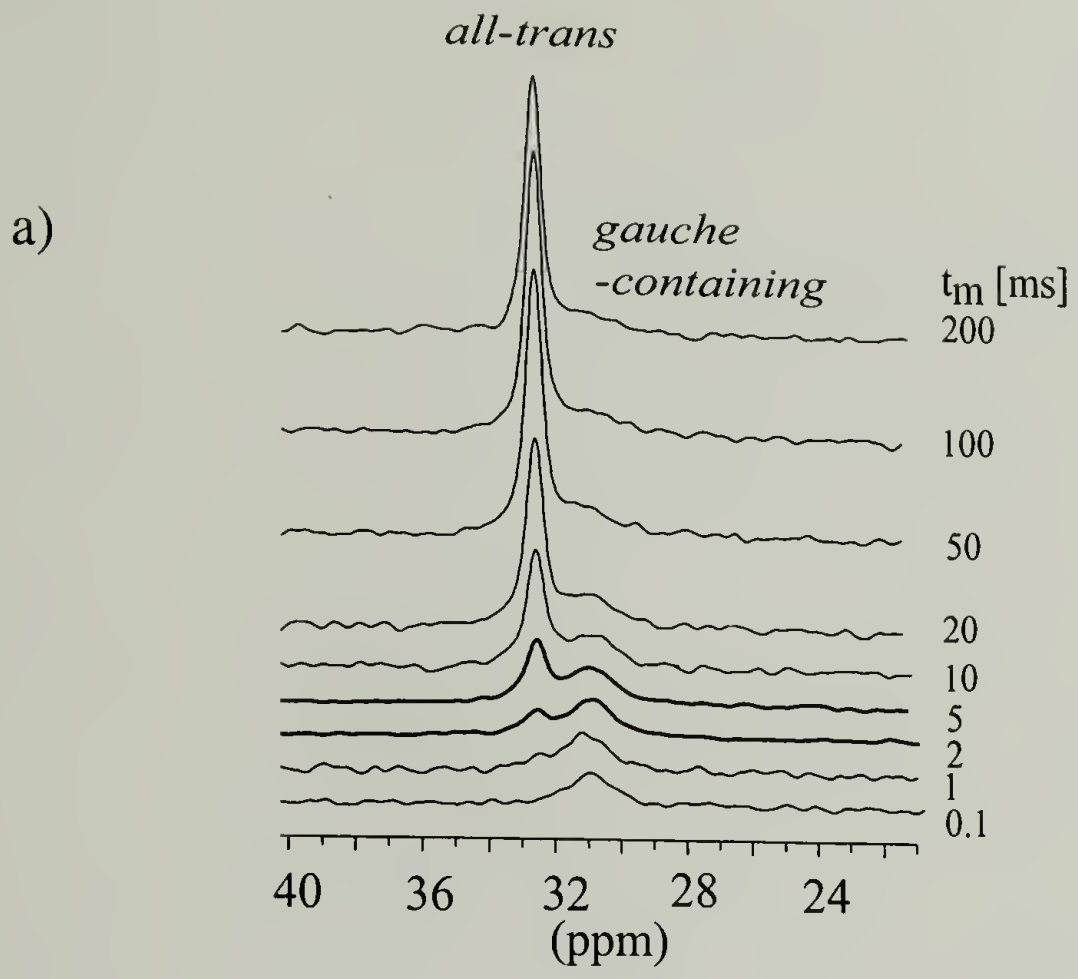

Figure 6.12 ^{1}H spin-diffusion with ^{13}C detection in PE-M b.q. Corresponding pulse sequence described in Fig.6.1a. t_f = 250 µs; CP =28µs. (a) Dependence of the ^{13}C lineshape on the mixing time t_m. t_m = 2 ms and 5 ms correspond to spin diffusion into the crystalline-amorphous interface. (b) Dependence of the normalized integral intensity of all-trans and gauche-containing components on the mixing time t_m.

a)

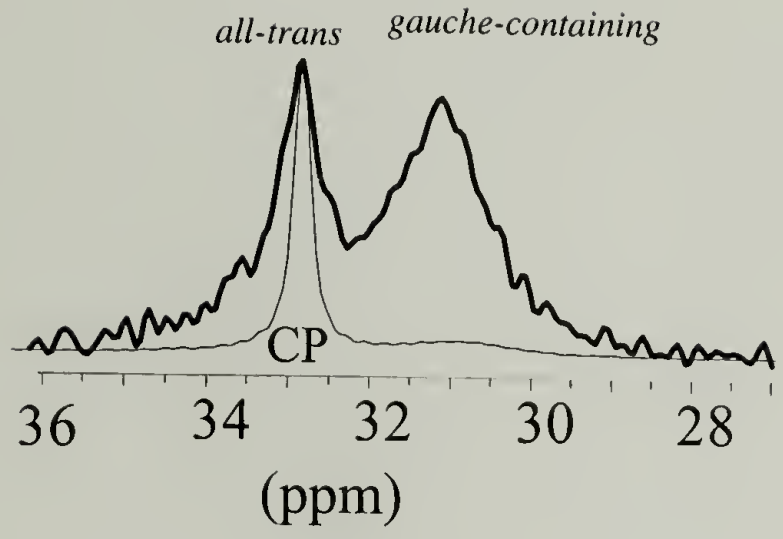

b)

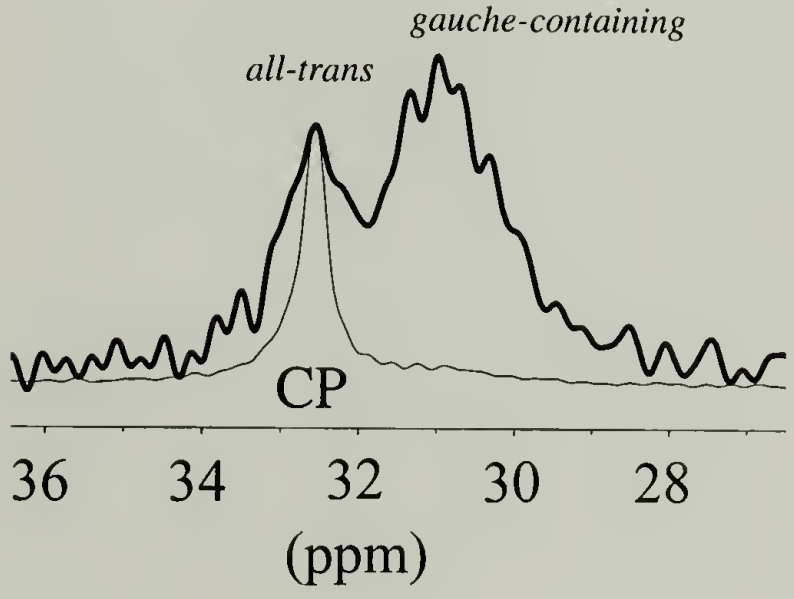

Figure 6.13 Interfacial (heavy line) vs. crystalline (thin line) lineshape in the methylene region . The interfacial signal was acquired using ^{1}H spin-diffusion with ^{13}C detection technique (Fig.6.1.a), t_m = 2 ms, CP=28 μs. The crystalline spectrum was obtained by cross-polarization. CP=28 μs. (a) PE-ZN b.q.; (b) PE-M b.q. The broad lineshape of the all-trans interfacial signal indicates that at the interface all-trans chains are surrounded by molecules in a disordered conformation.

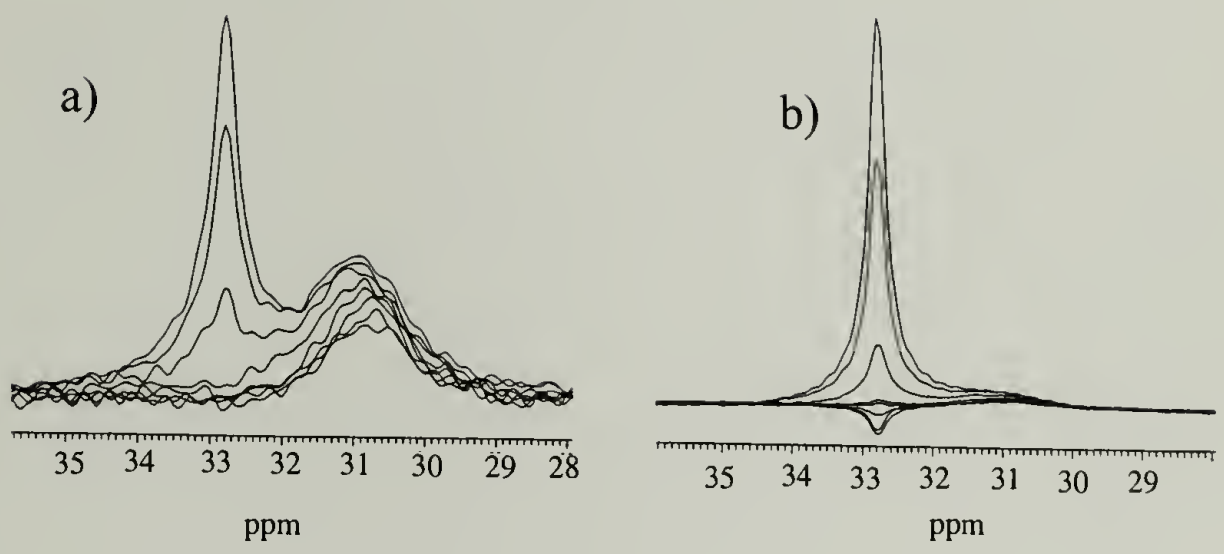

Figure 6.14 ^{1}H T_2 relaxation behavior in PE-ZN b.q. Spectra acquired using combined ^{1}H spin-diffusion - ^{1}H T_2 relaxation technique ; (Fig.6.1.b.) t_1 increments of 5ms were used in all measurements. (a) Interfacial component. t_f=195 μs; t_m = 5ms; CP=28μs. (b) Crystalline core (reference) t_f=1 μs; t_m = 5ms; CP=28μs (no ^{1}H T_2 selection). (c) ^{1}H T_2 relaxation curves for the interfacial component and core crystallites.

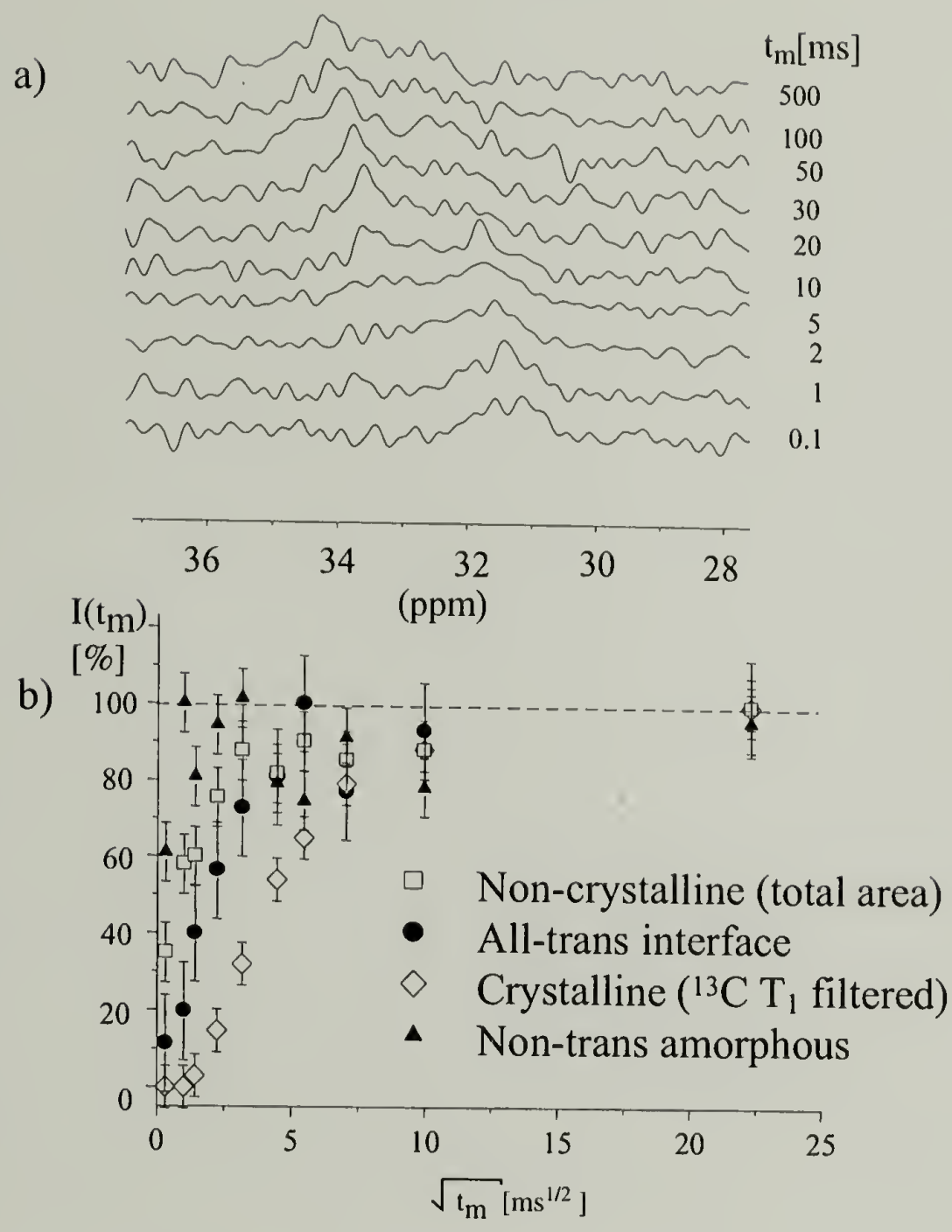

Figure 6.15 Investigation of the interfacial domain in PE-M b. q. using the combined ^{1}H spin-diffusion-^{13}C T_1 selection technique with ^{13}C detection (Fig.6.1.c). For each t_m two spectra were acquired: ^{13}C T_1 filtered crystalline spectrum (t_{fl} = 3s) and the reference spectrum (t_{fl} = 10 ms).
The difference (non-crystalline) spectrum was obtained by subtraction of the crystalline from the reference spectrum, without a scaling factor. The region 28.5-31.8 ppm in the non-crystalline spectrum corresponds to the disordered non-trans interface, the region 31.8-34.5 ppm - to the all-trans interfacial domain. (a) Dependence of the lineshape of the difference spectra on t_m.
(b) Dependence of the normalized integral intensity on t_m

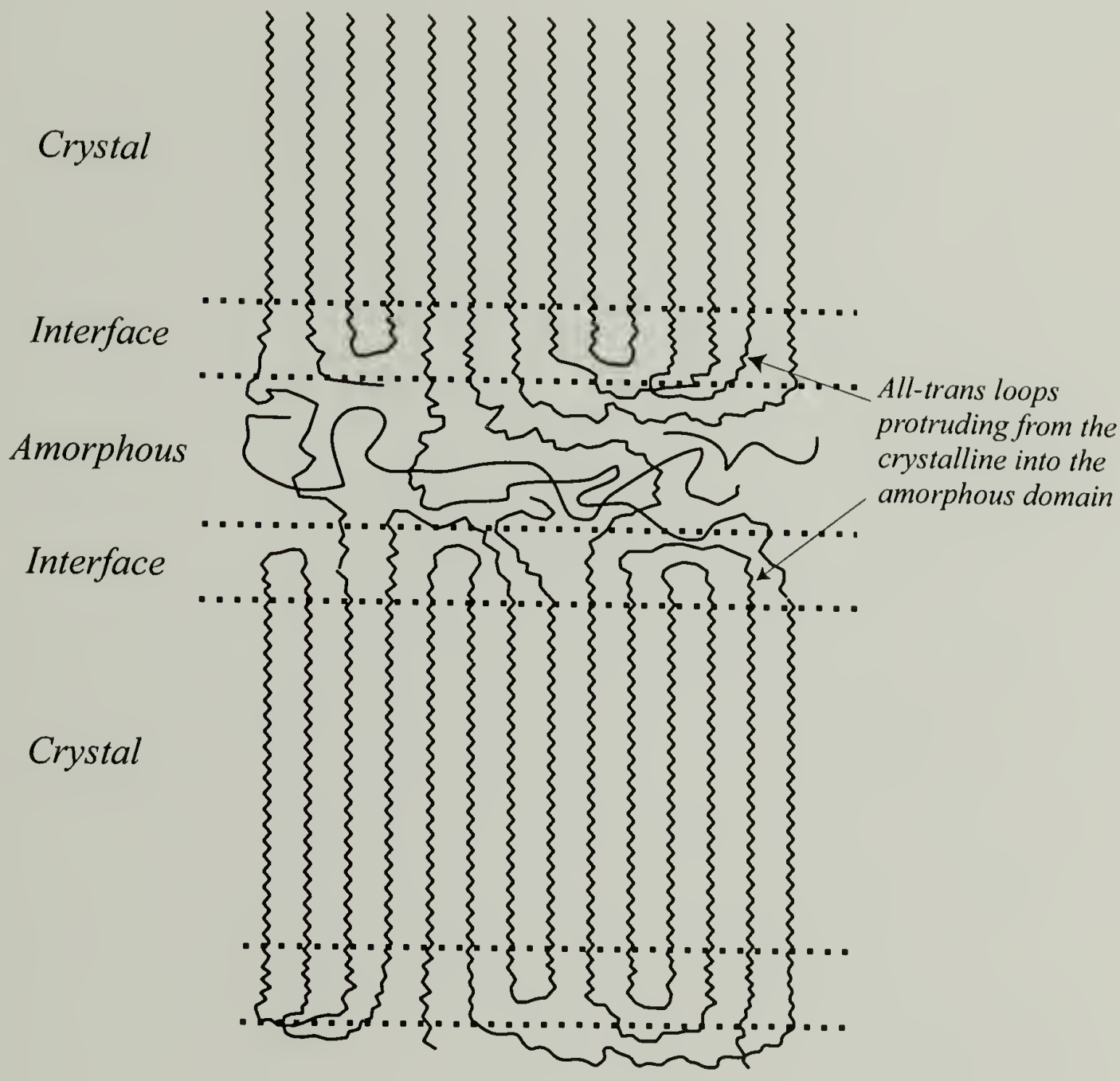

Figure 6.16 Proposed morphological structure of semi-crystalline ethylene co-polymers (branched units not shown).

CHAPTER 7

CONCLUSIONS AND PROPOSED SUBSEQUENT RESEARCH

The experimental work described in this thesis conclusively demonstrates the strong effects of the branch distribution on crystallization behavior, morphology and molecular mobility of LLDPEs. This chapter contains the specific conclusions drawn from each experimental chapter as well as some new questions and possible research avenues discovered in the course of thesis research.

7.1. Effect of Branch distribution on the evolution of viscoelastic properties of LLDPEs during isothermal and non-isothermal crystallization and partial melting

7.1.1 Conclusions

The experimental results of chapter 3 confirm that the intermolecular branch distribution controls the crystallization kinetics and the evolution of viscoelastic properties of LLDPEs during melting and crystallization.

Indeed, the heterogeneous Ziegler-Natta LLDPEs contain a significant fraction of molecules with very low branch content. These almost linear chains determine the behavior of heterogeneous LLDPEs during the melt-solid transition. In contrast, metallocene LLDPEs contain a variety of chains with gradually changing branching. As a result, the melting and solidification interval

may be broader for metallocene co-polymers than for their Ziegler-Natta analogs with similar or even higher average branching.

In heterogeneous LLDPEs, the long linear methylene sequences are found in the low branched chains, while the short methylene sequences are predominantly confined to highly branched molecules. In homogeneous metallocene LLDPEs long and short linear segments belong to the same molecules. During the non-isothermal crystallization of metallocene LLDPEs, the crystallites formed at high temperatures by long methylene sequences are covalently bound to the shorter linear sequences, which remain in the melt. The presence of the crystalline "anchors" decreases the mobility of short methylene sequences and limits their access to the centers of crystallization, so the crystallization of shorter segments becomes kinetically hindered. On the other hand, in heterogeneous systems the crystallization of long linear segments does not have a significant effect on the crystallization behavior of shorter methylene sequences. As a result, the effect of the thermal history on the crystallization behavior is more pronounced in metallocene than in Ziegler-Natta copolymers.

For the early stages of the isothermal crystallization of LLDPEs, the dependence of viscoelastic properties on the crystallinity ϕ was defined by correlating the rheological properties of the crystallizing melt with the crystallization kinetics measured by DSC. Based on the slope of the $G'(\phi)$ and $tan\delta(\phi)$ dependencies, three periods of the structure development in crystallizing LLDPEs were described: the initial structure formation

($0<\phi<0.002$), the development of a physical network ($0.002<\phi<\phi_{gel}$), and the tightening of the physical network ($\phi>\phi_{gel}$.). It was shown that for the isothermal crystallization of LLDPEs, the overall crystallinity at the melt-solid transition (gel point) is rather low, $\phi_{gel}< 5\%$ [w/w].

The thermal programs for the preparation of stable critical gels from the slightly crystallized LLDPEs by partial melting and step-crystallization were developed during this investigation. Mechanical properties of stable critical gels formed from the metallocene LLDPE were characterized by the steady-shear and dynamic rheological techniques. It was proven that the appearance of the "plateau region" in the *tan* $\delta(\omega)$ dependence indeed corresponds to the formation of physical structures in the crystallizing melt.

The stable critical gel prepared from the metallocene LLDPE by partial melting was characterized using Raman spectroscopy. It was shown that the crystallinity at the gel point does not exceed $5 \pm 3\%$ [w/w]. These results are consistent with the data obtained during the isothermal crystallization experiments.

7.1.2 Proposed further research.

There are several sets of experiments which are proposed to further map the factors controlling the relationship between the branch distribution and the solidification behavior of the ethylene co-polymers.

Commercial LLDPEs usually have a rather broad branch distribution; however, narrow-distributed LLDPE fractions can be prepared from the commercial samples using the preparative TREF (Temperature Raising Elution Fractionation) technique. The simple device for preparative TREF can be built from standard laboratory equipment.[1] The investigation performed on the narrow-distributed LLDPE fractions will allow to separate the effects of the overall branching on the solidification behavior from the influence of the branch distribution. Desired branch distributions can be created by blending several narrow-distributed LLDPE fractions with different branch content.

The type of the intermolecular branch distribution may be different in polymers manufactured by different companies. For instance, the intermolecular branch distribution in the metallocene ethylene-octene LLDPE, manufactured by DOW is distinctly bimodal. Thus the further investigation should include LLDPEs produced by DOW, Union Carbide, and Phillips.

The information about the morphology of physical gels near the critical point is paramount for the understanding of the mechanism of physical gelation in LLDPEs. However the structural investigation of critical and near-critical gels presents a significant challenge because of the low overall crystallinity at the gel point. The thermal protocols for the preparation of stable physical gels developed during this investigation allow to approach the critical gel from the solid side. The conclusions about the structure of physical gel may be made based on the evolution of the crystalline structure during partial melting. The

tendencies defined at lower temperatures can be extrapolated to the gel point. Because of the existing controversy in the assignment of Raman bands[2-3] the morphological investigation of the LLDPE during the partial melting has to be performed using a combination of Raman, solid-state NMR and WAXS experiments, performed under the identical thermal protocols.

7.2. Effect of the branch distribution on the morphology and local molecular mobility in LLDPEs

7.2.1 Conclusions

The experimental results obtained in the chapters 4 and 5 reveal the strong effect of the branch distribution on the morphology and molecular mobility in LLDPEs. Indeed, in highly heterogeneous Ziegler-Natta co-polymers the crystalline domain is enriched by almost linear chains, while the amorphous domain is formed by highly branched molecules. In contrast, in homogeneous metallocene systems both crystalline and amorphous domains are formed by segments belonging to the same chains. Consequently, in a metallocene co-polymer the average thickness of the crystalline and amorphous domains is lower, the rate of chain diffusion in the crystalline region is higher, and the molecular mobility in the amorphous domain is lower than in its Ziegler-Natta analog.

A novel non-destructive solid-state NMR technique for the determination of the lamellar thickness distribution in non-polar ethylene co-polymers was developed, its validity was proven by comparison with the results of SAXS,

Raman and independent NMR investigations.

7.2.2 Proposed further research

The morphological structure controls various important macroscopic properties in LLDPEs. Thus, the qualitative understanding of the tendencies in the branch distribution-morphology relationship established in Chapters 4 and 5 may be very useful for the successful optimization of ethylene co-polymers.

Further investigations should bring the understanding of the effects of the branch distribution on the LLDPE morphology to the more quantitative level. This can be accomplished by expanding the range of samples under investigation. For instance, different types of co-monomers and various types of branch distributions occurring in commercial LLDPEs should be investigated using the assortment of techniques successfully applied in this study. All studied samples have to be characterized by analytic TREF, so the corresponding branch distributions will be known in great detail.

A variety of blends with desired branch distributions can be prepared from narrow-distributed LLDPE fractions. Investigation of such "artificial LLDPEs" will enable researchers to answer a variety of questions related to the branching-morphology relationship.

Another important direction in the investigation of LLDPEs is the relationship between the branch distribution and macroscopic properties. Using solid-state NMR techniques, the molecular mechanisms determining the

relationship between the morphology and mechanical properties of LLDPEs can be characterized. Then, the effect of the branch distribution on the molecular mobility and on the local morphology can be correlated with the influence of the branch distribution on the mechanical properties of LLDPEs.

7.3. Morphological partitioning of branched units and structure of the interfacial domain in LLDPEs

7.3.1 Conclusions

Using solid-state NMR techniques based on ^{1}H spin diffusion with ^{13}C detection, it was proven that a developed crystalline-amorphous interface exists in LLDPEs. The average thickness of the interfacial domain both in metallocene and in Ziegler-Natta LLDPE was estimated as 10-15% of the average crystallite thickness. For the first time, a resolved ^{13}C NMR signal related to the interfacial domain was observed. Based on the chemical shift and on the lineshape of the interfacial signal, it was shown that the interfacial domain is predominantly formed by all-trans yet partially mobile chains. It was proposed that all-trans chains form loops, which protrude from the crystalline into the amorphous domain in a comb-like fashion.

Using a combined ^{1}H spin-diffusion-^{13}C selection technique it was proven that the structure of the interfacial domain is rather heterogeneous. It contains both all-trans and disordered regions.

The morphologieal partitioning of branehed units was studied using WAXS and solid-state NMR teehniques. It was determined that 20 % of propene segments are ineluded into the erystalline phase, while no evidenee of the inelusion of butyl branches into the crystalline lattiee was found. The loeal ehain eonformation in the vieinity of erystalline braneh defeets in the ethylene-propene eo-polymer was eharaeterized using 2D exehange, ^{13}C direet polarization, CP T_1 selection and CODEX teehniques. It was shown that erystalline defeets may not be deseribed in a satisfaetory way by the simple 3-bond model. Based on the results of 2D-exehange and CODEX experiments, it was proposed that the adequate model should account for the distribution of ehain conformations and motional modes.

7.3.2 Proposed further researeh

The experimental results of ehapter 6 prove that valuable information about the interfaeial structure may be obtained by solid-state NMR teehniques, based on ^{1}H spin-diffusion. However, the factors affeeting the interfaeial structure in LLDPEs still are not understood in a great detail.

As the next step, the influenee of the braneh eontent and braneh distribution on the interfaeial content and structure of the interfaeial domain ean be studied. This can be aeeomplished by expanding the range of samples studied, so it will include a variety of eo-monomers and branch distributions. By using narrow-distributed LLDPE fractions manufactured by preparative TREF it

will be possible to separate the effect of the overall branching on the interfacial structure from the influence of the branch distribution.

Another important subject for future investigations is the relationship between the content and the structure of the interfacial domain and the mechanical properties of LLDPEs. Thus, during the future studies the phase composition has to be correlated with the mechanical characteristics of LLDPEs, such as modulus, toughness and crack resistance.

The solid-state NMR investigation involving ^{13}C labeling is a very efficient approach for the direct characterization of the morphological partitioning of branched units. While the inclusion of methyl branches into the crystalline lattice was proven by a variety of techniques, the morphological partitioning of ethyl branches in LLDPEs still remains a subject of controversy.[4-5] The ^{13}C signal for the methyne carbon at the branch site is well resolved from the methylene backbone signal. By using ethylene-butene co-polymer ^{13}C-labeled at the methyne site, the morphological partitioning of the ethyl branches can be determined with great precision.

During the current study, it was shown that the local structure of the crystalline branch defects is rather complex, so the morphological models used in the further investigations should account for the distribution of chain conformations in the vicinity of the branch defects. A higher degree of ^{13}C labeling (20-30%) will allow to enhance the sensitivity in the NMR experiments and to obtain more information about the crystalline defect structure.

7.4 References

1. Francuskiewicz, F. *Polymer fractionation*; Springer-Verlag: Berlin ; NY, 1994.

2. Naylor, C. C.; Meier, R. J.; Kip, B. J.; Williams, K. P. J.; Mason, S. M.; Conroy, N.; Gerrard, D. L."Raman Spectroscopy Employed for the Determination of the Intermediate Phase in Polyethylene." *Macromolecules*, **28**, 2969 (1995).

3. Mandelkern, L.; Alamo, R. G.; M.A.Kennedy."Comments on Paper "Raman Spectroscopy Employed for the Determination of the Intermediate Phase in Polyethylene"." *Macromolecules*, **28**, 2988 (1995).

4. Alamo, R.G.; Mandelkern, L."The crystallization behavior of random copolymers of ethylene." *Thermochimica Acta*, **238**, 155 (1994).

5. VanderHart, D.L.; Perez, E."A ^{13}C NMR Method for Determining the Partitioning of End Groups and Side Branches between the Crystalline and Noncrystalline Regions in Polyethylene." *Macromolecules*, **19**, 1902 (1986).

BIBLIOGRAPHY

Adisson, A.; Ribeiro, M.; Deffieux, A.; Fontanille, M."Evaluation of the heterogeneity in linear low-density polyethylene comonomer unit distribution by differential scanning calorimetry characterization of thermally treated samples." *Polymer*, **33**, 4337 (1992).

Akpalu, Y.; Kielhorn, L.; Hsiao, B. S.; Stein, R. S.; Russell, T. P.; VanEgmond, J.; Muthukumar, M."Structure development during crystallization of homogeneous copolymers of ethene and 1-octene: Time-resolved synchrotron X-ray and SALS measurements." *Macromolecules*, **32**, 765 (1999).

Alamo, R.; Domszy, R.; Mandelkern, L."Thermodynamic and Structural Properties of Copolymers of Ethylene." *J. Phys Chem*, **88**, 6587 (1984).
Alamo, R.; Mandelkern, L."Origins of Endothermic Peaks in Differential Scanning Calorimetry." *J. Polym Sci. B. Polym. Phys*, **24**, 2087 (1986).

Alamo, R.; Mandelkern, L."Origins of Endothermic Peaks in Differential Scanning Calorimetry." *J.Polymer Science B:Polymer Phys.*, **24**, 2087 (1986).

Alamo, R. G.; Chan, E. K. M.; Mandelkern, L."Influence of Molecular Weight on the Melting and Phase Structure of Random Copolymers of Ethylene." *Macromolecules*, **25**, 6381 (1992).

Alamo, R. G.; Graessley, W. W.; Krishnamoorti, R.; Loshe, D. J.; Londono, J. D.; Mandelkern, L.; Stehling, F. C.; Wignall, G. D."Small Angle Neutron Scattering Investigations of Melt Miscibility and Phase Segregation in Blends of Linear and Branched Polyethylenes as a Function of the Branch Content." *Macromolecules*, **30**, 561 (1997).

Alamo, R. G.; L.Mandelkern."Thermodynamic and Structural Properties of Ethylene Copolymers." *Macromolecules*, **22**, 1273 (1989).

Alamo, R. G.; Londono, J. D.; Mandelkern, L.; Stehling, F. C.; Wignall, G. D."Phase Behavior of Blends of Linear and Branched Polyethylenes in the Molten and Solid States by Small-Angle Neutron-Scattering." *Macromolecules*, **27**, 411 (1994).

Alamo, R. G.; Mandelkern, L."The crystallization behavior of random copolymers of ethylene." *Thermochimica Acta*, **238**, 155 (1994).
Alamo, R. G.; Viers, B. D.; Mandelkern, L."Phase Structure of Random Ethylene Copolymers: A Study of Counit Content and Molecular Weight as Independent Variables." *Macromolecules*, **26**, 5740 (1993).

Albrecht, T.; Strobl, G."Temperature-Dependent Crystalline-Amorphous Structures in Linear Polyethylene: Surface Melting and the Thickness of the Amorphous Layers." *Macromolecules*, **28**, 5827 (1995).

Alizadeh, A.; Richardson, L.; Xu, J.; McCartney, S.; Marand, H."Influence of Structural and Topological Constraints on the Crystallization and Melting Behavior of Polymers. 1.Ethylene/1-Octene Copolymers." *Macromolecules*, **32**, 6221 (1999).

Armistead, K.; G.Goldbeck-Wood."Polymer Crystallization Theories." *Advances in Polymer Science*, **100**, 223 (1992).

Ashcraft, C. R.; Boyd, R. H."A Dielectric Study of Molecular Relaxation in Oxidized and Chlorinated Polyethylenes." *Journal of Polymer Science: Polymer Physics*, **14**, 2153 (1976).

Axelson, D. E."Crystalline Order in Polyethylene: A ^{13}C NMR CP/MAS Solid-State T_1 study." *J. Polym. Sci: Polym.Phys.*, **20**, 1427 (1982).

Axelson, D. E.; Levy, G. C.; Mandelkern, L."A Quantitative Analysis of Low-Density (Branched) Polyethylenes by Carbon-13 Fourier Transform Nuclear Magnetic Resonance at 67.9 MHz." *Macromolecules*, **12**, 41 (1979).

Axelson, D. E.; Mandelkern, L.; Levy, G. C."^{13}C Spin Relaxation Parameters of Branched Polyethylenes. Ramification of Quantitative Analysis." *Macromolecules*, **10**, 557 (1977).

Axelson, D. E.; Mandelkern, L.; Popli, R.; Mathieu, P."Carbon-13 NMR of Polyethylenes: Correlation of the Crystalline Component T1 with Structure." *J. Polym.Sci: Polym. Phys*, **21**, 2139 (1983).

Baker, C. H.; Mandelkern, L."The Crystallization and Melting of Copolymers II-Variations in Unit-cell Dimensions in Polymethylene Copolymers." *Polymer*, **7**, 71 (1966).

Balbontin, G.; Camurati, I.; Dalll'Occo, T.; Finotti, A."Determination of 1-Butene distribution in LLDPE by DSC analysis after thermal fractionated crystallization." *Angew. Makromol. Chem.*, **219**, 139 (1994).

Balta-Calleja, F. J.; Vonk, C. G. *X-ray scattering of synthetic polymers*; Elsevier: NY, 1989.

Banks, W.; Gordon, M.; Sharples, A."The Crystallization of Polyethylene after Partial Melting." *Polymer*, **4**, 289 (1963).

Bark, M.; Zachmann, H. G.; Alamo, R.; Mandelkern, L."Investigations of the crystallization of polyethylene by means of simultaneous small-angle and wide-angle X-ray scattering." *Makromol. Chem,*, **193**, 2363 (1992).

Bassett, D. C. *Principles of Polymer Morphology*; Cambridge University Press: Oxford, 1981.

Bassett, D. C.; Hodge, A. M."On the morphology of melt-crystallized polyethylene II. Lamellae and their crystallization conditions." *Proc.Roy.Soc.*, **A377**, 39 (1981).

Baumgaertel, M.; Winter, H. H."Interrelation between continious and discrete relaxation time spectra." *Journal of Non-Newtonian Fluid Mechanics*, **44**, 15 (1992).

Bensason, S.; Minick, J.; Moet, A.; Chum, S.; Hiltner, A.; Baer, E. "Classification of Homogeneous Ethylene-Octene Copolymers Based on Comonomer Content." *J. Polym.Sci., B: Polym.Phys.*, **34**, 1301 (1996).

Boutahar, K.; Carrot, C.; Guillet, J."Crystallization of Polyolefins from Rheological Measurements-Relation between the transformed fraction and dynamic moduli." *Macromolecules*, **31**, 1921 (1998).

Boyd, R. H."Relaxation process in crystalline polymers: Molecular interpretation -a review." *Polymer*, **26**, 1123 (1985).

Boyd, R. H.; Billiyar, K."The effect of melting on the alpha relaxation process in some crystalline polymers." *Polymer pre-prints*, 329 (1973).

Brown, G. M.; Butler, J. H."New method for the characterization of domain morphology of polymer blends using ruthenium tetroxide staining and low voltage scanning electron microscopy (LVSEM)." *Polymer*, **38**, 3937 (1997).

Bunn, C. W.; Renffew, A.; Morgan, P. . In *Polyethylene;* Illife Ed.: London, 1975.

Chambon, F.; Winter, H. H."Stopping of Crosslinking Reaction in a PDMS Polymer at the Gel Point." *Polymer Bull.*, **13**, 499 (1985).

Chambon, F.; Winter, H. H."Linear Viscoelasticity at the Gel Point of a Crosslinking PDMS with imbalanced Stochiometry." *Journal of Rheology*, **31**, 683 (1987).

Channel, A. D.; Clutton, E. Q.; Capaccio, G."Phase segregation and impact toughness in linear low density polyethylene." *Polymer*, **35**, (1994).

Channell, A. D.; Clutton, E. Q."The effect of short chain branching and molecular weight on the impact toughness of polyethylene." *Polymer*, **33** (1992).

Cheung, T. T. P.; Gerstein, B. C."^{1}H nuclear magnetic resonance studies of domain structures in polymers." *J.Appl.Phys.*, **52**, 5517 (1981).

Colquhoun, I. J.; Packer, K. J."Nuclear Magnetic Resonance in Solid Ethylene/α-Olefin Copolymers: Relaxation, Spin-diffusion and Lamellar Widths." *British Polymer Journal*, **19**, 151 (1987).

Crist, B."Small-Angle X-ray Scattering of Semicrystalline Polymers. I. review of Existing Models." *J.Polym.Sci., Polym.Phys.Edn*, **11**, 635 (1973).

Crist, B.; Hill, M. J."Recent Developments in Phase Separation of Polyolefin Melt Blend." *J.Polym.Sci.,B:Polym. Phys.*, **35**, 2329 (1997).

Crist, B.; Rhee, J. Polyethylene-copolymer model blends: morphology and mechanical properties. In *New Advances in Polyolefins;* Chung, T. C. Ed.; Plenum Press: NY, 1993.

Cudby, M. E. A.; Packer, K. J.; Hendra, P. J."Proton n.m.r. spin-lattice relaxation in the rotating frame and the thickness of the crystalline lamellae in some polyethylenes." *Polymer Communications*, **25**, 303 (1984).

Davis, G. T.; Weeks, J. J.; Martin, G. M.; Eby, R. K."Cell Dimensions of hydrocarbon crystals: Surface effects." *J.Appl.Phys.*, **45** (1974).

deAzevedo, E. R.; Hu, W.-G.; Bonagamba, T. J.; Schmidt-Rohr, K. "Centerband-Only detection of Exchange: Efficient Analysis of Dynamics in solids by NMR." *JACS*, **121**, 8411 (1999).

Defoor, F.; Groenickx, G.; Reynaers, H.; Schouterden, P.; Heijden, B. V. D."Thermal and Morphological Characterization of Binary Blends of Fractions of 1- Octene LLDPE." *J. Appl. Polym. Sci*, **47**, 1839 (1993).

Djabourov, M."Gelation-A Review." *Polymer International*, **25**, 135 (1991). Doi, M.; Edvards, S. F. *The Theory of Polymer Dynamics*; Clarendon Press: Oxford, 1995.

Dunbar, M. G.; Novak, B. M.; Schmidt-Rohr, K."Trans content in atactic polystyrene estimated by double-quantum solid-state NMR." *Solid State Nuclear Magnetic Resonance*, **12**, 119 (1998).

Eby, R. K."Determination of the Propagation Constants for Ultrasonic Waves in Melting and Molten Polyethylene." *The Journal of The Acoustical Society of America*, **36**, 1485 (1964).

Flory, P. J."Thermodynamics of Crystallization in High Pollymers IV. A Theory of Crystalline States and Fusion in Polymers,Copolymers, and Their Mixtures with Diluents." *J. Chem. Phys.*, **17**, 223 (1947).

Flory, P. J."Theory of Crystallization in Copolymers." *Trans Far Soc.*, **51**, 848 (1955).

Flory, P. J.; Yoon, D. Y.; Dill, K. A."The Interphase in Lamellar Semicrystalline Polymers." *Macromolecules*, **17**, 862 (1984).

Francuskiewicz, F. *Polymer fractionation*; Springer-Verlag: Berlin ; NY, 1994.

Fu, Q.; Chiu, F.-C.; McCreight, K. W.; Guo, M.; Tseng, W. W.; Cheng, S. Z. D.; Keating, M. Y."Effects of the Phase-separated Melt on Crystallization Behavior and Morphology in Short Chain Branched Metallocene Polyethylenes." *J. Macromol.Sci.,Phys.*, **B36**, 41 (1997).

Gaber, B. P.; Peticolas, W. L."On the Quantitative Interpretation of Biomembrane Structure by Raman Spectroscopy." *Biochimica et Biophysica Acta*, **465**, 260 (1977).

Gabriel, C.; Kaschta, J."Comparison of different shear rheometers with regard to creep and creep recovery measurements." *Rheologica Acta*, **37**, 358 (1998).

Gabriel, C.; Munstedt, H."Creep recovery behavior of metallocene linear low-density polyethylenes." *RHEOLOGICA ACTA*, **38**, 393 (1999).

Gelfer, M.; Beyer, F.; Gido, S. P.; Alamo, R.; Schmidt-Rohr, K."Polyethylene Crystallite Thickness Distribution from 1H NMR Relaxation, Calibrated by Electron Microscopy and Raman LAM." *Submitted to Macromolecules*

Gelfer, M.; Schmidt-Rohr, K."Investigation of Morphology and Molecular Mobility in Ethylene-Hexene Copolymers by Solid-State NMR." *Abstr. Papers Amer. Chem. Soc.*, **217**, 266 (1999).

Gelfer, M. Y.; Winter, H. H."Effect of branch distribution on rheology of LLDPE during early stages of crystallization." *Macromolecules*, **32**, 8974 (1999).

Gillet, S.; Delpuech, J.-J."Optimum Conditions for Nondestructive Quantitative Analysis by Carbon-13 NMR." *Journal of Magnetic Resonance*, **38**, 443 (1980).

Goldman, M.; Shen, L."Spin-Spin Relaxation in LaF_3." *Phys.Rev.*, **144**, 321 (1966).

Harris, D. J.; Bonagamba, T. J.; K.Schmidt-Rohr."Conformation of Poly(ethylene oxide) Intracalated in Clay and MoS_2 Studied by Two-Dimensional Double-Quantum NMR." *Macromolecules*, 1436 (1999).

Hashemi, S.; Williams, J. G."A fracture toughness of low density and linear low density polyethylenes." *Polymer*, **27**, 384 (1986).

Hausner, G.; Schmidtke, J.; Strobl, G. "The Role of Co-Units in Polymer Crystallization and Melting: New Insights from Studies on Syndiotactic Poly(propene-co-octene)." *Macromolecules*, **31**, 6251 (1998).

Hess, W.; Vilgis, T. A.; Winter, H. H."Dynamic Critical Behavior during Chemical Gelation and Vulcanization." *Macromolecules*, **21**, 2536 (1988).

Hill, M. J.; Barham, P. J."Liquid-liquid phase separation in melts of blends of linear with branched polyethylenes: morphological exploration of the phase diagram." *Polymer*, **33**, 4099 (1992).

Hill, M. J.; Barham, P. J."Absence of phase separation effects in blends of linear polyethylene fractions of different molecular weight." *Polymer*, **36**, 1523 (1995).

Hill, M. J.; Barham, P. J."Liquid-liquid phase separation in blends containing copolymers produced using metallocene catalysts." *Polymer*, **38**, 5595 (1997).

Hill, M. J.; Barham, P. J."Morphology maps of binary blends of copolymers produced using the metallocene catalyst process." *Polymer*, **41**, 1621 (2000).

Hill, M. J.; Barham, P. J.; Keller, A."Phase segregation in blends of linear with branched polyethylene: the effect of varying the molecular weight of the linear polymer." *Polymer*, **33**, 2530 (1992).

Hill, M. J.; Barham, P. J.; Keller, A.; Rosney, C. C. A."Phase segregation in melts of blends of linear and branched polyethylene." *Polymer*, **32**, 1384 (1991).

Hill, M. J.; Morgan, R. L.; Barham, P. J."Minimum branch content for detection of liquid-liquid phase separation , using indirect techniques, in blends of polyethylene with ethylene-octene and ethylene-butene copolymers." *Polymer*, **38**, 3003 (1997).

Hingmann, R.; Rieger, J.; Kersting, M."Rheological Properties of a Partially Molten Polypropylene Random Copolymer During Annealing." *Macromolecules*, **28**, 3801 (1995).

Hlatky, G. G."Metallocene catalysts for olefin polymerization - Annual review for 1996." *Coordination Chemistry Reviews*, **181**, 243 (1999).

Horst, R. H.; Winter, H. H."Stable critical gels of a crystallizing copolymer of ethene and 1-butene." *Macromolecules*, **33**, 130 (2000).

Hosoda, S."Structural Distribution of Linear Low-Density Polyethylenes." *Polymer Journal*, **20**, 383 (1988).

Hosoda, S.; Nomura, H.; Gotoh, Y.; Kihara, H."Degree of branch inclusion into the lamellar crystal for various ethylene /α-olefin copolymes." *Polymer*, **31**, 1999 (1990).

Hosoda, S.; Uemura, A."Effect of the Structural Distribution on the Mechanical Properties of Linear Low-Density Polyethylenes." *Polymer Journal*, **24**, 939 (1992).

Howard, P. R.; Crist, B."Unit Cell Dimensions in Model Ethylene-Butene-1 Copolymers." *J.Polym.Sci.,B:Polym.Phys*, **27**, 2269 (1989).

Hsieh, E. T.; Randall, J. C."Ethylene-1-Butene Copolymers. 1. Comonomer Sequence Distribution." *Macromolecules*, **15**, 353 (1982).

Hsieh, E. T.; Randall, J. C."Monomer Sequence Distributions in Ethylene-1-Hexene Copolymers." *Macromolecules*, **15**, 1402 (1982).

Hu, S.-R.; Kyu, T.; Stein, R. S."Characterization and Properties of Polyethylene Blends I. Linear Low-Density Polyethylene with High-Density Polyethylene." *J.Polym.Sci.,B: Polym.Phys.*, **25**, 71 (1987).

Hu, W. G.; Boeffel, C.; Schmidt-Rohr, K."Chain Flips in Polyethylene Crystallites and Fibers Characterized by Dipolar ^{13}C NMR." *Macromolecules*, **32**, 1611 (1999).

Hu, W.-G.; Schmidt-Rohr, K."Characterization of ultradrawn polyethylene fibers by NMR: crystallinity, domain sizes and a highly mobile second amorphous phase." *Polymer*, **41**, 2979 (2000).

Huang, J.; Prasad, A.; Marand, H."Study of the temperature dependence of isothermal spherulitic growth rate data for poly(pivalactone) in blends with poly(vinylidene fluoride): a link between coherent secondary nucleatio theory and mixing thermodynamics." *Polymer*, **35**, 1896 (1984).

Huang, Y.-L.; Brown, N."Dependence of Slow crack Growth in Polyethylene on Butyl Branch Density: Morphology and Theory." *J.Polym.Sci.,B:Polym.Phys*, **29**, 129 (1991).

Jackson, J. B.; Flory, P. J.; Chaing, R.; Richardson, M. J."Shear modulus in Relation to Crystallinity in Polymethylene and its copolymers." *Polymer*, **4**, 237 (1963).

Kaminsky, W."New polymers by metallocene catalysis." *Macromol. Chem.Phys.*, **197**, 3907 (1996).

Kavanagh, G. M.; Ross-Murphy, S. B."Rheological Characterization of Polymer Gels." *Prog.Polym.Sci.*, **23**, 533 (1998).

Keating, M. Y.; McCord, E. F."Evaluation of the comonomer distribution in ethylene copolymers using DSC fractionation." *Thermochimica Acta*, **243**, 129 (1994).

Keller, A.; Machin, M. J."Oriented Crystallization in Polymer." *J. Macromol. Sci.,Phys.*, **B1**, 41 (1967).

Kilian, H. G."Small-strain elastic moduli of quasi-isotropic semicrystalline eutecoid copolymers and aspects of universality." *Colloid and Polymer Sci*, **262**, 374 (1984).

Kim, M. H.; Phillips, P. J."Nonisothermal Melting and Crystallization Studies of Homogeneous Ethylene/a-olefin Random Copolymers." *Journal Applied Polymer Science*, **70**, 1893 (1998).

Kim, M. H.; Phillips, P. J.; Lin, J. S."The equilibrium melting points of random ethylene-octene copolymers: A test of Flory and Sanchez-Eby theories." *J.Polym.Sci B Polymer Physics*, **38**, 154 (2000).

Kim, Y.-M.; Park, J.-K."Effect of Short Chain Branching on the Blown Film Properties of Linear Low Density Polyethylene." *Journal of Applied Polymer Science*, **61**, 2315 (1996).

Kimura, K.; Shigemura, T.; Yuasa, S."Characterization of Ethylene-1-Butene Copolymer by Differential Scanning Calorimetry and ^{13}C-NMR Spectroscopy." *J.Appl.Polym.Sci.*, **29**, 3161 (1984).

Kimura, K.; Yuasa, S.; Maru, Y."Carbon-13 nuclear magnetic resonance study of ethylene-1-octene and ethylene-4-methyl-1-pentene copolymers." *Polymer*, **25**, 441 (1984).

Kimura, T.; Neki, K.; Tamura, N.; Horii, F.; Nakagawa, M.; Odani, H."High-resolution solid-state ^{13}C nuclear magnetic resonance study of the combined process of 1H spin diffusion and 1H spin-lattice relaxation in semicrystalline polymers." *Polymer*, **33**, 493 (1992).

Kitamaru, R.; Horii, F.; Murayama, K."Phase Structure of Lamellar Crystalline Polyethylene by Solid-State High-Resolution ^{13}C NMR: detection of the Crystalline-Amorphous Interphase." *Macromolecules*, **19** (1986).

Kitamaru, R.; Nakaoki, T.; Alamo, R. G.; Mandelkern, L."A Carbon-13 NMR Study of the Phase Structure of Semicrystalline Polymeers: Hydrogenated Polybutadiene." *Macromolecules*, **29**, 6847 (1996).

Krause, S. Polymer-Polymer Compatibility. In *Polymer Blends;* Paul, D. R.; Newman, S. Eds.; Acad.Press: NY, 1978; Vol. 1; pp. 16.

Kuchanov, S. I.; Panyukov, S. V."Molecular theory of solutions and blends of heteropolymers. I. Thermodynamics of amorphous multicomponent polymer systems." *J.Polym.Sci.,B:Polym. Phys.*, **36**, 937 (1998).

Kumar, S. K.; Yoon, D. Y."Lattice Model for Crystal-Amorphous Interphases in Lamellar Semicrystalline Polymers: Effects of Tight-Fold Energy and Chain." *Macromolecules*, **22**, 3458 (1989).

Kuwabara, K.; Kaji, H.; Horii, F.; Bassett, D. C.; Olley, R. H."Solid -State ^{13}C NMR Analyses of the Crystalline-Noncrystalline Structure for Metallocene-Catalyzed Linear Low-Density Polyethylene." *Macromolecules*, **30**, 7516 (1997).

Kyu, T.; Hu, S.-R.; Stein, R. S."Characterization and Properties of Polyethylene Blends II. Linear Low-Density with Conventional Low-Density Polyethylene." *J.Polym.Sci.,B:Polym.Phys.*, **25**, 89 (1987).

Lacher, R. C.; Bryant, J. L."Time-resolved SAXS on Crystallization of a Low-Density Polyethylene/High-Density Poluethylene Polymer Blend." *Macromolecules*, **21**, 1180 (1988).

Lambert, W. S.; Phillips, P.J. "Regime Transitions in a Nonreptating Polymer: Cross-Linked Linear Polyethylene." *Macromolecules*, **23**, 2075 (1990).

Lambert, W. S."Structural and melting studies of crosslinked linear polyethylenes." *Polymer*, **31**, 2077 (1990).

Lambert, W. S.; Phillips, P. J."Crystallization kineticsof low-molecular weight fractions of branched polyethylenes." *Macromolecules*, **27**, 3537 (1994).

Lambert, W. S.; Phillips, P. J."Small-angle X-ray scattering studies of crystallization in crosslinked linear polyethylene." *Polymer*, **35**, 1810 (1994).

Lambert, W. S.; Phillips, P. J."Crystallization kinetics of fractions of branched polyethylenes .2. Effect of molecular weight." *Polymer*, **37**, 3585 (1996).

Larson, R. G. *The Structure and Rheology of Complex Fluids*; Oxford Univ. Press: NY, 1999.

Laupretre, F.; Monnerie, L.; Barthelemy, L.; Vairon, J. P.; Sauzeau, A.; Roussel, D."Influence of Crystallization conditions on the Location of Side-Chain Branches in Ethylene Copolymers as Studied by High-Resolution Solid-State ^{13}C NMR." *Polymer Bulletain*, **15**, 159 (1986).

Lee, Y. D.; Phillips, P. J.; J.S.Lin."The Influence of Crystallinity Distribution on Small-Angle X-ray Scattering from Semicrystalline Polymers." *Journal of Polymer Science B: Polymer Physics*, **29**, 1235 (1991).

Lin, L.; Argon, A. S."ReviewStructure and plastic deformation of polyethylene." *Journal of Materials Science*, **29**, 294 (1994).

Lin, Y. G.; Mallin, D. T.; Chien, J. C. W.; Winter, H. H."Dynamic Mechanical Measurement of Crystallization-Induced Gelation in Thermoplastic Elastomeric Poly(propylene)." *Macromolecules*, **24**, 850 (1991).

Lindsey, C. P.; Patterson, G. D."Detailed Comparison of the Williams-Watts and Cole-Davidson functions." *J.Chem.Phys*, **73**, 3348 (1980).

Lu, L.; Alamo, R. G.; Mandelkern, L."Lamellar Thickness Distributions in Linear Polyethylene and Ethylene Copolymers." *Macromolecules*, **27**, 6571 (1994).

Lustiger, A.; Markham, R. L."Importance of tie molecules in preventing polyethylene fracture under long-term loading conditions." *Polymer*, **24**, 1647 (1983).

Mandelkern, L."The melting of crystalline polymers." *Rubber. Chem. tech*, **32**, 1392 (1959).

Mandelkern, L. *Crystallization of Pollymers*; McGraw-Hill: NY, 1964.

Mandelkern, L."The Relation between Structure and Properties of Crystalline polymers." *Polymer Journal*, **17**, 337 (1985).

Mandelkern, L.; Alamo, R. G. Crystallization Kinetics. In *Physical Properties of Polymers Handbook;* Mark, E. J. Ed.; American Institute of Physics: Woodbury, NY, 1996; pp. 417.

Mandelkern, L.; Alamo, R. G. Thermodynamic Quantities Governing Melting. In *Physical Properties of Polymers Handbook;* NY, A. Ed.; J.E. Mark: Woodbury, NY, 1996; pp. 119.

Mandelkern, L.; Alamo, R. G.; Kennedy, M.A. "Comments on Paper "Raman Spectroscopy Employed for the Determination of the Intermediate Phase in Polyethylene"." *Macromolecules*, **28**, 2988 (1995).

Mandelkern, L.; Alamo, R. G.; M.A.Kennedy."Interphase Thickness of Linear Polyethylene." *Macromolecules*, **23**, 4721 (1990).

Mandelkern, L.; M.Glotin; Benson, R. A."Supermolecular Structure and Thermodynamic Properties of Linear and Branched Polyethylenes under Rapid Crystallization Conditions." *Macromolecules*, **14**, 22 (1981).

Mandelkern, L.; Stack, G. M."Equilibrium Melting Temperature of Long-Chain Molecules." *Macromolecules*, **17**, 871 (1984).

Mansfield, M.; Boyd, R."Molecular Motion, the Alpha Relaxation, and Chain Transport in Polyethylene Crystals." *J. Polym. Sci.,:Polym. Phys.Ed.*, **16**, 1227 (1978).

Mansfield, M. L."Monte Carlo Study of Chain Folding in Melt-Crystallized Polymers." *Macromolecules*, **16**, 914920 (1983).

Marega, C.; Marigo, A.; Cingano, G.; Zanetti, R."Small-angle X-ray scattering from high-density polyethylene: lamellar thickness distributions." *Polymer*, **37**, 5549 (1996).

Margio, A.; Marega, C.; Zanetti, R.; Scarzi, P."A Study of the Lamellar Thickness Distribution in 1-Butene, 4-Methyl-1-Pentene and 1-Hexene LLDPE by Small and Wide Angle X-ray Scattering and Transmission Electron Microscopy." *Eur.Polym.J.*, **34**, 597 (1998).

Marigo, A.; Cingano, G.; Marega, C.; Zanetti, R."Small- and wide-angle X-ray scattering characterization of -hexene linear low-density polyethylene." *Macromol.Chem.Phys.*, **196**, 2537 (1995).

Marigo, A.; Cingano,G. ; Zanetti,R.; Ferrara,G.; Paganetto,G. "Small-and wide-angle X-ray scattering characterization of 1-hexene linear low-density polyethylene." *Macromol Chem Phys*, **196**, 2537 (1995).

Markis, M."Chemically Crosslinked High-Density Polyethylene." *J. Appl. Polym. Sci*, **13**, 713 (1969).

Marqusee, J. A."Chain Configuration in Semicrystalline Interphases: Chain Stiffness." *Macromolecules*, **22**, 472 (1989).

Marqusee, J. A.; Dill, K. A."Chain Configuration in Lamellar Semicrystalline Polymer Interphases." *Macromolecules*, **19**, 2420 (1986).

Mathot, V. B. F. Structure, crystallization and melting of linear, branched and copolymerized polyethylenes as revealed by fractionation methods and DSC. In *New Advances in Polyolefins;* Chung, T. C. Ed.; Plenum Press: NY, 1993; pp. 121.

Mathot, V. B. F.; Pijpers, M. F. J."Molecular Structure, Melting Behavior, and Crystallinity of 1-Octene Based Very Low Density Polyethylenes (VLDPEs) as Studied by Fractionation and Heat Capacity Measurements with DSC." *J.Appl.Polym.Sci*, **39**, 979 (1990).

Mathot, V. B. F.; Scherrenberg, R. L.; Pipjers, T. F. J."Metastability and order in linear, branched and copolymerized polyethylenes." *Polymer*, **39**, 4541 (1998).

Maxfield, J.; Mandelkern, L."Crystallinity, Supermolecular Structure, and Thermodynamic Properties of Linear Polyethylene Fractions." *Macromolecules*, **10**, 1141 (1977).

McFaddin, D. C.; Russell, K. E.; Kelusky, E. C."^{13}C nmr solid-state studies of relaxation behavior of branches in homogeneous 1-alkene-ethylene copolymers." *Polymer Communications*, **27**, 204 (1986).

McGrum, N. G.; Read, B. E.; Williams, G. *Anelastic and Dielectric Effects in Polymer Solids*; John Willey & Sons: London-New York-Sydney, 1967.

Minick, J.; Moet, A.; A.Hiltner; E.Bar; Chum, S. P."Crystallization of Very Low Density Copolymers of Ethylene with alpha-Olefins." *Journal of Applied Polym Sci.*, **58**, 1371 (1995).

Mirabella, F. M.; Westphal, S. P.; Fernando, R. L.; Ford, E. A."Morphological Explanation of the Extraordinary Fracture Toughness of Linear Low Density Polyethylenes." *J. Polym.Sci.,B:Polym.Phys.*, **26**, 1995 (1988).

Mours, M.; Winter, H. H."Relaxation Patterns of Nearly Critical Gels." *Macromolecules*, **29**, 7221 (1996).

Mueller, K. T.; Jarive, T. P.; Aurentz, D. J.; Roberts, B. W."The REDOR transform: direct calculation of internuclear coupling from dipolar-dephasing NMR data." *Chemical Physics Letters*, **242**, 553 (1995).

Mumby, S. J.; Sher, P.; Ruiten, J. v."Liquid-liquid phase separation in blends of polydisperse linear and branched polyethylenes." *Polymer*, **36**, 2921 (1995).

Mutter, R.; W.Stille; Strobl, G. "Transition Regions and Surface Melting in Partially Crystalline Polyethylene - a Raman-Spectroscopic Study." *J.Polym.Sci.,B:Polym.Phys*, **31** (1993).

Naylor, C. C.; Meier, R. J.; Kip, B. J.; Williams, K. P. J.; Mason, S. M.; Conroy, N.; Gerrard, D. L."Raman Spectroscopy Employed for the Determination of the Intermediate Phase in Polyethylene." *Macromolecules*, **28**, 2969 (1995).

Naylor, K. L.; Phillips, P. J."Optimization of Permanganic Etching of Polyethylenes for Scanning Electron Microscopy." *J.Polym.Sci.,Polym.Phys.Ed*, **21**, 2011 (1983).

Nesarikar, A.; Crist, B.; Davidovich, A."Liquid-Liquid Phase Separation in Linear Low-Density Polyethylene." *J. Polym. Sci.,B: Polym.Phys.*, **32**, 641 (1994).

Nielsen, L."Transitions in Ethylene Polymers." *J.Polym Sci*, **42**, 357 (1960).

Nijenhuis, K.; Winter, H. H."Mechanical Properties at the Gel Point of a Crystallizing Poly(vinyl chloride) Solution." *Macromolecules*, **22**, 411 (1989).

Noid, D. W.; Sumpter, B. G.; B.Wunderlich."Molecular Dynamics Simulation of Twist Motion in Polyethylene." *Macromolecules*, **24**, 4148 (1991).

Odian, G. G. *Principles of polymerization*; McGraw-Hill: New York, 1970.

Packer, K. J.; Pope, J. M.; Yeung, R. R.; Cudby, M. E. A."The Effect of Morphology on ^{1}H NMR Spectra and Relaxation in Semicrystalline Polyolefins." *J. Polym.Sci: Polym. Phys.*, **22**, 589 (1984).

Parker, J. A.; Bassett, D. C.; Olley, R. H."On high pressure crystallization and the characterization of linear-low density polyethylenes." *Polymer*, **35**, 4140 (1994).

Perez, E.; Bello, A.; Perena, J. M.; Benavente, R.; Martinez, M. C.; Aguilar, C."Solid-state nuclear magnetic resonance study of linear-low density polyethylenes: 1. Ethylene-1-butene copolymers." *Polymer*, **30**, 1508 (1989).

Perez, E.; Vanderhart, D. L."Morphological Partitioning of Chain Ends and Methyl Branches in Melt-crystallized Polyethylene by ^{13}C-NMR." *J. Polym. Sci.: Part B: Polym.Phys.*, **25**, 1637 (1987).

Peters, M.; Goderis, B.; Vonk, C.; Reynaers, H.; Mathot, V."Morphology of Homogeneous Copolymers of Ethene and 1-Octene. Influence of Thermal History on Morphology." *J. Polym.Sci.,b:Polym.Phys.*, **35**, 2689 (1997).

Phillips, P. J."Polymer Crystals." *Rep.Prog.Phys.*, **53**, 549 (1990).

Pink, D. A.; Green, T. J.; Chapman, D."Raman Scattering in Bilayers of Saturated Phosphatidylcholines." *Biochemistry*, **19**, 349 (1980).

Pogodina, N. V.; Winter, H. H."Polypropylene crystallization as a physical gelation process." *Macromolecules*, **31**, 8164 (1998).

Point, J. J."New Approach to the Mechanism of Oligomer Crystallization." *J. Chem. Soc. Faraday Trans.*, **91**, 2565 (1995).

Point, J. J."Experimental Study of Mechanism of Crystallization of Poly(ethylene oxide) and an Alternative to the Standart kinetic Theory of crystallization of Long-Chain Compounds." *Macromolecules*, **30**, 1375 (1997).

Point, J. J."Experimental Study of the mechanism of Crystallization of Poly(ethylene oxide) and an Alternative to the Standard Kinetic Theory of Crystallization of Long-Chain Compounds." *Macromolecules*, **30** (1997).

Point, J.-J.; Janimak, J. J."An evaluation of the theories of regimes of nucleation controlled crystal growth as applied to polymers." *J. Crystal Growth*, **131**, 501 (1993).

Popli, R.; L.Mandelkern."Influence of Structural and Morphological Factors on the Mechanical Properties of the Polyethylenes." *J. Polymer Science B; Polymer Physics*, **25**, 441 (1987).

Rana, D.; Lee, C. H.; Cho, K.; Lee, B. H.; Choe, S."Thermal and Mechanical Properties for Binary Blends of Metallocene Polyethylene with Conventional Polyolefins." *J. Appl. Polym.Sci.*, **69**, 2441 (1998).

Randall, J. C."Carbon-13 NMR of Ethylene-1-Olefin Copolymers: Extension to the Short-Chain Branch Distribution in a Low-Density Polyethylene." *J.Polym.Sci: Polym.Phys.Ed*, **11**, 275 (1973).

Reding, F. P.; Faucher, J. A.; Whitman, R. D."Glass Transitions in Ethylene copolymers and Vinyl Homopolymers and Copolymers." *Journal of Polymer Science*, **57**, 483 (1962).

Ree, M.; Kyu, T.; Stein, R. S."Quantitative Small Angle Light-Scattering Studies of the Melting and Crystallization of LLDPE/LDPE Blends." *J.Polym.Sci.,B:Polym.Phys*, **25**, 105 (1987).

Reneker, D. H.; Mazur, J."Dispirations, disclinations, dislocations and chain twist in polyethylene crystals." *Polymer*, **24**, 1387 (1983).

Reneker, D. H.; Mazur, J."Dispirations, disclinations, dislocations and chain twist in polyethylene crystals." *Polymer*, **24**, 1387 (1983).

Richardson, M. J.; Flory, P. J.; Jackson, J. B."Crystallization and Melting of Copolymers of Polyethylene." *Polymer*, **4**, 221 (1963).

Righetti, M. C."Influence of branching on melting behavior and isothermal crystallization of poly(butylene terephtalare)." *Macromol.Chem. Phys.*, **198**, 363 (1997).

Rodrigues-Cabello, J. C.; Martin-Monge, J.; Lagaron, J. M.; Pastor, J. M."Determination of the content of extended chain segments in isotropic and uniaxially stretched polyethylenes by Raman spectroscopy." *Macromolecular Chemistry and Physics*, **199**, 2767 (1998).

Rouse, P. E."A Theory of the Linear Viscoelastic Properties of Dilute Solutions of Coiling Polymers." *J.Chem.Phys.*, **21**, 1272 (1953).

Rull, F.; Prieto, A. C.; Casado, D. M.; Sobron, F.; Edwards, H. G. M."Estimation of Crystallinity in Polyethylene by Raman-Spectroscopy." *J. Raman. Spec.*, **24**, 545 (1993).

Ryan, A. J.; Fairclough, J. P. A.; Terrill, N. J.; Olmstead, P. D.; Poon, W. C. K."A scattering study of nucleation phenomena in polymer crystallisation." *Faraday Disc.,*, **112**, 13 (1999).

Sakaguchi, F.; L.Mandelkern; J.Maxfield."The Specific Heat of Linear Polyethylene After Annealing at Low Temperatures." *Journal of Polymer Science. Polymer Physics Edition*, **14**, 2137 (1976).

Sakiewicz, P.; Phillips, P. J."Peroxide Crosslinking of Linear Low-Density Polyethylenes with Homogeneous Distribution of Short Chain Branching." *J. Polym. Sci. A: Polym. Chem.*, **33**, 853 (1995).

Salazar, J. M. D.; Calleja, F. J. B."Influence of Chain Defects on the Crystallization of Polyethylene with Reference to Crystal Size and Perfection." *J. Crystal Growth*, **48**, 283 (1979).

Sasaki, S.; Tashiro, K.; Kobayashi, M.; Izumi, Y.; Kobayashi, K."Microscopically viewed structural change of PE during the isothermal crystallization from the melt - II. Conformational ordering and lamellar formation mechanism derived from the coupled interpretation of time-resolved SAXS and FTIR data." *Polymer*, **40**, 7125 (1999).

Schmidt-Rohr, K."A Double-Quantum Solid-State NMR Technique for Determining Torsion Angles in Polymers." *Macromolecules*, **29**, 3975 (1996).

Schmidt-Rohr, K."Complete Dipolar Decoupling of ^{13}C and Its Use in Two-dimensional Double-Quantum Solid-State NMR for Determining Polymer Conformations." *J. Magn.Resonance*, **131**, 209 (1998).

Schmidt-Rohr, K.; Spiess, H. W. *Multidimensional Solid-State NMR of Polymers*; Acad.Press: NY, 1994.

Schmidt-Rohr, K.; Wilhelm, M.; Spiess, H. W."Determination of Chemical-Shift Tensor Orientation in Methylene Groups by Separated-Local-field NMR." *Magnetic Resonance in Chemistry*, **31**, 352 (1993).

Schouterden, P.; Groenickx, G.; Hejden, B. V. d.; Jansen, F."Fractionation and thermal behavior of linear low density polyethylene." *Polymer*, **28**, 2099 (1987).

Schwittay, C.; M.Mours; Winter, H. H."RheologicalnExpression of Physical Gelation in Polymers." *Faraday Discussions*, **101**, 93 (1995).

Seguella, R.; F.Rietsch."On the Isomorphism of Ethylene/α-olefin Copolymers." *J.Polym.Sci.,Polym.Lett.,*, **45**, 4175 (1974).

Shirayama, K.; Kita, S.-I.; Watabe, H."Effects of Branching on Some Properties of Ethylene/a-olefin Copolymers." *Makromol.Chem*, **151**, 97 (1972).

Snyder, R. G.; Krause, S. J.; Scherer, J. R."Determination of the Distribution of Straight-Chain Segment Lengths in Crystalline Polyethylene from the Raman Lam-1 Band." *J. Polym. Sci.,Polym.Phys. Edn.*, **16**, 1593 (1978).

Snyder, R. G.; Scherer, J. R."Interpretation of Longitudial-Acoustical Mode Spectra of Polymers." *J.Polym.Sci.,Polym.Phys*, **18**, 421 (1980).

Song, H. H.; Stein, R. S.; Wu, D.--. Q.; Ree, M.; Phillips, J. C.; LeGrand, A.; Chu, B."Time-Resolved SAXS on Crystallization of a Low Density Polyethylene/High-Density Polyethylene Polymer Blend." *Macromolecules*, **21**, 1180 (1988).

Song, H. H.; Wu, D.--. Q.; Chu, B.; Satkowski, M.; Ree, M.; Stein, R. S.; Phillips, J. C."Time-Resolved Small-Angle X-ray Scattering of a High Density Polyethylene/Low density Polyethylene Blend." (1990).

Sperling, L. H. *Introduction to physical polymer science*; Wiley: New York, 1986.

Starck, P."Dynamic Mechanical Thermal Analysis on Ziegler-Natta and Metallocene type ethylene co-polymers." *European polymer journal*, **33**, 339 (1997).

Stark, P."Studies of the Comonomer Distributions in Low Density Polyethylenes Using Temperature Rising Elution Fractionation and Stepwise Crystallization by DSC." *Polymer International*, **40**, 111 (1996).

Stribeck, N.; Alamo, R. G.; Mandelkern, L.; Zachmann, H. G."Study of the Phase Structure of Linear polyethylene by Means of Small-Angle X-ray Scattering and Raman Spectroscopy." *Macromolecules*, **28**, 5029 (1995).

Strobl, G. R. *Physics of Polymers*; Springer-Verlag: Berlin, 1996.

Strobl, G. R.; Hagedorn, W."Raman Spectroscopic Method for Determining Crystallinity of Polyethylene." *J.Polym.Sci: Polym.Phys*, **16**, 1181 (1978).

Tarazona, A.; Koglin, E.; Coussens, B. B.; Meier, R. J."Conformational dependence of Raman frequencies and intensities in alkanes and polyetyhylene." *Vibrational Spectroscopy*, **14**, 159 (1997).

Tashiro, K.; Sasaki, S.; Kobayashi, M."Structural Investigation of Orthorombic- to Hexagonal phase transition in Polyethylene Crystal: The Experimental Confirmation of the Conformationally Disordered Structure by X-ray Diffraction and Infrared/Raman Spectroscopic Measurements." *Macromolecules*, **29**, 7460 (1996).

Teh, J. W.; Blom, H. P.; Rudin, A."A Study on the Crystallization Behavior of Polypropylene, Polyethylene and their Blends by Dynamic-Mechanical and Thermal Methods." *Polymer*, **35**, 1680 (1994).

Tritto, I.; Fan, Z.-Q.; Locatelli, P.; Sacchi, M. C."13C NMR Studies of Ethylene-Propylene Copolymers Prepared with Homogeneous Metallocene-based Ziegler-Natta Catalysts." *Macromolecules*, **28**, 3342 (1995).

Usami, T.; Takayama, S."Fine-Branching Structure in High-pressure, Low-Density Polyethylenes by 50.10-MHz ^{13}C NMR Analysis." *Macromolecules*, **17**, 1756 (1984).

VanderHart, D. L.; Khoury, F."Quantitative determination of the monoclinic crystalline phase content in polyethylene by $^{1}3C$ NMR." *Polymer*, **25**, 1589 (1984).

VanderHart, D. L.; Perez, E."A ^{13}C NMR Method for Determining the Partitioning of End Groups and Side Branches between the Crystalline and Noncrystalline Regions in Polyethylene." *Macromolecules*, **19**, 1902 (1986).

Vega, J. F.; MunozEscalona, A.; Santamaria, A.; Munoz, M. E.; Lafuente, P."Comparison of the rheological properties of metallocene-catalyzed and conventional high-density polyethylenes." *Macromolecules*, **29**, 960 (1996).

Vonk, C. G.; Pijpers, A. P."An X-ray Diffruction Study of Nonlinear Polyethylene.I. Room-Temperature Observations." *J.Polym.Sci.,Polym.Phys,Ed.*, **23**, 2517 (1985).

Wagener, K. B.; Valetti, D."ADMET Modeling of Branching in Polyethylene. The Effect of a Perfectly-Spaced Methyl Group." *Macromolecules*, **30**, 6688 (1997).

Wagner, J.; Abu-Iqyas, S.; Monar, K.; Phillips, P. J."Crystallization of ethylene-octene copolymers at high cooling rates." *Polymer*, **40**, 4717 (1999).

Wahslstrand, K. J."Computer simulation studies of soliton model for dielectric relaxation in crystalline polyethylene and related polymers. I continuum and pinnedlimits." *J.Chem Phys.*, **82**, 5247 (1985).

Wasserman, S. H.; Graessley, W. W."Effects of Polydispersity on linear viscoelasticity in entangled polymer melts." *polymer Engineering and Science*, **36**, 543 (1992).

Wasserman, S. H.; Graessley, W. W."Prediction of linear viscoelastic responce of entangled polyolefin melts from molecular weight distribution." *polymer Engineering and Science*, **36**, 852 (1996).

Whittall, K. P."Innvestigation of Analysis Techniques for Complicated NMR Relaxation Data." *J. Magnetic Resonance*, **95**, 221 (1991).

Whittall, K. P.; Mackay, A. L."Quantitative Interpretation of NMR Relaxation Data." *J. Magn.Reson.*, **84**, 134 (1989).

Wignall, G. D.; Alamo, R. G.; Londono, J. D.; Mandelkern, L.; Kim, M. H.; Lin, J. S.; Brown, G. M."Morphology of blends of linear and short-chain branched polyethylenes in the solid state by small-angle neutron and X-ray scattering, differential scanning calorimetry, and transmission clectron microscopy." *Macromolecules*, **33**, 551 (2000).

Wignall, G. D.; Alamo, R. G.; Londono, J. D.; Mandelkern, L.; Stehling, F. C."Small-Angle Neutron Scattering Investigations of Liquid-Liquid Phase Separation in Heterogeneous Linear Low-Density Polyethylene." *Macromolecules*, **29**, 5332 (1996).

Wignall, G. D.; Londono, J. D.; Lin, J. S.; Alamo, R. G.; Galante, M. J.; Mandelkern, L. "Morphology of Blends of Linear and Long-Chain Branched Polyethylenes in the Solid State-a Study by SANS,SAXS, and DSC." *Macromolecules*, **28**, 3156 (1995).

Wild, L."Composition Distributions in Polyolefins: A Job for TREF." *Trends in Polymer Science*, **1**, 50 (1993).

Winter, H. H."Analysis of dynamic mechanical data:inversion into a relaxation time spectrum and consistency check." *J. Non-Newtonian Fluid Mech.*, **68**, 225 (1997).

Winter, H. H.; Chambom, F."Analysis of Linear Viscoelasticity of a Crosslinking Polymer at thc Gel Poin." *Journal of Rheology*, **30**, 376 (1986).

Winter, H. H.; Mours, M."Rheology of Polymers near Liquid-Solid Transitions." *Advances in Polymer Science*, **134**, 166 (1997).

Wunderlich, B. *Macromolecular physics*; Academic Press: New York, 1980; Vol. 2.

Zhang, F."Motion of twist defects in crystalline polyethylene: A molecular – dynamics study." *Physical Review B-condensed matter*, **59**, 792 (1999).

Zhao, Y.; Liu, S.; Yang, D."Crystallization behavior of blends of high-density polyethylene with novel linear low-density polyethylene." *macromol. Chem.Phys.*, **198**, 1427 (1997).

Zuniga, I.; Rodrigues, K.; Mattice, W. L."Analytical and Monte Carlo Studies of the Interfacial Region in Semicrystalline Polymers with First- and Second-Order Intrachain Interactions." *Macromolecules*, **23**, 4108 (1990).